

D180-22876-7

Solar Power Satellite

SYSTEM DEFINITION STUDY

FINAL BRIEFING
DECEMBER 13, 1977

Approved



G. R. Woodcock
Study Manager

Boeing Aerospace Company
Missiles And Space Group
Space Division
P.O. Box 3999
Seattle, Washington 98124

D180-22876-7

FOREWORD

The SPS systems definition study was initiated in December 1976. Part I was completed on May 1, 1977. Part II technical work was completed October 31, 1977.

The study was managed by the Lyndon B. Johnson Space Center (JSC) of the National Aeronautics and Space Administration (NASA). The Contracting Officer's Representative (COR) was Clarke Covington of JSC. JSC study management team members included:

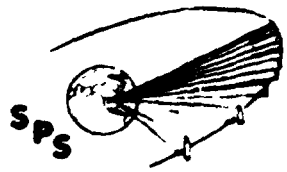
Lou Livingston	System Engineering and Analysis	Dick Kennedy	Power Distribution
Lyle Jenkins	Space Construction	Bob Ried	Structure and Thermal Analysis
Jim Jones	Design	Fred Stebbins	Structural Analysis
Sam Nassiff	Construction Base	Bob Bond	Man-Machine Interface
Buddy Heineman	Mass Properties	Bob Gundersen	Man-Machine Interface
Dickey Arndt	Microwave System Analysis	Ilu Davis	Transportation Systems
R. H. Dietz	Microwave Transmitter and Rectenna	Harold Benson	Cost Analysis
Lou Leopold	Microwave Generators	Stu Nachtwey	Microwave Biological Effects
Jack Seyl	Phase Control	Andrei Konradi	Space Radiation Environment
Bill Dusenbury	Energy Conversion	Alva Hardy	Radiation Shielding
Jim Cioni	Photovoltaic Systems	Don Kessler	Collision Probability
		Bill Simon	Thermal Cycle Systems

The Boeing study manager was Gordon Woodcock. Boeing technical leaders were:

Vince Caluori	Photovoltaic SPS's	Walt Lund	Microwave Transmitter
Dan Gregory	Thermal Engine SPS's	Owen Denman	Microwave Design Integration
Eldon Davis	Construction and Orbit-to-Orbit Transportation	Jack Gwin	Power Distribution
Hal DiRamio	Earth-to-Orbit Transportation	Don Grim	Electric Propulsion
Dr. Joe Gauger	Cost	Henry Hillbrath	Propulsion
Bob Conrad	Mass Properties	Dr. Ted Kramer	Thermal Analysis and Optics
Rod Darrow	Operations	Keith Miller	Human Factors and Construction Operations
Bill Emsley	Flight Control	Jack Olson	Configuration Design
Ottis Bullock	Structural Design	Dr. Henry Oman	Photovoltaics
Dr. Ervin Nalos	Microwave Subsystem	John Perry	Structures

The General Electric Company Space Division was the major subcontractor for the study. Their contributions included Rankine cycle power generation, power processing and switchgear, microwave transmitter phase control and alternative transmitter configurations, remote manipulators, and thin-film silicon photovoltaics.

Other subcontractors were Hughes Research Center - gallium arsenide photovoltaics, Varian - klystrons and klystron production, SPIRE - silicon solar cell directed energy annealing.



D180-22876-7

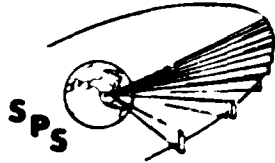
BOEING

**Solar Power Satellite
System Definition Study
Executive Summary**

GUIDELINES AND ASSUMPTIONS

Guidelines and assumptions used during the course of the study are summarized here. It is emphasized that the approach taken to this study was to maximize confidence in results, rather than to minimize mass and cost projections by using optimistic or far-future technology extrapolations. This is reflected in the selection of energy conversion systems, in the selection of transportation systems, in the mass and cost estimating techniques and in the uncertainty analysis approach.

A significant factor in overall cost characteristics is the maximum ionosphere beam intensity stated. This intensity limit strongly influences the cost characteristics of the ground receiving system, which represents approximately 25% of total costs.



SPS-1668

D180-22876-7

Guidelines & Assumptions

BOEING

GUIDELINES

- JSC INHOUSE STUDY (JSC-11568, THE "GREEN BOOK") SHOULD BE USED AS A POINT OF DEPARTURE.
- SPS SYSTEM DESIGNED AND ANALYZED SHOULD REPRESENT THE EARLY PART OF A MATURE OPERATIONAL PROGRAM.
- SPS SYSTEM DESIGNS SHOULD MAXIMIZE CONFIDENCE IN RESULTS RATHER THAN MINIMIZING MASS AND COST THROUGH MAJOR TECHNOLOGY EXTRAPOLATIONS.

ASSUMPTIONS

- INITIAL SPS'S DEPLOYED IN 1990'S
- 1977 DOLLARS THROUGHOUT
- SPACE TRANSPORTATION OPERATIONS KSC-BASED
- SPS'S OPERATE AT GEO
- NOMINAL DESIGN OUTPUT 10,000 MEGAWATTS THROUGH TWO MICROWAVE LINKS AT 2.45 GHz
- MAXIMUM INOSPHERE BEAM INTENSITY 23 MW/CM²

SPS SYSTEM DEFINITION STUDY DESIGN EVOLUTIONS

Design evolutions of the principal types of SPS systems and space support systems are shown.

The photovoltaic SPS began with the JSC truss configuration at a geometric concentration ratio of 2. This configuration was sized for beginning-of-life output capability. The configuration was resized to allow maintenance of output capability throughout the thirty-year design life system, by periodic array addition. At the completion of part 1 of the study, a total of 10 photovoltaic options had been defined as shown. These included silicon and gallium arsenide energy conversion at concentration ratios 2 and 1 and various power maintenance methods. The lowest cost silicon system was selected for continuance into part 2. This system employed no concentration and used in situ annealing of the solar cells for power maintenance. The configuration was further defined during part 2. The system output, with the optimum rectenna size, was reduced to 9.3 GW as a result of final definitions of the efficiency chain.

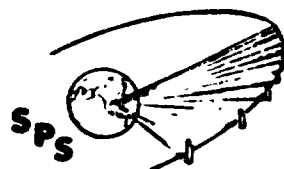
The thermal engine analyses began with the 10 GW Brayton system defined under an earlier contract. Early in the subject study, an analysis of available data on plastic film reflector degradation in the space environment suggested that a 30% degradation might occur. Consequently, the concentrators were enlarged to compensate. The configuration was next divided into 16 modules with trough-shaped concentrators as shown under "constructionized Brayton." During part 1 Rankine and Thermionic systems were also evaluated. Initial evaluations indicated the Rankine system to be more massive than the Brayton system. However, a cycle temperature ratio optimization resulted in a lower overall mass. Additional design changes introduced at this point eliminated steerable facets from the concentrator by flying the system always exactly facing the sun.

Toward the end of the study, new information became available on plastic film reflectors indicating that degradation impact would not occur and the final system configuration was, therefore, resized to reflect nondegradation of the concentrator.

The principal evolution in space transportation systems was in the launch vehicle. The study began with the 230 ton payload heavy lift launch vehicle at a projected cost for transportation to orbit of \$33 per kilogram. Packaging indicated that higher payload densities could make possible a reusable shroud. Staging optimization studies led to a 400 ton heavy lift launch vehicle that went through the evolution shown. Also, a two-stage winged vehicle option, based on earlier JSC studies, was added.

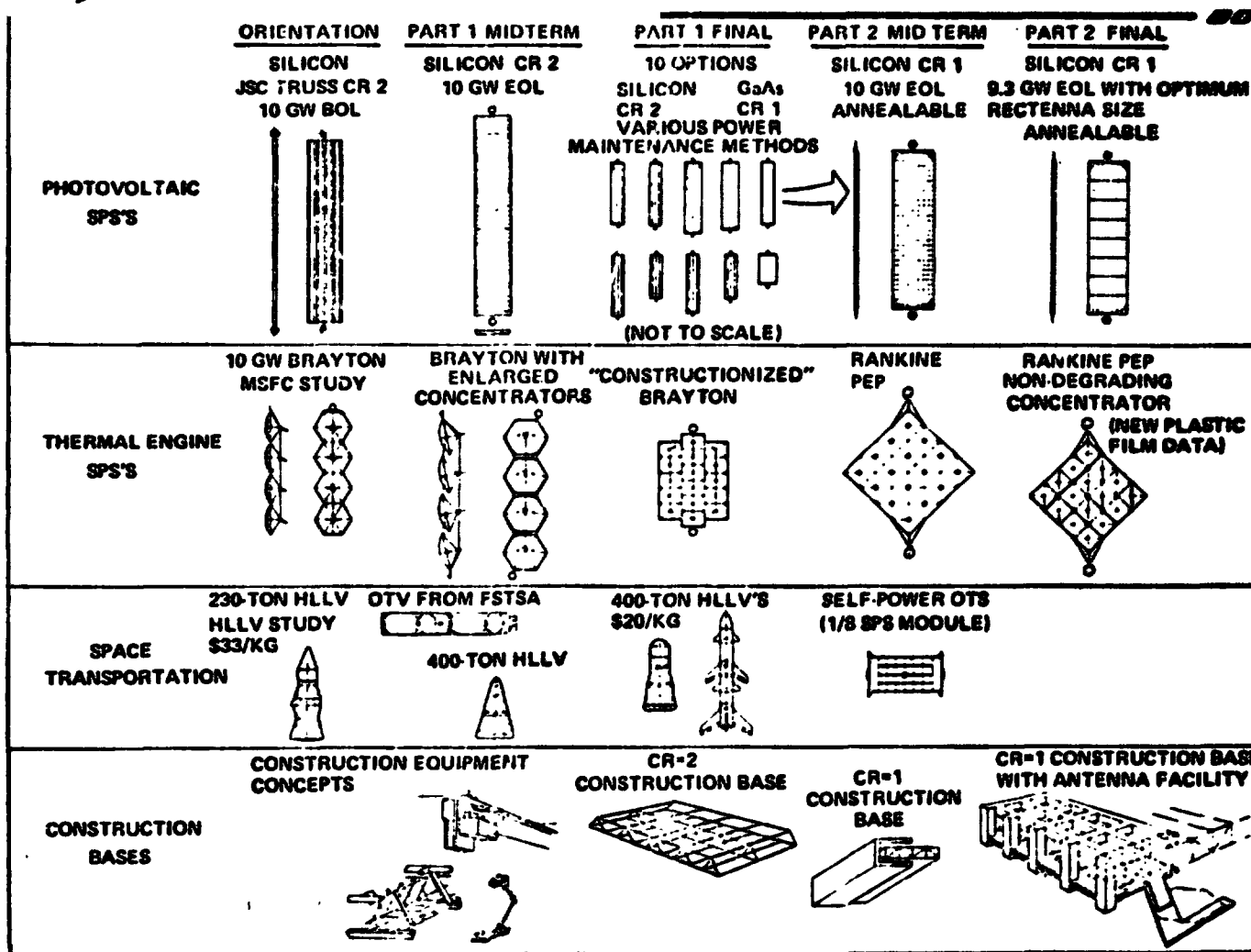
Studies of chemical orbit transfer vehicles included space based and earth launched options. The orbit transfer option taken from the Future Space Transportation System Analyses study was found to be least cost and was retained. Investigation of the means of moving the SPS hardware itself from low earth orbit to geosynchronous orbit continued to indicate a significant cost advantage to the self-power concept.

The evolution of construction concepts began with equipment concepts. The initial construction base concept was for the concentration ratio 2 satellite and included little detail other than overall size and shape. This construction base concept evolved to the illustration shown at the lower right hand corner of the chart. Most of the structure is shown blocked in with structural detail only on one small portion of the construction base. This construction base includes capabilities to construct satellite modules and transmitter antennas. Analogous construction base concepts were developed for the thermal engine system also, but are not shown on this chart.



SPS System Definition Study Design Evolutions

SPS-1548



BEING

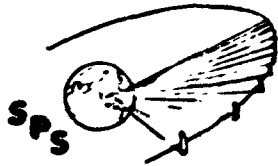
ORIGINAL PAGE IS
OF POOR QUALITY

D180-22876-7

PRINCIPAL FINDINGS

Principal findings of the study are summarized on this chart. The remainder of the executive summary section of this briefing follows this general outline and provides substantiation of the statements.

**ORIGINAL PAGE IS
OF POOR QUALITY**



D180-22876-7

Principal Findings

BOEING

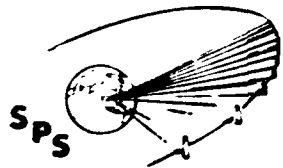
SPS-1650

- | | |
|--|---|
| POWER TRANSMISSION | <ul style="list-style-type: none">- CONSTRAINTS DICTATE THE DESIGN- DETAILED MICROWAVE LINK ERROR ANALYSIS CONFIRMED ATTAINABILITY OF ACCEPTABLE LINK EFFICIENCY |
| ENERGY CONVERSION | <ul style="list-style-type: none">- SILICON PHOTOVOLTAIC BEST OVERALL CHOICE- POTASSIUM RANKINE BACKUP CHOICE |
| SPACE CONSTRUCTION OPERATIONS | <ul style="list-style-type: none">- ASSEMBLY LINE FACILITY KEY TO HIGH PRODUCTIVITY- LEO CONSTRUCTION LOWEST COST |
| SPACE TRANSPORTATION OPERATIONS | <ul style="list-style-type: none">- LOW COST DUE TO TRAFFIC LEVEL, NOT NEW TECHNOLOGY- PAYLOAD VOLUME IS LAUNCH VEHICLE DESIGN DRIVER |
| SPS SYSTEM COSTS | <ul style="list-style-type: none">- POWER COST IN 4 CENTS/kwh RANGE, COMPETITIVE BY YEAR 2000- SYSTEM DESIGN FLEXIBILITY KEY TO COST CONFIDENCE |

CONSTRAINTS DICTATE POWER TRANSMITTER DESIGN

A systems analysis of power transmitter design considerations was conducted. The design process illustrated here controls the determination of transmitter design. The desired power distribution voltage of 40 kv is a compromise between distribution efficiency and mass, and problems and risk associated with high voltage distribution. Power distribution is matched to klystron operating conditions to minimize the amount of power processing required. Experience in developing and operating klystrons has indicated that tube maximum efficiency occurs in a relatively narrow range of perveance. Perveance and distribution voltage dictate beam current and the voltage and beam current dictate klystron power. Tube efficiency and thermal dissipation limits in terms of heat rejection capability then establish the maximum klystron installation density. The current value for this parameter is approximately 23 kw RF per square meter.

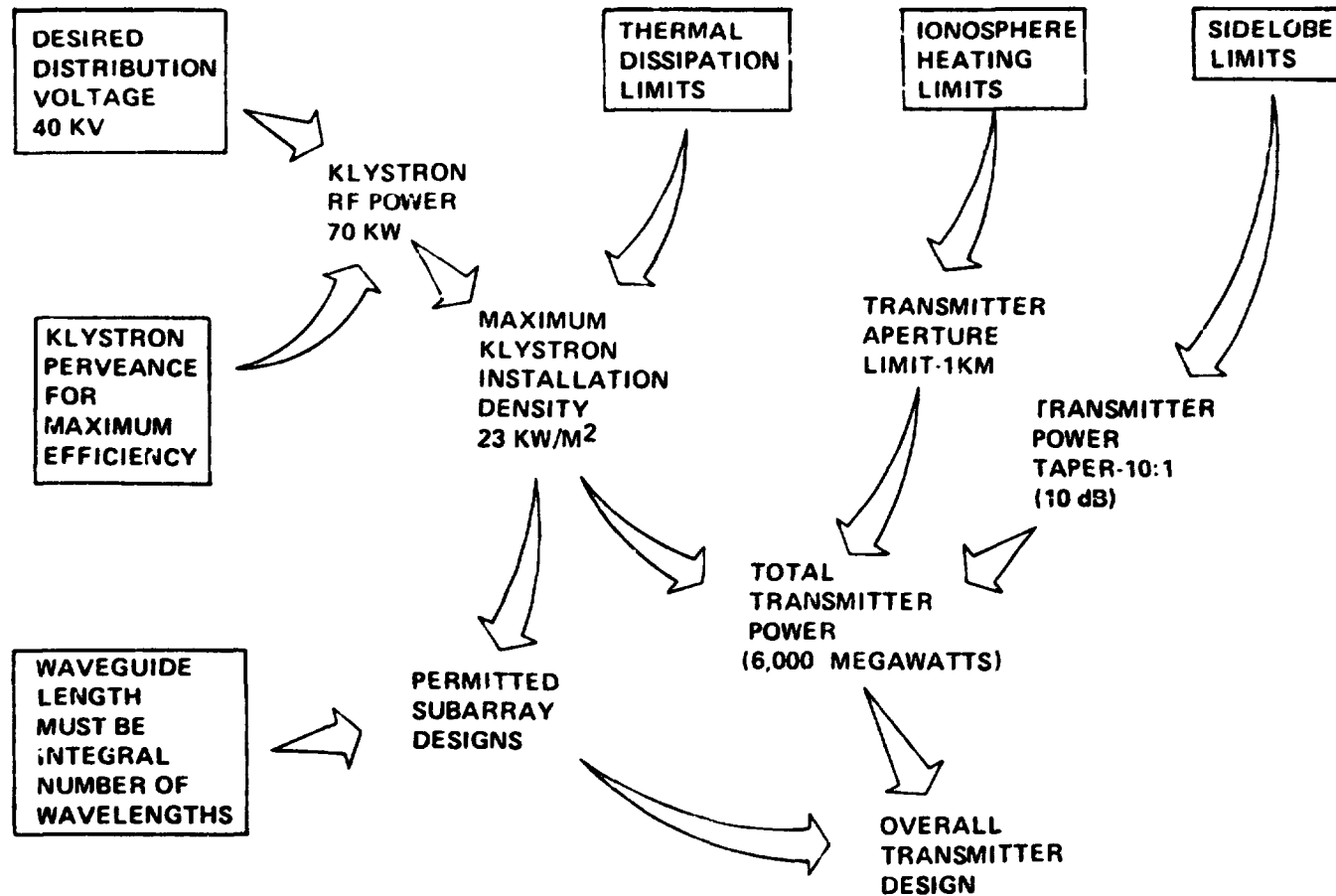
Ionosphere heating limits determine the transmitter aperture limits (larger aperture results in a smaller beam, to increase the ionosphere power density above whatever heating limit is established). Sidelobe limits are quite uncertain at present but will probably establish a transmitter power taper of at least 10:1. Power taper, aperture limit, and maximum klystron installation density combined to determine the total transmitter power. This power and the subarray design limits, together with power taper, establish the overall transmitter design.



Constraints Dictate Power Transmitter Design

SPS 1670

BOEING

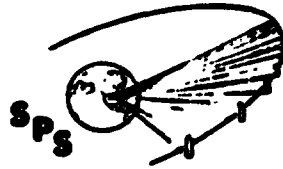


MICROWAVE POWER TRANSMITTER DESIGN

The main features of the power transmitter design is illustrated on the facing page. The basic power amplifier element is a 70 kw heat-pipe-cooled klystron. Each transmitter element includes one klystron, its control and support circuitry, its thermal control equipment, its distribution waveguides and its section of radiating waveguide. The subarray is the basic Earth-manufactured unit. It is approximately 10 meters square and will contain from 4 to 36 klystron elements. The subarrays, in turn, are integrated in the overall transmitter. Each transmitter includes 6,932 subarrays supported on a two-tier structure. At the back of the structural assembly are the power processors that provide the necessary voltage changes and voltage regulation required by the RF systems. Approximately 15% of the total power is processed, the other 85 % being used directly by the klystrons without processing or regulation. Power interrupters and switch gear are provided for all power supplied to the transmitter, so that the sector supplied by any power processor assembly can be isolated or shutoff in the event of failures or malfunctions.

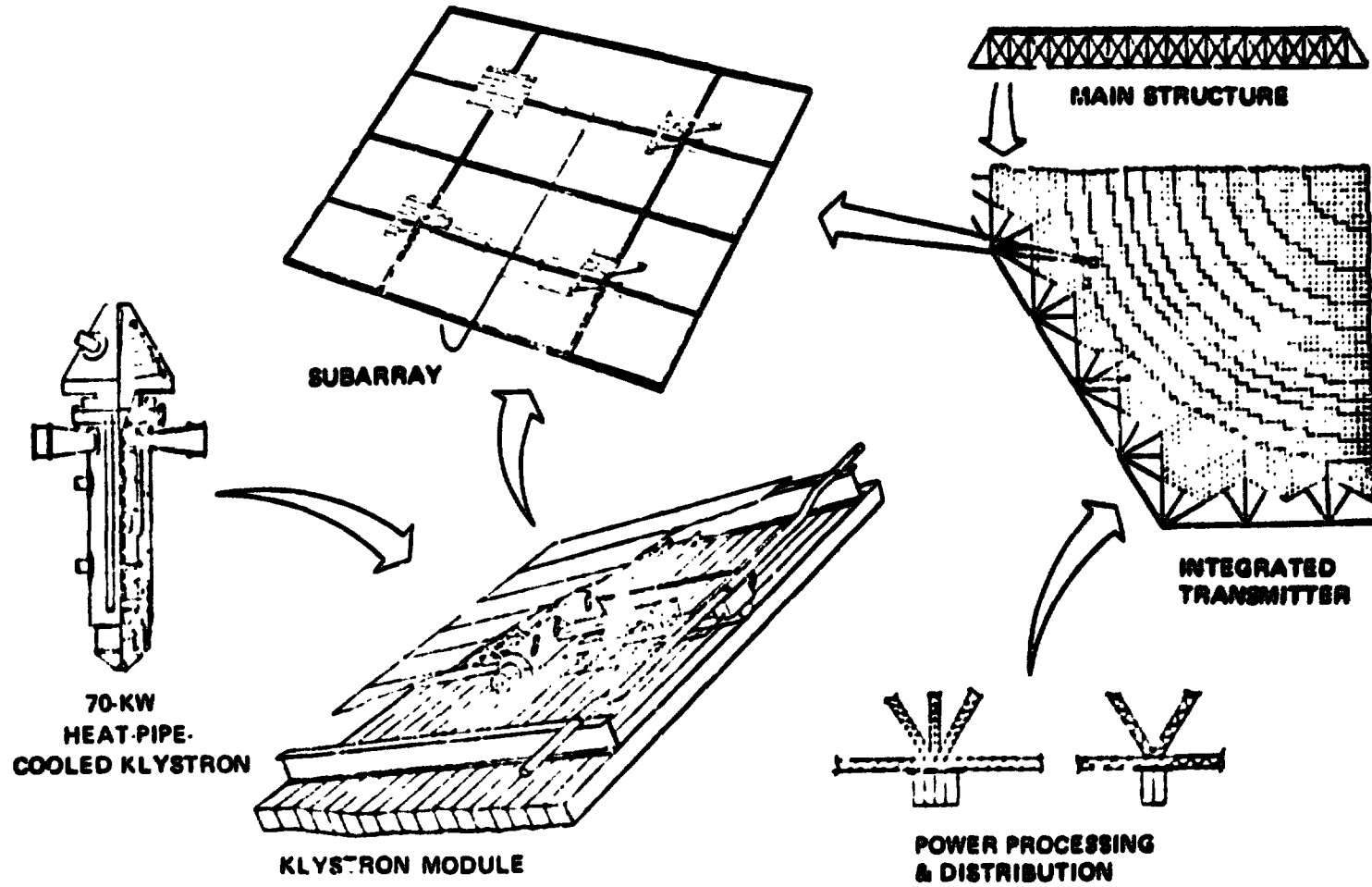
The power transmitter design illustrated is an integrated design meeting the structural, thermal, electrical, and RF requirements of the SPS power transmission system.

Microwave Power Transmitter Design Concept



SPS-1051

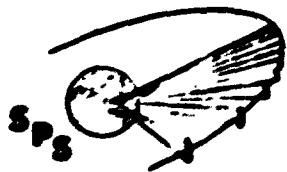
SCENE



D180-22876-7

POWER TRANSMISSION SYSTEM HIGHLIGHTS

The principal features of the power transmission system are indicated on the facing page. The reference system employs a 10 dB taper in ten steps with an option being a fourteen-step, 17-dB taper providing an additional 10 dB of sidelobe suppression.



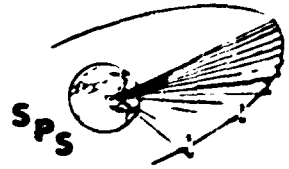
SPS-1802

Power Transmission System Highlights

	39C GREEN BOOK	CURRENT REFERENCE	REASON FOR CHANGE
OUTPUT POWER TO GRID FROM EACH RECTENNA	50W	4.880W	EFFICIENCY CHAIN VARIANCE
ARRAY APERTURE ILLUMINATION	10-STEP TRUNCATED 10-dB GAUSSIAN	SAME	
(ALTERNATE ILLUMINATION)		(14-STEP) (17-dB)	PROVIDES ADDITIONAL 10dB OF SIDELobe SUPPRESSION
SUBARRAY SIZE	100m²	113.8m²	GEOMETRIC CONSTRAINTS
NUMBER OF SUBARRAYS	7860	6932	LARGER AREA PER SUBARRAY
ERROR BUDGET -			
PHASE CONTROL	±10°	SAME	
AMPLITUDE	±1db	SAME	
SUBARRAY MECHANICAL	±3 ARC MIN	±1 ARC MIN	REDUCE LOSSES
RF DISTRIBUTION	NONE	2% TOTAL LOSS	DETAILED SUBARRAY ANALYSIS
PHASE CONTROL	ACTIVE RETRO-DIRECTIVE	SAME	
RECTENNA SIZE	10 x 14km	9.4 x 13 km	HIGHER RECTENNA UNIT COSTS YIELD SMALLER OPTIMUM SIZE
MAXIMUM BEAM POWER DENSITY	23 mw/m²	SAME	

MICROWAVE POWER TRANSMISSION SYSTEM REFERENCE 10 dB TAPER

The left-hand plot illustrates the 10 step, 10 dB taper for the reference system. The right-hand plot shows the actual power density delivered to the ground by this taper pattern including the first 4 sidelobes. The reference taper is shown in solid lines and optional ways of providing the same amount of taper are shown as dotted lines. As can be seen, differences between the reference and the options are slight. The sidelobe suppression provided by the reference system is 24 dB resulting in a first sidelobe at 0.1 M/Wcm^2 . The ideal beam efficiency is 96.5% (With no errors in the production of the beam, 96.5% of the energy is in the main lobe with the remainder in the sidelobes.)

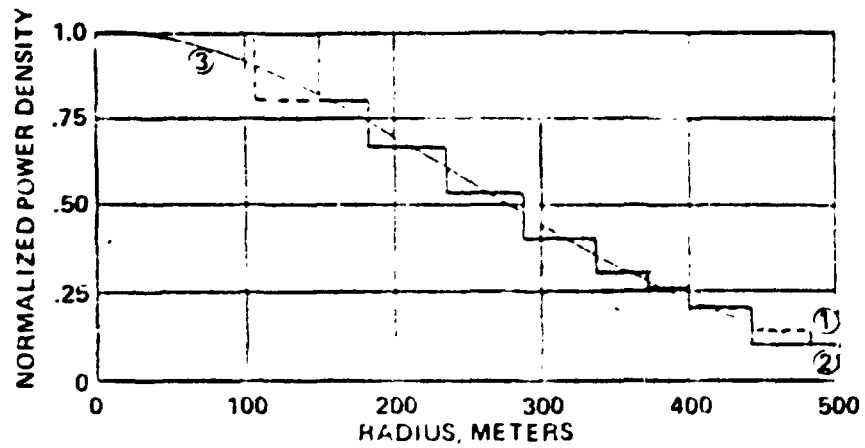


D180-22876-7

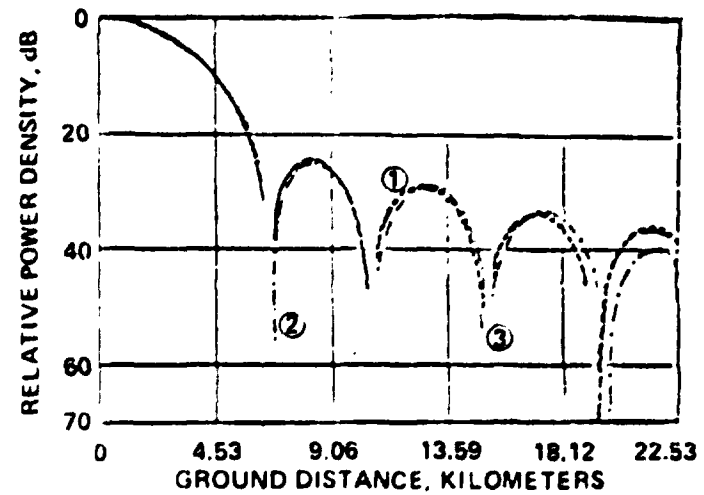
MPTS - Reference 10 dB Taper

SPS-1311

BOEING



(A) TRANSMITTER DISTRIBUTION FUNCTIONS

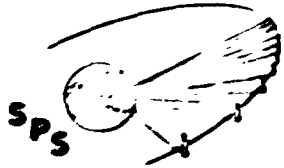


(B) FAR FIELD GROUND DISTRIBUTION

D180-22876-7

MICROWAVE POWER TRANSMISSION SYSTEM , 7 DB POWER DENSITY TAPER

It may be desirable to provide additional sidelobe suppression. The pattern shown here provides an additional 10 dB of sidelobe suppression resulting in a first sidelobe level of 0.1 MW cm^{-2} . The 17 dB power taper is quantized in 14 steps and a slightly larger antenna is required to accommodate the additional power taper without excessive thermal power to be dissipated at the center of the array.

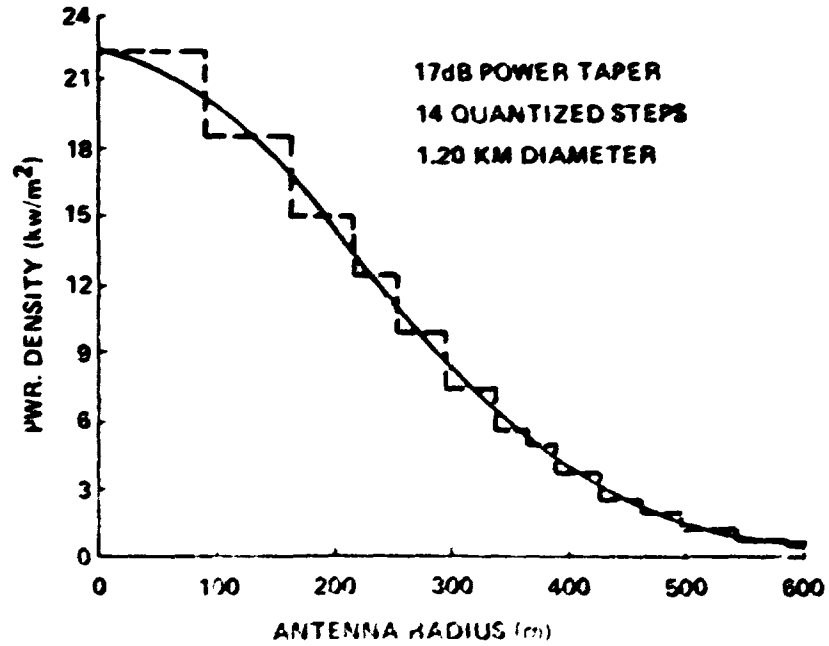


D180-22876-7

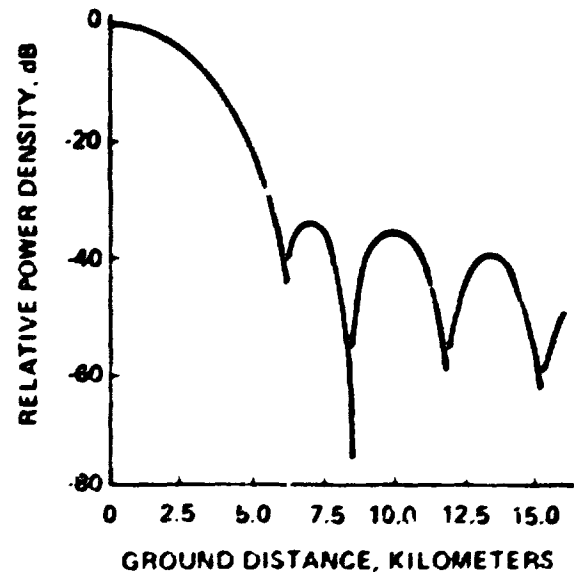
MPTS 17 dB Power Density Taper

SPS-1200

BOEING



(A) ANTENNA POWER TAPER

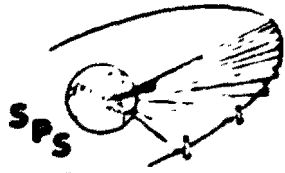


(B) FAR FIELD GROUND DISTRIBUTION

D180-22876-7

THE MICROWAVE BEAM – A SAFE POWER CARRIER

The customary engineering manner of plotting the beam pattern in decibels tends to leave the impression that the sidelobe level is significant as compared to the main beam level. This plot shows the pattern on an approximately linear scale. (The height of the sidelobes has been exaggerated to some degree so that they can be seen at all.) Also indicated are representative receiving antenna sizes and power levels at different locations within the beam.

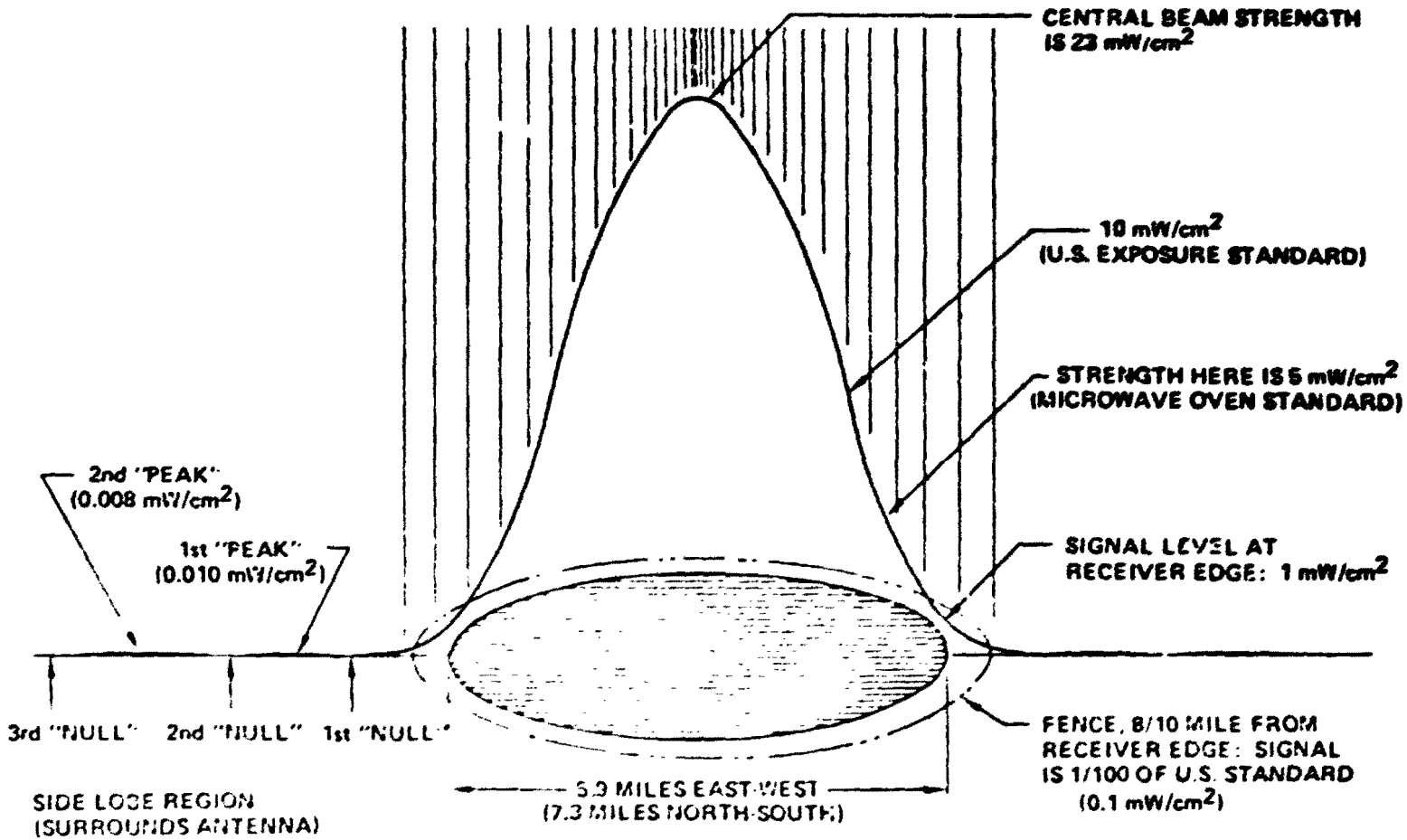


SPS 1638

The Microwave Beam: A Safe Power Carrier

BOEING

(A CROSS-SECTION THROUGH THE BEAM)

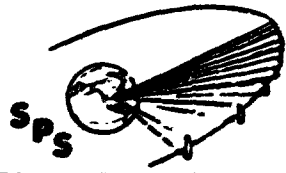


(mW/cm² = 1/1000 WATT PER SQUARE CENTIMETER)

D180-22876-7

DESIGN CONSTRAINTS ILLUSTRATION

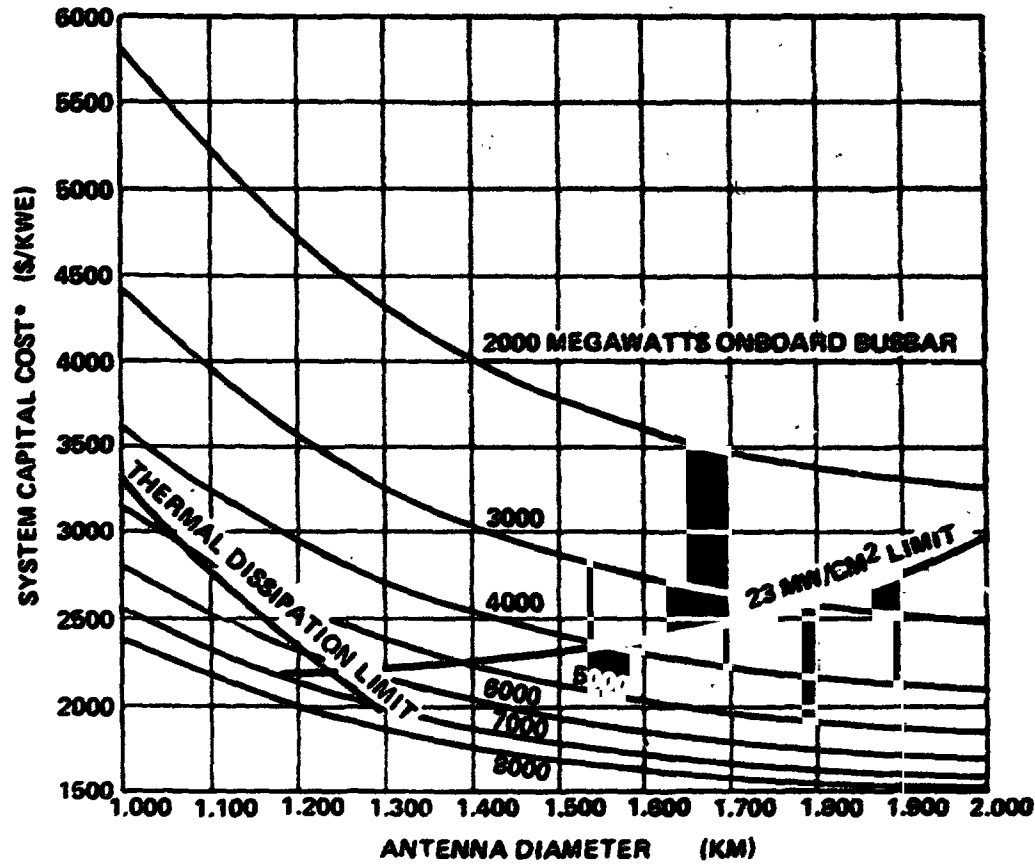
A graphic example of the effect of design constraints is shown in this computer plot of transmitter system performance. The example shown is for the 17 dB taper option to better illustrate the effect of the thermal dissipation limit and the ionosphere heating limit. The free design parameters accessible to the designer are power fed to the transmitter and transmitter diameter. It is evident that the system minimum cost occurs at the intersection of the two constraint limit lines at a transmitter diameter slightly greater than 1.0 km and a feed power of slightly over 6,000 mw. For the 10 dB taper reference case the thermal dissipation limit is moved down and to the left so that the minimum cost system is at one km diameter and approximately 8,000 Mw of electric feed power.



SF-1671

D180-22876-7

Transmitter Constraints Determine Minimum Cost Design Point

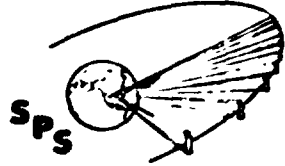


* ASSUMES BEAM-DIAMETER RECTENNA

REFERENCE PHOTOVOLTAIC SPS CONFIGURATION

Shown here is an artist's illustration of the reference photovoltaic configuration. It consists of 128 structural bays, 660 meters square, with each structural bay supporting a planar photovoltaic array consisting of 50 micron solar cells integrated with a 75 micron borosilicate glass front cover and 50 micron borosilicate glass back cover. The satellite structure is a two-tier graphite epoxy tubular truss structure.

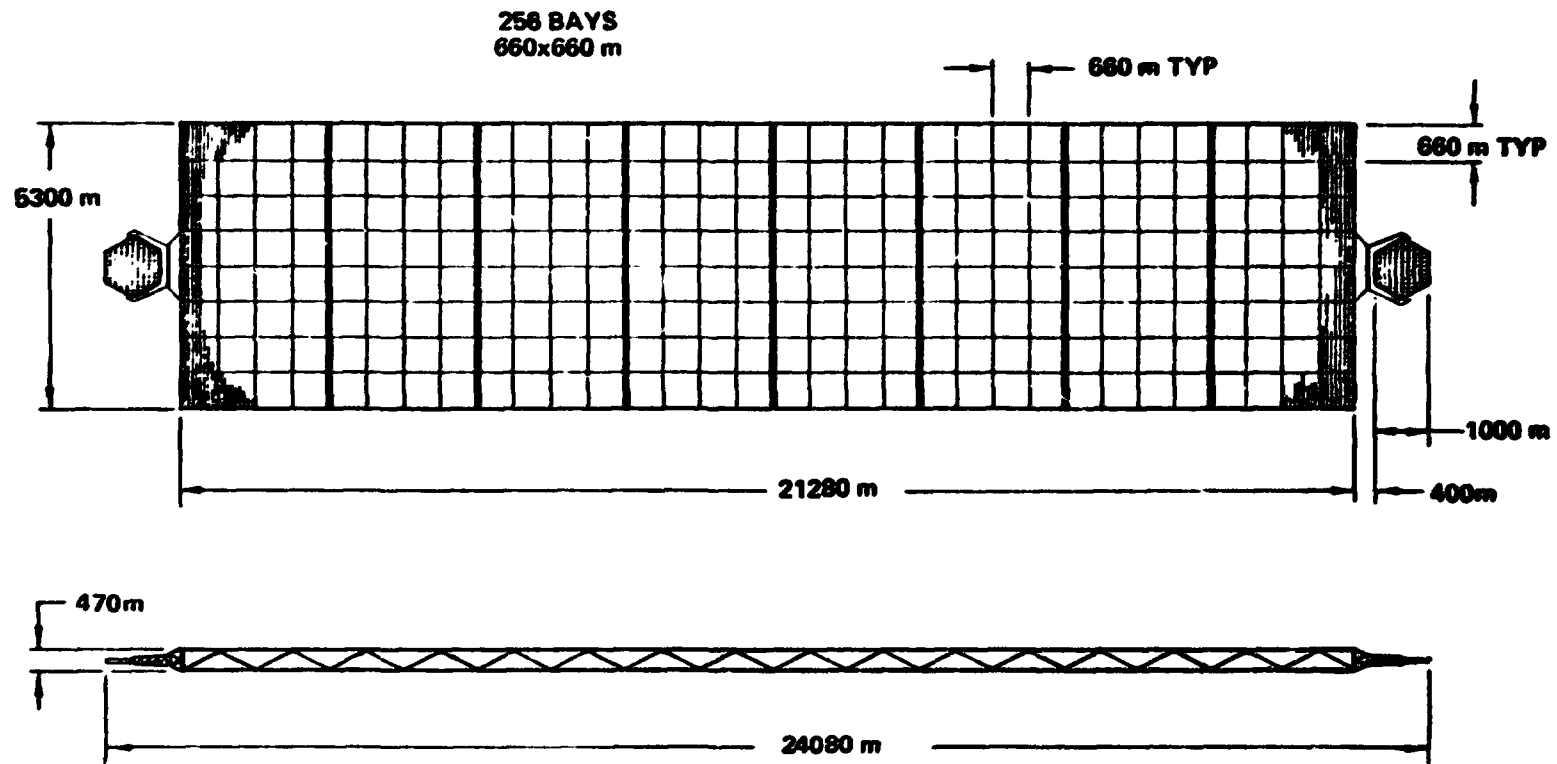
Considerable discussion has ensued over the details of the structural configuration. One concept calls for assembly of the structured beams, from parts entirely prefabricated on earth, by an "assembler" beam machine. Another concept calls for fabrication of the beams from specially prepared stock by a "thermal former" beam machine. The choice of these options has no noticeable effect on overall construction operations. The prefabricate/assemble option provides a more ideal structural section that reduces SPS structure mass by about 1,000,000 kg ($\approx 20\%$ of structure mass) as compared to thermally formed beams made of closed-section members. Open-section members do not provide adequate compressive strength for this size of structure.



SPS-1004

Photovoltaic Reference Configuration

BOEING



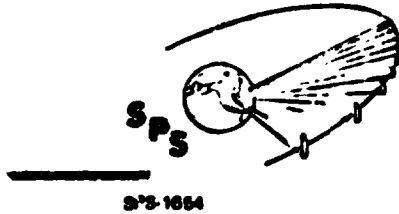
TOTAL SOLAR CELL AREA: 97.34 Km²
TOTAL ARRAY AREA: 102.51 Km²
TOTAL SATELLITE AREA: 112.78 Km²
OUTPUT: 16.43 GW MINIMUM TO SLIPRINGS

D180-22876-7

PHOTOVOLTAIC SYSTEM HIGHLIGHTS

Tabulated on the facing page are highlights of the reference photovoltaic system configuration

D180-22876-7



Photovoltaic System Highlights

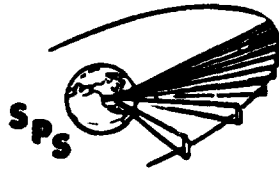
BOEING

SOLAR CELL EFFICIENCY	17.3% (15.6% CELL WITH SAW-TOOTH COVER)
SOLAR CELL THICKNESS	50 μm
COVER THICKNESS	75 μm
SUBSTRATE THICKNESS	50 μm
BLANKET UNIT MASS	0.427 kg/m²
CELL AREA	97.3 km²
BLANKET AREA	102.5 km²
OVERALL AREA	112.8 km²
SOLAR BLANKET COST	\$35/m²
STRUCTURE COST	\$80/kg
FLIGHT MODE	POP WITH ELECTRIC THRUST
POWER DISTRIBUTION	40 KV WITH 208 ISOLATABLE POWER SECTORS; PASSIVELY-COOLED DEDICATED ALUMINUM SHEET CONDUCTORS
POWER MAINTENANCE	PERIODIC ANNEALING

D180-22876-7

NOMINAL EFFICIENCY CHAIN

The normal efficiency change for the photovoltaic system and microwave power transmission system is compared here with the JSC "greenbook" values at the initiation of the study. Reasons for significant differences are indicated.



SPS-1053

Nominal Efficiency Chains Photovoltaic SPS

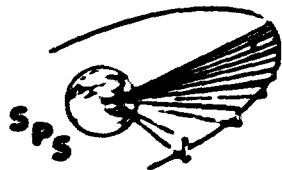
BOEING

ITEM	JSC GREEN BOOK	CURRENT NOMINAL	REASON FOR DIFFERENCE
SUMMER SOLSTICE FACTOR	NOT INCLUDED	.9765	} THESE WERE INCLUDED IN ENERGY INTENSITY ON SPS
COSINE LOSS (POP)	NOT INCLUDED	.919	
SOLAR CELL EFFICIENCY	0.103	.173	} SLIGHTLY BETTER CELL; CR = 1
RADIATION DEGRADATION		.97	
TEMPERATURE DEGRADATION		.954	
		0.151	
COVER UV DEGRADATION	NOT INCLUDED	.956	} DISTRIBUTION OPTIMIZATION
CELL-TO-CELL MISMATCH		.99	
PANEL LOST AREA		.961	
STRING I ² R		.998	
BUS I ² R		.934	
	.932		
ROTARY JOINT	1.0	1.0	} PROCESSING & TEMPERATURE VARIAN ESTIMATE
ANTENNA POWER DISTR	.98	.97	
DC-RF CONVERSION	.87	.85	
WAVEGUIDE I ² R	.98	.985	
IDEAL BEAM		.985	
INTER-SUBARRAY ERRORS	.88	.946	} .88
INTRA-SUBARRAY ERRORS		.961	
ATMOSPHERE ABSORP.	.98	.98	} INTRA-SUBARRAY EFFECTS NOT INCLUDED IN GREEN BOOK
INTERCEPT EFFICIENCY		.95	
RECTENNA RF-DC	.90	.848	
GRID INTERFACING	.99	.97	
			} NUMERICAL INTEGRATION INCLUDES DC-DC PROCESSORS
PRODUCTS/SUMS SIZES (Km ²)	.0608	.0679 108.8	

D180-22876-7

REFERENCE PHOTOVOLTAIC SYSTEM MASS STATEMENTS

The current reference mass statement is compared here with the original JSC "greenbook" statement for the photovoltaic system. Reasons for significant changes are noted.



Silicon Photovoltaic Mass Properties Summary

BOEING

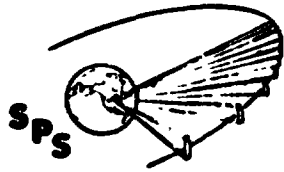
SPS 1673

ITEM	JSC "GREEN BOOK" MASS	CURRENT MASS	REASON FOR CHANGE
MULTIPLE/Common USE EQUIPMENT	(3467)	(5634)	
PRIMARY STRUCTURE	2973	5396	• DESIGN LOADS
OTHER	484	249	
ENERGY COLLECTION	(5736)	(0)	• CHANGE TO CR - 1
ENERGY CONVERSION (SOLAR BLANKETS)	(29877)	(43750)	• CHANGE TO CR - 1 • GLASS CELL COVERS
POWER DISTRIBUTION	(3000)	(2388)	
POWER TRANSMISSION	(15371)	(25212)	
STRUCTURE	1210	500	• SUBARRAY STRUCTURE IN SUBARRAYS
POWER DISTR	167	5866	• PROCESSORS & THERMAL CONTROL
MICROWAVE GENERATORS	8946	13490	• THERMAL CONTROL
SUBARRAY STR & WAVEGUIDES	4002	4314	
CONTROL ELEX	358	970	
OTHER	788	72	• GREEN BOOK CARRIED ROTARY JOINT IN AJTENIJA MASS
SUBTOTAL	56240	78994	• DETAILED UNCERTAINTY ANALYSIS
GROWTH	(50%) (28120)	(26.6%) (20506)	
TOTAL	84360	97499	

REFERENCE PHOTOVOLTAIC SPS MASS ESTIMATE HISTORY

The mass estimate history for the photovoltaic SPS, through the conduct of the system definition study, is shown here. The point of departure estimates come from the JSC green book. Energy conversion system detailed mass estimates were available by the Part I mid-term. The principal reason for increase was the addition of borosilicate glass covers on the solar cells, increasing the unit mass of the solar blankets substantially.

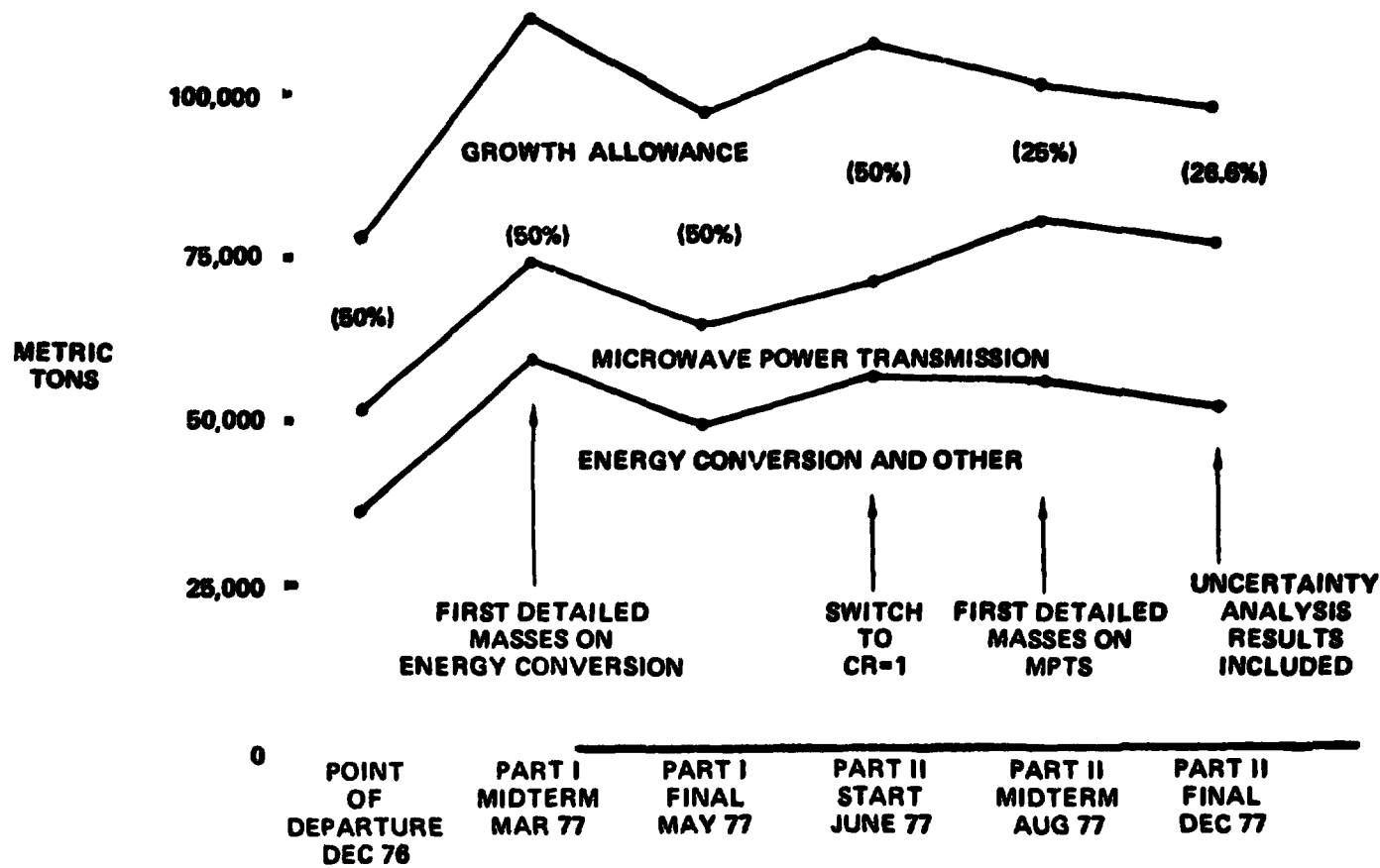
Some reduction of structure mass for the energy conversion system resulted in the values shown for the Part I, final. During this time, an arbitrary 50% mass growth allowance was carried. With initiation of Part II of the study, effort was begun on the power transmission system. By the mid-term of Part II, detailed mass estimates were available. These mass estimates resulted in a significant increase in the power transmission system primarily due to mass requirements determined for thermal control systems. This time also, a mass properties review suggested that with the availability of comparatively detailed mass estimates and the general lack of escalating factors internal to the SPS design, a 25% mass growth allowance would be more appropriate. During the final part of the Part II effort, a detailed uncertainty analyses was conducted and predicted a mass growth of 26.6%. This growth allowance was incorporated in the final mass statement.



SPS-1399

Reference Photovoltaic SPS Mass Estimate History

BOEING

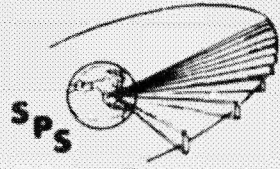


D180-22876-7

THERMAL ENGINE REFERENCE CONFIGURATION

The artist's illustration shows the thermal engine configuration. (The illustration shows the module arranged in a 3 x 5 pattern, whereas the current configuration is a 4 x 4 pattern.) Each module consists of a faceted plastic film concentrator supported by a tubular truss graphite structure, a cavity absorber with 36 Rankine turbogenerators and pumps per absorber, and the necessary thermal radiators for waste heat rejection.

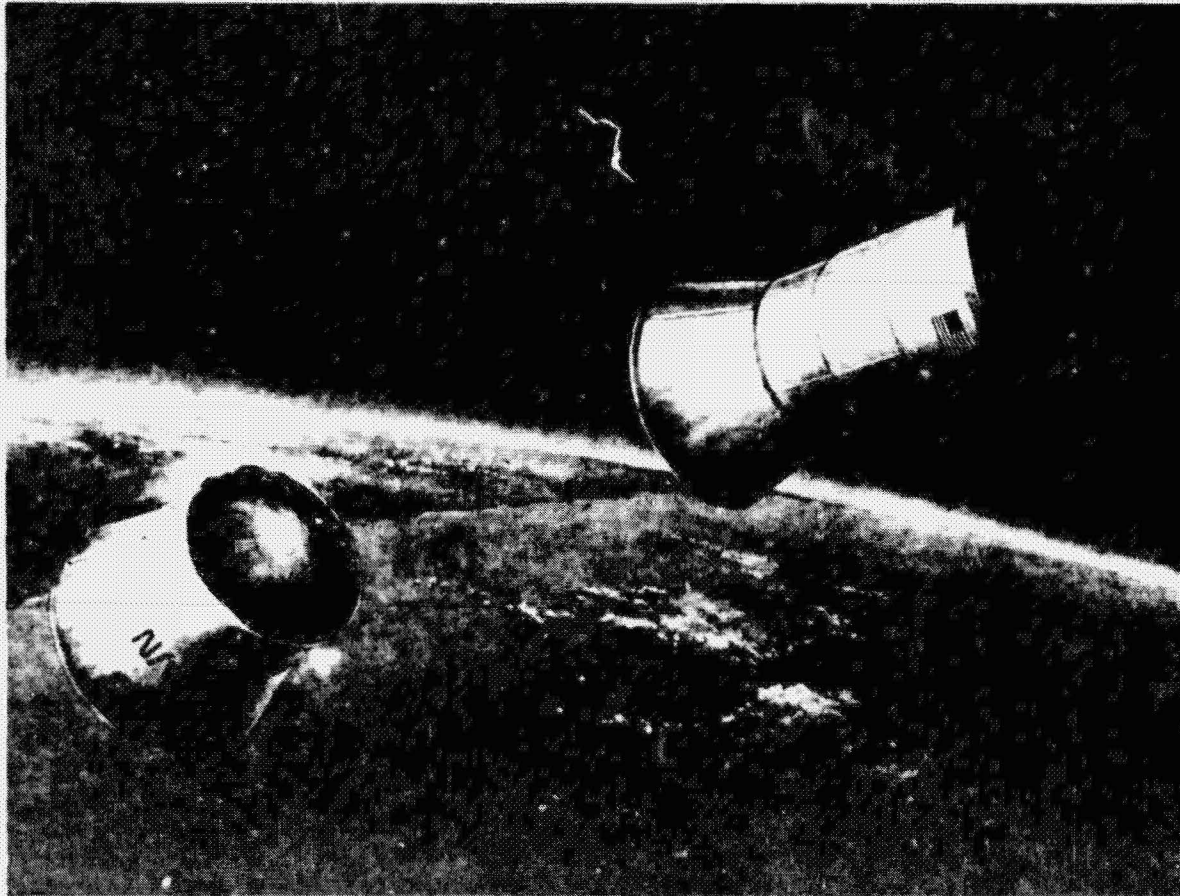
D180-22876-7



Thermal Engine Reference Configuration

BOEING

SPS-1701

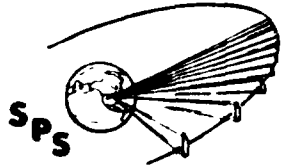


ORIGINAL PAGE IS
OF POOR QUALITY

D180-22876-7

THERMAL ENGINE HIGHLIGHTS

Tabulated here are the principal features of the thermal engine system design.



SPS-1674

D180-22876-7

Thermal Engine Highlights

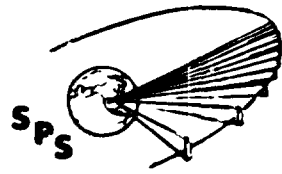
BOEING

TURBINE INLET TEMPERATURE	1242K (1778°F)
TURBINE EXHAUST TEMPERATURE	932K (1218°F)
TURBOGENERATOR SIZE (NOMINAL)	31.4 MW
TURBOGENERATORS PER SPS	576 (6 ARE "RESERVE")
MODULES PER SPS	16
RADIATOR PROJECTED AREA	1.15 KM²/SPS
CYCLE EFFICIENCY	0.189
REFLECTOR FACETS	116,000
SATELLITE ORIENTATION	PERPENDICULAR TO ECLIPTIC, ELECTRIC THRUST
REFLECTOR FACET THICKNESS	2.5 μM (ALUMINIZED KAPTON)
TOTAL FACET AREA	119 KM²
POWER DISTRIBUTION	40 KV, PASSIVELY COOLED DEDICATED ALUMINUM SHEET CONDUCTORS, ANTENNA JOINTS INCORPORATE DIURNAL AXIS WITH SLIP RINGS AND ANNUAL AXIS WITH WIND-UNWIND CABLES.
MAINTENANCE	MALFUNCTION DETECTION SYSTEM FOR SHUTDOWN OF INDIVIDUAL TURBOGENERATORS AS REQUIRED, PERIODIC MAINTENANCE.

D180-22876-7

THERMAL ENGINE MASS PROPERTIES SUMMARY

A mass statement for the thermal engine reference system is presented here. There was no comparable "greenbook" reference at the beginning of the study. With growth included, the two mass statements are essentially equivalent. The growth allowances resulted from the detailed uncertainty analysis. Because of the somewhat greater maturity of the thermal engine technology the predicted growth was slightly less



D180-22876-7

SPS Thermal Engine Mass Properties Summary

SPS-1676

BOEING

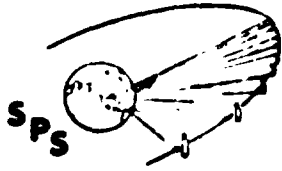
ITEM	RANKINE THERMAL ENGINE
MULTIPLE/Common USE EQUIPMENT	<u>2662</u>
PRIMARY STRUCTURE	774
SATELLITE CONTROL	1450
COMM. & DATA	4
MECH SYS & OTHER	200
ANTENNA YOKE	234
ENERGY COLLECTION	<u>8091</u>
SUPPORT STRUCTURE	6254
REFLECTOR FACETS	1837
ENERGY CONVERSION	<u>40084</u>
CPC & LIGHT DOORS	324
CAVITY ABSORBER	1000
THERMAL ENGINES	21933
RADIATORS	10769
FLUIDS	6058
POWER DISTRIBUTION	<u>4978</u>
MICROWAVE POWER TRANSMISSION	<u>25212</u>
TOTAL	<u>81027</u>

REFERENCE THERMAL ENGINE SPS MASS ESTIMATE HISTORY

The thermal engine mass estimate history goes back to Boeing IR&D work conducted beginning in 1972. The specific values shown for 1973 and 1975 came from papers published in the technical literature. These papers did not address the mass of microwave power transmission systems and early estimates available from the literature were quite optimistic as can be seen.

The point of departure mass estimate represented the first completely integrated thermal engine design with all interrelationships in this complex system properly represented. The power transmission system mass at that time was taken from Raytheon publications. Brayton system cycle optimization brought the mass down slightly by the Part I mid-term, where also the JSC microwave power transmitter mass was adopted. By the Part I final, additional mass reductions resulted from the adoption of the 16 module configuration as compared to the 4 module configuration.

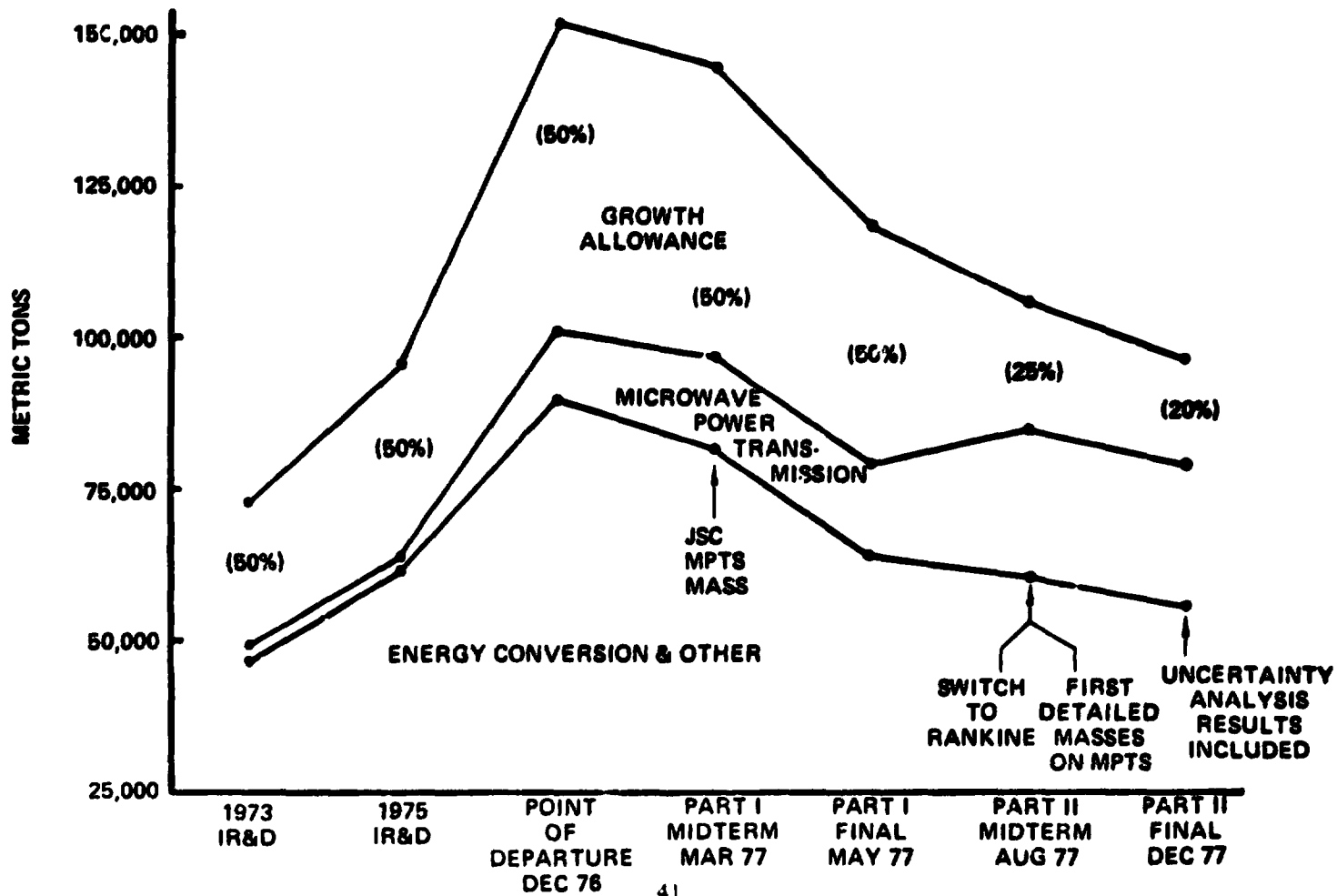
The continuing reduction in energy conversion systems mass was due to first, the switch to the Rankine system and secondly, elimination of the oversized concentrator originally thought necessary to compensate for the degradation of plastic film reflectors. The power transmission system masses for the thermal engine and photovoltaic systems are equivalent. The uncertainty analyses predicted a 20% mass growth for the thermal engine system, somewhat less than for the photovoltaic system, as might be expected due to the somewhat greater maturity of the technology.



SPS-1388

Reference Thermal Engine SPS Mass Estimate History

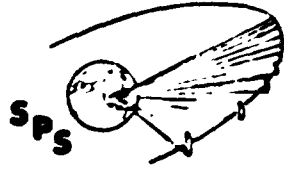
BOEING



D180-22876-7

PHOTOVOLTAIC vs THERMAL ENGINE ASSESSMENT

Highlights of the overall assessment are summarized.



SPS-1655

Photovoltaic vs Thermal Engine Assessment

BOEING 

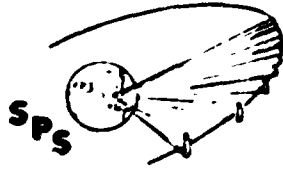
- **NO SIGNIFICANT DIFFERENCES IN SATELLITE MASSES OR COSTS**
 - Photovoltaic is simpler but thermal engine technology is more mature

- **COMPLEXITY OF THERMAL ENGINE SPS INCREASES OPERATING COSTS**
 - Larger construction crew and facility
 - Lower packaging density

- **OVERALL 5% TO 10% SYSTEM COST ADVANTAGE FOR PHOTOVOLTAIC**
 - But advantage is sensitive to solar blanket production costs

PHOTOVOLTAIC PREFERENCE IS SENSITIVE TO SOLAR BLANKET COST

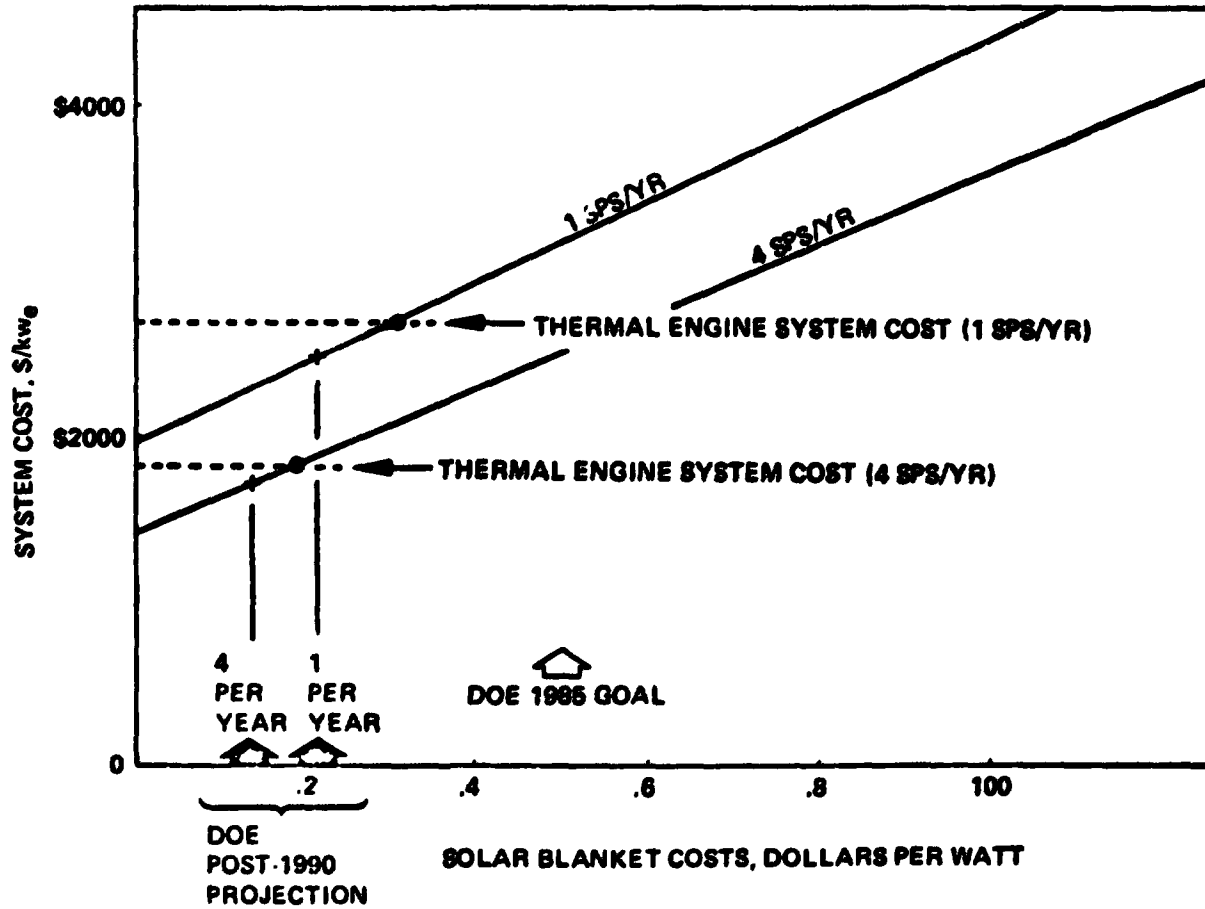
Because of the uncertainty and controversy regarding solar blanket cost projections, the sensitivity of the photovoltaic system to solar blanket cost is important. Shown here are the study median projections for one SPS per year and four SPSs per year compared to the Department of Energy 1985 goal and Department of Energy post-1990 projections. Influence on SPS total system cost is shown for each case. Also shown are the comparative thermal engine system costs which indicate at what point an increase in solar blanket cost would motivate a change to the thermal engine system. This change occurs long before an unacceptable cost level is reached.



SPS 1656

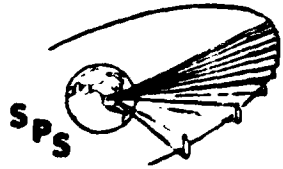
Photovoltaic Preference is Sensitive to Solar Blanket Costs

BOEING



PHOTOVOLTAIC SPS CONSTRUCTION FACILITY ARRANGEMENT

Illustrated here is the construction facility arrangement that arose from the construction base definition effort. It is a combined power transmitter antenna and photovoltaic energy conversion construction facility. The facility is comprised of a C-clamp-shaped truss structure. The structure is shown boxed in for most of the facility to clarify the illustration but would actually appear as indicated by the "actual structure" callout. Overall facility dimensions are 1.4 x 2.8 km. Crew modules and launch vehicle docking stations are shown approximately to scale. The crew modules are sized for 100 people (17 meters diameter by 23 meters length). The facility includes 4 bays dedicated to structure manufacture and 4 bays dedicated to solar blanket and equipment installation. Additional details of the various construction concepts, operations and timelines are described in more detail later in this briefing book.

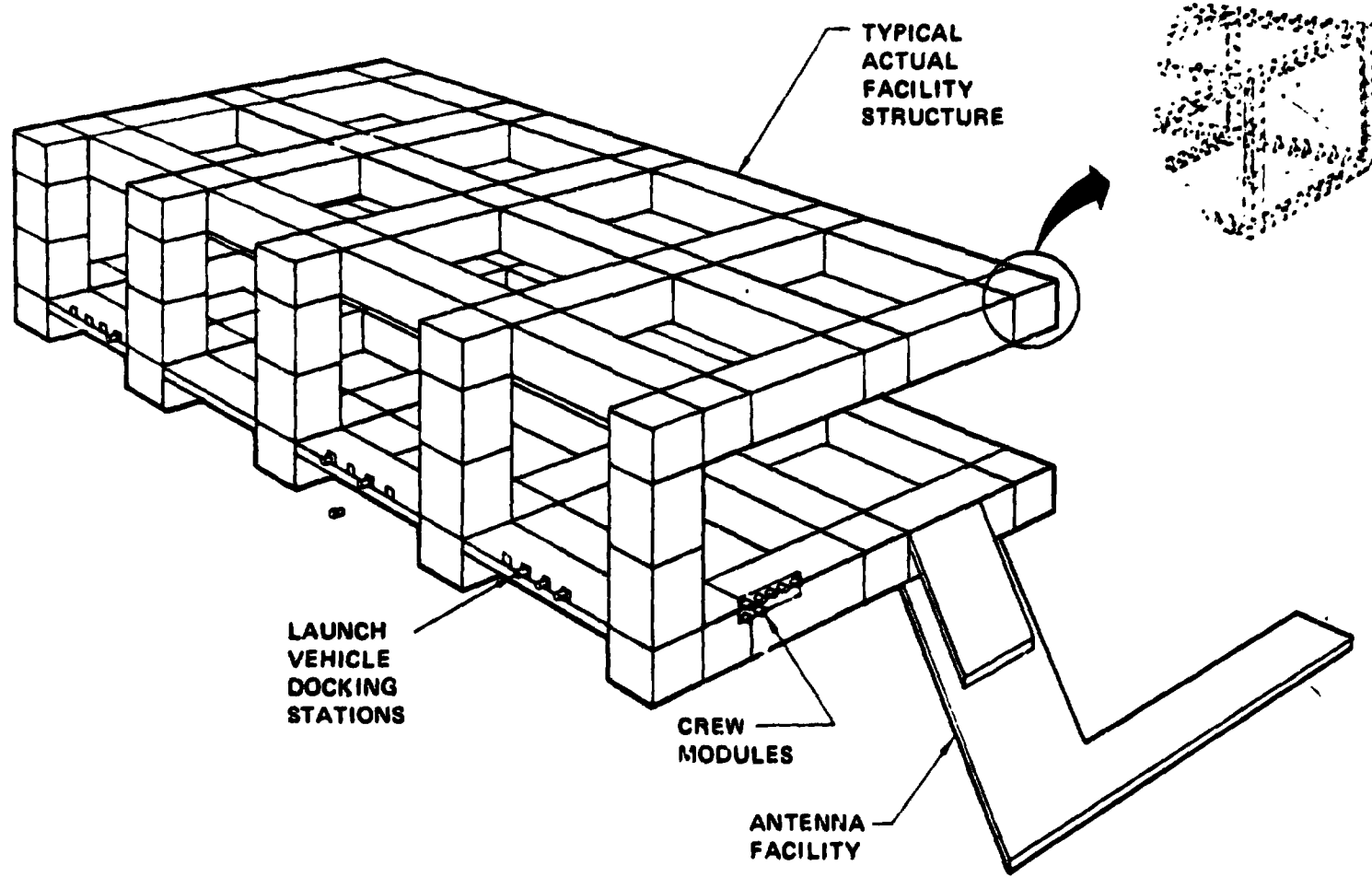


D180-22876-7

Photovoltaic Construction Facility Arrangement

BOEING

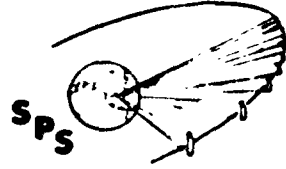
SPS 1657



D180-22876-7

CONSTRUCTION HIGHLIGHTS

The most significant comparative construction factors for the principal options are compared.



SPS-1658

Construction Highlights

BOEING

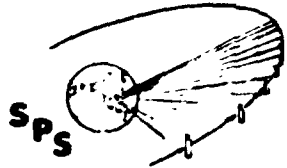
- CREW SIZE
 - AT LEO
 - AT GEO
 - TOTAL
- CONSTRUCTION TIME FOR 1 SPS
- CREW WORK SCHEDULE
- CREW STAYTIME
- MAIN BASE SIZE
- BASE MASS (METRIC TONS)
 - AT LEO
 - AT GEO
- BASE COST (LEO & GEO)
- HLLV LAUNCHES TO DELIVER

<u>PHOTOVOLTAIC</u>		<u>THERMAL</u>	
<u>LEO CONSTRUCTION</u>	<u>GEO CONSTRUCTION</u>	<u>LEO CONSTRUCTION</u>	<u>GEO CONSTRUCTION</u>
540	550	815	835
480	70	760	105
60	480	55	730
540			
1 YEAR	1 YEAR	1 YEAR	1 YEAR
10 HOURS/DAY, 6 DAYS/WEEK, 2 SHIFTS			
90 DAYS	90 DAYS	90 DAYS	90 DAYS
2.8 x 1.8 x 1.0 km		2.8 x 1.8 x 1.0 km	
5870	750	9350	1150
770	6535	850	10040
8.2 BILLION		12.4 BILLION	
61	93	96	144

D180-22876-7

CONSTRUCTION RESULTS

Principal results of the construction analysis are summarized here.



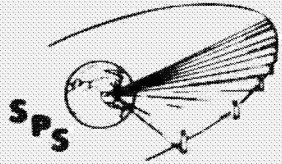
Construction Results

- **REQUIRED CONSTRUCTION RATE DETERMINES BASE SIZE AND QUANTITY**
 - Bases analyzed were sized for 1 SPS per year
- **BASE AND EQUIPMENT COSTS ARE SIGNIFICANT**
 - Effective Utilization is Essential
- **LARGE PAYLOAD VOLUME AIDS CONSTRUCTION BASE TRANSPORTATION**
 - Packaging density is about 40% that for SPS Hardware
- **FACILITY DESIGN HAS EVOLVED TO ASSEMBLY LINE CONCEPT**
 - Maximizes crew and machine productivity; minimizes satellite design impact problems
- **CREW ARE PRIMARILY MACHINE SUPERVISORS**
 - Little or no spacesuit work
- **ONBOARD LOGISTICS IMPORTANT DESIGN FACTOR**
 - Hardware throughput is 15 tons per hour

REFERENCE HEAVY LIFT CARGO LAUNCH VEHICLE

This artist's illustration shows the reference heavy lift launch vehicle at the time of second stage separation. The booster is an oxygen/hydrocarbon system equipped for down-range powered soft landing at sea. The upper stage employs oxygen/hydrogen propellants and includes a retractable telescoping payload shroud to provide large-volume accommodation for the low-density SPS payload. The payload bay size is 17 meters diameter by 23 meters cylindrical length. The upper stage is also equipped for down-range sea landing.

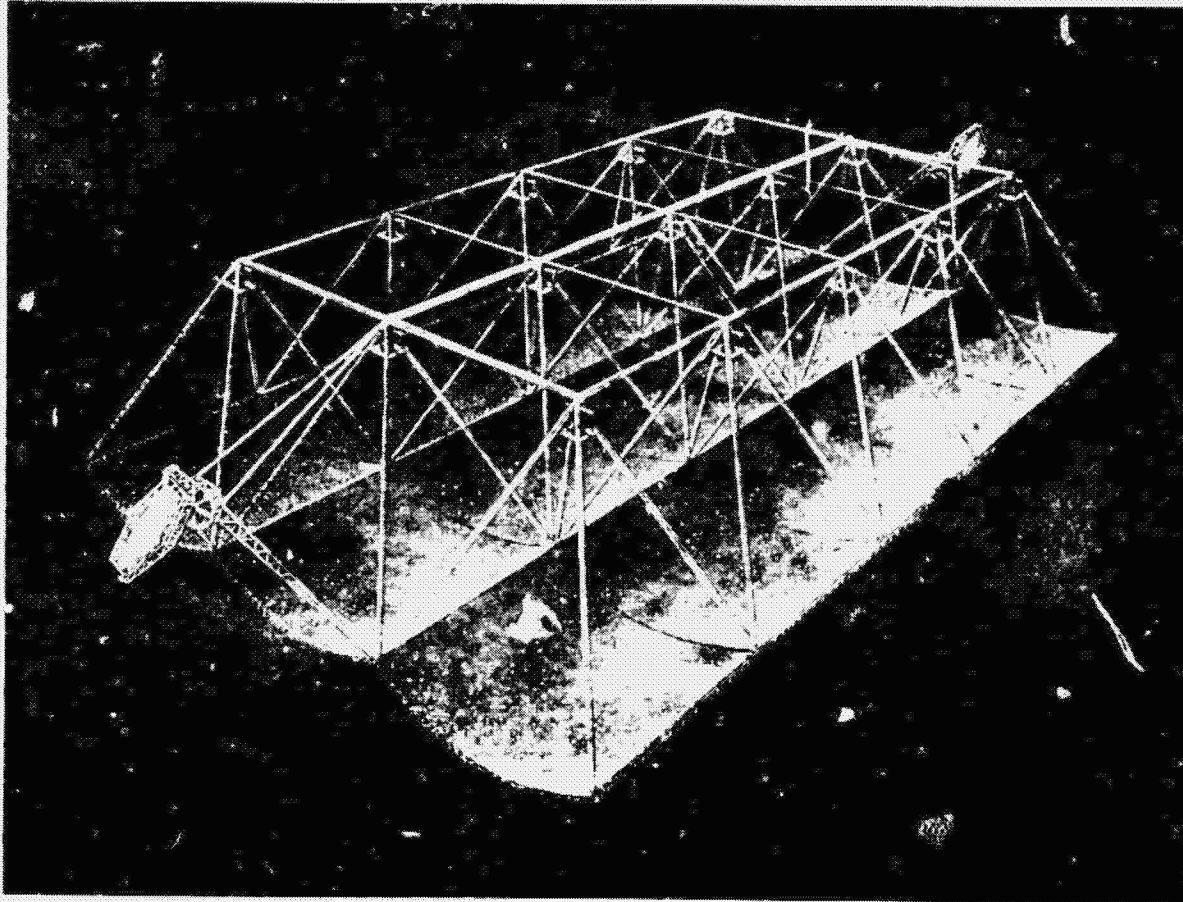
D180-22876-7



Reference Earth Launch Vehicle Depicted at Stage Separation

BOEING

SPS-1702

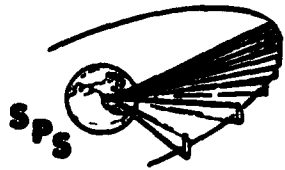


ORIGINAL PAGE IS
OF POOR QUALITY

LAUNCH SYSTEM OPTIONS

Two primary launch system options were characterized, a ballistic two-stage heavy lift vehicle illustrated on a previous page, and a winged two-stage heavy lift vehicle. The differences in performance between these two options were well within the uncertainty of performance estimation.

The identified advantages of each are indicated on the chart. The winged vehicle indicated somewhat higher development and unit cost. The principal issue between the two systems is sea landing versus land landing. The sea landing mode requires restart of some of the rocket engines (or start of special landing engines) for the powered letdown into the water and the hardware is exposed to the sea saltwater environment. There is also some uncertainty associated with landing loads to be experienced upon water contact. The winged land landing vehicle avoids these issues. Because of the sonic boom profiles for ascent and reentry of the vehicles, and because the booster requires down range land landing, the winged system introduces significant launch and recovery siting issues. No suitable down range land landing sites are available for KSC launch. Potentially attractive sites, with regions of significant sonic boom overpressure being under government control, exist in the southwestern United States. These sites are further north than KSC and introduce additional performance penalties associated with the plane change required to achieve a zero-inclination geosynchronous orbit. Other alternative sites have not been identified.

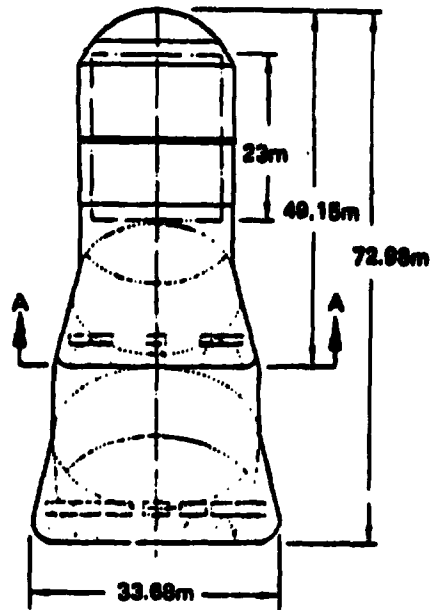


D180-22876-7

Launch System Options

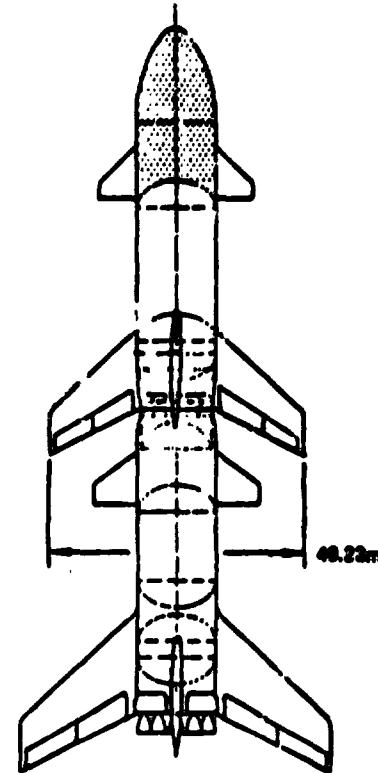
BOEING

8 11



BALLISTIC VTOVL

- LARGE PAYLOAD VOLUME READILY PROVIDED
- SEA LANDING AVOIDS RECOVERY SITING ISSUES
- SLIGHTLY LOWER COST PER FLIGHT



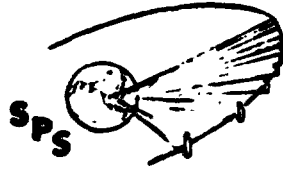
WINGED VTOHL

- LAND LANDING AVOIDS SEA LANDING & RECOVERY ISSUES
- ENGINE START/RESTART NOT REQUIRED FOR LANDING

PAYLOAD DENSITY IS DESIGN DRIVER

The payload densities achieved for the photovoltaic and thermal engine configurations are compared here. Except for the power transmission system, the difference in photovoltaic and thermal engine systems would be far more striking.

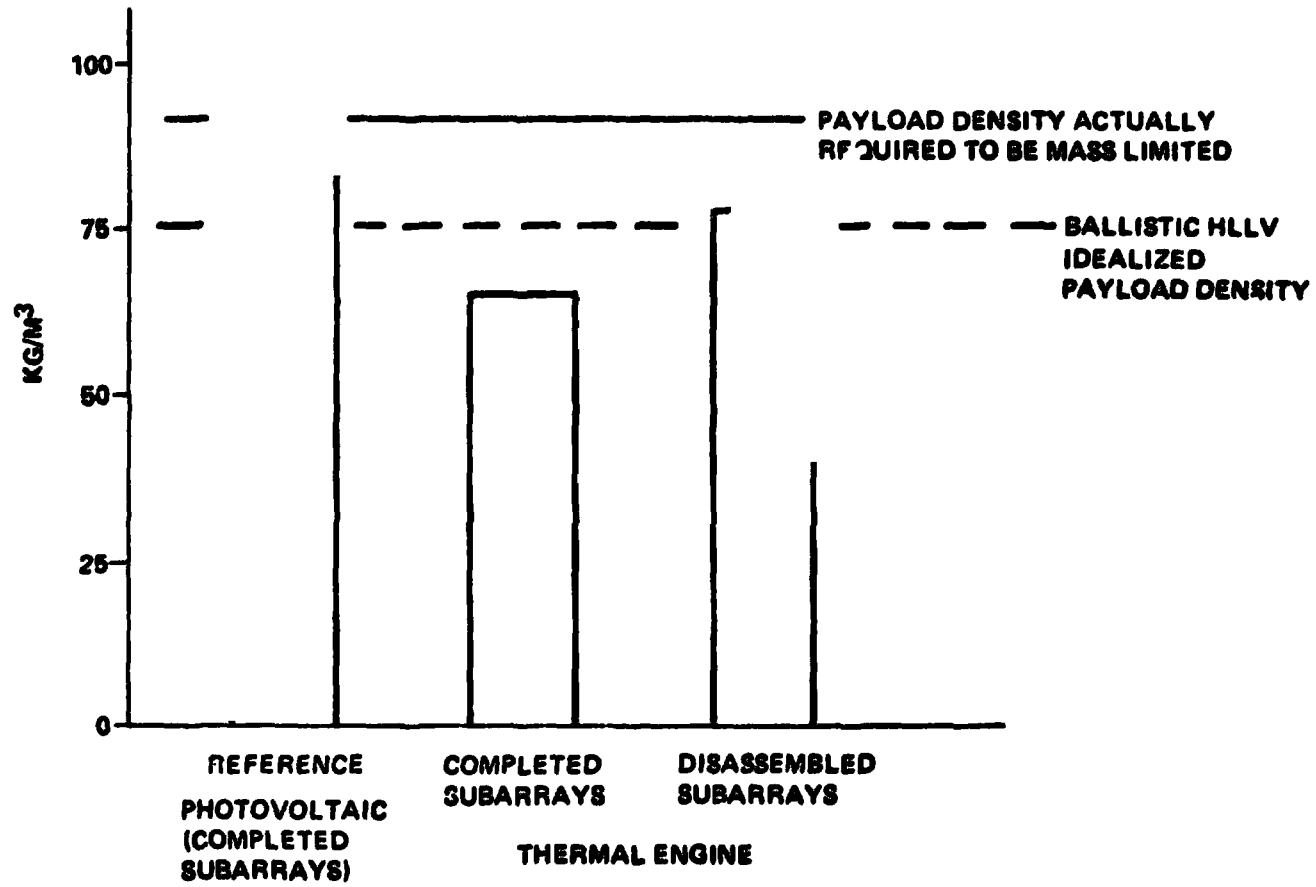
The ballistic launch vehicle system has a theoretical payload density of 75 kg per cubic meter based on the available cylindrical volume within the payload shroud. However, actual payloads are more rectangular or irregular in shape and the payload density required for payload packages to reach a mass limited condition in this shroud is approximately 92 kg per cubic meter. As indicated, the photovoltaic system slightly exceeded this value whereas the thermal engine system does not reach it. As discussed in more detail in the transportation section of the briefing, the least cost solution to the thermal engine volume problem was to use expendable shrouds of considerably increased volumetric capability.



SPS-1676

Payload Density is Design Driver

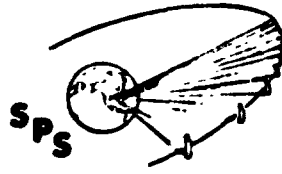
BOEING



D180-22876-7

TRANSPORTATION SYSTEM HIGHLIGHTS

Tabulated on the facing page are the principal features of the SPS transportation systems.



SPS-1660

Transportation Highlights

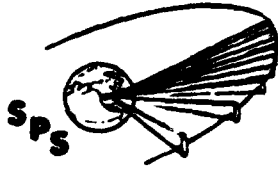
BOEING

- **CARGO LAUNCH VEHICLE (REFERENCE)**
 - 2-STAGE BALLISTIC FULLY REUSABLE
 - VERTICAL TAKEOFF, POWERED VERTICAL SEA LANDING
 - GROSS MASS 10,000 TONS WITH 390 TONS NET PAYLOAD
 - PAYLOAD VOLUME 17 x 23 M (13.3 M³/TON; 75 kg/M³)
 - LO₂/KEROSENE BOOSTER; LO₂/LH₂ SECOND STAGE
- **ALTERNATE OPTION IS 2-STAGE WINGED VERTICAL TAKEOFF, UNPOWERED HORIZONTAL LAND LANDING**
- **PERSONNEL LAUNCH VEHICLE—MODIFIED SHUTTLE, 75 PASSENGERS**
- **PERSONNEL ORBIT TRANSFER VEHICLE**
 - 2-STAGE FULLY REUSABLE LO₂/LH₂ OTV
 - 75 TO 100 PASSENGERS DEPENDING ON CONSTRUCTION LOCATION AND SPS TYPE
- **CARGO ORBIT TRANSFER—ELECTRIC-PROPELLED SELF-TRANSPORT OF SPS MODULES; 180-DAY TRIP**
- **OPTION IS FULLY REUSABLE LO₂/LH₂ OTV FOR GEO CONSTRUCTION**

HLLV ASCENT OVERPRESSURES

This figure shows the sonic boom overpressure generated by the Heavy Lift Launch Vehicle (HLLV) during ascent as a function of ground location. This figure is applicable to either the winged vehicle or to the ballistic vehicle, since the plumes and trajectories of these two vehicles are nearly the same, and it is the plume rather than vehicle size which controls the magnitude of the boom.

The combination of vehicle trajectory and acceleration results in the generation of a caustic or "focal zone" region in which the sonic boom overpressures are much larger than they would be for steady flight. Overpressures in this very localized region will be about 25 psf. The beginning of the "focal zone" is located 31 nmi downrange from the launch site. The overpressure decreases rapidly to 10 psf at a point 34 nmi downrange from the launch site. It has dropped to 2 psf 65 nmi downrange from the launch site. These overpressures are about three times as large as those generated by the Saturn V.

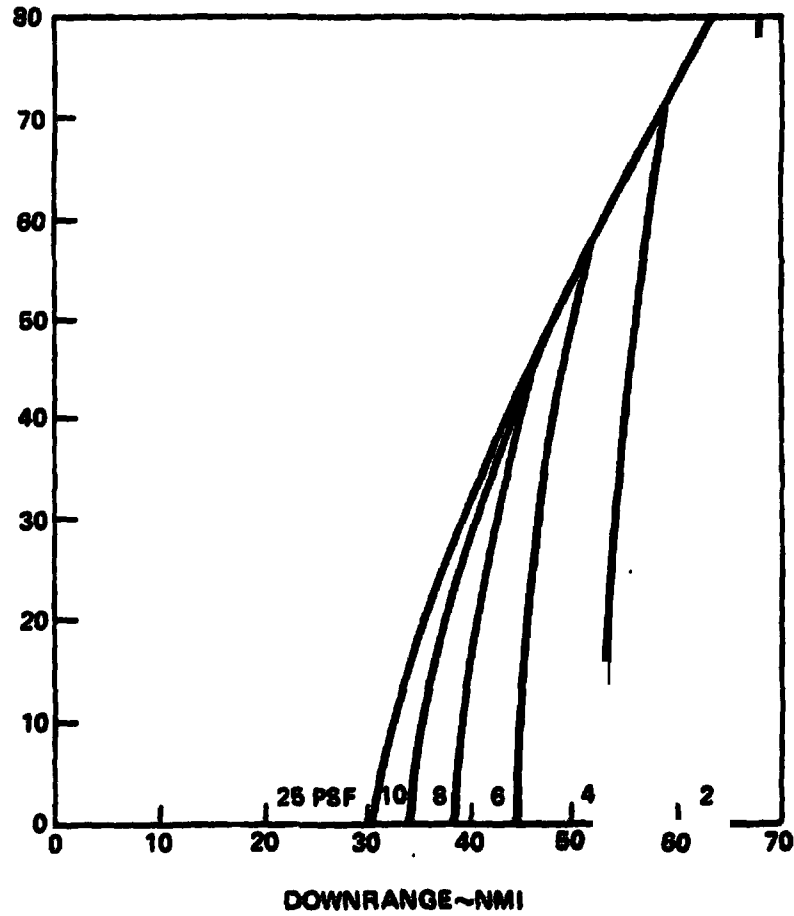


SPS-1032

HLLV Ascent Sonic Boom Overpressures

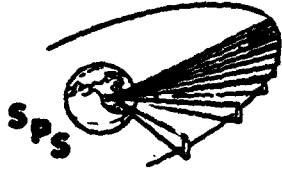
BOEING

LATERAL RANGE
~ NMI



SENSITIVITY OF HLLV ASCENT SONIC BOOM OVERPRESSURES TO VEHICLE SIZE

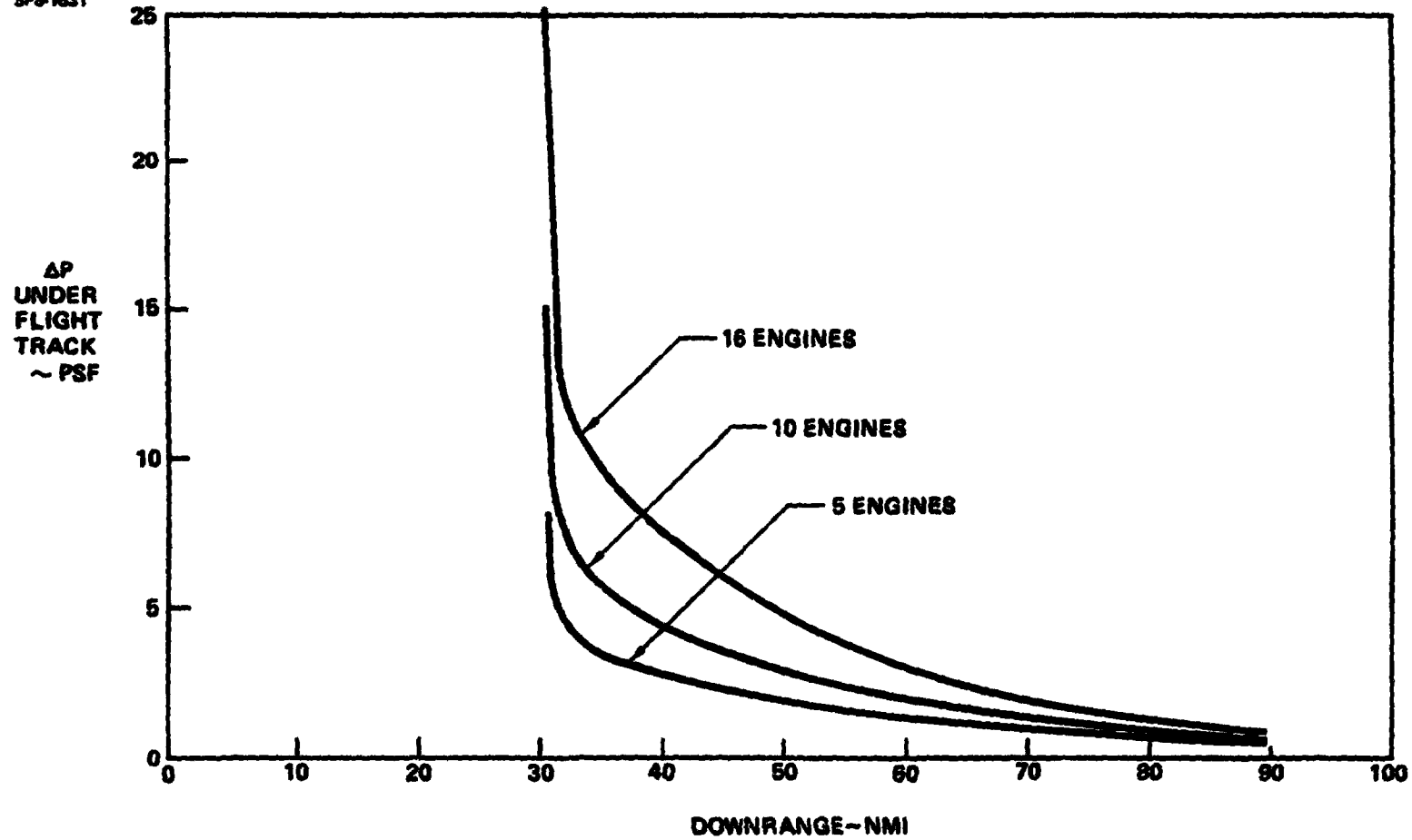
This figure shows the sensitivity of the sonic boom overpressures under the ascent flight track to the size of the HLLV. HLLV size was varied by varying the number of engines and, thereby, the plume size. The overpressure in the "focal zone" decreases from 25 psf to 15 psf when the number of engines is reduced from 16 to 10 and from 25 psf to 8 psf when the number of engines is reduced from 15 to 5.



Sensitivity of HLLV Ascent Sonic Boom Overpressures to Vehicle Size

BOEING 

SP8-1631

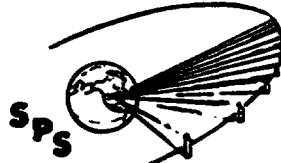


LEO/GEO DIFFERENCES

One of the principal issues addressed by this study was relative evaluation of construction in low earth orbit versus construction in the geosynchronous operational orbit. The summary table presented here provides an evaluation of the differences in terms of qualitative factors and projected cost differences associated with these factors. In terms of recurring costs, by far the most significant difference is associated with the launch rate. A slight advantage to LEO construction is seen in construction requirements. This difference is associated primarily with difference in the transportation costs for the construction facilities and crews at LEO as compared to GEO.

Principal design impacts on the SPS include oversizing of the solar arrays to compensate for radiation degradation and mismatch in solar cell performance associated with this degradation. It is estimated that most of the degradation will be recovered by annealing. Solar cells degraded by the orbit transfer after annealing would have about 95% of the output of those not degraded. Although only 25% of the solar cells are so degraded, the mismatch loss is additive to the degradation loss and results in a 5% oversize requirement. In addition, there is a difference in structural mass due to the redundancy in structure required to modularize the satellite. Satellite modifications associated with power distribution to the electric thrusters are included in orbit transfer system costs.

A total differential of \$16 million per SPS has been associated with operational complexities of the self-powered transfer operation. Additional significant factors are the differences in interest during construction associated with longer overall construction time required for LEO construction and differences in the cost growth resulting from its application as a constant factor on overall costs.



SPS-1677

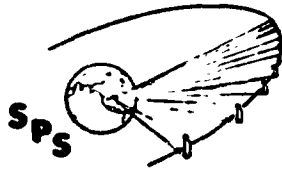
LEO versus GEO Construction Summary of Differences

RFP REF		DELTA COST IN MISSIONS PER SPS (GEO - LEO)		
		RECURRING (4 SPS/YR)	INITIAL NON- RECURRING	
A)	TRANSPORTATION REQUIREMENTS (INCLUDES CREW)	<ul style="list-style-type: none"> HLLV LAUNCH RATE, 1400/YR VS 3064/YR @ 4 YR, 350/YR VS 766/YR @ 1/YR 	HLLV = 2,548 OTV = 206	-1,431 (OTS) 2,223 (FLEET INVESTMENT)
B)	CONSTRUCTION REQUIREMENTS	<ul style="list-style-type: none"> FACILITY DELTA COSTS STATIONKEEPING PROPELLANT 800 KG/DAY CREW SUPPORT 	24 -9 9	530
C)	SPS DESIGN REQUIREMENTS	<ul style="list-style-type: none"> OVERSIZING FOR RADIATION DEGRADATION DELTA STRUCTURAL MASS - 854 TONS LESS FOR GEO 	-139 -70	-350 -175
D)	DEGRADATION POTENTIAL	<ul style="list-style-type: none"> INCLUDED IN SPS DESIGN REQUIREMENTS (OVERSIZING COMPENSATES FOR OUTPUT AND MISMATCH LOSS) 		
E)	LAUNCH SITE DIFFERENTIAL EFFECTS	<ul style="list-style-type: none"> HIGHER LAUNCH RATE FOR GEO 	-	1,715 LAUNCH FACILITY COSTS
F)	STARTUP	<ul style="list-style-type: none"> ORBIT TRANSFER HARDWARE IN OTS COST DELTA INTEREST DURING CONSTRUCTION 	-303	
G)	OPERATIONS CONSIDERATIONS	<ul style="list-style-type: none"> NO DIFFERENCE IN NUMBERS OF VEHICLES IN FLIGHT. MORE COMPLEX MONITORING FOR OTS. BERTHING EQUIPMENT INCLUDED IN GEO FACILITY FOR LEO CONSTRUCTION 	-10	
H)	COLLISION	<ul style="list-style-type: none"> COLLISION AVOIDANCE PROPELLANT OBJECT MONITORING COST 	-1 -5	
I)	COST DIFFERENTIALS	<ul style="list-style-type: none"> OTHER FACTORS ITEMIZED IN THIS TABLE DELTA GROWTH (FACTOR ON DELTA COST) 	156	
J)	ORBIT TRANSFER	<ul style="list-style-type: none"> HARDWARE/SOFTWARE COSTS REFLECTED AS OTS COSTS 	-	
TOTAL COST DIFFERENTIALS			1,995	2,512

D180-22876-7

SPS COST FACTORS

Although the SPS's are big, they are relatively simple designs employing highly repetitive elements. The combination of size and simplicity achieved in an SPS is probably only attainable in a space system. It allows the economies of scale to be combined with the economies of mass production to minimize the hardware costs. An additional factor in minimizing the hardware cost is that the design loads and other design conditions in space are of minimal effect on the system. Consequently, these systems are comprised predominantly of directly useful elements, i.e., solar blankets, with the investment in support systems such as structure and controls being a very small part of the total cost. A further attractive feature of the space location is that the very small differential gravity loads allow easy movement of SPS's under construction with respect to the construction facility, allowing an assembly line approach to construction.



SPS-1662

D180-22876-7

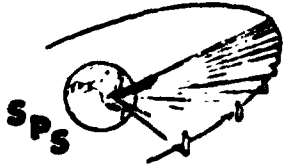
SPS Cost Factors

BOEING

- **SPS'S ARE BIG BUT SIMPLE DESIGNS EMPLOYING REPETITIVE ELEMENTS**
 - Economics of scale combine with economics of mass production
- **DESIGN LOADS IN SPACE ARE MINIMAL**
 - Overhead costs associated with support systems are a small part of the total
 - Assembly operations use production line approach
- **SUNLIGHT MORE THAN 99% OF THE TIME**
 - Solar collectors "work hard" for maximum cost effectiveness
 - Little or no storage required
- **TRAFFIC LEVELS ALLOW REALIZATION OF LOW-COST POTENTIALS FOR SPACE TRANSPORTATION**
 - Fully reusable vehicles economically justified
 - Frequent flights allow cost-effective operations

PROGRAM ASSUMPTIONS FOR COST ANALYSES

In order to develop cost data for the SPS systems, several program assumptions were necessary. These assumptions correspond to a direct development of the SPS systems studied under this contract. They do not represent recommendations as to a most desirable or most practicable SPS program. The last assumption relates to the fact that most of the mass growth seen in these systems (as a result of the uncertainty analyses) came from the efficiency chain, with the reference design efficiency being somewhat more optimistic than the median value resulting from the assignment of uncertainty ranges to the efficiency chain. (Under the bivariate normal distribution assumption used in the uncertainty analyses, the most probable value for any item is the mean of the extremes. This is believed to be a realistic model for this kind of uncertainty analysis.) It is expected that the losses in efficiency in the early systems will be recoverable through a normal process of product improvement. Therefore, the growth allowances applied to the 1-SPS-per-year case were reduced for the 4-SPS-per-year case.



SPS-1681

Program Assumptions for Cost Analyses

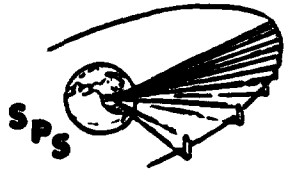
BOEING

- **AFTER A TECHNOLOGY VERIFICATION PROGRAM, INVOLVING GROUND AND FLIGHT PROGRAMS BUT NO NEW SPACE VEHICLES, DEVELOPMENT OF THE 10,000 MEGAWATT SPS, AND ITS ASSOCIATED SYSTEMS, BEGINS.**
- **THE PRODUCTION CAPACITY INITIALLY DEVELOPED IS SIZED FOR A PRODUCTION RATE OF ONE SPS PER YEAR, BUT DOES NOT INITIALLY ACHIEVE THAT RATE.**
- **THE EARLY SPS'S INCUR THE MASS GROWTH PREDICTED BY THE UNCERTAINTY ANALYSIS.**
- **BY THE TIME A PRODUCTION RATE OF FOUR PER YEAR HAS BEEN REACHED, MASS GROWTH HAS BEEN REDUCED BY PRODUCT IMPROVEMENT.**

D180-22876-7

COST ANALYSIS METHODOLOGY

The overall cost analysis methodology is diagrammed on the facing page. It begins with mass estimates and system descriptions for the reference systems. The system descriptions allow selection of cost estimating relationships. These are used to exercise the Boeing parametric cost model to generate an aerospace cost estimate for DDT&I and first unit cost. The aerospace first unit costs are then run through a mature industry analysis that applies production rate factors according to the production rate required for each system element. The totaled mature industry estimates are then adjusted for interest during construction and for cost growth corresponding to mass growth as predicted by the uncertainty analyses. These provide the final production unit costs for 1 SPS per year and 4 SPS's per year.

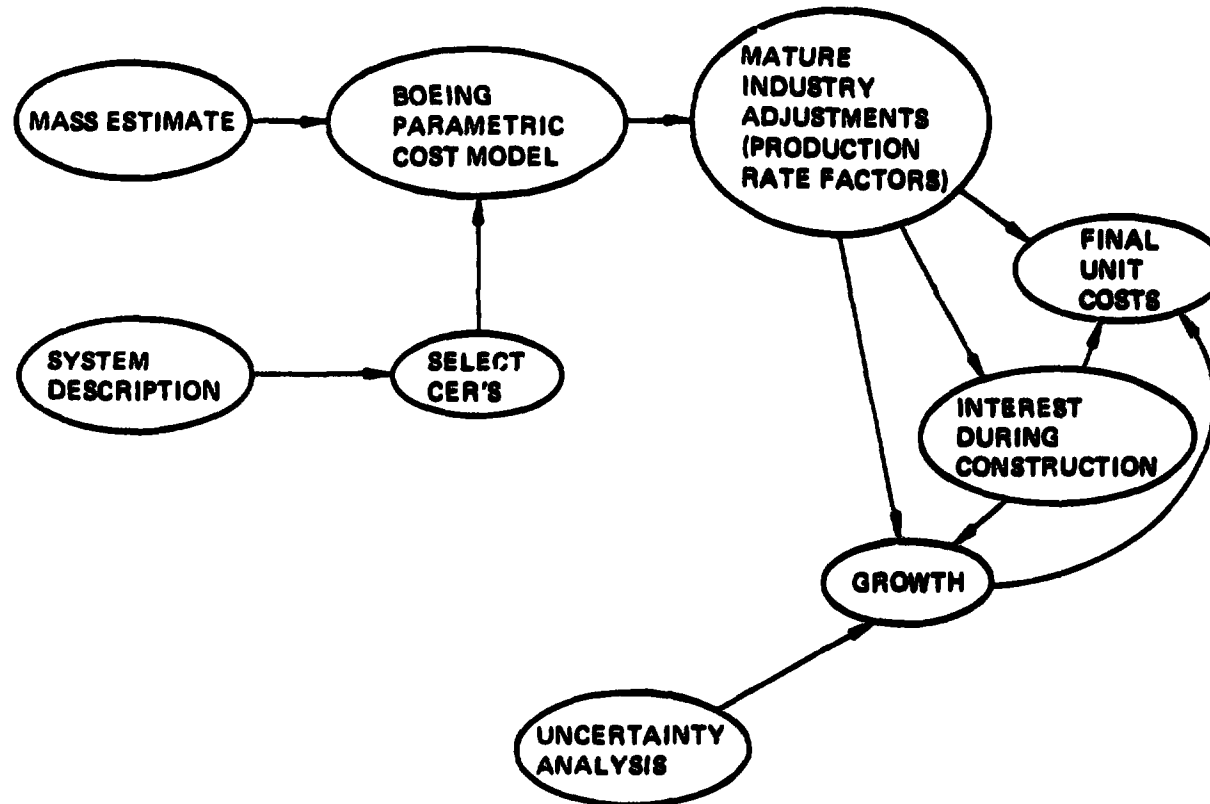


D180-22876-7

Cost Analysis Methodology

SPS-1882

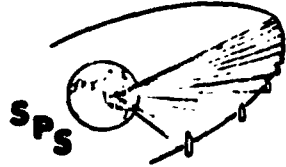
BOEING



D180-22876-7

MATURE INDUSTRY METHODOLOGY CONFIRMATION

The mature industry costing approach was developed by Dr. Joe Gauger based on information developed during IR&D analyses of design-to-cost, experienced costs for commercial aircraft and other systems, and statistical correlations for financial and production factors for a wide variety of commercial industries. It was judged to be desirable to spot-check the mature industry predictions. A total of five spot checks were made as indicated on the facing page. These included solar blankets, graphite structures, klystrons, potassium vapor turbines, and electromagnetic liquid potassium feed pumps. In all cases, the mature industry projection was well within the uncertainties that would be expected for the kind of cost estimates being made. Based on these examples, we believe the mature industry methodology to be an appropriate cost estimating procedure for SPS systems.



SPS-1663

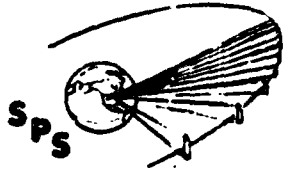
Mature Industry Methodology Confirmation

BOEING ———

	<u>MATURE INDUSTRY PROJECTION</u>	<u>INDUSTRY ESTIMATES</u>
SOLAR BLANKETS	\$22 to \$37/m ²	\$25 to \$50/m ² (RCA, TI, GE, MOTOROLA)
GRAPHITE EPOXY STRUCTURE	\$60/kg	\$50/kg (BOEING)
KLYSTRONS	\$3000/TUBE	\$1750 to \$2700/TUBE (VARIAN)
TURBINES	\$40 to \$50/kg	\$62/kg (GE)
PUMPS	\$75 to \$150/kg	\$66/kg (GE)

RECTENNA SIZE OPTIMIZATION

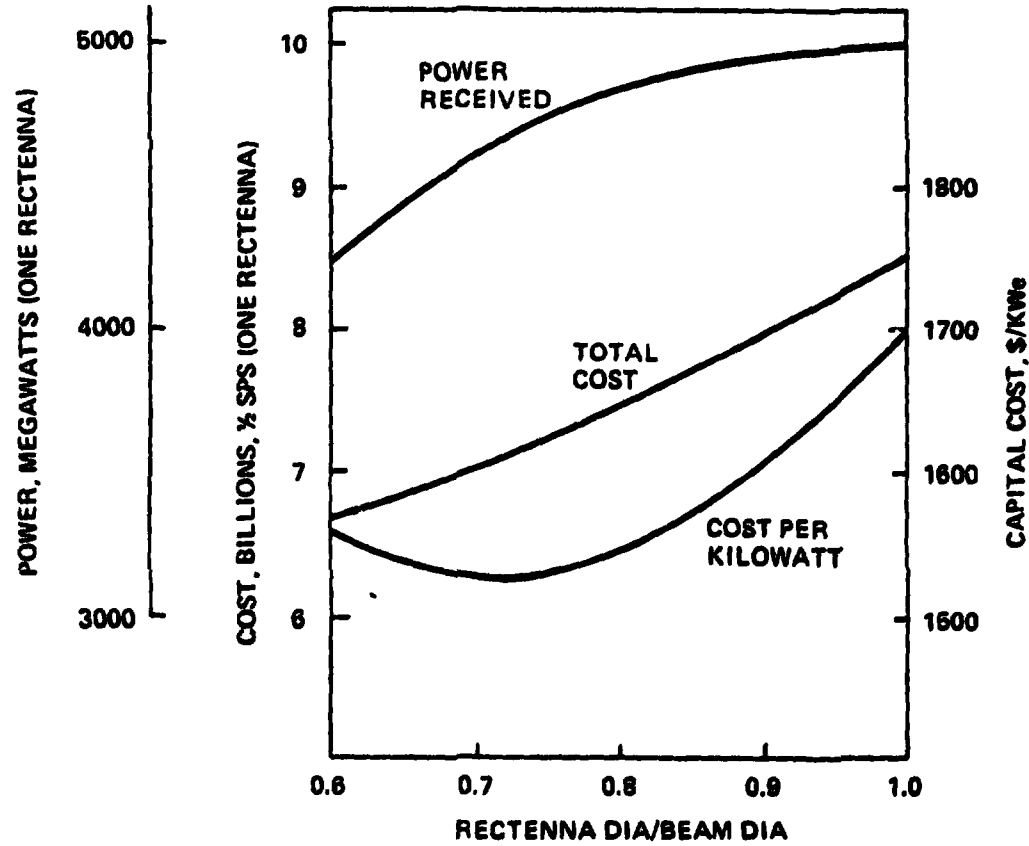
Illustrated here is an example of system design flexibility adjustment to reduce system cost sensitivity to a particular cost problem. Until late in the study effort it was assumed that the receiving antennas would be full main-beam diameter. (This is the optimum if receiving antennas are low in cost.) However, receiving antenna cost estimates were surprisingly high, resulting in a significant cost problem. The nature of the transmitted beam is that very little of the total power is in the outer regions of the main beam. Consequently, a cost optimization of rectenna size reduced its area by approximately half, reduced the received power by about 5% and reduced the cost per kw by 20 percent. (Cost values shown here do not include interest during construction or growth.)



SPS-1366

Rectenna Size Optimization

BOEING

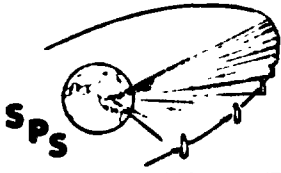


(Note: Beam diameter is the entire main lobe to the first null.)

PRODUCTION COST RESULT SUMMARY

Total production costs are summarized in these bar charts for eight combinations of energy conversion system, production rate, and construction location. The silicon photovoltaic system has a modest cost advantage over the thermal engine and low Earth orbit construction has a significant cost advantage over geosynchronous construction. The most important cost change occurs with the production rate increase from 1 SPS per year early in the program, to 4 SPS's per year in a more mature operation. Principal cost reductions with system maturity occur in SPS hardware production, space transportation, and projected product improvement. The lowest capital cost is achieved with the silicon photovoltaic system at 4 SPS's per year with LEO construction. The figure is approximately \$1,700 per kilowatt electric including interest during construction and projected growth. Still lower figures might be projected for advanced systems, such as thin film gallium arsenide.

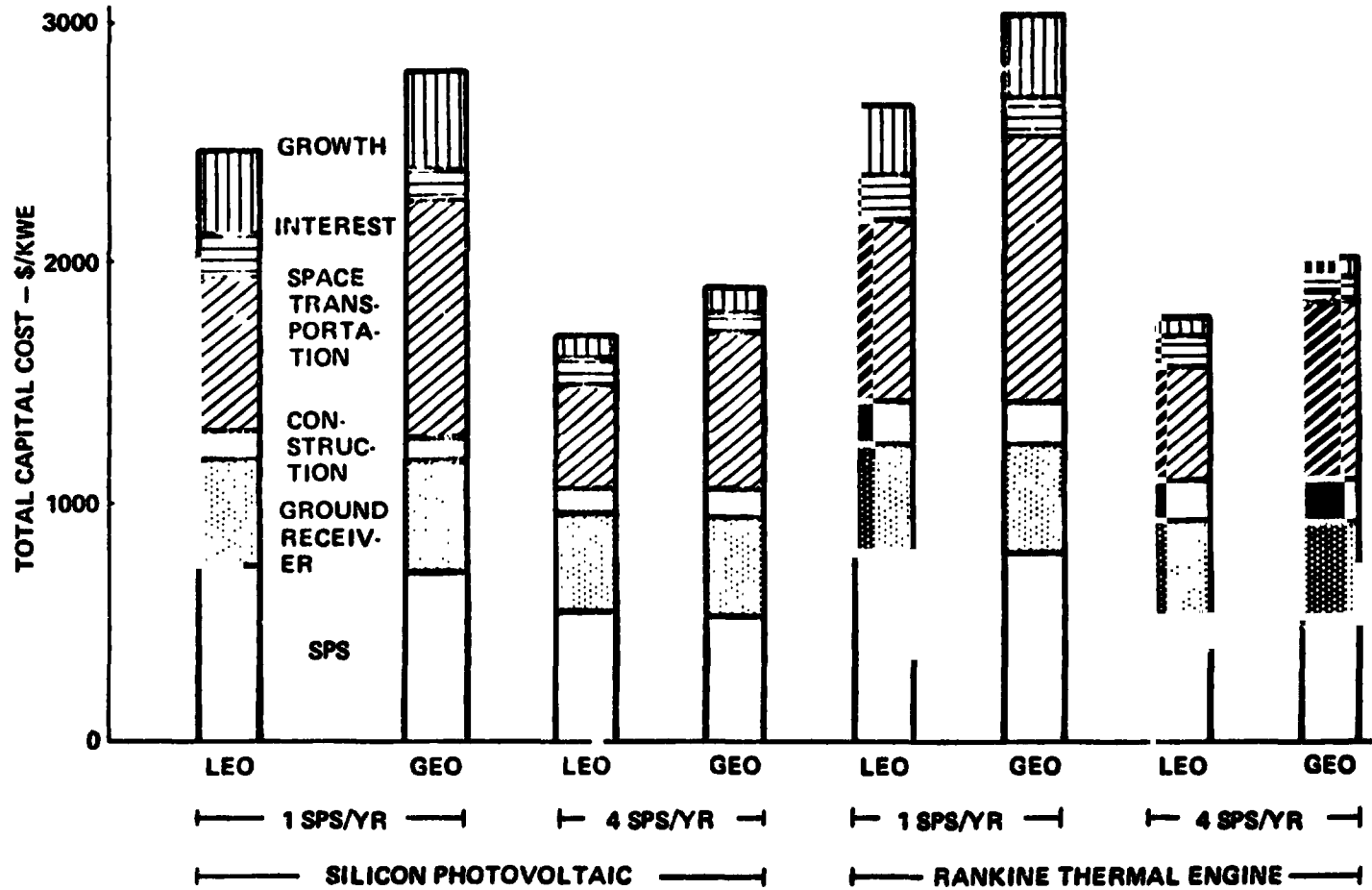
Achievement of the projected silicon photovoltaic costs is critically dependent on the development of a satisfactory mass production technology for single crystal silicon solar cells and blankets. This mass production technology may require continuous growth processes but recent indications of improvements in the technology presently used for solar cell manufacture, indicate that automation of this technology may provide greater cost reduction than commonly supposed.



Production Cost Results Summary

BOEING

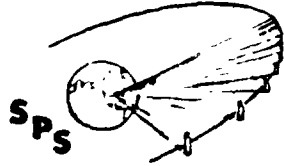
SPS-1700



D180-22876-7

LEO TRANSPORTATION COSTS FOR FOURTEEN YEAR PROGRAM

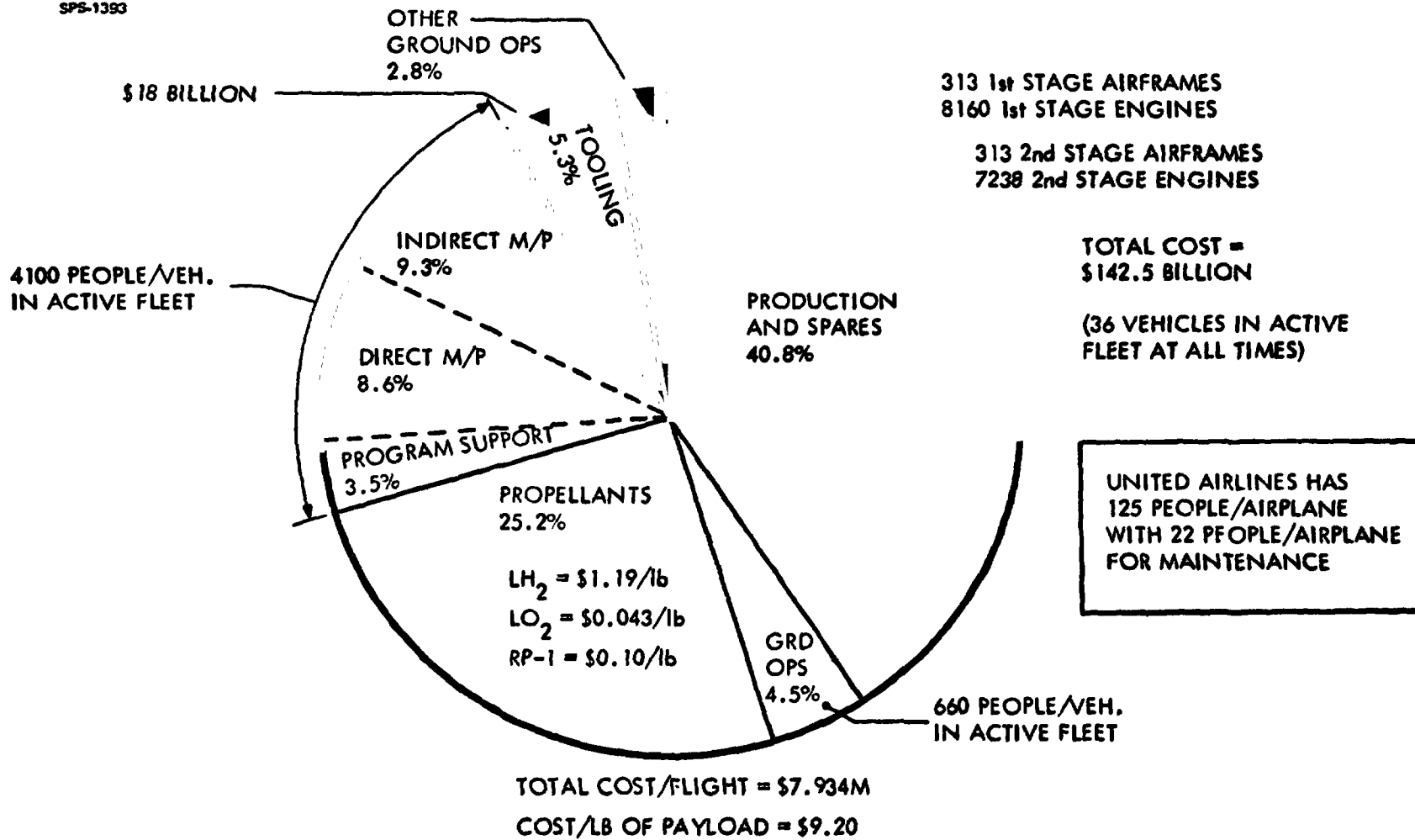
One of the principal issues of overall SPS costs is the cost of space transportation. The projections made during this study have indicated a low earth transportation cost on the order of \$20 per kilogram, including amortization of the vehicle fleet investment, total operations manpower, and propellant costs. The distribution of this cost over the assumed 14 year program is shown on this chart. Vehicle production hardware is the greatest factor; manpower is second in importance, and propellants are third. The propellant cost is about 1/3 of the total, typical of a mature transportation system.



SPS-1393

LEO Transportation Costs for 14 Year Program at 4 Satellites/Year

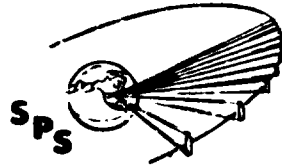
BOEING



D180-22876-7

COST PER FLIGHT WORK BREAKDOWN STRUCTURE

Cost per flight analyses used the work breakdown structure tabulated here. This structure is patterned after the shuttle user charge cost analyses but includes two principal differences: (1) Because the large traffic model will wear out many vehicles, the production of vehicles and their spares is amortized in the cost per flight. (2) Production rates required will demand several ship-sets of tooling. The tooling required to achieve the required rates is also amortized against cost per flight.



SPS-530

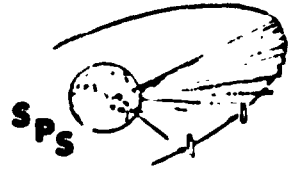
Cost/Flight WBS

BOEING

WBS ELEMENT
OPERATIONS COST
PROGRAM DIRECT PROGRAM SUPPORT PRODUCTION AND SPARES STAGE 1 AIRFRAME ENGINES STAGE 2 AIRFRAME ENGINES
TOOLING STAGE 1 STAGE 2
GROUND OPS/SYS GROUND OPS GROUND SYS GSE SUSTAINING ENGR GSE SPARES PROPELLANT OTHER
DIRECT MANPOWER CIVIL SERVICE SUPPORT CONTRACTOR
INDIRECT MANPOWER CIVIL SERVICE SUPPORT CONTRACTOR

FLIGHT VEHICLE PRODUCTION HARDWARE COSTS

Since vehicle production is the most important component of space transportation costs, it is important to compare the estimates to other similar systems. Shown here are costs in terms of dollars per pound for several aerospace vehicles including commercial aircraft and launch vehicles, as well as the calculated costs for the second stage and first stage of the winged launch vehicle systems. All costs here are expressed as the average costs over 300 units with learning curves applied as appropriate. The commercial aircraft are similar in complexity to the launch vehicles, but a significantly smaller fraction of the overall investment is in propulsion. The S-1C Saturn booster stage is comparable in complexity to the first stage of the wing-wing vehicle. Shuttle costs are seen to be somewhat higher than would be expected from the cost estimates here. However, there are several reasons for that as expressed on the following page.

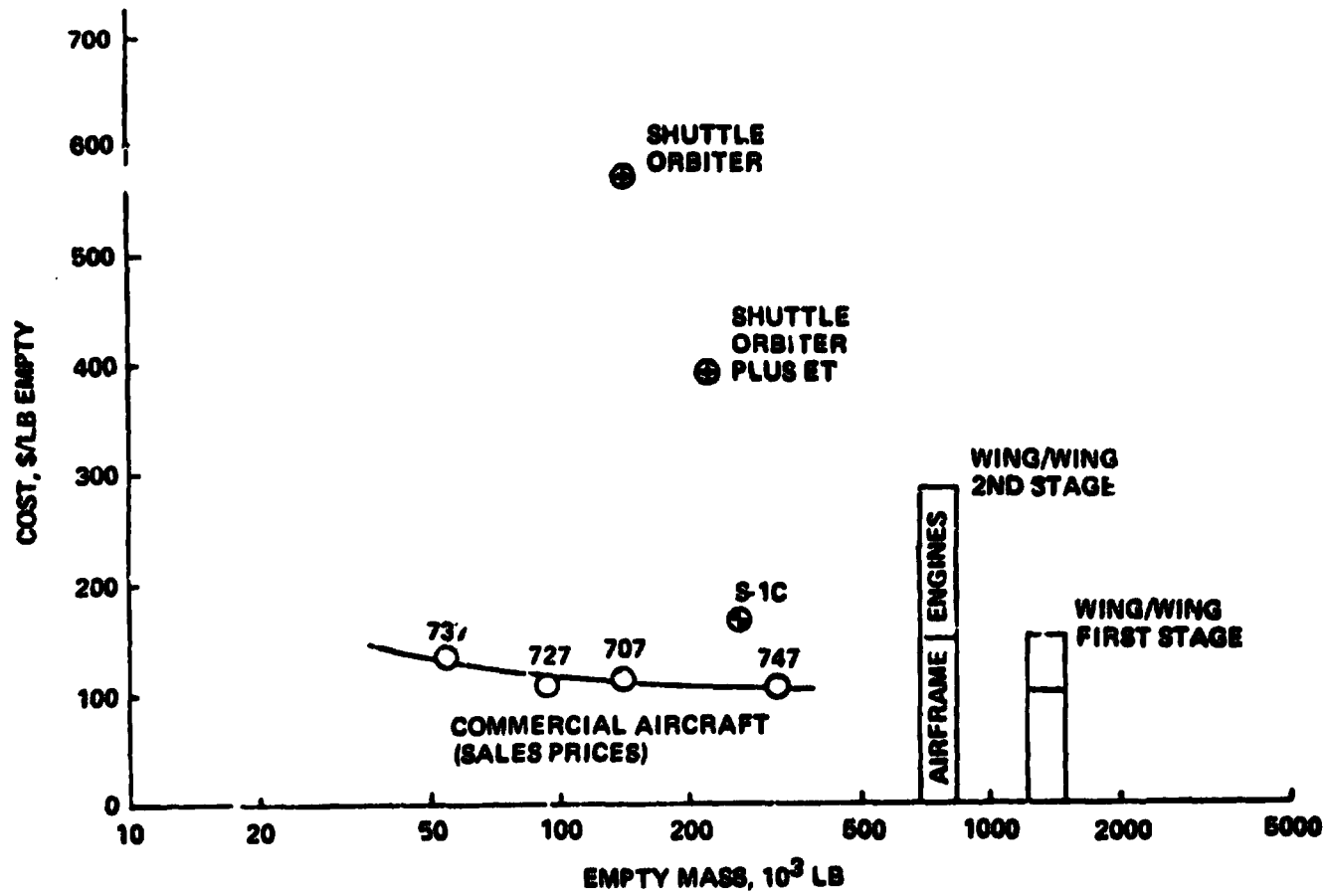


Flight Vehicle Production Hardware Costs

(NORMALIZED TO 300 UNITS)

SPS-1594

BOEING

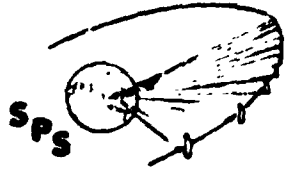


D180-22876-7

DIFFERENCES BETWEEN SHUTTLE ORBITER AND SPS LAUNCH VEHICLE SECOND STAGE

Cost driver differences between the shuttle orbiter and the SPS vehicles are summarized here. These differences are sufficient to rationalize the difference in unit cost expressed on the previous page. However, even if shuttle unit costs were used, the cost of payload transportation would be increased very little.

D180-22876-7



SPS-1664

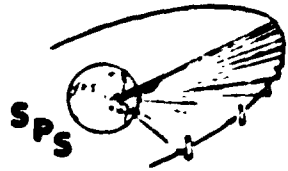
Differences Between Shuttle Orbiter and Wing/Wing 2nd Stage

BOEING

- WING/WING HAS LESS STRUCTURAL COMPLEXITY (INCLUDES PROPELLANT TANKS)
- HIGH \$/MASS COMPONENTS (ENGINES & AVIONICS) LESSER % OF WING/WING EMPTY MASS
- PRODUCTION RATHER THAN PROTOTYPE TOOLING & RATES
- IF WE USED SHUTTLE ORBITER \$/LB FOR WING/WING 2ND STAGE IT WOULD INCREASE PAYLOAD TRANSPORTATION COST LESS THAN \$2/LB

MAJOR MANPOWER COST DATA AND COMPARISONS

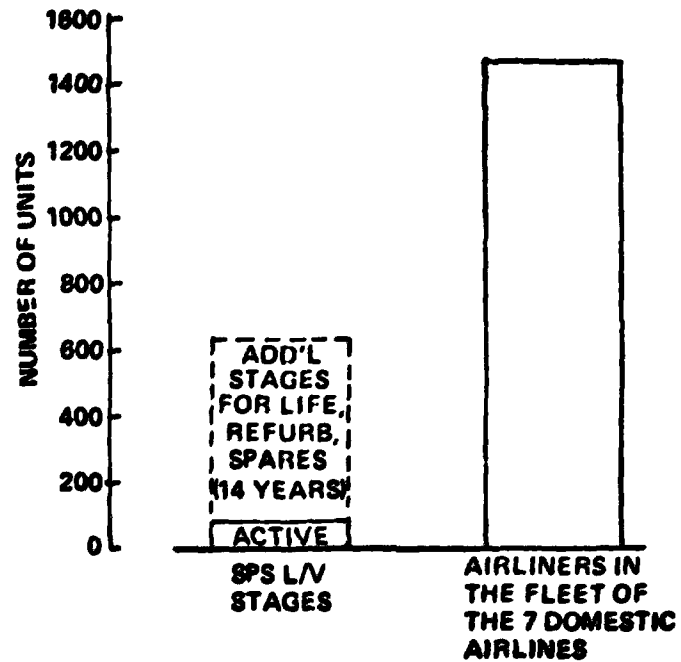
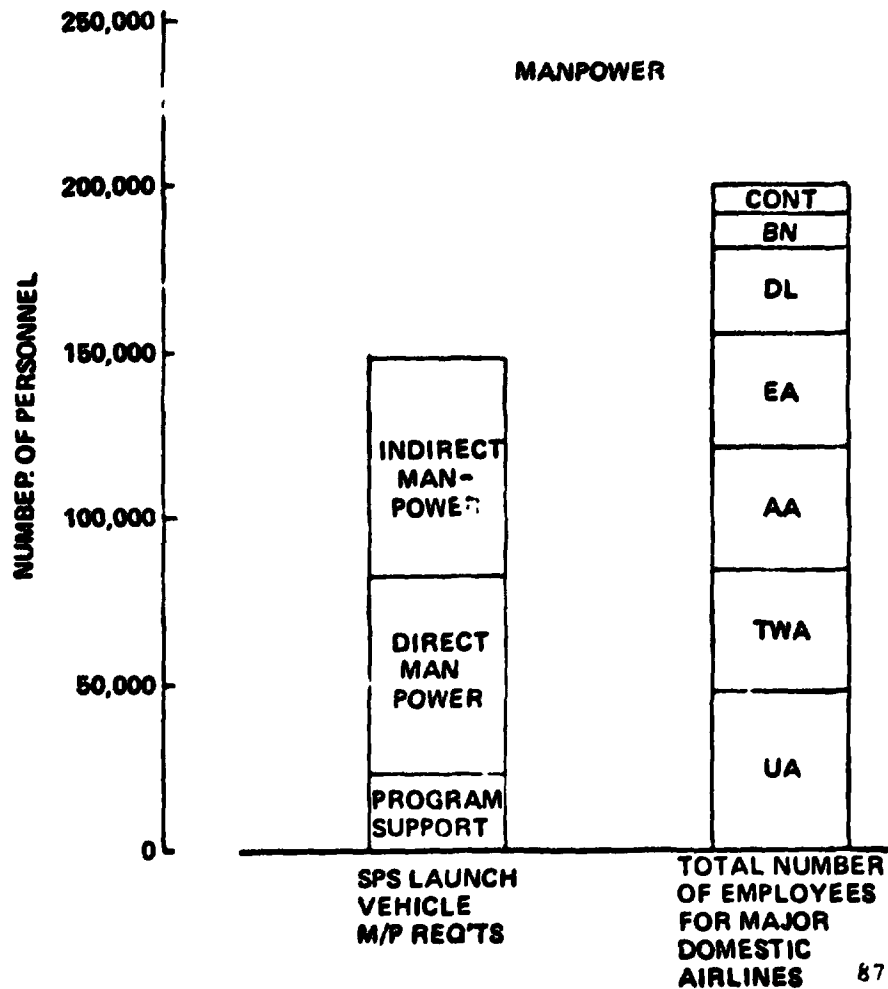
Manpower cost estimates for conducting the SPS transportation operations were made on a detailed task/timeline/headcount basis including all indirect and direct tasks. The estimates are summarized on this chart. They were derived from analogies and extensions of the cost estimating base used to derive space shuttle user charges. In this illustration they are compared with the manpower requirements and fleet sizes for major domestic airlines. The level of overall operations is seen not to be beyond the experience of commercial aerospace vehicle operators today and the fleet size active at any one time is very small by comparison to commercial airline operations. The vehicles, of course, are larger, but even if the left-hand bar is scaled according to vehicle size, the comparison of manpower and fleet size between the SPS operations and commercial airlines indicates the manpower allocations for SPS transportation to be quite generous.



SPS-1397

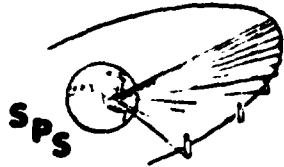
Major Manpower Cost Data and Comparisons

BOEING



PROPELLANT COST BASIS

Propellant costs are energy costs and, therefore, are of considerable significance in SPS transportation costs. At the left of this chart are shown the propellant mass and cost distributions for the SPS vehicle. On the right hand side, the SPS propellant cost estimates used are compared with more recent data arrived from Boeing and JSC studies of large-scale propellant cost production. Significantly, the propellant cost estimates used were higher than the more recent estimates, except in the case of RP-1, where the cost was commensurate with production of RP-1 from oil. In the timeframe considered, it may be necessary to use synthetic hydrocarbons produced from coal. This might increase the RP-1 cost significantly, but the RP-1 cost contribution to overall propellants was relatively small and this low estimate is more than compensated by the higher estimates for the other two propellants. Further, if synthetic propellants are employed, a synthetic hydrocarbon such as methane or propane can be produced at lower cost than a synthetic heavy hydrocarbon, such as RP-1.

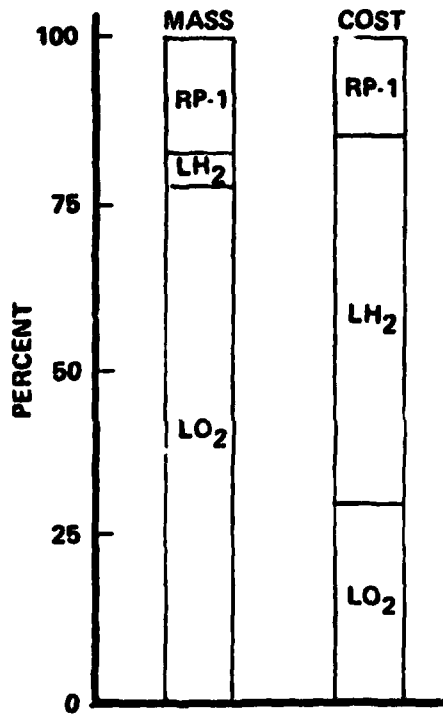


SPS-1396

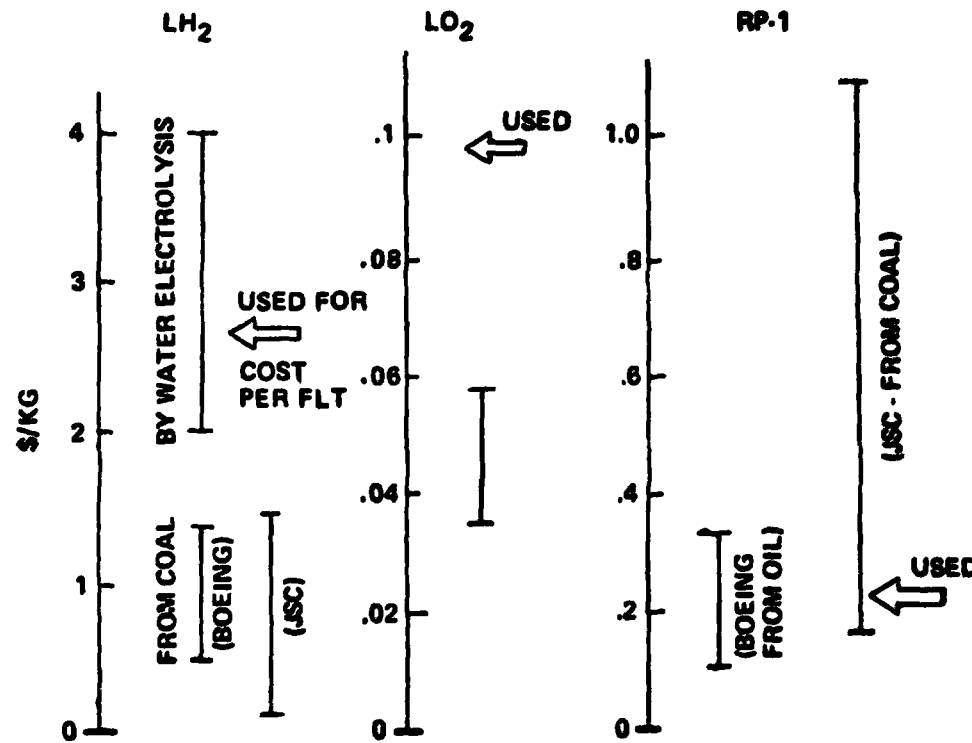
Propellant Cost Basis

BOEING

PROPELLANT DISTRIBUTION



PROPELLANT COST ESTIMATES

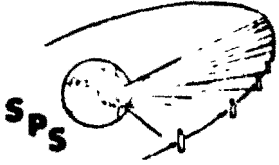


D180-22876-7

COST PER FLIGHT PARAMETRICS

The cost per flight for the heavy lift launch vehicle is dependent upon annual launch rate, being lower at high launch rates. Actual cost for the SPS systems described in this briefing used the parametric cost per flight data shown on this chart. Values ranged from about 13 million dollars per flight for the one SPS per year case with LEO construction to about 7½ million dollars per flight for the four SPS per year case with GEO construction.

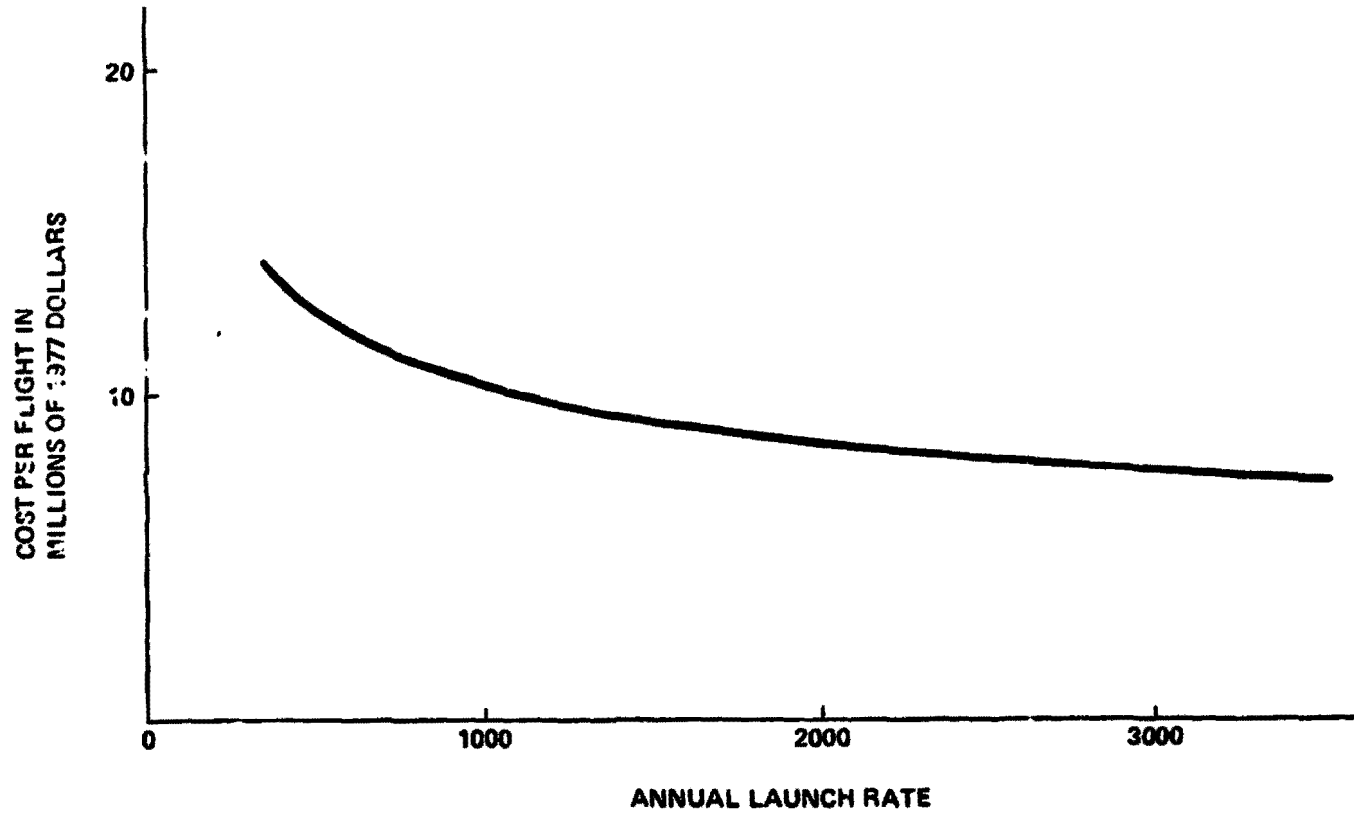
D180-22876-7



SPS-1693

HLLV Launch Costs

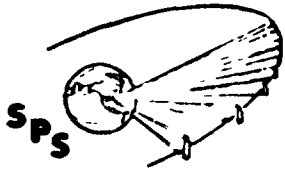
BOEING



UNCERTAINTY ANALYSES METHODOLOGY

An important objective of the SPS systems study was to make the best possible estimates of uncertainty in size, mass and costs, for the SPS systems characterized. The methodology employed was newly developed for the study and included the principal steps indicated on the chart. The basis for the uncertainty analyses was itemized estimates in the uncertainties of component performance, masses, and cost. A typical example would be the uncertainty in solar cell efficiency and degradation. This is an example of the case where correlation exists between the two factors: i.e., more efficient cells tend to experience somewhat greater degradation because the greater efficiency tends to be associated with greater thickness and experimental data indicate thicker cells degrade more. In developing the statistics in size, mass and cost, these kinds of correlations were taken into account through use of a bivariate normal distribution probability model.

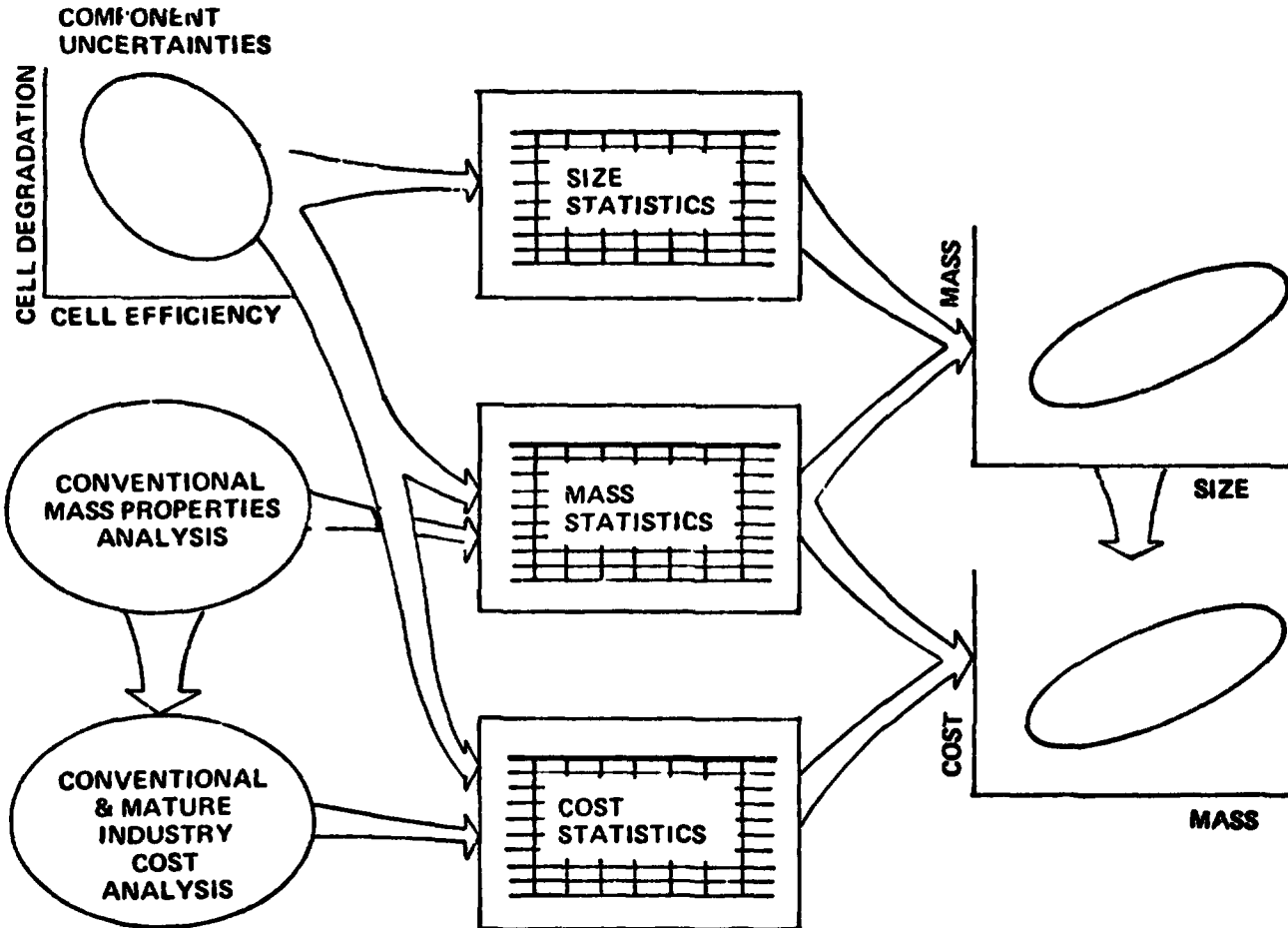
Also providing input data to the uncertainty analyses was a conventional mass property analyses for the systems with estimated uncertainties in such factors as structural crippling criteria, solar cell thickness, and turbomachinery unit masses. Additional uncertainties were developed in system costs, such as uncertainty in solar cell cost per unit area and uncertainties in machinery costs. These uncertainties were coupled with the cost analyses discussed later to prepare the cost statistics. Size statistics and mass statistics were combined to develop a joint mass/size uncertainty estimate and mass statistics and cost statistics were combined to generate combined cost/mass uncertainties. The bivariate normal distribution model was used to statistically combine the uncertainties, with recognition of correlations between component uncertainties where significant correlations were determined to exist.



Uncertainty Analysis Methodology

BOEING

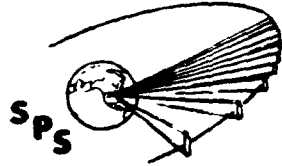
SPS-1395



D180-22876-7

COMPARISON OF EFFICIENCY CHAINS

The reference system efficiency chains are compared on the facing page. The power transmission system efficiency chain is the same for each energy conversion concept and is not repeated. As indicated, the projected overall efficiency of the silicon system is very slightly higher than that of the Rankine thermal engine system.



SPS-1678

Comparison of Efficiency Chains

BOEING

SILICON PHOTOVOLTAIC

ITEM	NOMINAL	MINIMUM	MAXIMUM
SUMMER SOLSTICE FACTOR	.9675	.9675	.9675
COSINE LOSS (POP)	.919	.919	.919
SOLAR CELL EFFICIENCY	.173	.148	.18
RADIATION DEGRADATION	.97	.90	1.0
TEMPERATURE DEGRAD	.954	.954	.954
COVER UV DEGRADATION	.956	.956	1.0
CELL-TO-CELL MISMATCH	.99	.99	.99
PANEL LOST AREA	.961	.961	.961
STRING I ² R	.998	.995	.999
BUS I ² R	.934	.91	.961
ROTARY JOINT	1.0	1.0	1.0
ANTENNA POWER DISTR	.97	.95	.98
DC-RF CONVERSION	.85	.80	.88
WAVEGUIDE I ² R	.985	.985	.985
IDEAL BEAM	.985	.985	.99
INTER-SUBARRAY ERRORS	.956	.88	.97
INTRA-SUBARRAY ERRORS	.981	.97	.99
ATMOSPHERE ABSORP.	.98	.98	.98
INTERCEPT EFFICIENCY	.95	.90	.98
RECTENNA RF-DC	.848	.79	.92
GRID INTERFACING	.97	.96	.98
PRODUCTS SIZES (KM ²)	.0679 108.8	.0385 193	.095 77.8

RANKINE THERMAL ENGINE

ITEM	NOMINAL	MINIMUM	MAXIMUM
CONCENTRATOR	.877	.83	.95
REFLECT DEGR	1.0	.70	1.0
CPC	.885	.80	.885
CAVITY OPTICAL	.950	.95	.98
CAVITY RERADIATION	.917	.917	.934
CAVITY THERMAL	.995	.990	.997
CYCLE	.189	.189	.200
GENERATOR	.984	.984	.986
PARASITIC	.962	.944	.98
POWER DISTR	.948	.93	.96
MPTS (FROM P/V)	.563	.412	.683
PRODUCTS SIZES	.0628 118 KM ²	.027 274 KM ²	.095 77.8 KM ²

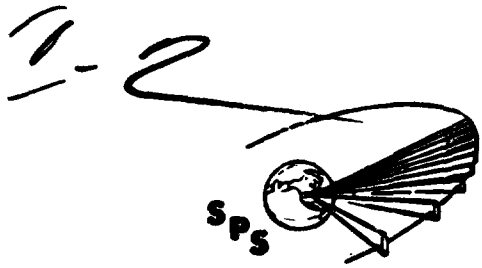
ORIGINAL PAGE IS
OF POOR QUALITY

PHOTOVOLTAIC SPS RELATIVE UNCERTAINTY CONTRIBUTIONS

Uncertainty analyses (to be described more fully later) resulted in the relative uncertainty contributions illustrated here. Also shown are the statistical combinations of all energy conversion effects and all power transmission effects. The energy conversion effect is slightly less than the power transmission effect because a significant correlation between solar cell efficiency and radiation degradation reduces the combined effect of these two parameters considerably below what a simple root sum square would indicate. The uncertainty in power transmission link efficiency is a principal driver on overall system mass and cost uncertainty because it influences more of the system than does solar blanket performance.

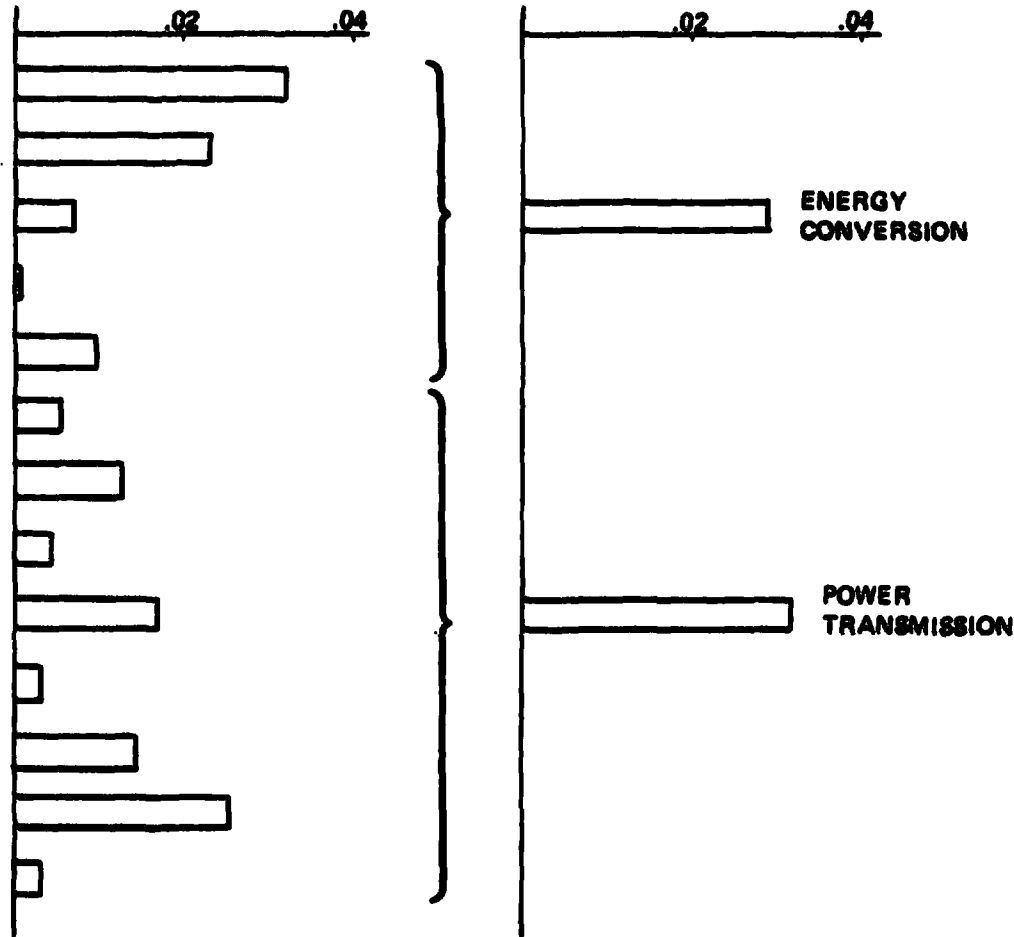
Photovoltaic SPS Efficiency: Relative Uncertainty Contributions

BOEING



SPS-1672

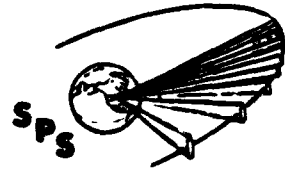
- SOLAR CELL EFFICIENCY
- RADIATION DEGRADATION
- COVER UV DEGRADATION
- STRING I²R
- BUS I²R
- ANTENNA POWER DISTR
- DC-RF CONVERSION
- IDEAL BEAM EFF'Y
- INTER-SUBARRAY ERRORS
- INTRA-SUBARRAY ERRORS
- INTERCEPT EFF'Y
- RECTENNA RF-DC
- GRID INTERFACE



PHOTOVOLTAIC SYSTEM MASS/SIZE UNCERTAINTY ANALYSIS RESULTS

This chart compares the statistically-derived result with the worst-on-worst and best-on-best results defined by combining all the most optimistic component uncertainties and all the most pessimistic component performances. It is demonstrably true that as increased detail is developed in this kind of analysis, the worst-on-worst and best-on-best extremes will continue to become further apart, while the statistical uncertainties will tend to change little and will approach a representation of true uncertainties. Significantly, the reference point design was outside the projected 3 sigma range for mass and size. This resulted primarily because the efficiency chain assigned to the reference design was more optimistic than the most probable efficiency chain defined by the statistical analyses. An example is as follows: In dc/RF conversion, the nominal efficiency assigned to the reference design was 85% with extremes of 80% and 86%. It is a consequence of the bivariate normal distribution model that the most probable value must be the median between the extremes. This resulted in the most probable size being significantly greater than the reference design size.

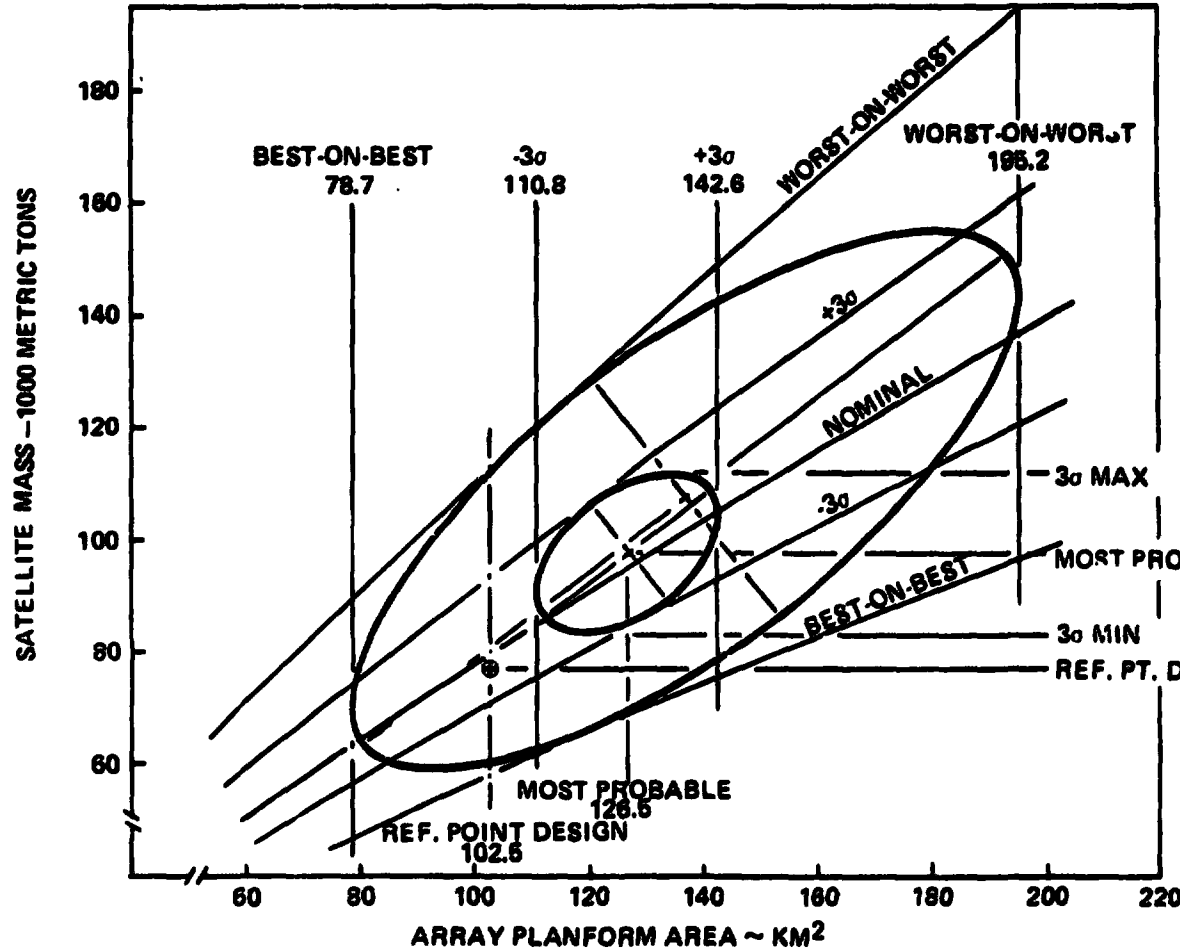
The reference design point is slightly below the nominal line because the nominal line is associated with 10,000 MW output, whereas the reference design, with the final efficiency chain assessment, provided 9,300 MW output. The projected mass growth is the difference between the most probable point and the reference point and is equivalent to 26.6%. This growth is very close to the 25% projected by historical correlations of comparable systems.



Photovoltaic SPS Mass/Size Uncertainty Analysis Results

SPS-1679

BEING



ORIGINAL PAGE IS
OF POOR QUALITY

112,000(+45.5%)

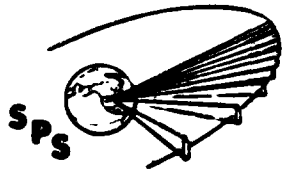
MOST PROBABLE 97,500(+26.6%)

83,000(+ 7.8%)

REF. PT. DESIGN 77,000 METRIC TONS

THERMAL ENGINE MASS SIZE UNCERTAINTY ANALYSES RESULTS

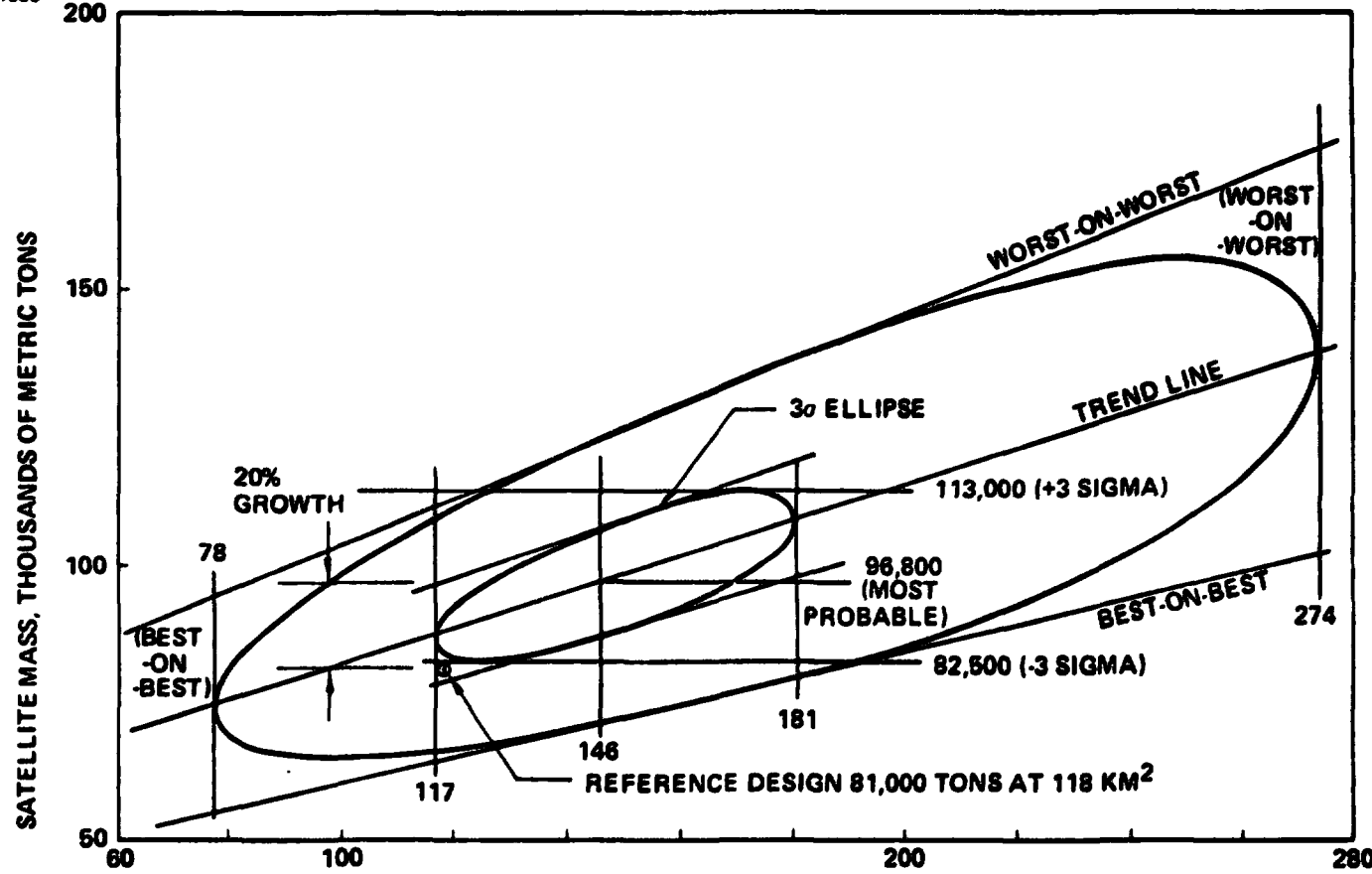
Presented here is an uncertainty estimate for the thermal engine comparable to the previous one for the photovoltaic system. Because the technology of the thermal engine system is somewhat more mature, it would be expected to estimate somewhat less mass growth and that turned out to be the case. An additional factor in the reduced mass growth projection is that a significant part of the size escalation is associated with the size of the concentrator which is a low-mass component of the thermal engine system.



Rankine Thermal Engine Size/Mass Uncertainty Analysis Results

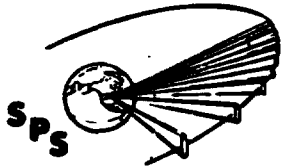
BOEING —————

SPS-1686



MASS/COST UNCERTAINTY ANALYSES RESULTS

With costs included in the uncertainty analyses, it is necessary to discriminate between the 1 SPS per year case and the 4 SPS per year case. As discussed under cost analyses, for the 4 SPS per year case, an estimate was made that about 60% of the predicted mass growth could be removed by product improvement. Similarly to the size and mass estimates, the reference design trended towards the optimistic side of the median of the cost uncertainties. Consequently, one sees first a cost escalation at the reference design point and then a further cost growth associated with the mass growth projection. Note the very high correlation between cost and mass uncertainties. This corresponds to the historical indications that cost growth is frequently associated with mass growth, and especially with the compensation for (or removal of) mass growth in a system when performance requirements dictate that mass growth be limited to predetermined values.



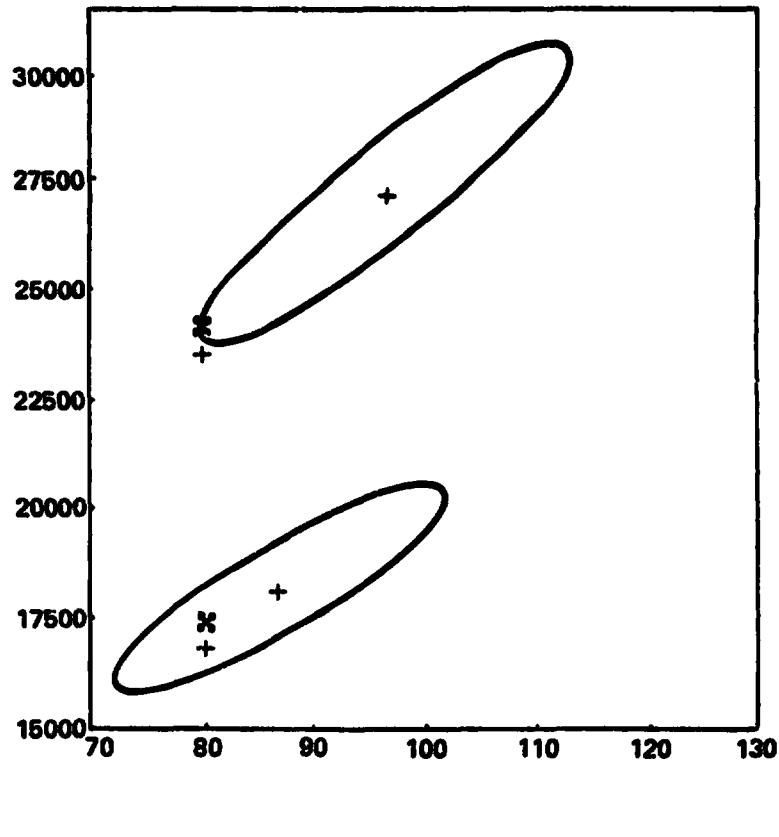
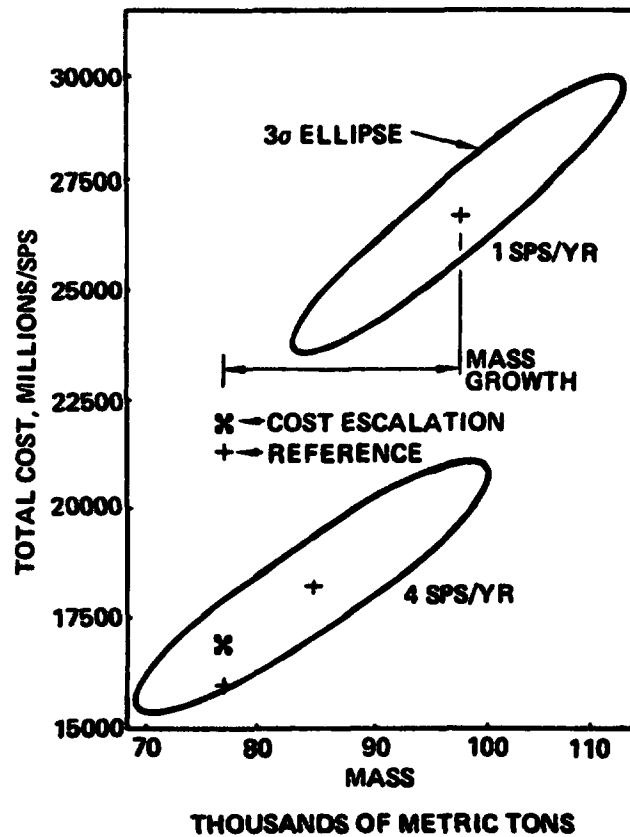
SPS-1680

Mass/Cost Uncertainty Analysis Results

BOEING

SILICON PHOTOVOLTAIC

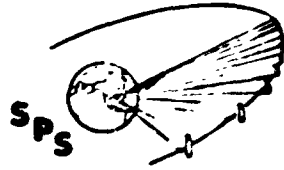
RANKINE THERMAL ENGINE



TOTAL COSTS THROUGH NO. 1 SPS PHOTOVOLTAIC SYSTEM

The actual hardware development costs for SPS hardware represent a small portion of the overall nonrecurring cost required to initiate the program. This is because the SPS hardware is highly repetitive; individual elements are not extremely large and the development of the basic hardware can be primarily carried out on the ground. The total nonrecurring cost includes a technology verification effort including ground-based and flight-based test activities, the development of SPS energy conversion and power transmission/reception hardware, and a significant investment in development of space operations capability including space transportation and space construction systems.

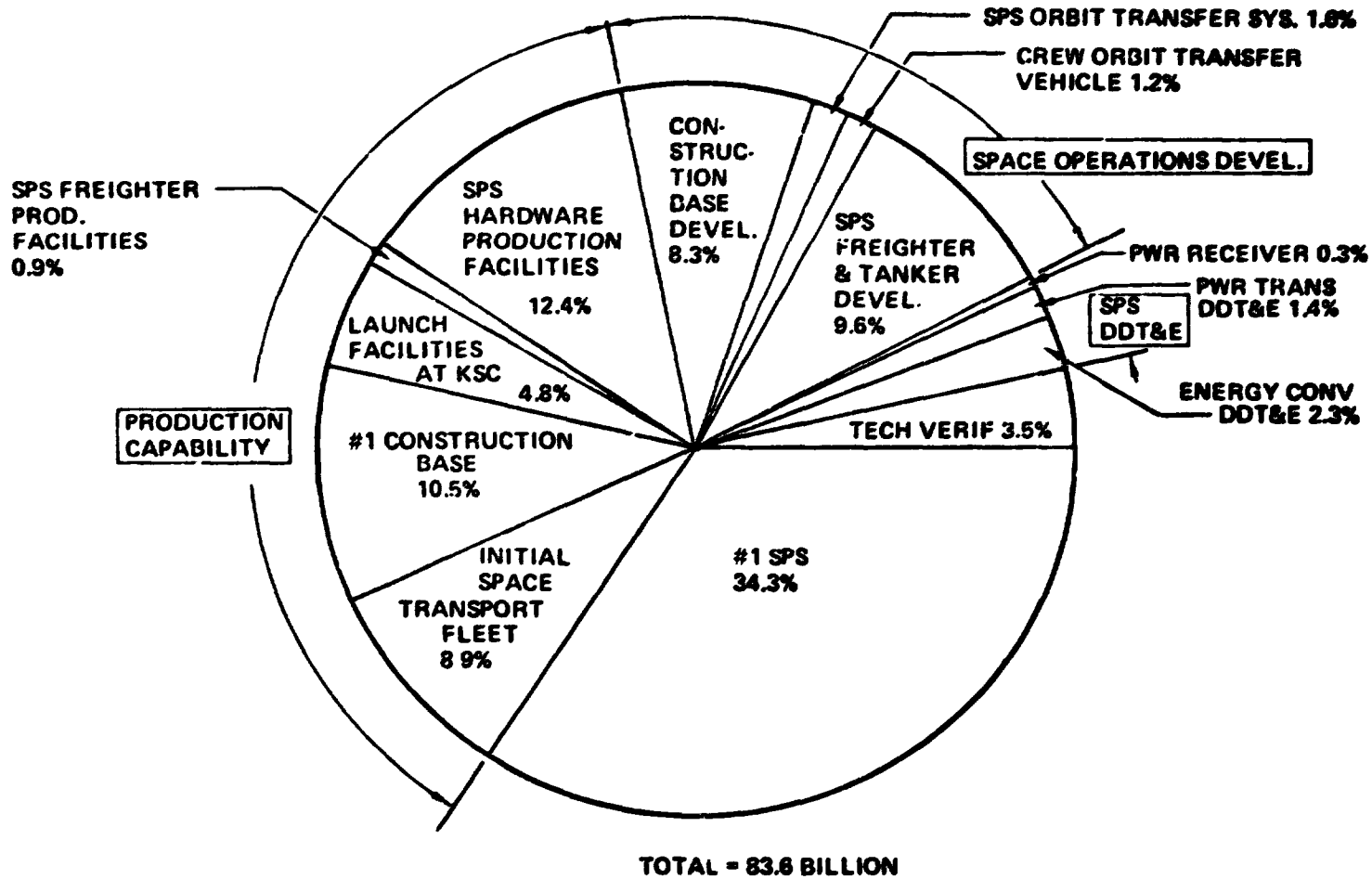
The largest slice of the total nonrecurring costs is for installation of a production capability sufficient for production of 1 SPS per year, i.e., 10,000 MW a year, and for the production of the first SPS. The production cost estimate for the first SPS does not include the production capability amortization factors included in SPS costs on prior charts. It does include a 50% prototype factor penalty cost. The overall total is slightly more than \$80 billion in 1977 dollars. A similar estimate for the thermal engine SPS was about \$8 billion greater, primarily due to the additional cost of the more complex construction base system.



SPS-1549

Total Costs Through #1 SPS Photovoltaic System

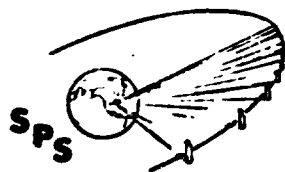
BOEING



D180-22876-7

PREDICTED BUSBAR POWER COSTS AND UNCERTAINTIES

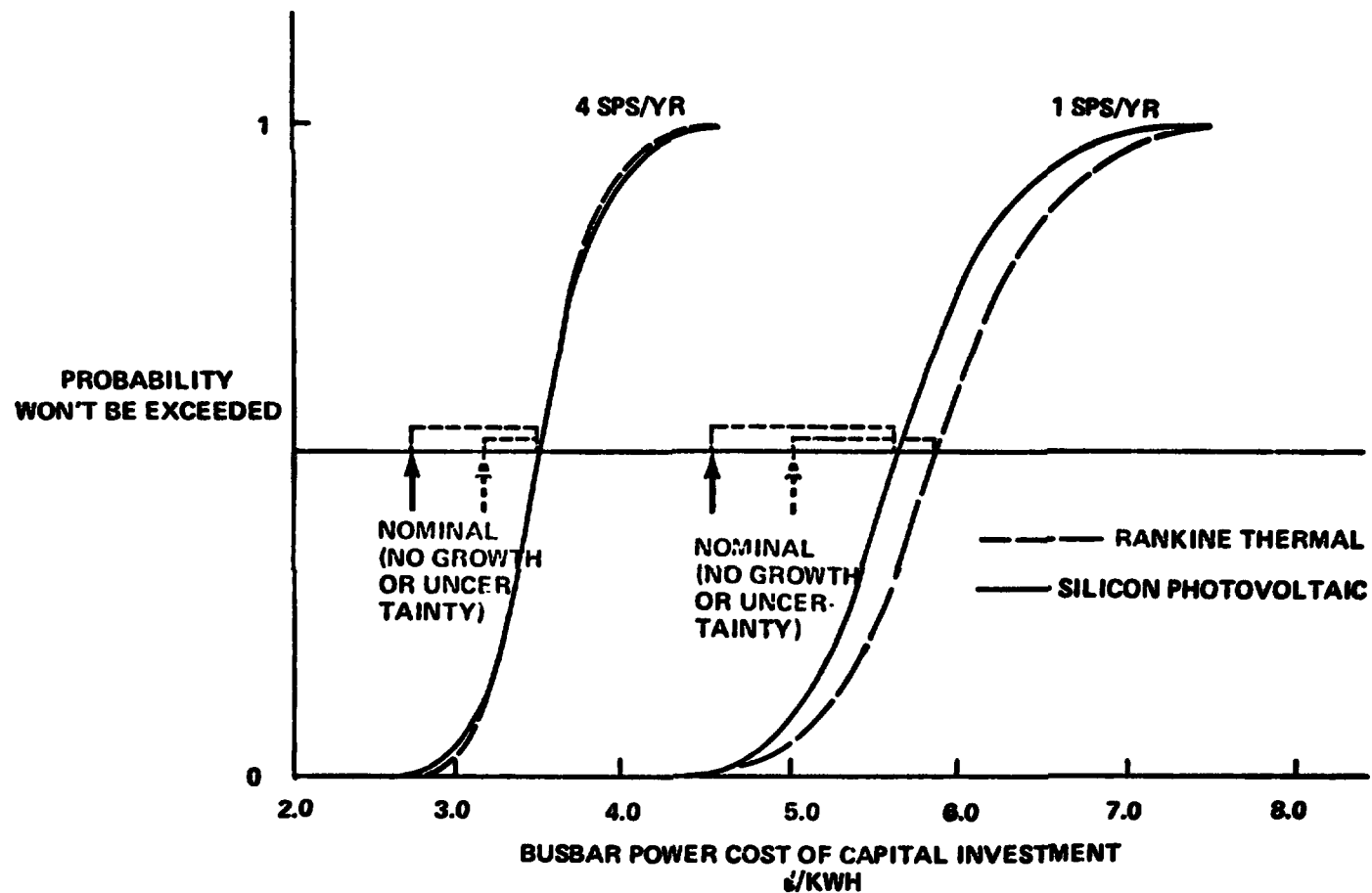
The bottom line for an SPS system is its capability to produce power at an acceptable cost. The result shown on this chart represents the final result of the costing and uncertainty analyses. Uncertainties for busbar power costs include the uncertainties in unit costs as well as uncertainties in the appropriate capital charge factor to be applied and the plant factor at which the SPS can operate. Capital charge factors from 12-18 percent were considered and the plant factor uncertainty was taken as 70%-90% at one SPS per year and 85%-95% for four SPS's per year. These uncertainties were statistically combined with the cost uncertainties derived by the cost uncertainty analyses.



SPS-1684

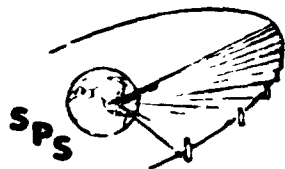
Predicted Busbar Power Cost & Uncertainties

BOEING



PROJECTIONS INDICATE SPS COST COMPETITIVENESS BY THE YEAR 2000

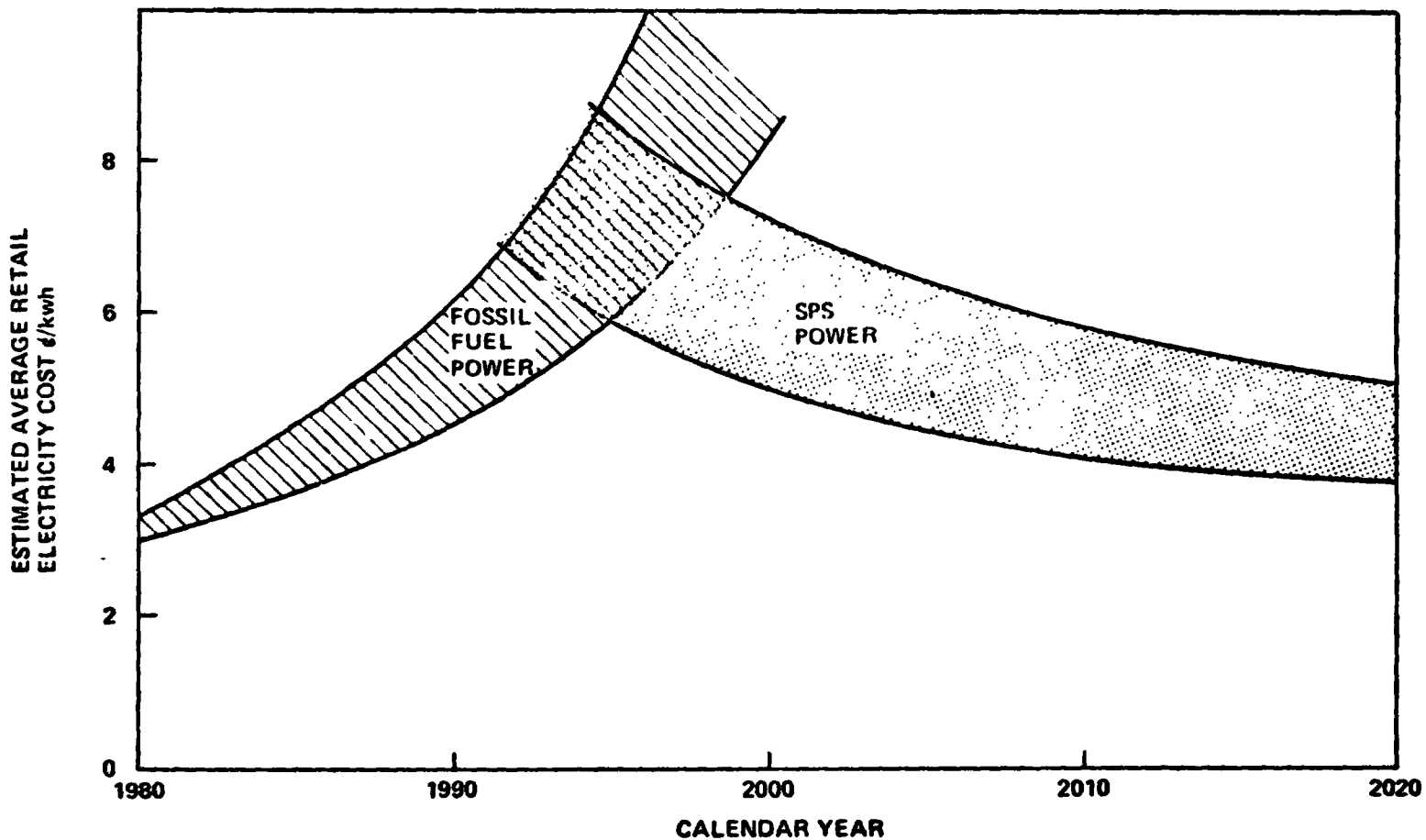
A study of energy and power cost conducted on IR&D indicated an approximate projection of increase in electrical power costs illustrated in the left hand band on this chart. Results from this study are plotted in the right hand band. As indicated these two projections cross over in the general vicinity of the year 2000. This indicates that even with a relatively vigorous program to develop the solar power satellite, by the time production installations could begin the system would be cost competitive with alternative energy sources.

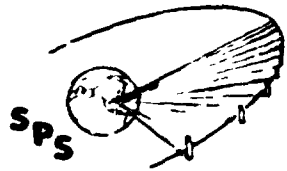


SPS-1667

Projections Indicate SPS Power will be Economically Attractive

BOEING



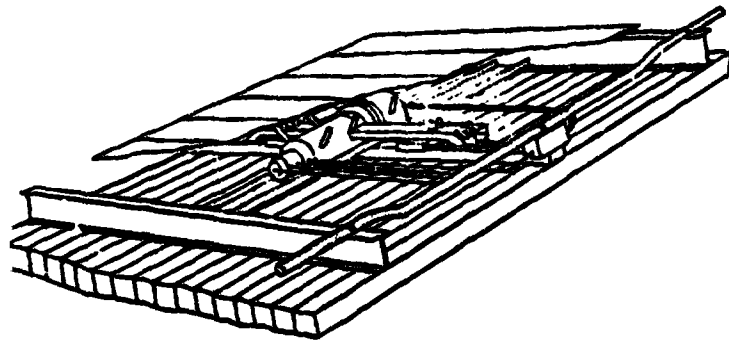
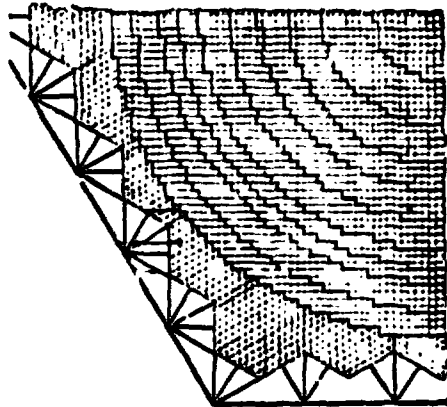


SPS-1667

D180-22876-7

MPTS Briefing

----- **BOEING** -----



- **ARRAY ANALYSIS**
W. LUND, & RATHJEN
- **RF TRANSMITTER**
E. J. NALOS
- **POWER DISTRIBUTION**
J. GEWIN
- **STRUCTURAL AND THERMAL INTEGRATION**
O. DENMAN
- **SUPPORTING WORK**
GENERAL ELECTRIC COMPANY, SYRACUSE NY
VARIAN ASSOCIATES, PALO ALTO, CA

Microprocessor Power
Transmission System

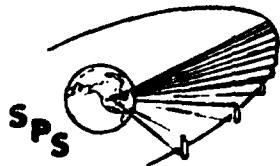
PRECEDING PAGE BLANK NOT FILLED

MPTS ROAD MAP

The study road map indicates the approach taken in establishing a baseline design for the spaceborne element of the MPTS. Highlights of this approach include a klystron transmitter selection study, an end-to-end system efficiency evaluation, spacetenna pattern analysis and structural integration. These combine to produce inputs and constraints to the overall SPS cost model which makes possible the SPS system evaluation. Follow-on topics are defined which will result in the next level of refinement of an improved SPS.

The klystron trade study encompasses klystron design, thermal analysis, manufacturing and reliability assessments, power distribution and X-ray assessment. Spacetenna integration is influenced by structural concepts, design validation, mass assessment, and finally end-to-end efficiency calculations which require a reference spacetenna design whose radiation pattern and impedance characteristics are known. Alternate candidates for the spacetenna radiating element have also been assessed to assist in a final antenna design selection.

D180-22876-7



SPS 1639

BOEING

Array Analysis

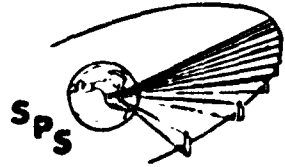
PRECEDING PAGE BLANK NOT FILLED

SPACETENNA SIZE AND POWER DENSITY

Collection efficiency and radiated power were calculated for a fixed rectenna size and power output. The spacetenna aperture distributions used in the study were:

- o **Uniform**
- o **10 db Gaussian**
- o **20 db Gaussian**
- o **Inflected Bessel**

The inflected Bessel produced a system with the highest efficiency and lowest power required at the spacetenna. However, it required a spacetenna with a radius in excess of 900 meters. The 10 db Gaussian was selected as the best compromise for further analysis.



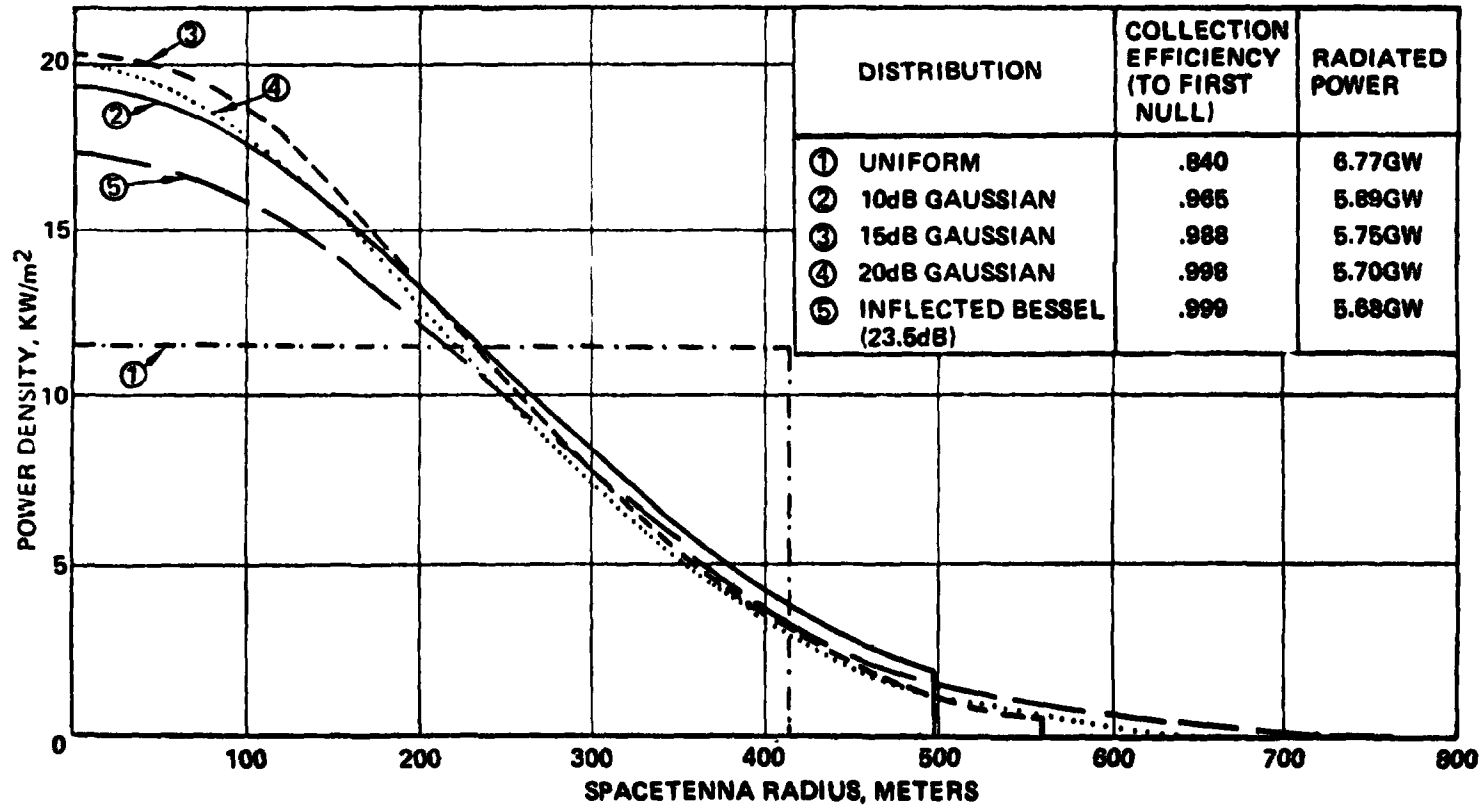
SPS 858

D180-22876-7

Spacenna Size and Power Density Required For Fixed Rectenna Size and Power Output

BOEING

- RECTENNA RADIUS TO FIRST NULL = 6,485 METERS
- DELIVERED GROUND POWER = 5GW
- ASSUMED RECTENNA EFFICIENCY = 88%

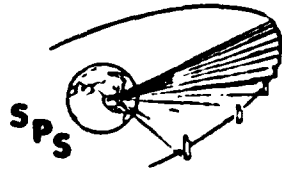


SIDELOBE DISTRIBUTIONS FOR FIXED RECTENNA CONSTRAINTS

This study was conducted to examine spaceborne transmitter aperture power tapers alternate to the 10 db Gaussian used as baseline. The distributions investigated were:

- o Uniform
- o 10 db Gaussian
- o 20 db Gaussian
- o Inflected Bessel

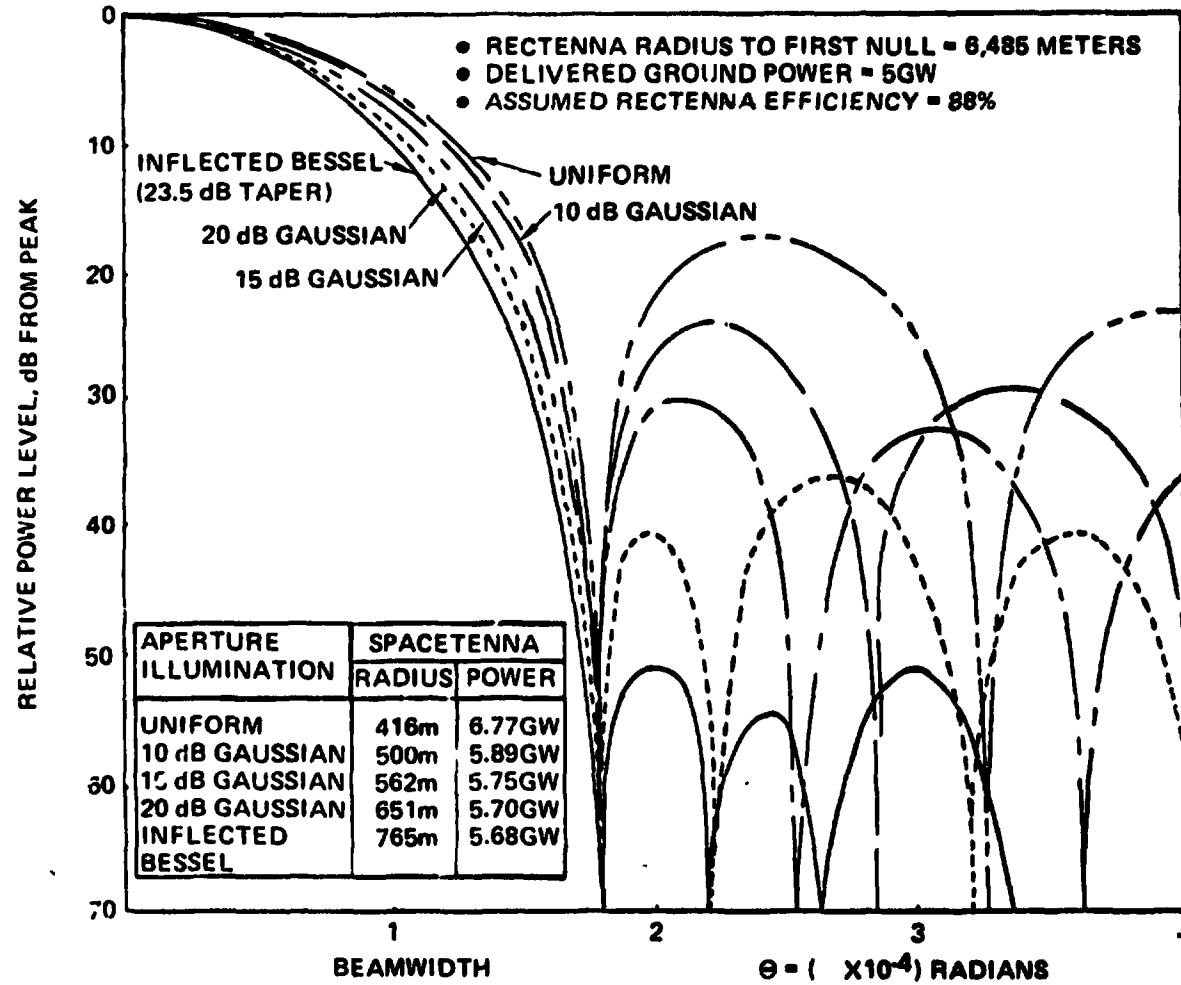
The resulting secondary antenna patterns were compared for beamwidth and sidelobe level. Because of power quantization techniques presently in use, the 9.5 db Gaussian taper was settled on as the new baseline giving an overall efficiency of 96.6 percent.



SPS 850

Sidelobe Distributions For Fixed Rectenna Constraints

BOEING

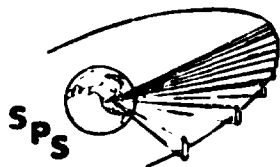


APERTURE FIELD DISTRIBUTION AND SPACETENNA PATTERN

This figure depicts the aperture power distribution produced by both the 10 db Gaussian taper and the inflected Bessel taper. The next figure graphs the secondary radiation patterns produced by these aperture distributions. The inflected Bessel distribution can be written as

$$f(\rho) = 1 + 4.35 J_0(3.84 \rho)$$

This expression is the sum of two distributions – a uniform distribution $f(\rho) = 1$ and a Bessel distribution $f(\rho) = J_0(U_1 \rho)$. The value of the constant U_1 controls the sidelobe level and edge illumination. This constant is adjusted to optimize the distribution. The usefulness of this type of distribution will be further investigated including the effect on rectification efficiency.

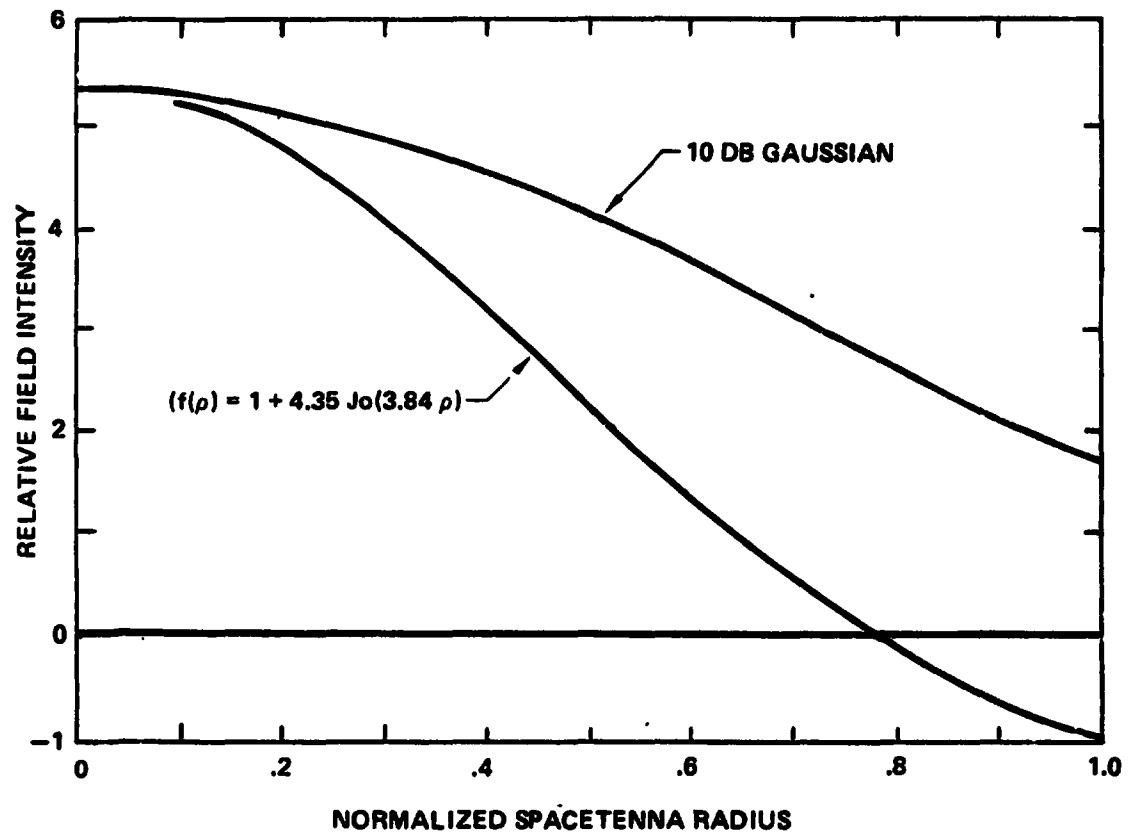


D180-22876-7

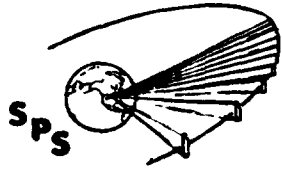
Aperture Field Distribution

SPS-1599

BOEING

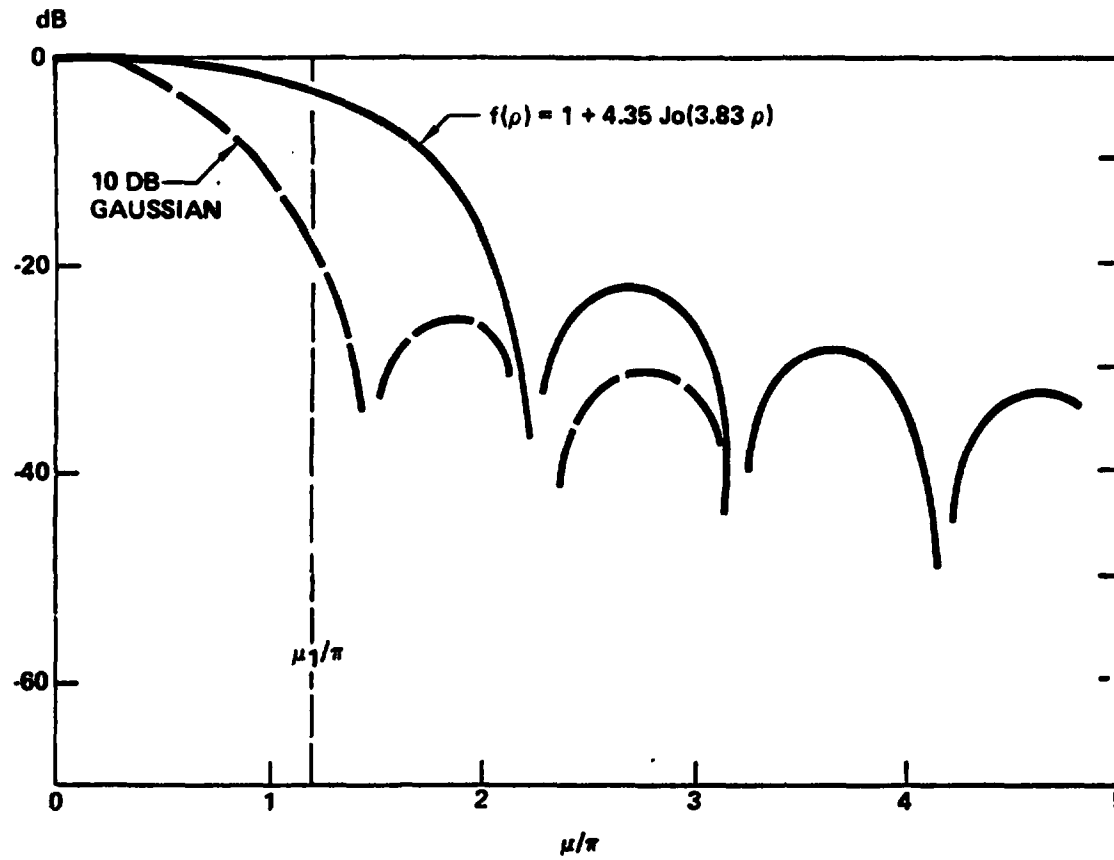


Spacetenna Pattern



SI-S-1600

BOEING

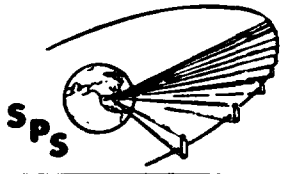


PRECEDING PAGE BLANK NOT FILMED

ARRAY PATTERN ROLL-OFF CHARACTERISTICS

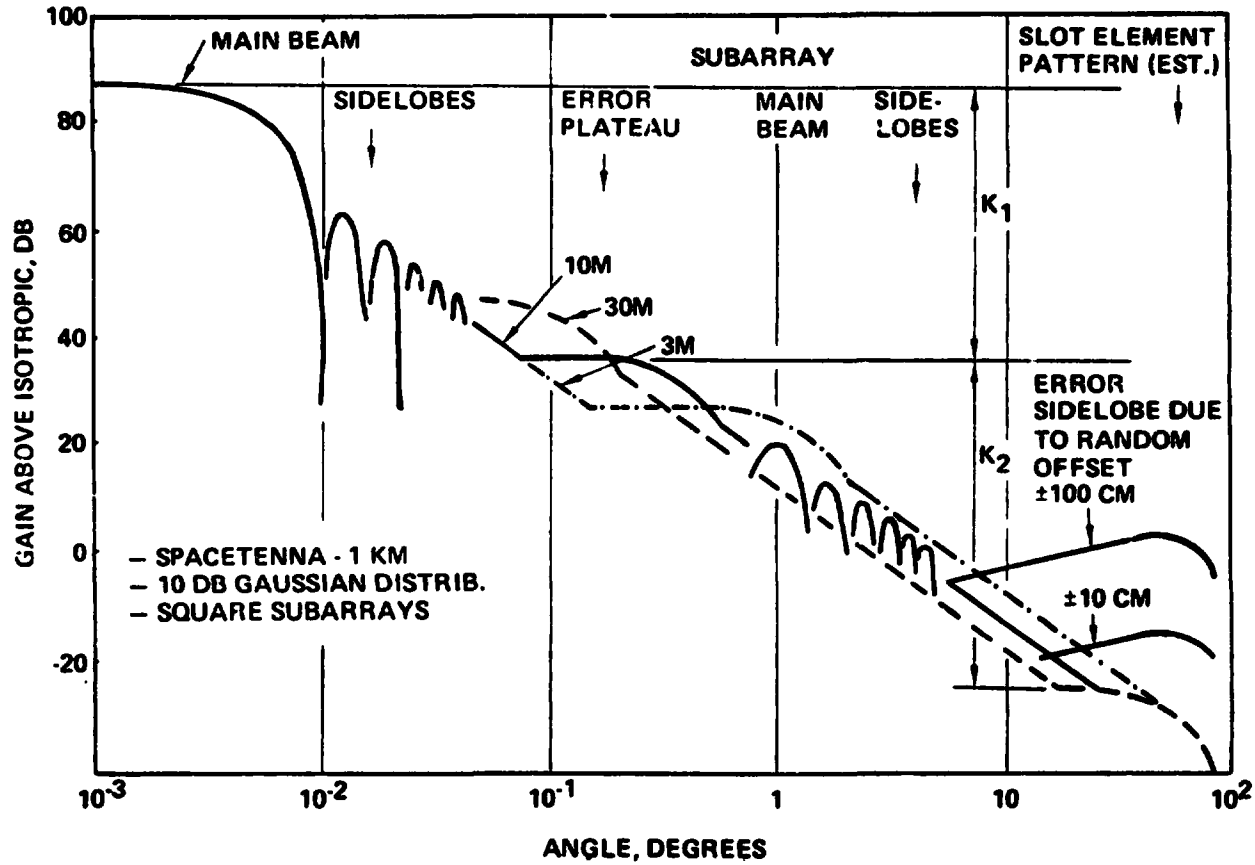
A numerical integration technique was used to obtain the radiation pattern of the 10 db Gaussian tapered distribution. It was established that the sidelobes rolled off at a 30 db/decade of angle rate. The chart shows the first five sidelobes and the average power line 3 db below the peaks. The error plateaus were computed from the assumed error magnitudes and the number of sub-arrays associated with three different subarray sizes. The aperture efficiency was also obtained by numerical integration. The sub-array roll-off characteristics were obtained by numerically integrating the square aperture distribution for each of 19 different cuts over a 45 degree sector of θ . These cuts were then averaged at each θ to give the pattern shown. The resultant subarray sidelobes also roll off at a 30 db/decade of angle.

Array Pattern Roll-Off Characteristics



SPS-1641

BOEING

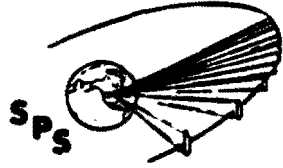


TOTAL RADIATED POWER VS ANGLE

To obtain a clearer view of how the total energy is distributed, the average pattern level as a function of angle can be integrated graphically. By weighting a $\sin \theta$ term with an additional multiplier proportional to θ , it is possible to take out the area bias produced by the logarithmic plot. Repeating this in terms of power rather than db, as shown in the facing chart, gives a curve, the area under which represents the radiated power.

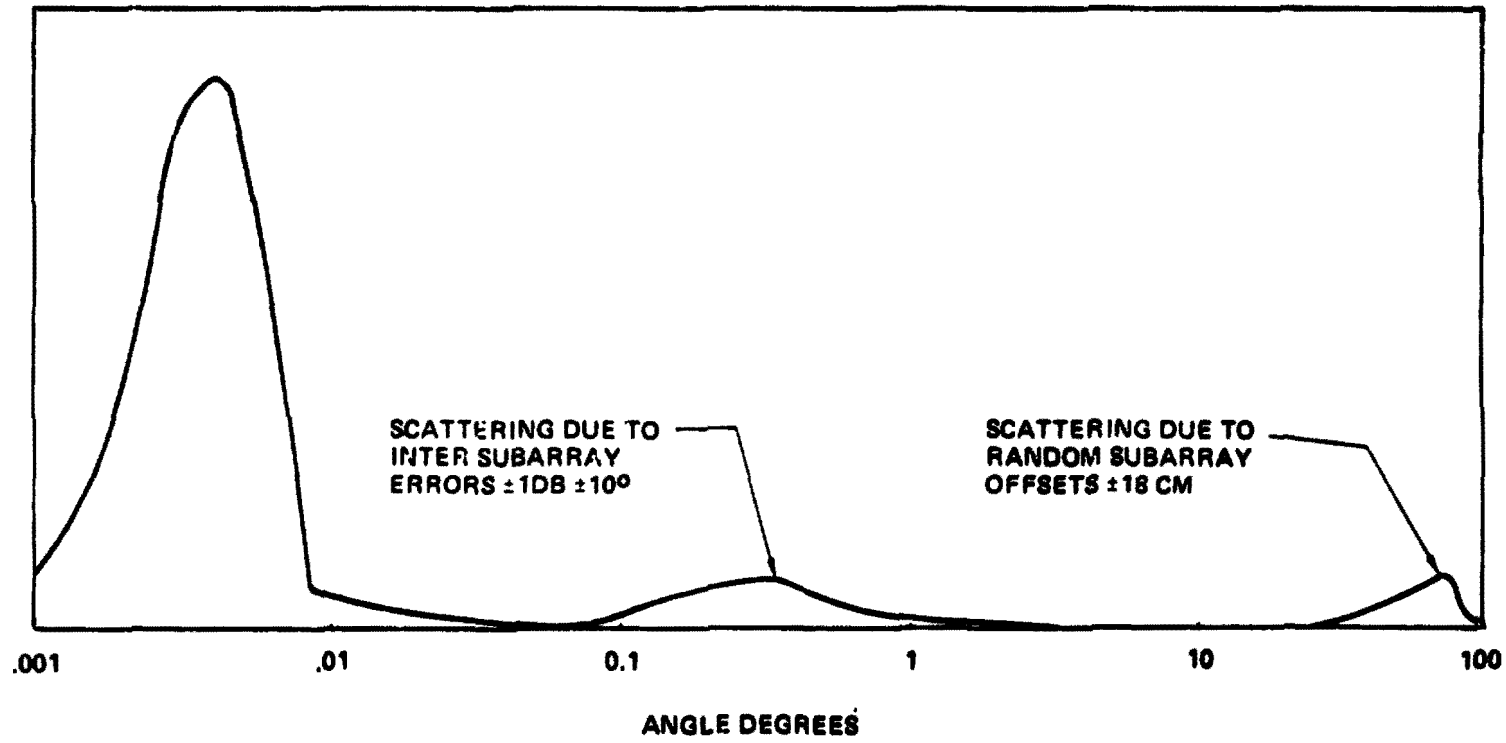
D160-22876-7

Total Radiated Power vs. Angle



SPS-1648

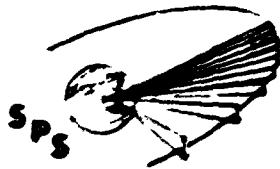
BOEING



D180-22876-7

**COMPARISON OF 10 DB GAUSSIAN DISTRIBUTION FUNCTIONS
AND THEIR FAR FIELD POWER DISTRIBUTIONS**

Power quantization from subarray to subarray is used to approximate the desired continuous 10 db Gaussian aperture distribution. In order to check the pattern sensitivity to quantization step size, quantization values were varied as shown on the figure. The secondary radiation patterns were calculated and examined for comparative beamwidth and side lobe level. As can be seen, the variations are negligible.

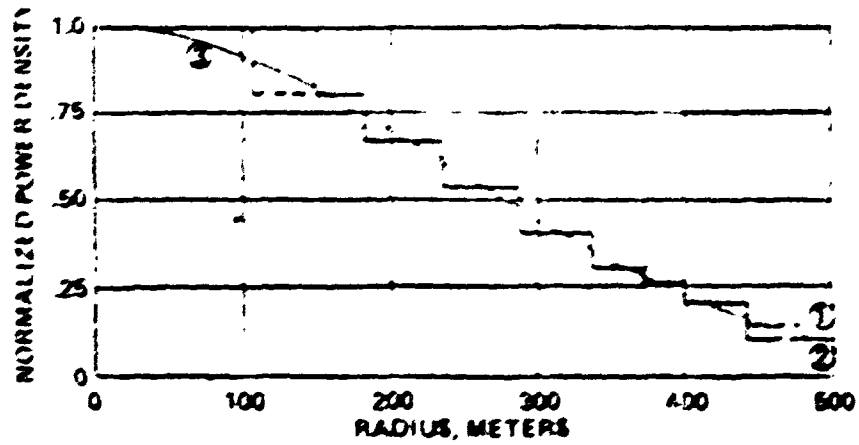


D1180-22876-7

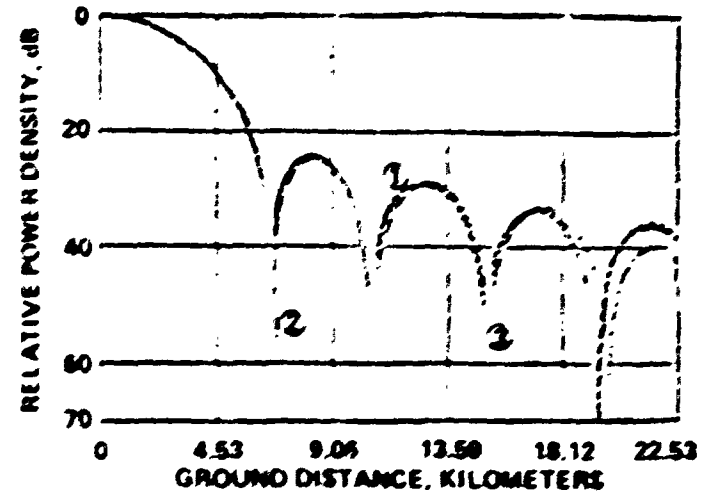
MPTS - Reference 10 dB Taper

DPL-1211

BOEING



(A) TRANSMITTER DISTRIBUTION FUNCTIONS



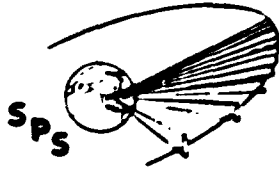
(B) FAR FIELD GROUND DISTRIBUTION

D180-22876-7

QUANTIZED ENHANCED SPACETENNA CONFIGURATION

In an attempt to improve the system efficiency and minimize any increase in spacetenna size, the concept shown is being investigated. Here the area of the aperture is increased only in selected locations (tabs are added). At present, an analytical evaluation is being conducted (BIGMAIN) to determine the appropriate aperture taper for optimum efficiency.

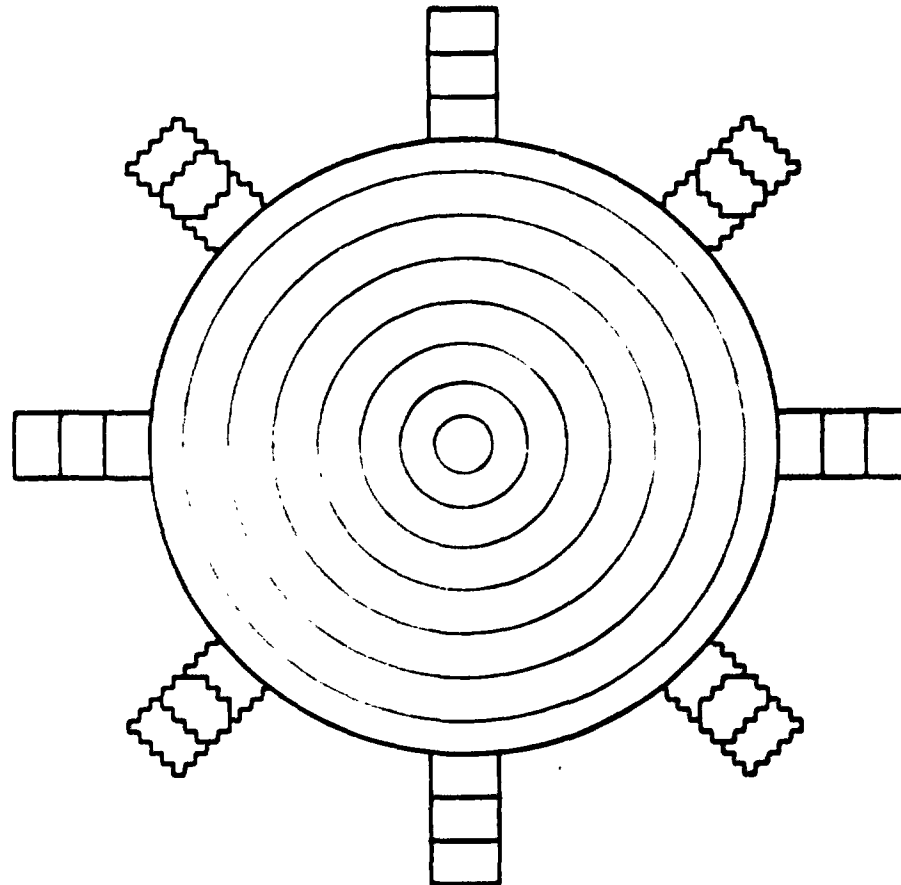
D180-22876-7



Quantized Enhanced Spacetenna Configuration

SPS 1690

BOEING



ALTERNATE CONCEPTS

Promising alternate candidates for the radiating elements of the space borne transmitter

- o Cylindrical Lens Horn Array
- o Traveling Wave End Fire Array
- o Enhanced Slot Element

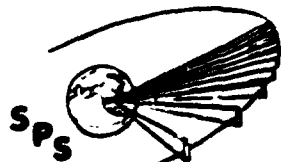
The lensed horn exhibits extremely high efficiency as a result of the lens in the horn aperture.

The traveling wave end fire array provides an open structure which is thermally transparent.

Using enhancing elements on each of the radiating slots in a planar array reduces mutual coupling and consequently losses due to edge effects. Although promising, structural complexity or increased mass have reinforced the selection of the slotted waveguide for the reference design for this phase of the study.

D180-22876-7

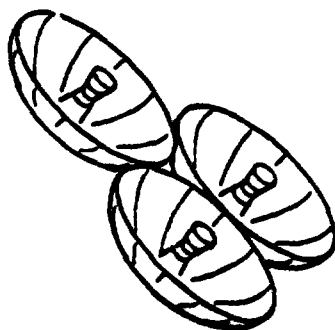
Alternate Array Candidates



SPS-1045

BOEING

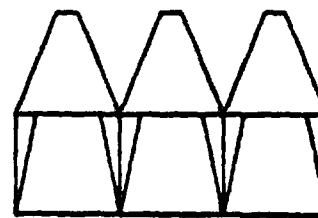
DEPLOYABLE PARABOLIC ARRAY



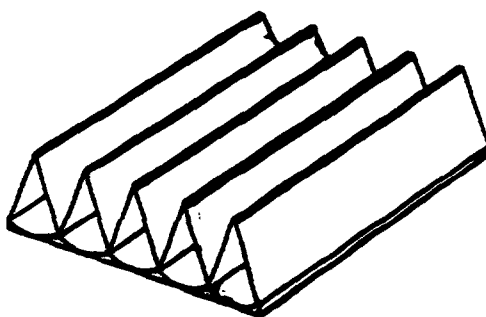
UNFURLABLE GORE TYPE PARABOLIC ARRAY



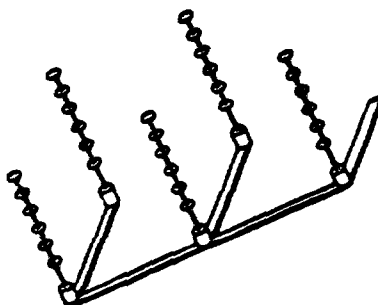
HORN ARRAY



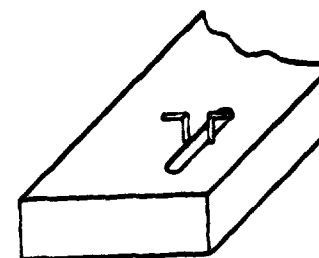
CYLINDRICAL LENS



TRAVELING WAVE END FIRE ARRAY



SLOT-DIPOLE ELEMENT

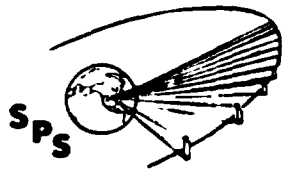


INPUT IMPEDANCE OF STANDING WAVE STICKS WITH 5 RESONANT SERIES SLOTS

The effect of stick length and slot spacing variation was approached from the standpoint of mismatch for the broadside resonant array. This is predominantly an impedance effect, the deviation of slot spacing from $\lambda_g/2$ due to lengthening of the entire stick or change of guide wavelength are primarily to build up the VSWR at the feed point of the stick. This is illustrated for a string of five series slots each deviating by $0.01\lambda_g$ from the resonant spacing of $\lambda_g/2$. From the Smith chart it can be seen that this deviation is equivalent to the introduction of a normalized susceptance of $B^i = .06$. The ratio of power delivered to that with the load matched can be written as a mismatch loss L_M

$$L_M = \frac{1}{2} (B^i)^2 = .02\%$$

where B^i = the total normalized susceptance introduced by all the slots.

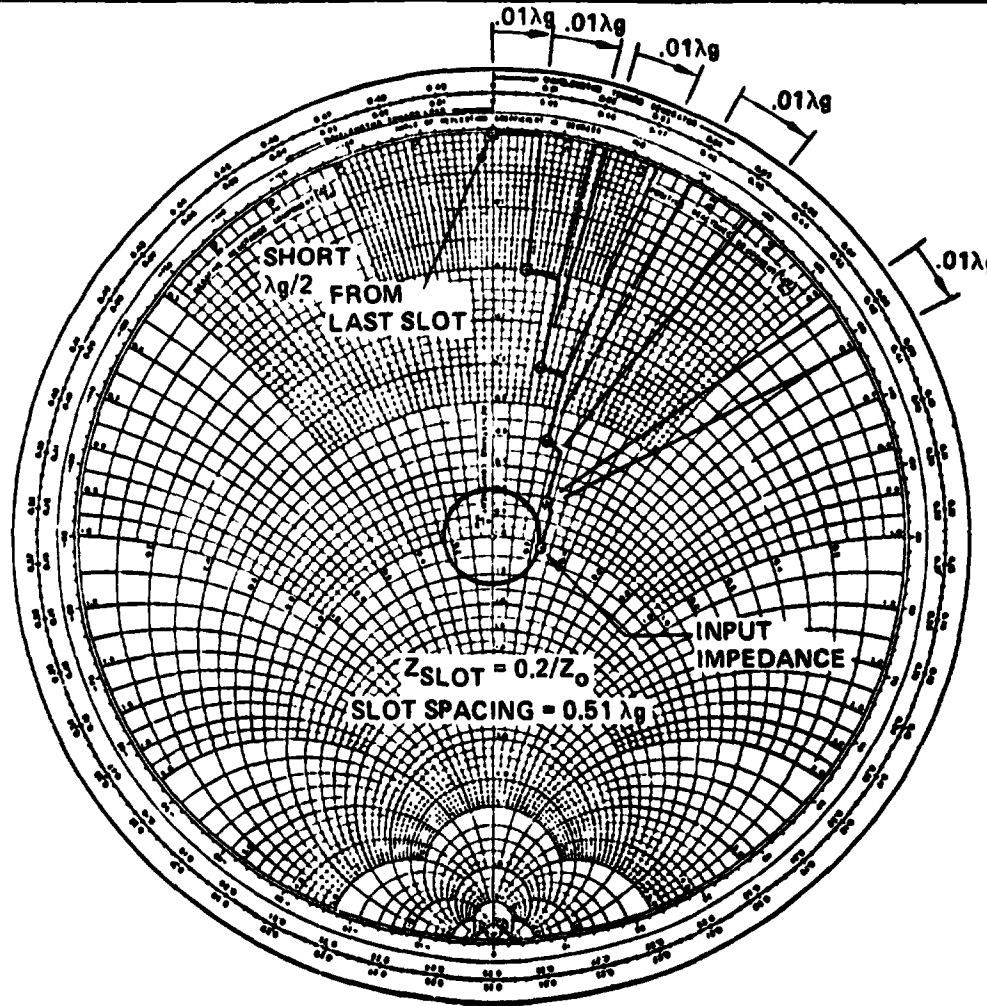


SPS-1688

D180-22876-7

Input Impedance of Standing Wave Stick with 5 Resonant Series Slots

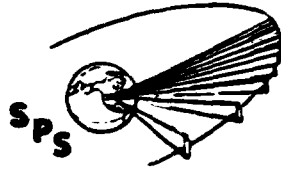
BOEING



PRECEDING PAGE BLANK NOT FILMED

SPS SUBARRAY LOSSES DUE TO DIMENSIONAL TOLERANCES

Because of manufacturing tolerances and thermal distortions, waveguide size as well as slot shape and position will be displaced from theoretical. These dimensional changes will produce unwanted scattering and impedance mismatch resulting in a reduction in efficiency. Factors affecting the losses in the Spacetenna were studied for a set of given manufacturing and control tolerances. These were found to produce non-dissipative power losses of 1.87% and dissipative power losses of 1.5% for Aluminum plated waveguide 9.09 x 6 cm I.D. Thermal effects were found to be negligible if composite waveguide was used. A number of factors including tolerance in the feeder guide from the klystrons and beam squint due to stick errors were found to produce negligible power losses.



SPS-1643

SPS Subarray Losses Due To Dimensional Tolerances

BOEING

<u>DIMENSION</u>	<u>TOLERANCE</u>	<u>EFFECT</u>	<u>MAIN BEAM POWER DEGRADATION</u>
SUBARRAY SURFACE	±50 MILS RMS	SCATTERING FROM PHASE VARIANCE	0.50% (1)
TILT OF SUBARRAY	0.1" AVERAGE	SUBARRAY PATTERN GAIN REDUCTION	0.50% (1)
GAP BETWEEN SUBARRAYS	±.25" AVERAGE	ARRAY FILLING LOSS (~ AREA LOSS)	0.13%
STICK LENGTH	±30 MILS	MISMATCH LOSS	0.02% (2)
WIDTH	±3 MILS	MISMATCH LOSS	0.12
CROSS GUIDE LENGTH	±30 MILS	MISMATCH LOSS	0.02% (2)
WIDTH	±3 MILS	MISMATCH LOSS	0.03%
SLOT OFFSET	±0.5 MILS	SCATTERING FROM AMPLITUDE VARIANCE	0.55% (4)
		TOTAL	1.87%

LEGEND: ALL LOSSES ARE ADDITIVE.

(1) INDEPENDENT OF SUBARRAY SIZE.

(2) INDEPENDENT OF STICK LENGTH.

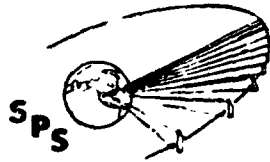
(3) REFERRED

(3) REFERRED TO AVERAGE STICK LENGTH OF $16.7 \lambda_g = 2.76$ METERS.

(4) ASSUMES MEAN SLOT OFFSET ERROR IS ZERO.

EFFECT OF DC-DC CONVERTER FAILURE

The "Bigman" computer program was exercised to provide estimates of performance degradation due to the failure of one DC-DC converter which supplies processed power to 420 Klystrons, each 70 KW RF. The results indicate an antenna efficiency degradation of roughly 0.4 to 0.5 percent and an increase in first sidelobe level of about 0.1 to 0.3 db depending on the location of the disabled converter. The total power loss thus approaches 0.9 percent, since additional disconnected RF power is added to the reduced array efficiency.



D180-22876-7

DIS 1640

BOEING

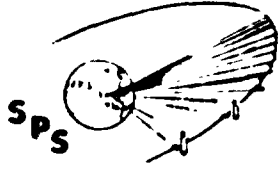
RF Transmitter

PRECEDING PAGE BLANK NOT FILMED

METHODS OF FOCUSING KLYSTRON BEAM

Conventional methods of focusing high power cw klystrons utilize an external electromagnet which usually weighs several times the tube weight. By designing the tube in a manner so that the solenoid can be wound directly on the tube and by selecting its OD to optimize the solenoid mass and power relationships, a low risk baseline design was arrived at having the highest probability of good efficiency. Alternate permanent Magnet (PM) and Periodic Permanent Magnet (PPM) schemes offer potential of some light weighting and elimination of solenoid power. These have not as yet been reduced to practice on high power CW tubes but merit additional consideration within the SPS time frame.

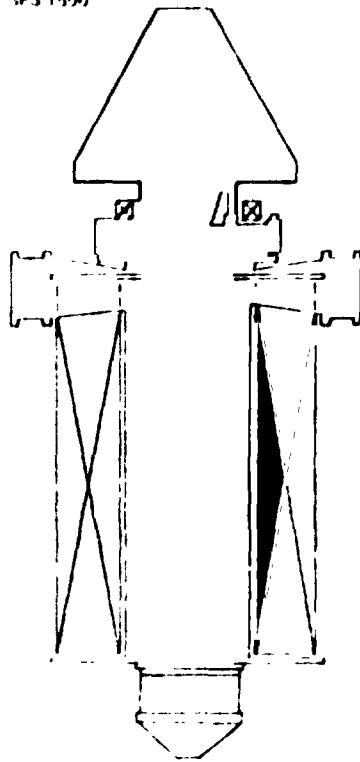
ORIGINAL PAGE IS
OF POOR QUALITY



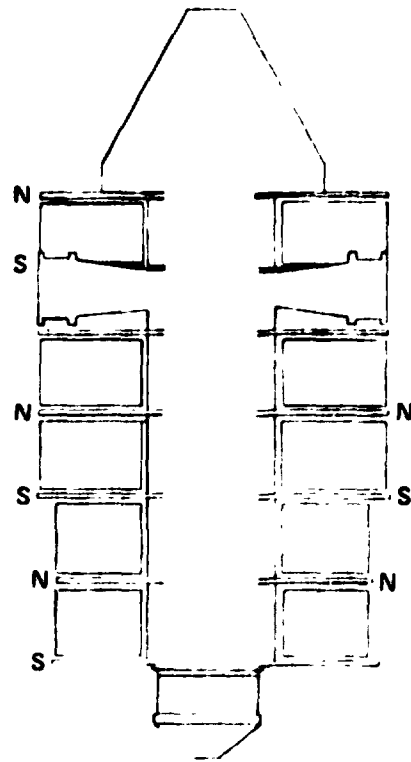
Methods of Focusing Klystron Beam

BOEING

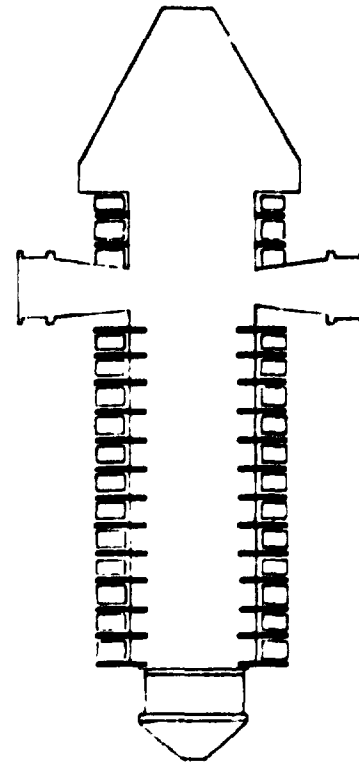
SPS 1590



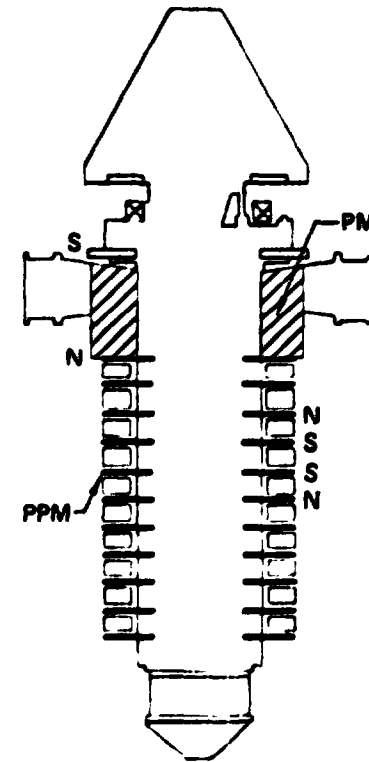
ELECTROMAGNETIC SOLENOID



MULTIPLE POLE EM



PPM

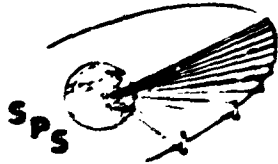


PM/PPM

BASELINE KLYSTRON DESIGN (70 KW)

The baseline design was arrived at on the following criteria:

- o Power level of 70 kw compatible with a maximum voltage of 42 kv and a perveance ($I_0/V_0^{3/2}$) of 0.25×10^{-6} , resulting in high efficiency.
- o RF Design. Single second harmonic bunching cavity resulting in short interaction length. 6 cavity design to give 40 db gain i.e., feasibility of solid state driver tube.
- o Focusing. Body-wound lightweight solenoid for low risk high efficiency approach.
- o Cathode: Coated powder or metal matrix medium convergence cathode to obtain an emission of $< 200 \text{ ma/cm}^2$ for 30 year life to emission wearout
- o Thermal Design. Heat pipe with passive radiators to obtain the desired CW level with conservative heat dissipation ratings.
- o Auxiliary Protection. Modulating anode to provide rapid protection shut off capability at the individual tube level, hopefully obviating the need for crow-bar type of turn-off

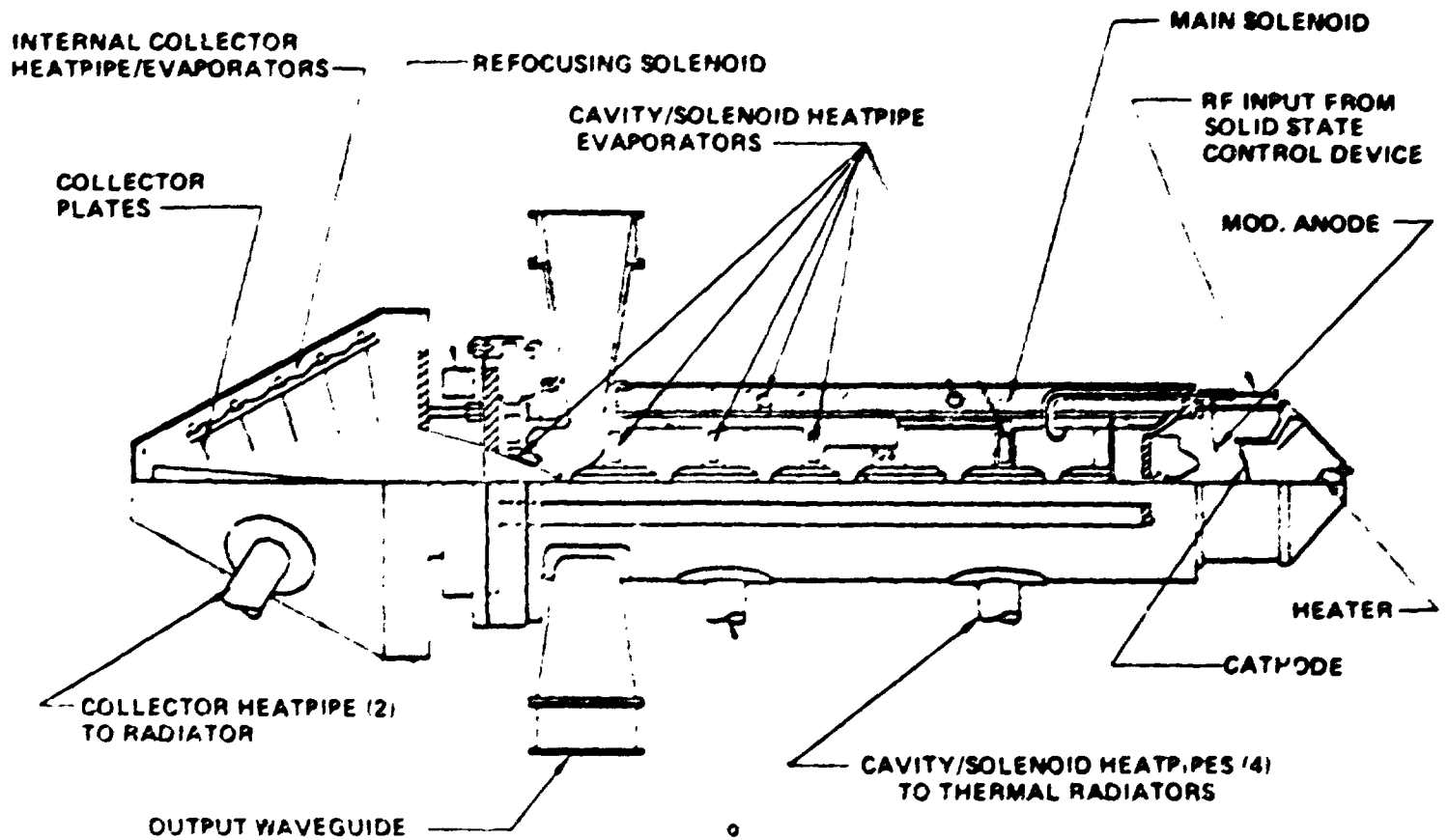


D140-22876-7

70 Kw Klystron

BOEING

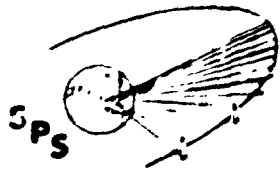
SPS 1564



D180-22876-7

ESTIMATED EFFECT OF COLLECTOR DEPRESSION

The relationships between klystron parameters required to optimize efficiency are shown. Although it is relatively easy to increase the overall efficiency from say 50 to 65% using a 3-stage depressed collector with a collector energy recovery of about 70%, the task of obtaining an 85% efficient klystron will likely require the use of a 5-stage collector. With an undepressed efficiency of 74% and a collector recovery of 50% a net efficiency of 85% would be realized. The design parameters for a 70 kw klystron, based on Equation (1), support this estimate.

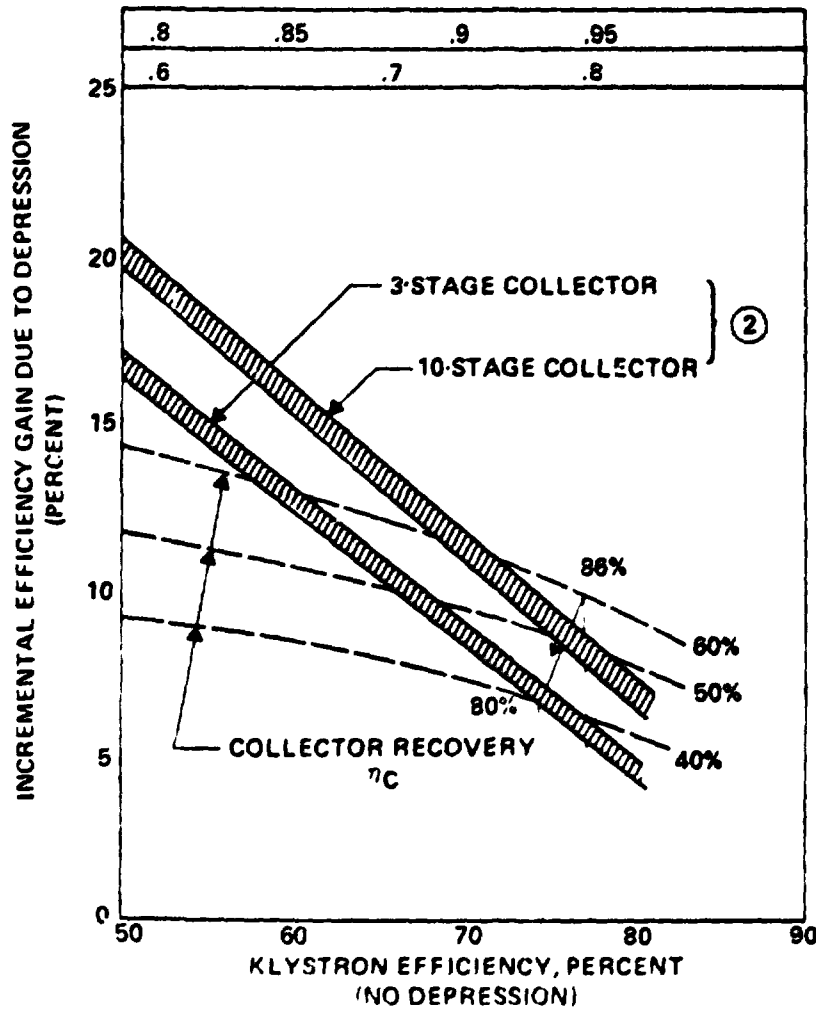


D180-22876-7

Estimated Effect of Collector Depression

SI'S 1587

BRIND



CIRCUIT EFFICIENCY, η_{CCT}
ELECTRONIC EFFICIENCY, η_e } ①

LEGEND:

① DESIGN VALUES BASED ON EXPERIENCE

$$\text{AND } \eta = \frac{\eta_{CCT} \eta_e}{1 - \eta_c (1 - \eta_e)}$$

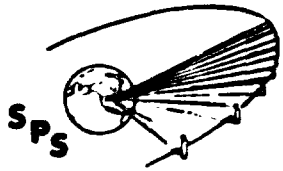
② INFERED VALUES PROJECTED FROM LOW EFFICIENCY TUBES
③ KLYSTRON EFFICIENCY (EXCL. SOLENOID)

INFERED FROM CHART	CALCULATED FROM 1
80 TO 86%	79 TO 85%

PROJECTED LIFE OF THERMIONIC CATHODES

Assurance of 30 year r.f. transmitter life will require continued testing and assessment to provide a credible data base from which to select either a cold cathode or a thermionic cathode operation. High secondary emission cold cathodes (Beryllium Oxide) have best known life of 18,000 hours and require oxygen replenishment. Best platinum cathode data is currently 10,000 hours at 5 GHz. Best thermionic cathode life data on the Intelsat transmitter TWTs and BMFWs is over 50,000 hours and cathode wearout due to emission can be designed to be 30 years with conservative current density. The candidate thermionic cathodes are proven oxide cathode operating below 900°C and Tungsten matrix cathodes at slightly over 1000°C. Actual cathode testing should be conducted in a realistic cathode-tube environment, not just a test diode. The SPS tube parameters are compatible with conservative cathode ratings with a cathode to beam convergence of less than 50.

To avoid excessive infant mortality, a burn-in period is recommended, which may be possible in space. The question of open envelope operation requires further assessment of space contaminants and can offer significant cost reduction if realizable.

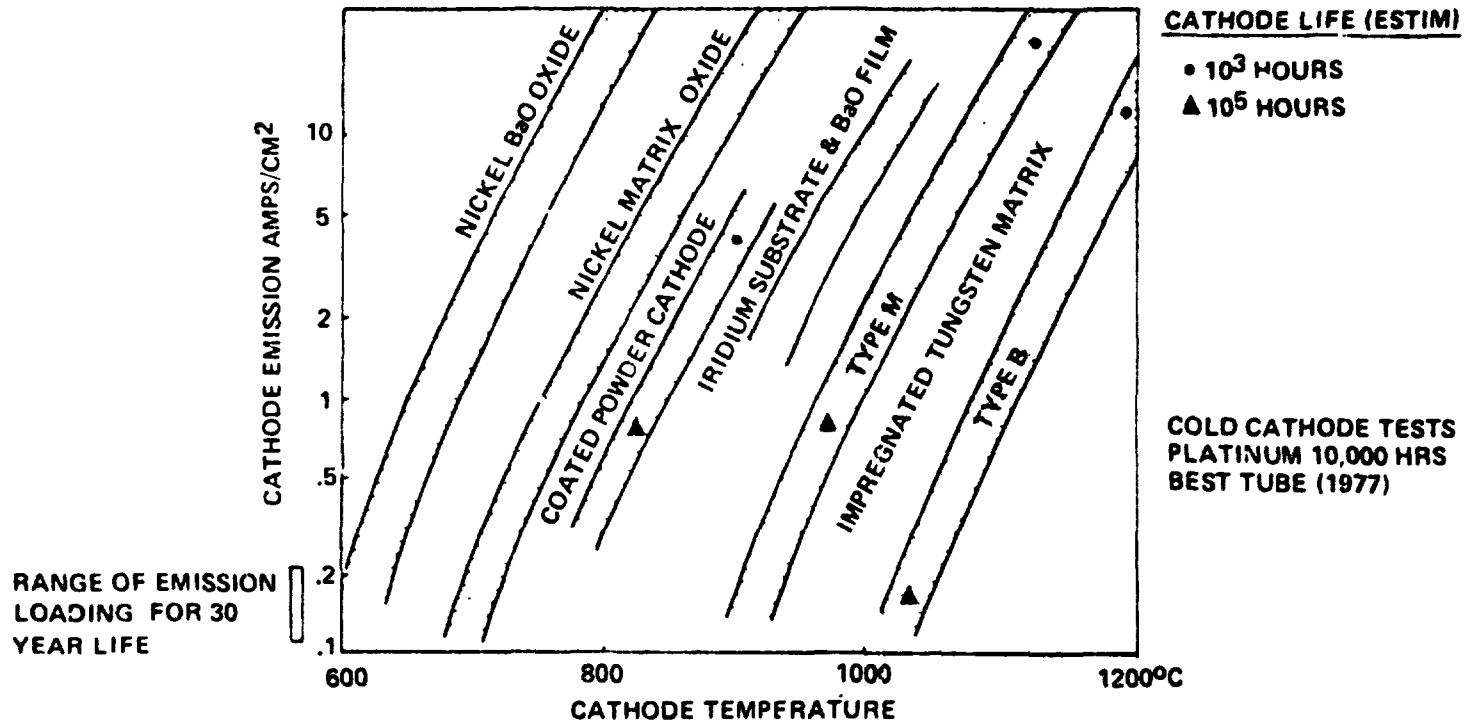


D180-22876-7

Cathode Emission Data

SPC-1585

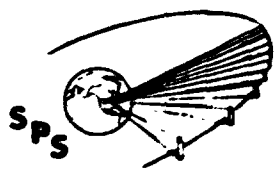
BOEING



KLYSTRON PROTECTIVE DEVICES

To assure reliable operation, hopefully in absence of a crowbar circuit, several features are proposed for incorporation into the klystron design and external circuit monitoring. These include:

- o Modulating anode which provides rapid shut-off feature should r.f. drive fail, or tube shut down in case of body or cathode-to-modulating anode arcing.
- o Arc detector in the output waveguide to shut off r.f. drive.
- o Body current monitors to assess cathode performance as a function of time.
- o Collector current monitors as possible indicators of internal arcing.

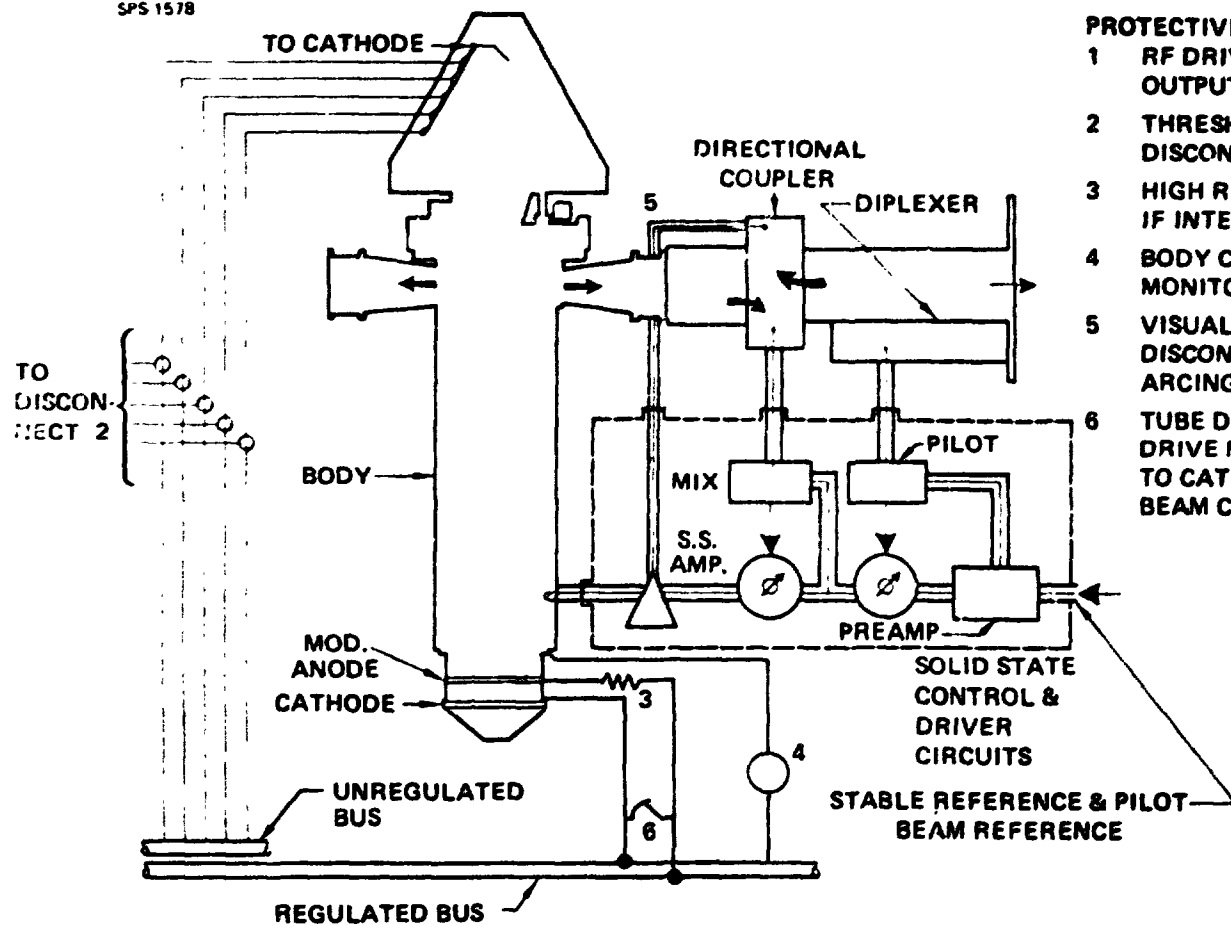


D180-22876-7

Klystron Protective Devices

SPS 1578

BOEING

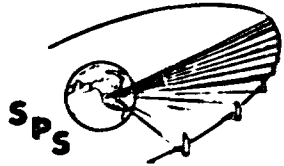


PROTECTIVE FEATURES

- 1 RF DRIVE SHUT OFF WITH OUTPUT WAVEGUIDE ARCING
- 2 THRESHOLD CURRENT DETECTORS DISCONNECT IF INTERNAL ARCING
- 3 HIGH RESISTANCE ARC QUENCHING IF INTERNAL ARCING
- 4 BODY CURRENT METER MONITORS CATHODE EMISSION
- 5 VISUAL ARC DETECTOR DISCONNECTS TUBE IF EXTERNAL ARCING
- 6 TUBE DISCONNECT DRIVE MOD ANODE VOLTAGE TO CATHODE—REMOVES BEAM CURRENT

SPECIFIC WEIGHT OF MICROWAVE TRANSMITTERS

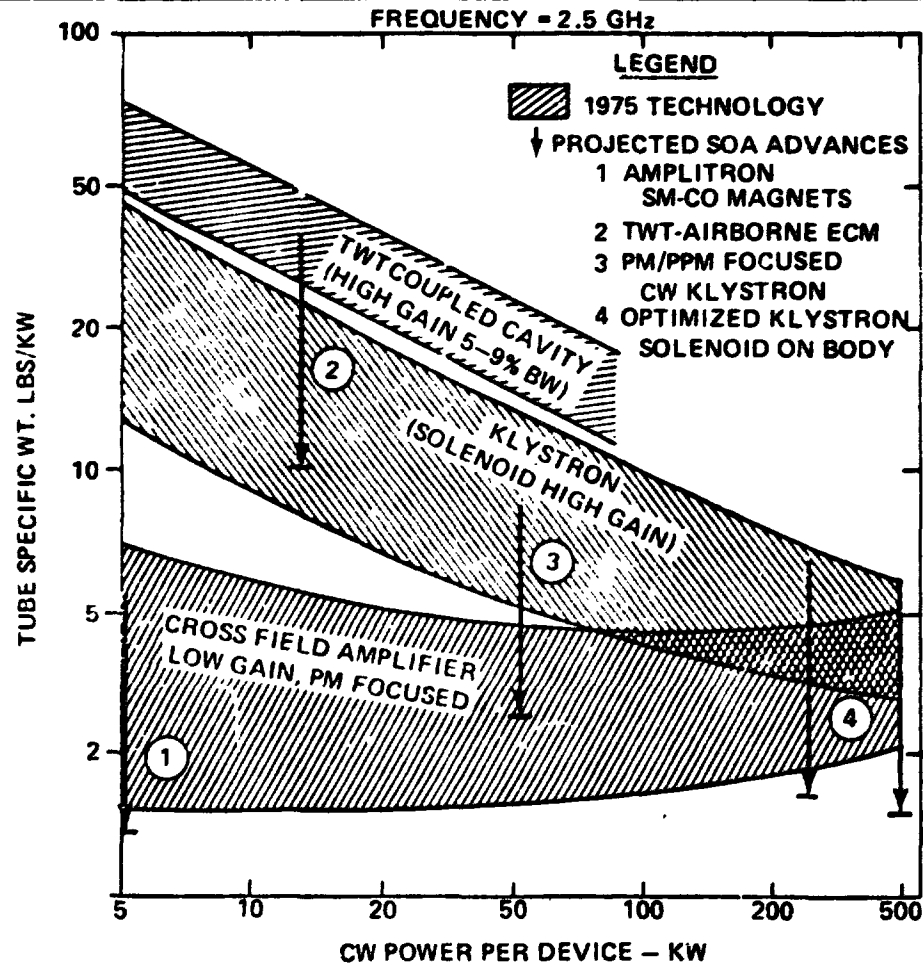
Specific weights of commercially available C W. transmitters vary over a large range of parameters. Crossed field services such as the amplitron, due to their compact interaction region are clearly superior in the regime below 100 kw CW. Broadband devices, such as the helix and coupled cavity TWT have never been optimized for low specific weight and are not directly applicable to SPS where the advantage of narrow bandwidth can be utilized. Amplitrons, utilizing relatively recent Samarium Cobalt improvements in permanent magnet technology are projected to have specific weights of below 1 lb. per Kw. CW klystrons at the 100 Kw level with conventional solenoid focusing are typically 5-10 lb/Kw but with a solenoid wound directly on the tube can approach 2 lb per Kw and probably below that at higher powers. At the 50 Kw CW level, a klystron design can be conceived using combined PM/PPM focusing with a specific weight of about 1.5 lb/kw. The choice between an amplitron and klystron will have to be based on realizing the above values and on other system considerations such as efficiency, gain, antenna integration and reliability.



Specific Weight of Microwave Transmitters

BOEING

SPS-1583

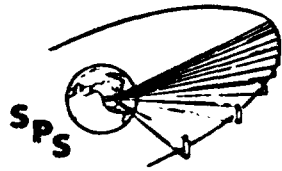


RF TRANSMITTER ACQUISITION COST

The attached chart points out the importance of proper power level selection to optimize r.f. transmitter acquisition and replacement cost. The indicated cost is based on the following estimated tube costs and MTBF's.

Tube Type	Power	Cost	MTBF (Years)	
			(1)	(2)
Amplitron	5KW	\$ 100	30	15
Klystron	50	2700	28	14
	250	6000	24	12
	500	7500	20	10

Cost of transportation to space is \$60/kg. Passive cooling is assumed. Other system factors such as efficiency, gain differential, maintenance cost and x-ray environment are not included. The analysis indicates that the higher power level klystrons are competitive with amplitrons on this basis and other system parameters will influence the ultimate transmitter selection.

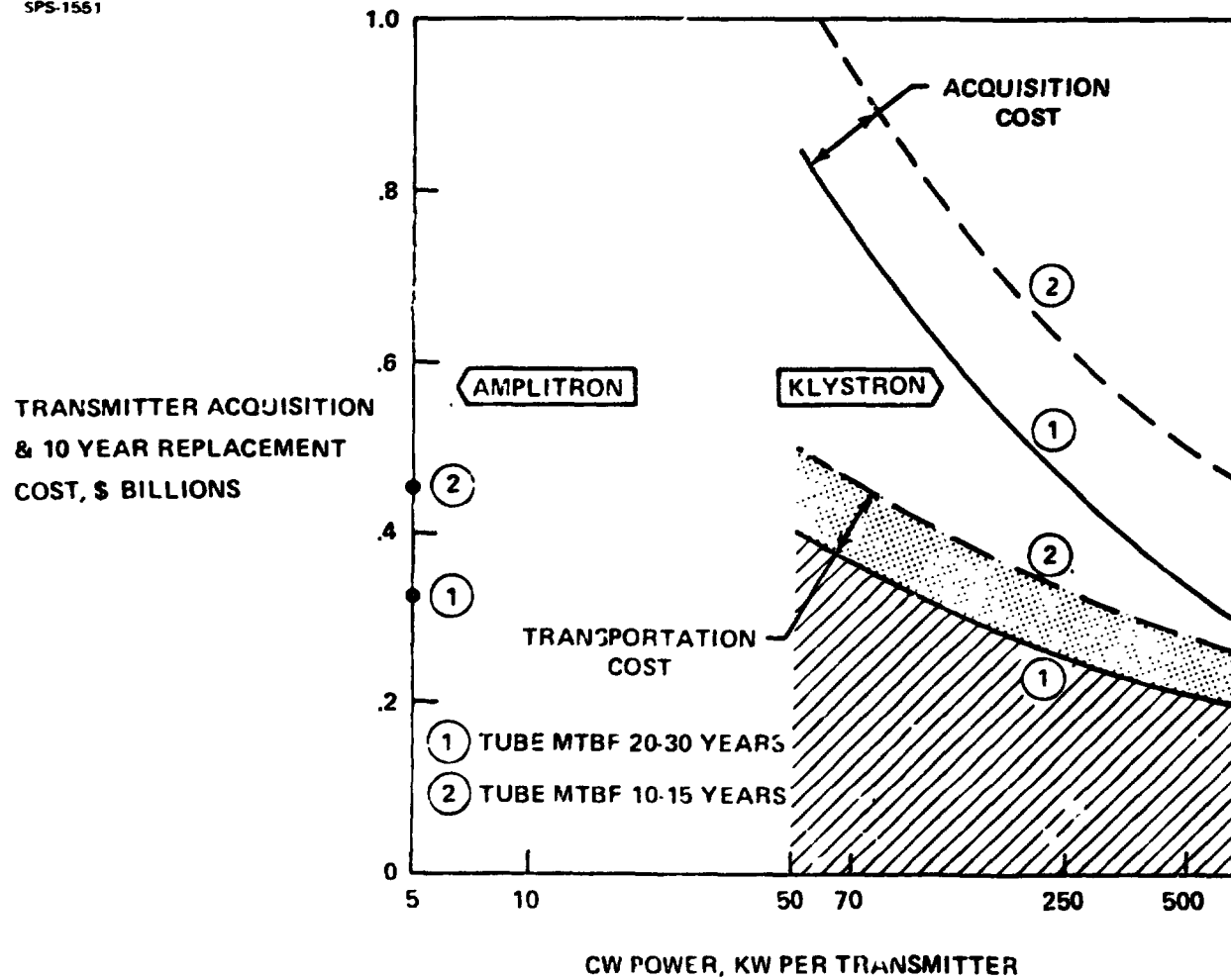


D180-22876-7

RF Transmitter Acquisition Cost for 6 Gigawatt System

BOEING

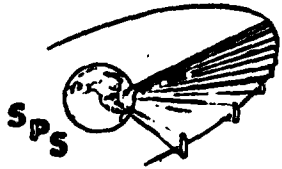
SPS-1551



D180-22876-7

MPTS POWER DISTRIBUTION SYSTEM BLOCK DIAGRAM

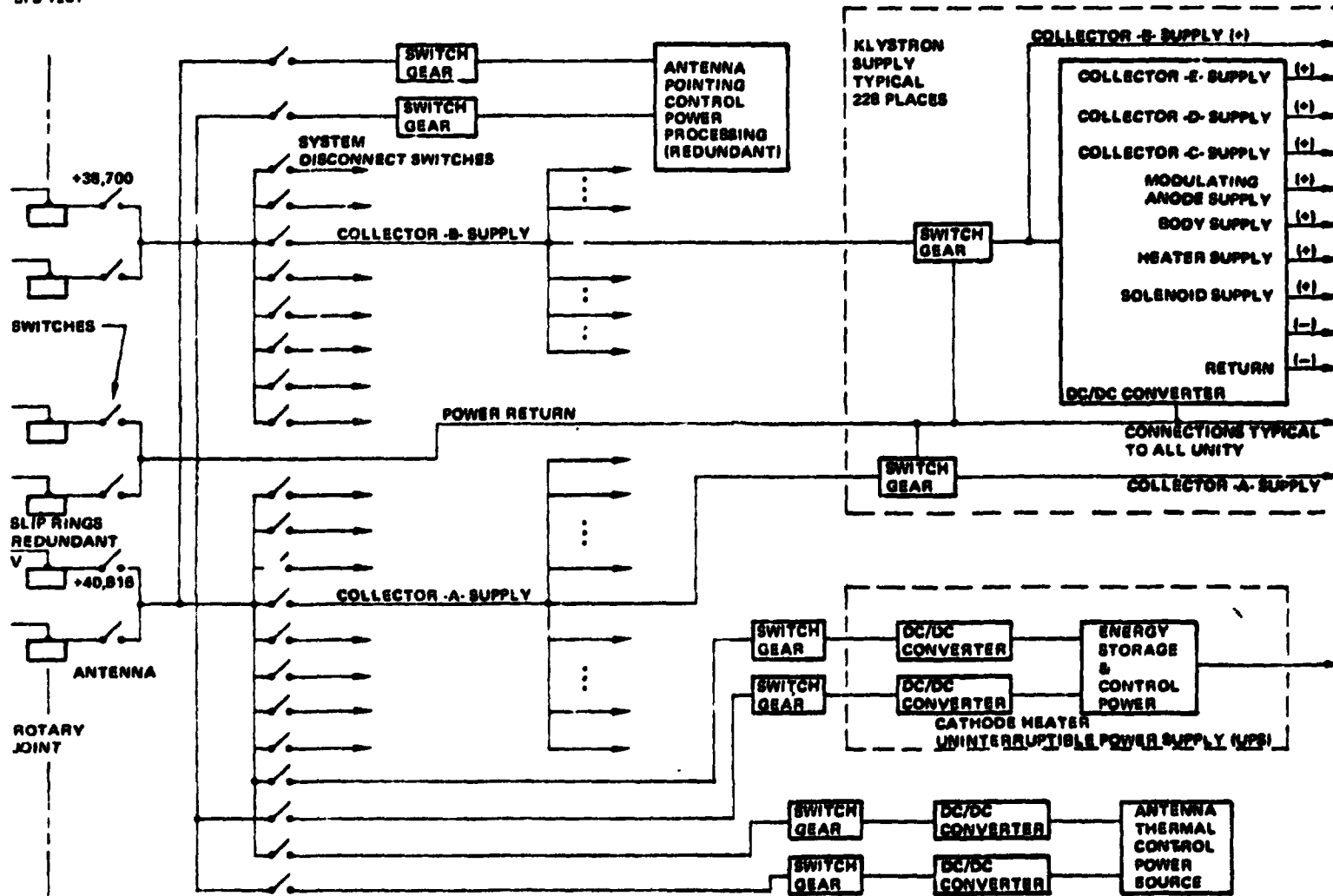
The MPTS power distribution system provides power transmission, conditioning, control, and storage for all MPTS elements. The antenna is divided into 228 power control sectors, each sector providing power to approximately 420 klystrons. The two klystron depressed collectors which require the majority of supplied power are provided with power directly from the power generation system to avoid the dc/dc conversion losses. All other klystron element power requirements are provided by the DC/DC converter. System disconnects are provided for isolation of equipment for repair and maintenance.



D180-22876-7

MPTS Power Distribution System Block Diagram

SPS-1201

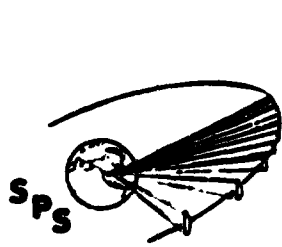


BEING

ORIGINAL PAGE IS
OF POOR QUALITY

MPTS CONDUCTOR DESIGN PROCEDURE

Aluminum sheet conductors were selected for routing power from the rotary joint to power sector control since they result in a minimum mass conductor system. For the conductor segment shown in the figures a conductor operating temperature can be selected which will minimize the satellite mass. A general case for selection of the optimum conductor temperature is shown in the figure. The conductor mass for the sheet conductors from the rotary joint to the power control substations was computed to be 270,577 kilograms with an I^2R loss of 145.5 megawatts for the entire antenna. The total mass which is attributable to the MPTS conductor system is the mass of the conductors plus the mass of the array required to compensate for the I^2R loss of the conductor system.



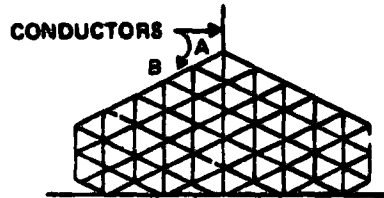
D180-22876-7

MPTS Conductor Design Procedure

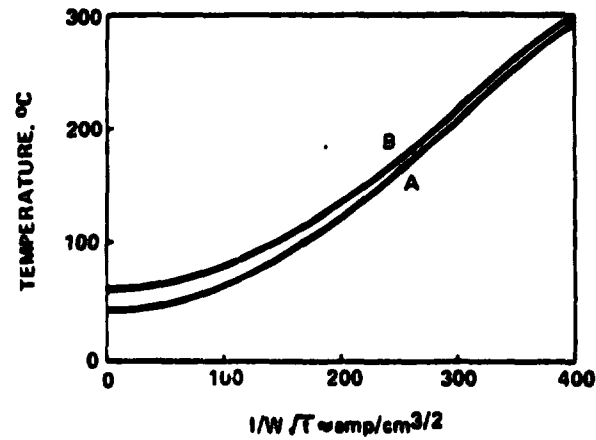
BOEING

SPS-1848

LOCATION & ROUTING

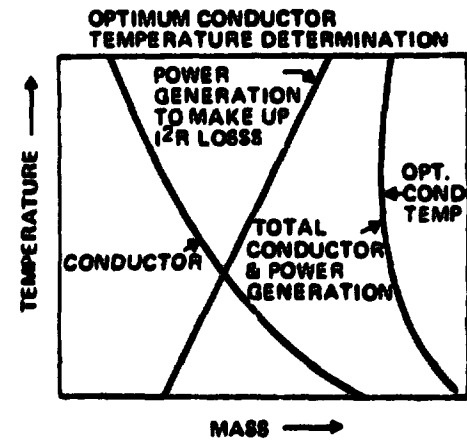


THERMAL ANALYSIS



FLAT ALUMINUM CONDUCTOR DIMENSIONS T & W

MASS OPTIMIZATION

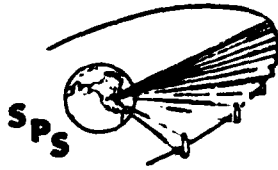


COMPARISON OF POWER DISTRIBUTION CONDUCTOR MASS

For a given d.c. power level at the r.f. transmitter, serious consideration must be given to the distribution voltage, not only on the basis of LEO/GEO plasma effects or nearby X-ray levels, but on the basis of I^2R losses within the satellite distribution network, as they are impacted by the conductor size/mass selection. The I^2R loss must be compensated by additional (photovoltaic) power generation capacity (@ 3.15 kg/kw), and if processed power is required, with redundant active thermal control (@ 14.5 kg/kw of thermal heat dissipated, with 96% efficient dc-dc converters).

The attached chart shows the result of an optimization for two types of distribution systems using flat aluminum conductors. It clearly shows that high current unprocessed power requirements can result in a large conductor mass penalty. This factor is of sufficient impact to warrant inclusion in any meaningful r.f. transmitter comparison.

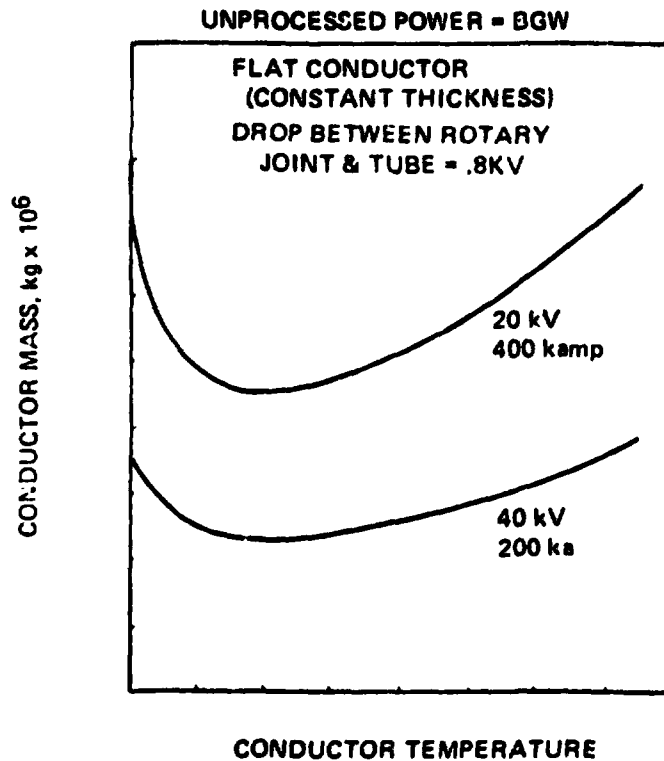
ORIGINAL PAGE IS
OF POOR QUALITY



Comparison of Power Distribution Conductor Mass for 20 KV & 40 KV System

SPS-1541

BOEING



EXAMPLE

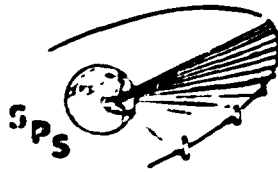
- **AMPLITRON @ 20 KV—UNPROCESSED POWER**
 OPTIMIZED CONDUCTOR MASS = $5.3 \times 10^6 \text{ kg}$
 I^2R LOSS = 12% = $3.75 \times 10^6 \text{ kg}$
 @3.15 kg/kW = $9.05 \times 10^6 \text{ kg}$

- **KLYSTRON @ 40 kV—15% PROCESSED POWER**
 OPTIMIZED CONDUCTOR MASS = $2.7 \times 10^6 \text{ kg}$
 WST OF PROCESSED POWER
 15% OF 4% THERMAL LOSS
 OF CONVERTER @ 14.5 kg/kW = $.71 \times 10^6$
 COST OF CONDUCTOR I^2R LOSS
 7.3% @ 3.15 kg/kW = 1.99×10^6
 = $5.3 \times 10^6 \text{ kg}$

- DIFFERENTIAL IS $75 \times 10^6 \text{ kg}$
 = 0.55 kg/kW RF

DC/DC CONVERTER OPTIMIZATION

The results of a DC/DC converter analysis, performed by the General Electric Company are shown in the figure. The total mass is composed of the DC/DC converter mass plus the mass of the radiator system required to cool the converter plus the additional satellite mass required to generate the power to compensate for converter electrical loss. The minimum total mass occurs at a converter switching frequency of approximately 20 kilohertz which corresponds to a converter specific mass of 1.0 kg/kw, and an efficiency of 96 percent. These values were used for the baseline MPTS power distribution system design.

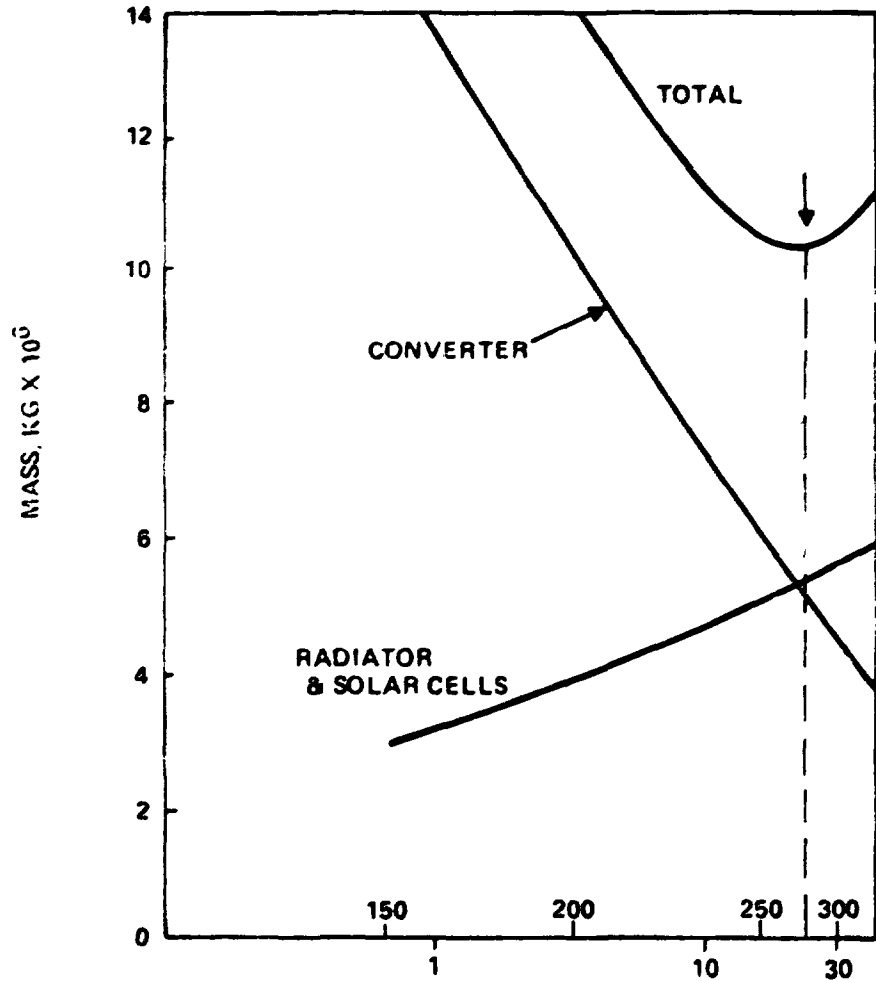


D180-22876-7

DC-DC Converter Optimization

BOEING

SPS 16-7



- RADIATOR MASS = 14.9 KG/KW (LOSSES)
- SOLAR CELL MASS = 3.15 KW/KW
- CONVERTER CHARACTERISTICS

FREQ KHZ	LOSSES KW	CONVERTER MASS KG	RADIATOR MASS KG
1	181	13,500	2,400
10	232	7,000	3,460
20	265	5,500	3,950
30	302	5,100	4,500

D180-22876-7

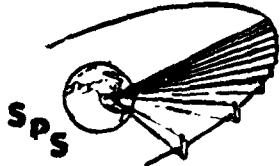
INTEGRATED KLYSTRON MODULE

An integrated klystron module, sized for installation near the center of the antenna, is shown. The major module components and their placement are noted.

This module configuration resulted in a very thin, 33 centimeter, subarray and is more conducive to earth fabrication, testing and transport to the antenna assembly location.

For this study, the subarray was the system LRU but with this type of structure, the module could be made the LRU with only slight modifications.

**ORIGINAL PAGE IS
OF POOR QUALITY**

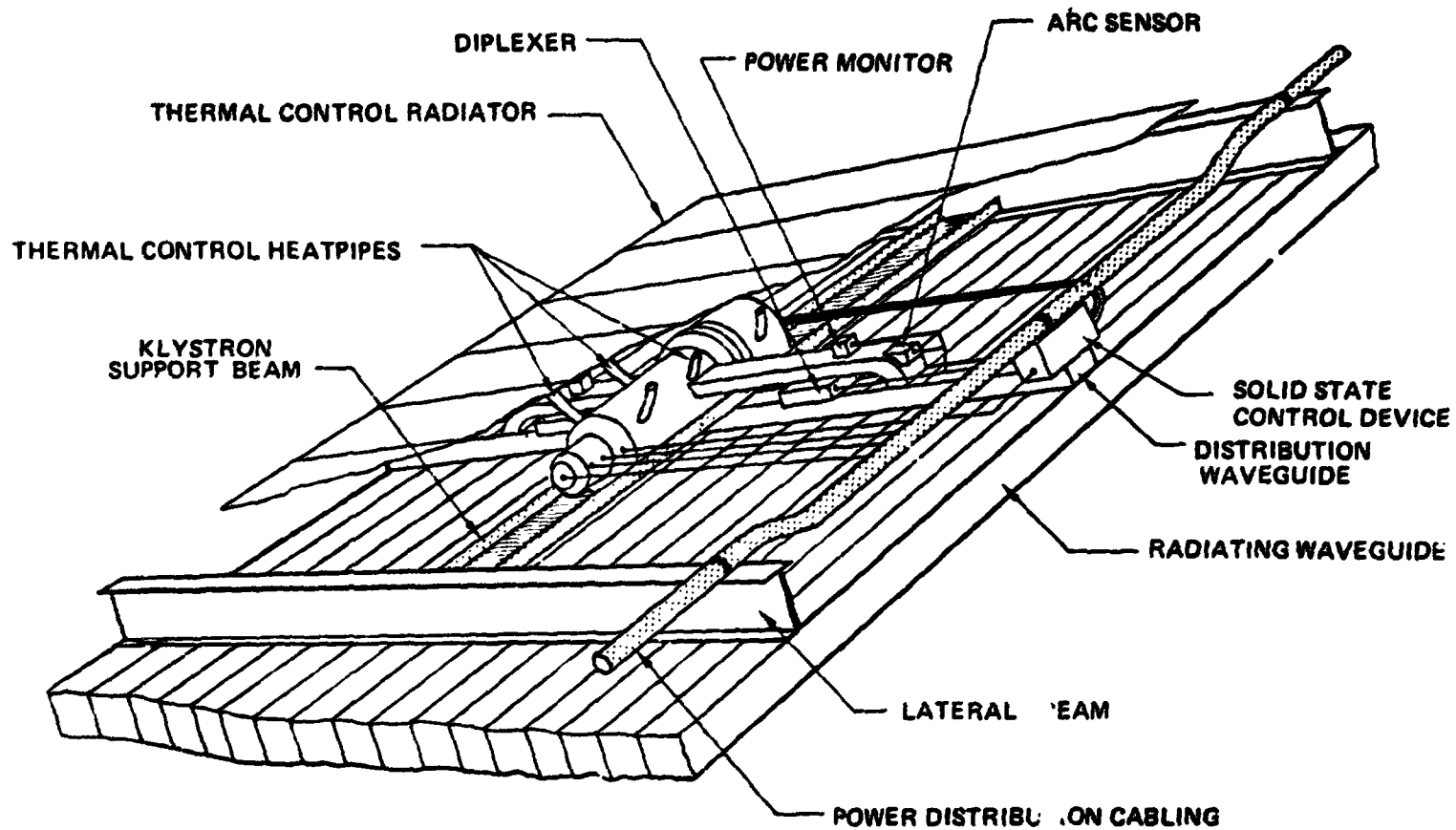


SPS-1576

D180-22876-7

Integrated Klystron Module

BOEING

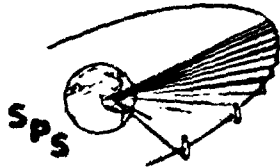


INTEGRATED SUBARRAY

An integrated subarray for the lowest power density near the spacetenna periphery is shown. This structural configuration shows where the module components are located and how the integral structure was achieved.

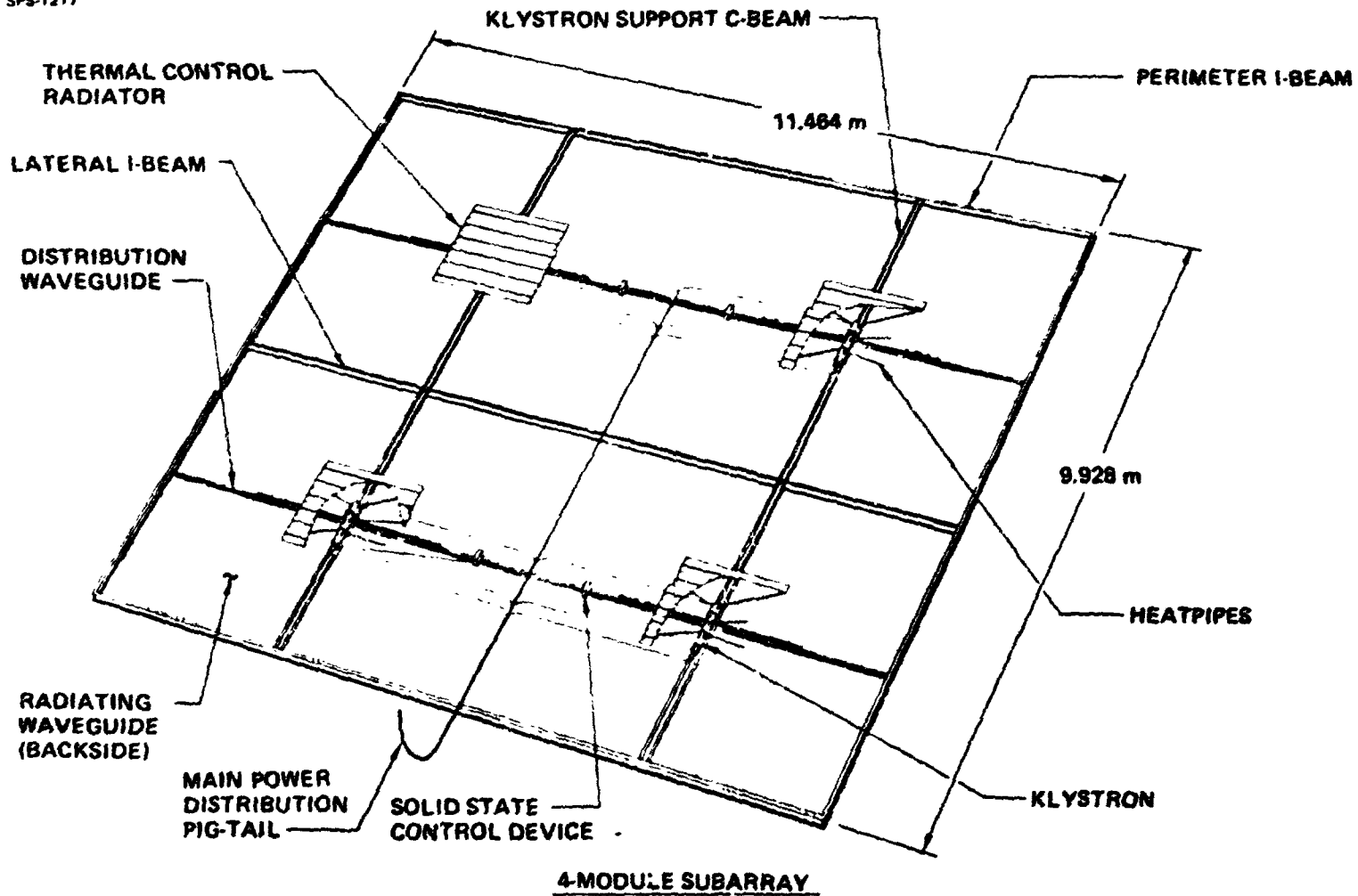
The structure supporting the klystron is designed to accept the variable number of modules per subarray necessary for output tapering. The same basic approach was used to lay out subarray structures and component locations for the other power densities.

Integrated Subarray



SPS-1217

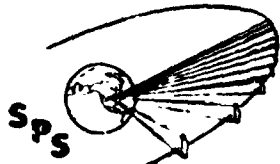
BOEING



POWER TAPER INTEGRATION

The actual integration of power density rings is illustrated on this view of one-fourth of the radiating face of the antenna. Listed for each step are the number of modules per subarray, the number of subarrays of that type and the number of klystrons in that step for one antenna.

To meet all of the design constraints shown previously, a power taper was achieved using the ten quantized steps available that would provide a ground output of 5.0 GW for a 1.00 kilometer diameter antenna with a 9.5 dB power density taper

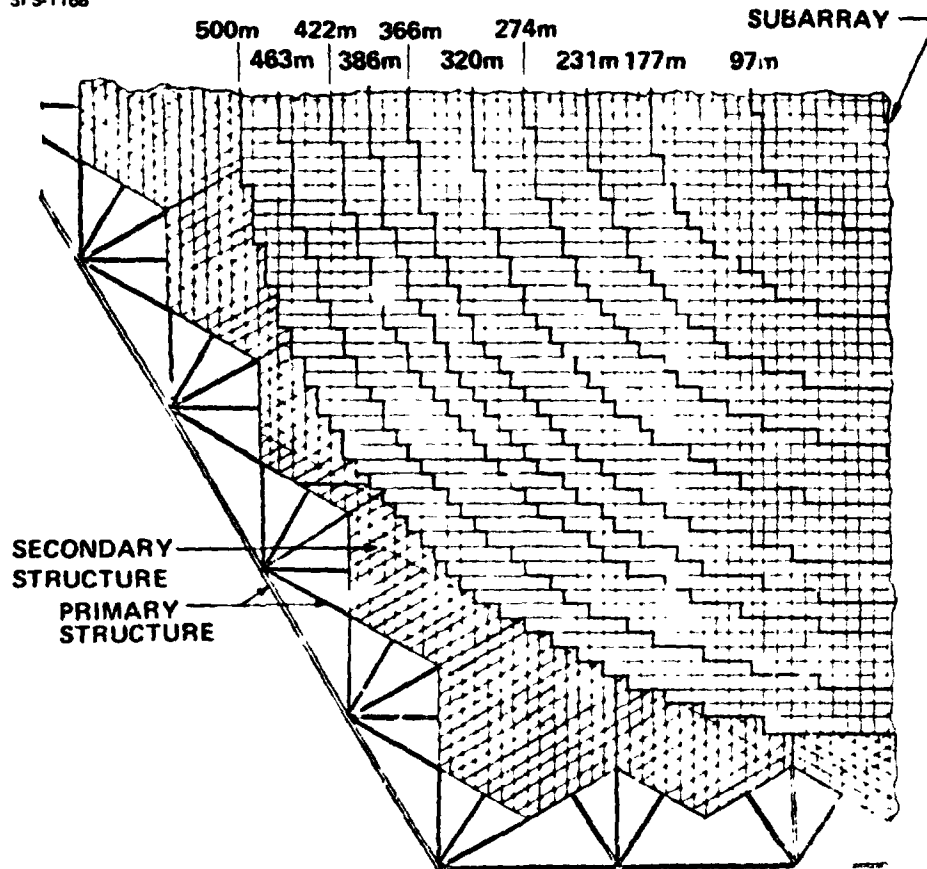


D180-22876-7

Power Taper Integration

BOEING

SPS-1168



STEP	NO. SUBARRAYS	NO. KLYSTRONS
1 @ 36	272	9792
2 @ 30	580	17420
3 @ 24	612	14688
4 @ 20	612	12240
5 @ 16	756	12096
6 @ 12	864	10368
7 @ 8	624	5652
8 @ 8	576	4608
9 @ 6	1032	6192
10 @ 4	1000	4000
TOTALS	6,932	97,056

POWER OUTPUT: (ANTENNA) 6.78 GW
(GROUND) 5.01 GW

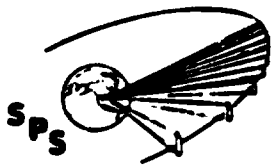
SPACETENN . STRUCTURAL CONCEPT

Primary Structure

The antenna primary structure is a tetrahedral planar truss and gives depth to the antenna for stiffness and stability. The primary structure supports the secondary structure, power distribution buses, power conditioning equipment, thermal control components and provides for antenna yoke attachment.

The primary structure is shown with secondary modules installed.

**ORIGINAL PAGE IS
OF POOR QUALITY**

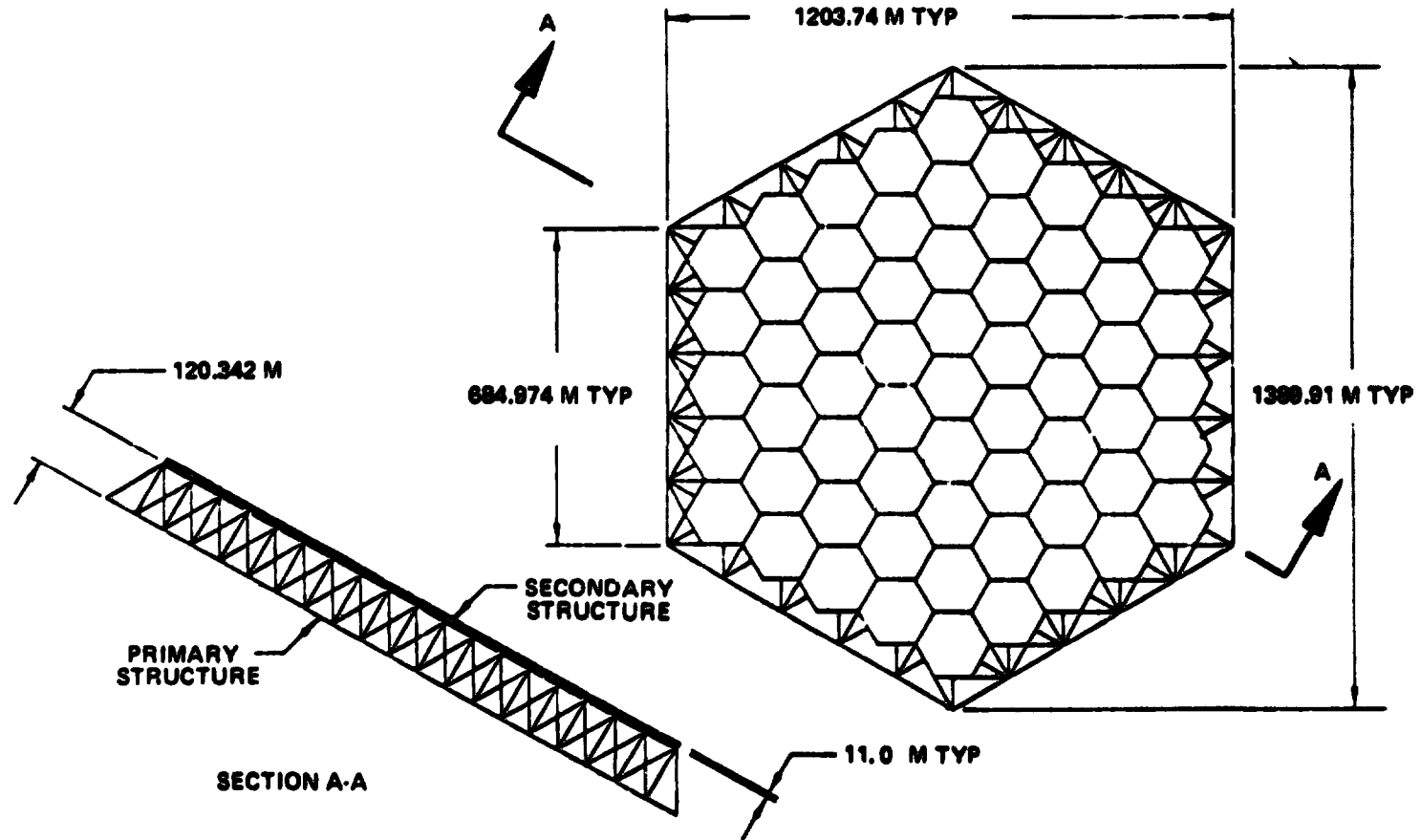


D180-22876-7

Primary Structure (Secondary Modules Shown)

SPS-1568

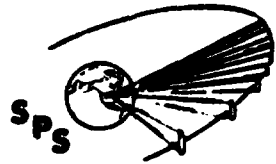
BOEING



D180-22876-7

SECONDARY TRUSS-MODULE

The antenna secondary structure, supporting the subarrays, is a tetrahedral planar truss. Individual modules may be built up in a planar fashion to form the planar radiating face of the antenna. Sixty-one of the hexagonal modules are arranged in five rings to complete the secondary structure.

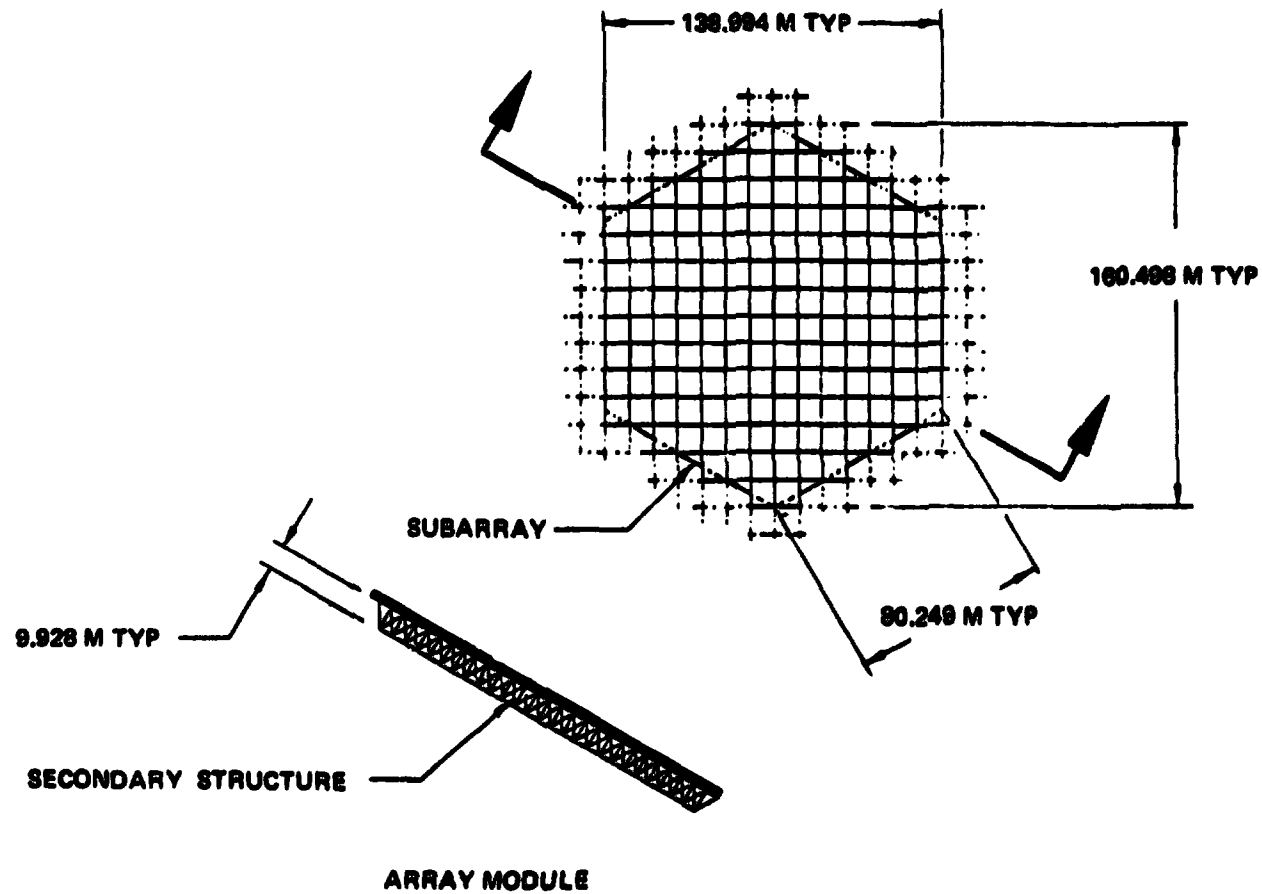


SPS-1666

D180-22876-7

Secondary Truss-Module (Subarrays Shown)

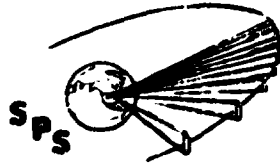
BOEING



MPTS MASS AND COST ESTIMATE

In order to obtain the desired power taper across the radiating aperture of the spaceteenna, the subarrays of which it is comprised must contain varying numbers of klystron modules. This chart depicts the estimates of mass and cost for the individual types of subarrays, the structure controls, power distribution system and command and control subsystem.

The antenna mass summary shown is significantly larger than previous mass estimates. The largest growth areas are power distribution (DC-DC converters including thermal control) and RF Generation (klystrons including thermal control).



D180-22876-7

Nominal MPTS Weight and Cost

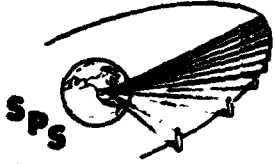
BOEING

SPS-1157

VIBS NUMBER		MASS (M.T.)	COST (10 ⁶ \$)
1.01.01.04	MPTS	13084	975.92
1.01.01.04.00	COMMON	3841	424.22
1.01.01.04.00.00	STRUCTURE	250.0	22.87
1.01.01.04.00.01	CONTROLS	(358)	62.51
1.01.01.04.00.02	POWER DISTR.	2933	230.21
1.01.01.04.00.03	COMM/DATA	(100)	108.64
1.01.01.04.01	TYPE 1 SUBARRAY	833.09	55.66
1.01.01.04.02	TYPE 2 SUBARRAY	1506.34	99.02
1.01.01.04.03	TYPE 3 SUBARRAY	1075.02	83.49
1.01.01.04.04	TYPE 4 SUBARRAY	1122.16	69.58
1.01.01.04.05	TYPE 5 SUBARRAY	1151.12	68.76
1.01.01.04.06	TYPE 6 SUBARRAY	1042.95	58.94
1.01.01.04.07	TYPE 7 SUBARRAY	613.57	32.13
1.01.01.04.08	TYPE 8 SUBARRAY	507.73	26.19
1.01.01.04.09	TYPE 9 SUBARRAY	750.55	35.20
1.01.01.04.10	TYPE 10 SUBARRAY	581.20	22.74

FOR 10 GW, 2 ANTENNAS, 26128 MT AND \$1951.8 x 10⁶

D180-22876-7



BEIND

Photovoltaic Conversion

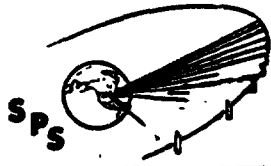
PRECEDING PAGE BLANK NOT FILMED

Photovoltaic Conversion

D180-22876-7

PHOTOVOLTAIC REFERENCE CONFIGURATION

This reference configuration represents the study starting point. Its size was based on the performance chain established during the JSC study and a ground output requirements of 10GW BOL.

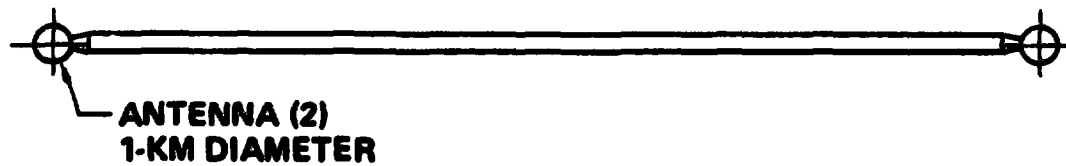
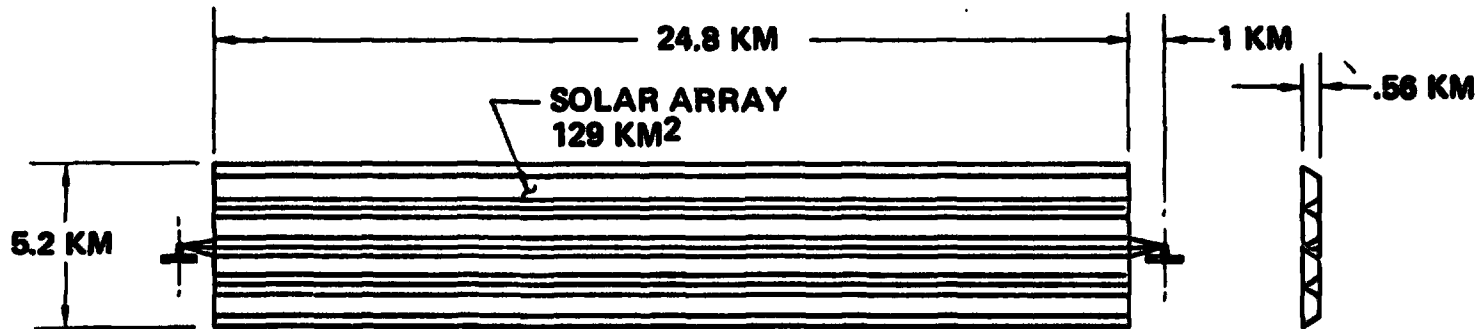


Initial Photovoltaic Reference Configuration

SP8-21

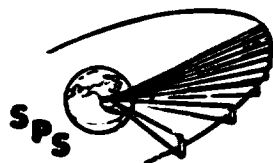
BOEING

- Silicon at CR = 2
- Nominal truss configuration with $\eta = .060$
- Orientation P.O.P.



PART I—PHOTOVOLTAIC STUDY REQUIREMENTS

The major objectives of Part I of this study are summarized here. These factors were used to analyze the various candidates for energy conversion and establish a system that could be defined to a greater depth in Part II.



SPS-1626

Part 1 – Photovoltaic Study Requirements

BEING _____

1. WHAT IS THE MOST OVERALL EFFECTIVE MEANS OF SPS ENERGY CONVERSION?
2. WHAT IS THE MOST DESIRABLE CONSTRUCTION/ASSEMBLY LOCATION(S)?

CANDIDATES

SINGLE CRYSTAL PHOTOVOLTAICS

- SILICON
- GALLIUM ARSENIDE

ADVANCED THIN FILM PHOTOVOLTAICS

- SILICON
- GALLIUM ARSENIDE
- CADMIUM SULFIDE
- COPPER INDIUM SELENIDE

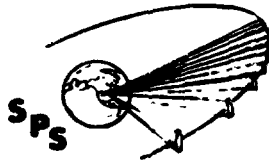
COMPARITORS

- SPS PERFORMANCE
- PERFORMANCE DEGRADATION
- SPS SIZE
- SPS MASS
- SYSTEM COMPLEXITY
- SYSTEM MAINTAINABILITY
- CONSTRUCTION REQUIREMENTS
- TRANSPORTATION REQUIREMENTS
- TECHNOLOGY ADVANCEMENT REQUIREMENTS
- SYSTEM COST DIFFERENTIAL FACTORS
- ENVIRONMENTAL EFFECTS DIFFERENTIAL FACTOR
- MATERIALS DIFFERENTIAL FACTORS

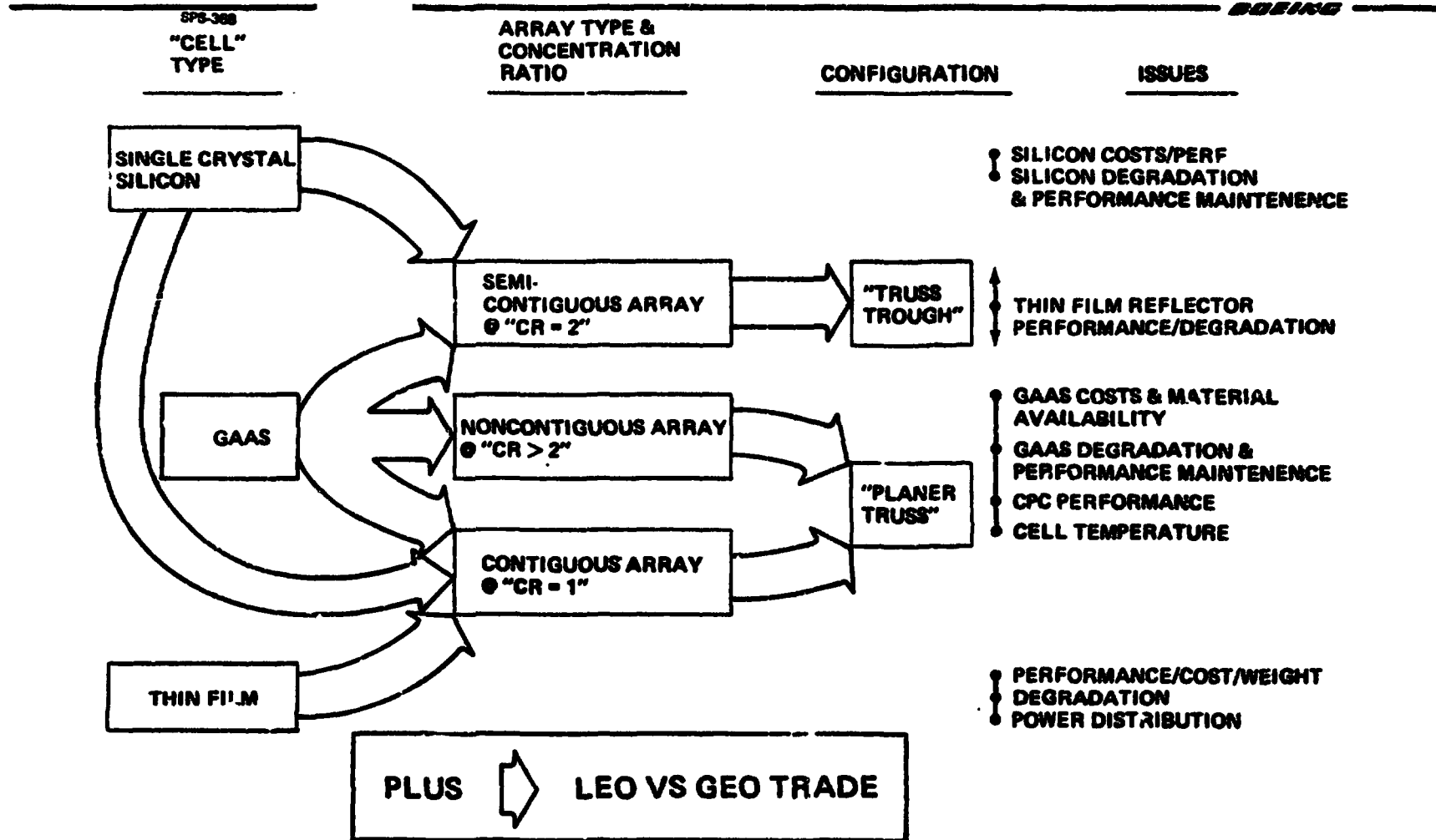
D180-22876-7

PHOTOVOLTAIC OPTIONS

Highlights of the Photovoltaic Study and its basic options and suboptions are shown together with the primary issues which required resolution during the first study phase. Effort was directed towards addressing these issues within the constraints of the satellite automated fabrication and assembly concept.



Part I – Photovoltaic Options

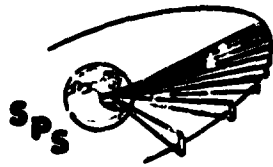


SOLAR CELL DEVELOPMENT—DECEMBER, 1976 STATUS

The "best achieved" cell efficiencies are those reported at the 1976 Photovoltaic Specialists Conference and the August, 1976 ERDA National Photovoltaic Conversion Program Review meeting. Only silicon solar cells are in production, with 14.6 percent efficiency reported by Spectrolab for a limited quantity of "sculptured" cells.

Efficiencies expected in 1978 are based on opinions by the investigators. For example, J. M. Woodall of IBM predicted that he would have 20 percent air-mass-zero gallium-arsenide cells within a year. Many workers predict 18-percent silicon cells.

The probable 1987 efficiencies are our own predictions, based on past progress and theoretical limits.



D180-22876-7

Solar-Cell Development--August, 1977 Status Cell Types Pertinent to Solar Power Satellites

SPS 28

BOEING

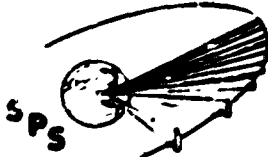
AIR MASS ZERO CONVERSION EFFICIENCY, PERCENT

<u>CELL</u>	<u>TYPE</u>	<u>PRODUCTION CELLS 1977</u>	<u>RESEARCH CELLS</u>			<u>THEORETICAL LIMIT</u>	<u>NOTES</u>
			<u>BEST ACHIEVED</u>	<u>1978</u>	<u>PREDICTABLE 1987</u>		
GALLIUM ARSENIDE	SINGLE CRYSTAL	17	18.5	21	22	25	HUGHES ACHIEVED 17.5% IN 2x2cm SPACE CELLS. BEING DEVELOPED BY JPL, VARIAN, SMU, MIT LINCOLN LABS FOR ERDA
	THIN FILM		12	15	17	25	
SILICON	SINGLE CRYSTAL	14.8	15.6	18	19	22	WOLF GIVES 19% GOAL
	POLYCRYSTAL		12.0	14	16	22	
	THIN FILM		7.2	12	13	22	
	METALLURGICAL VERTICAL JUNCTION		6.0 13	10 15	12 18	22 22	
CALCIUM SULFIDE		8.5	10	10			
InPCdS	SINGLE CRYSTAL THIN FILM		15 5.7	17 10			{ (?) IN RESOURCES
InP/InSnO	SINGLE CRYSTAL		15		17		{ SPLUTTERED, SCHOTTKY BARRIER, BELL LABS BEING DEVELOPED AT BOEING
CuInSe	THIN FILM		3			17	
Cd/CuInSe	THIN FILM		6.2			17	
Si/LaAs	TANDEM JUNCTION						34

D180-22876-7

SPECTRUM OF PROTONS INCIDENT ON SOLAR CELLS

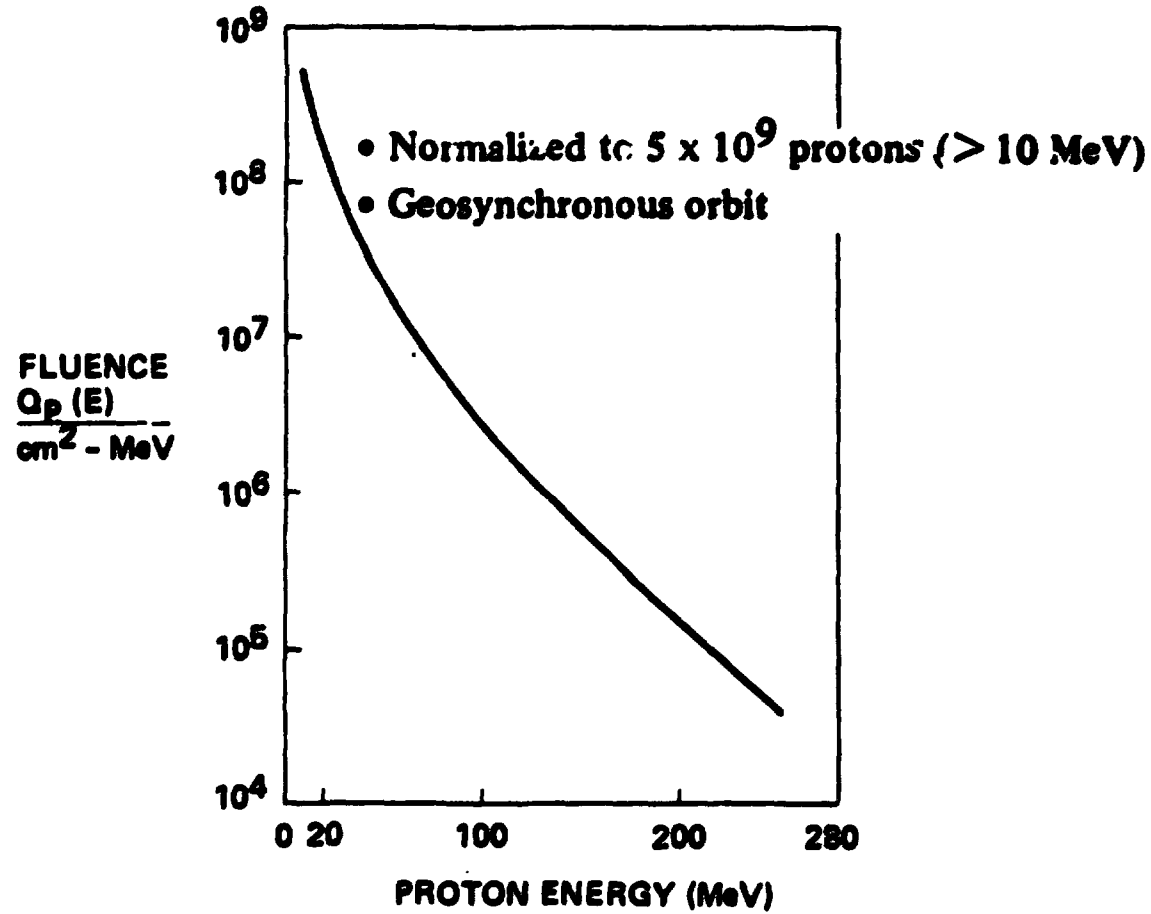
Using Prof. Webber's solar activity predictions, we calculate that in 30 years in geosynchronous orbit a silicon solar cell under a 150 μm (6 mil) fused silica cover will be exposed to the equivalent of 2.25×10^{11} protons having greater than 10 MeV energy. The spectrum of the protons is plotted here, with fluence as a function of proton energy. Note how copious are the low energy protons, when compared with the high-energy ones.



SP-728

Spectrum of Protons Incident on Solar Cells

BOEING

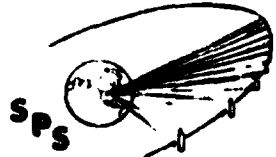


DAMAGE EQUIVALENT OF PROTONS

The previously derived proton fluence was converted into its equivalent one-MeV electron fluence by applying the I_p/I_e equivalence plotted here, in layer by layer of the solar cell. An alternate, but more gross, conversion could have been made with the curve from the solar cell Radiation Handbook, plotted as a dotted line for reference.

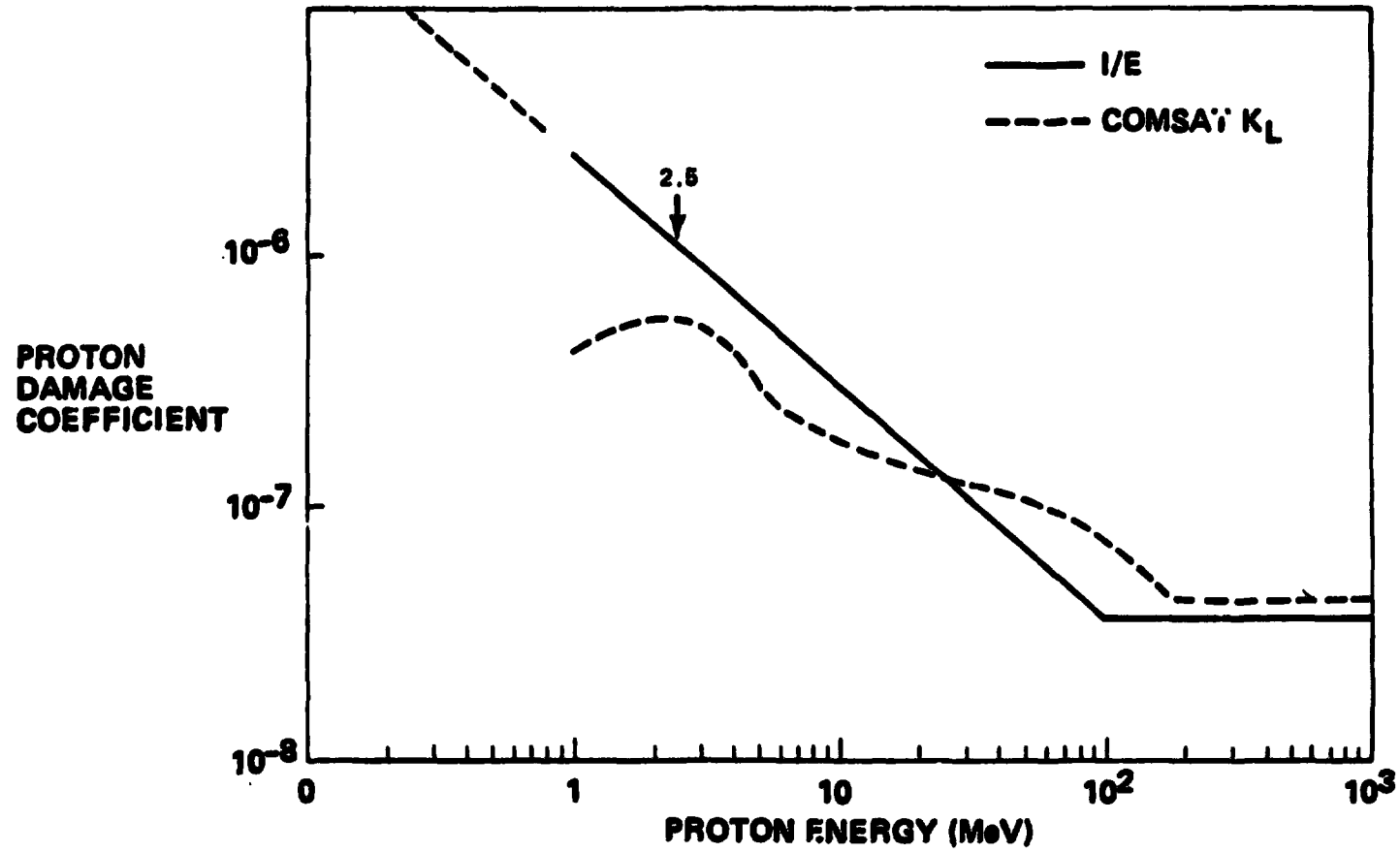
The one-MeV electron damage coefficient, when plotted in the units shown, would be around 10^{-10} , indicating that protons are some 1000 times as damaging as electrons.

Damage Equivalent of Protons



SPS-228

BEING

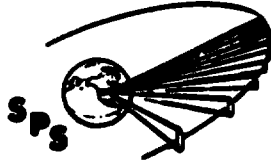


D180-22876-7

PART I ANNEALING SUMMARY

Although the data was somewhat limited, input data was received for every annealing issue and is summarized here.

A larger data base is needed on all annealing issues especially the temperature/time relations, percent recovery of radiation damage, and the effects of repeated annealing.



Annealing Summary

SPS 623

ISSUES:

- PROTON vs ELECTRON DAMAGE
- TEMPERATURE/TIME RELATIONSHIPS
- SUBSTRATE COMPATIBILITY
- % RECOVERY

DATA BASE:

SIMULATION PHYSICS: RESEARCH & TEST
HUGHES: RESEARCH*

INPUT:

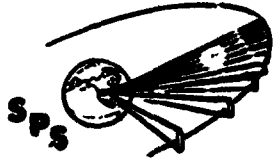
- ANNEALING IS FLUENCE DEPENDENT—PROTON DAMAGE REQUIRES HIGH TEMPERATURES (500°C+)
- TEMPERATURE IS PREDOMINANT PARAMETER
- DIRECTED ENERGY APPROACH PROMISING FOR BOTH EFFICIENCY & SUBSTRATE COMPATIBILITY
- RECOVERY WILL APPROACH 100% WITH PROPER DESIGN
- LOW TEMPERATURE GAAS ANNEALING PROBABLY NOT APPLICABLE TO PROTON DAMAGE

***HUGHES CURRENTLY INVOLVED IN RADIATION DEGRADATION TEST PROGRAM FOR USAF**

D180-22876-7

GaAs INPUT SUMMARY – HUGHES

The Hughes input on GaAs is summarized here in key areas. Of significance was the lack of data base in areas critical to SPS applications. The resolution of these issues could result in a GaAs SPS with significant cost and mass advantages.



SPS 635

GaAs Input Summary Hughes

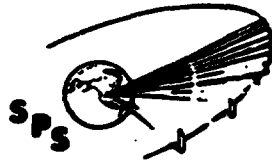
BOEING

- **SINGLE CRYSTAL EFFICIENCY @ AMO = 20%**
- **THIN FILM (10 μm) EFFICIENCY = SINGLE CRYSTAL EFFICIENCY**
- **GaAs MUCH MORE RESISTANT THAN SI TO HIGH ENERGY PROTON DAMAGE**
- **ELECTRON DAMAGE TO GAAS ANNEALS "OUT" @ 200-300°C**
- **GaAs \$\$ NOT EXPECTED TO EXCEED \$1/g**
- **DATA BASE LACKING FOR: THIN FILM; RADIATION DEGRADATION; ANNEALING**

THIN FILM REFLECTORS

A summary of the Part I reflector data used to evaluate the performance of a CR2 system is shown. Using the Project Able radiation degradation data and the "coupon data," an initial ideal reflectance of 0.85 will have degraded to 0.59 in 30 years. This resulted in a geometric concentration ratio of 2.0 ($CR_g = 2$), having an effective CR of 1.31 when compensated for solar cell thermal degradation.

Also shown are some of the problems that must be taken into account if a reflector is used to concentrate sunlight on solar cells.



SPS-367

Thin Film Reflectors

BOBING

- **"COUPON DATA"**
 - REFLECTANCE VS BEAM SPREAD
 - REFLECTANCE VS STRESS LEVEL
 - REFLECTANCE VS WAVE LENGTH
 - REFLECTANCE VS INCIDENCE ANGLE
 - REFLECTANCE VS RADIATION/TIME
 - REFLECTANCE VS ALUMINIZATION CHARACTERISTICS

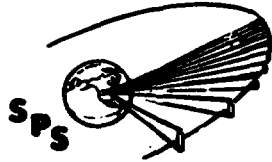
- **"REFLECTOR" PROBLEM/PERFORMANCE DEFINITION**
 - EDGE MARGIN FOR EVEN ILLUMINATION
 - STRESS LEVEL VS "FLATNESS"
 - MEMBRANE ANALYSIS
 - JOINTS ● EDGES ● TOLERANCES ● TEMP Δ 'S
 - REFLECTOR CREEP
 - MECHANICAL PROPERTIES' DEGRADATION

D180-22876-7

SHADOWING AFFECTS STRING PERFORMANCE

This illustration shows the effect of shadowing on solar cell string output. The percent shadowing can be interpreted as either the percent of the array that is completely shadowed, the percent of reference illumination provided to a string compared to other strings in the array or a combination of the two.

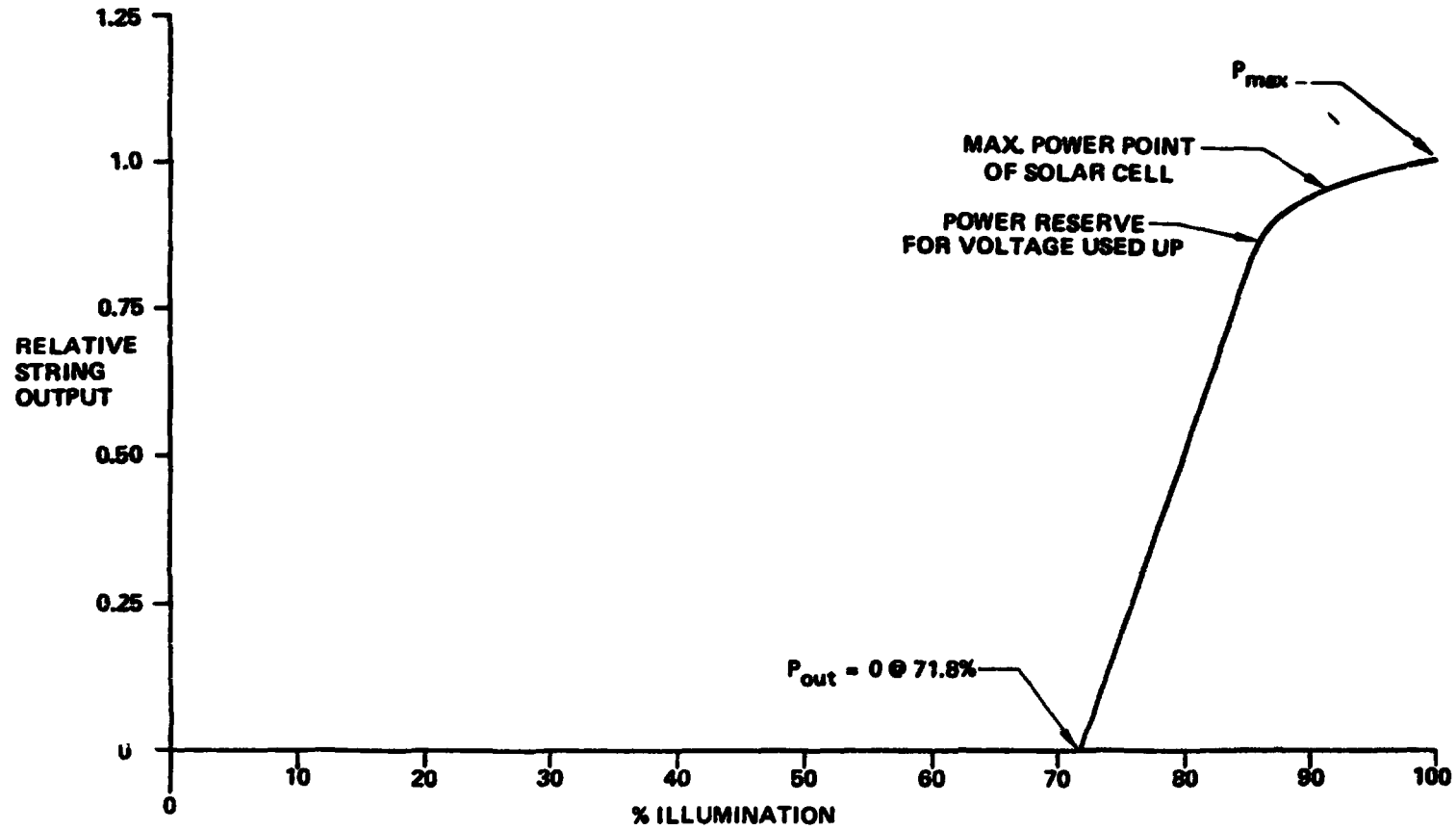
Uneven illumination may be caused by support members shadowing portions of the array, edge margins on thin film reflectors, or objects passing in front of and shadowing the solar array.



SPS-1625

Shadowing Affects String Output

BOEING

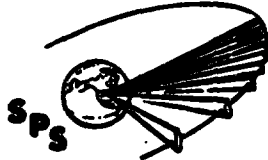


D180-22876-7

PART I SILICON SYSTEM COMPARISONS

Several silicon systems were developed in Part I to show the effect of the CR1 vs. CR2, LEO vs. GEO construction, and power maintenance scenarios. An illustration of some of the systems developed for GEO construction is shown.

The main conclusion that can be made from this comparison is that a CR1 system is more favorable and that annealing presents a large advantage in power maintenance. If annealing is not available, array addition would be the next logical choice.

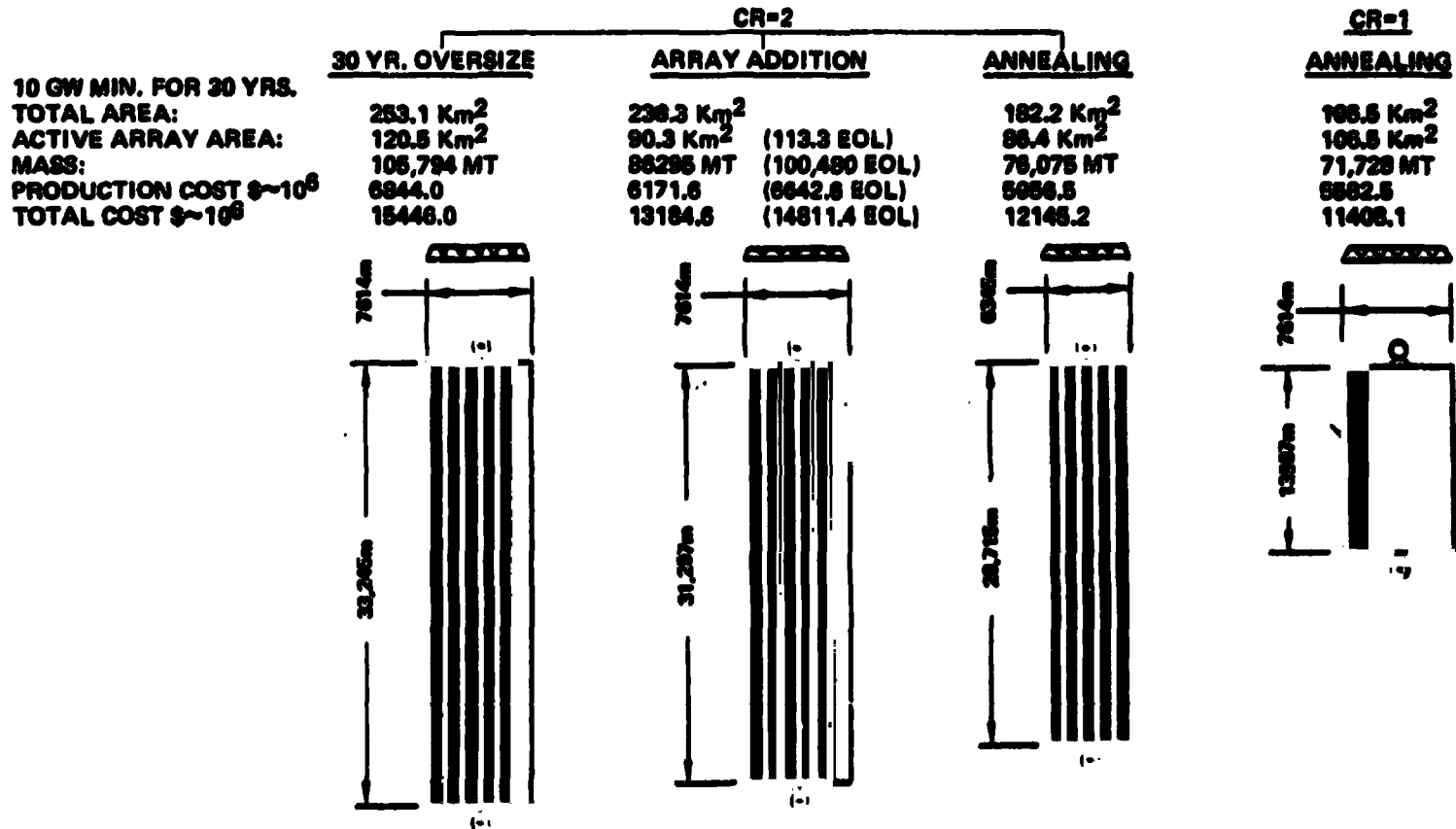


Part I – Silicon Configuration Summary

SPS-1828

BOEING

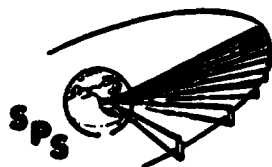
SILICON - GEO ASSEMBLY



D180-22876-7

CR1 SILICON SATELLITE SENSITIVITY TO CELL PERFORMANCE

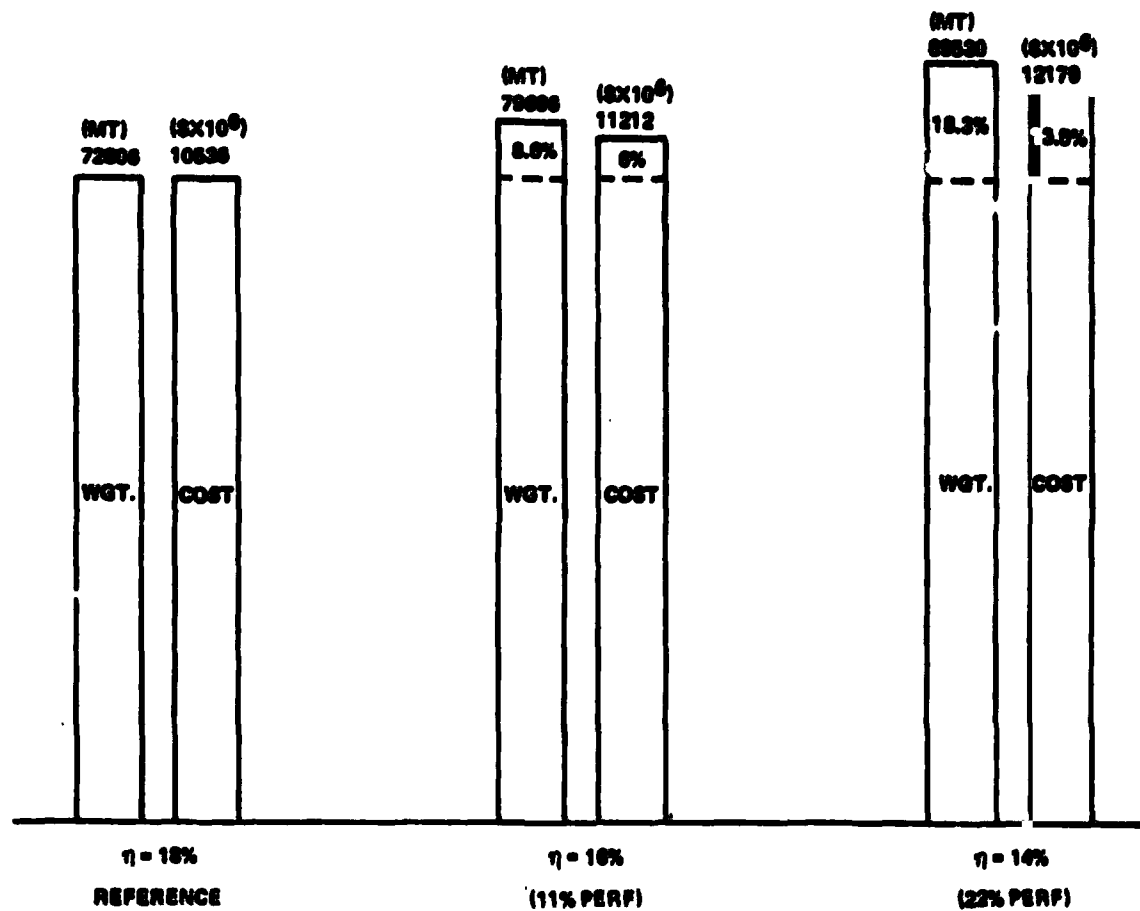
Silicon performance sensitivities, starting from a reference figure of 18% and dropping 2% per step, are shown here. Even at 14% efficiency there is not a dramatic change in either mass or cost. This indicates that achieving low cell costs is much more important than maximizing efficiency.



SPS 748

Silicon Satellite @ CR=1 Sensitivity To Cell Performance

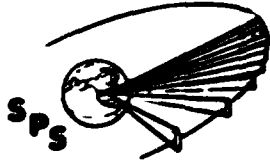
~~SECRET~~



D180-22876-7

PART I--GaAs SYSTEM COMPARISONS

A similar trade was made on GaAs systems with major conclusions shown here. The CR-1 vs. CR-2 trade is not as clear with GaAs systems, from a mass comparison. The lower gallium usage but higher system complexity and illumination problems with the CR-2 system must be taken into account for a fair comparison. The advantage of LEO construction is apparent in the cases shown.



D180-22876-7

Part I – GaAs Configuration Summary

SPS-1629

BOEING

GaAs – 10 GW MIN. FOR 30 YRS. V A ANNEALING

LEO ASSEMBLY

GEO ASSEMBLY

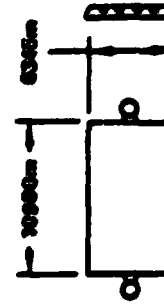
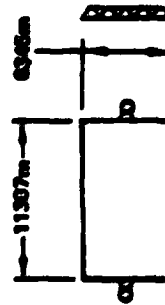
TOTAL AREA:
ACTIVE ARRAY AREA:
MASS:
PRODUCTION COST: $9 \sim 10^8$
TOTAL COST: $9 \sim 10^9$

CR=2

CR=1

104.9 Km ²	71.7 Km ²
86.9 Km ²	71.7 Km ²
46820 MT	46113 MT
5027.4	5197.9
8117.0	8313.0

66.4
66.4
42160 MT
5025.4
8442.7

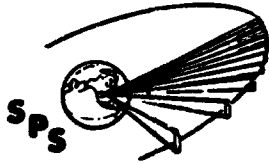


D180-22876-7

PHOTOVOLTAIC ENERGY CONVERSION COMPARISONS

A matrix of the photovoltaic energy conversion candidates and the major system comparators, shown previously, was developed. The viable candidates become apparent when compared in this fashion.

Single crystal silicon systems, CR1 and CR2, appear to be the best candidates for the least amount of extrapolation. Thin cell GaAs systems have the best overall characteristics but the question of gallium availability is currently unresolved.



Photovoltaic Energy Conversion Comparisons

SPS-1527

	PERFORMANCE	RADIATION DEGRADATION	THERMAL DEGRADATION	SYSTEM SIZE	SYSTEM MASS	SYSTEM COMPLEXITY	SYSTEM MAINTAINABILITY	MATERIAL AVAILABILITY	TECHNOLOGY ADVANCEMENT REQUIREMENTS
SINGLE CRYSTAL CELLS									
SILICON CR-1	MED	FAIR	FAIR	FAIR	MED	GOOD	GOOD	GOOD	LOW
SILICON CR-2	MFD	FAIR	FAIR	FAIR	MED	FAIR	MED	GOOD	LOW
GaAs CR-1	HIGH	FAIR	GOOD	GOOD	LOW	GOOD	GOOD	POOR	LOW
GaAs CR-2	HIGH	FAIR	GOOD	GOOD	LOW	FAIR	MED	POOR	LOW
GaAs CR>2	V. HIGH	FAIR	GOOD	GOOD	LOW	POOR	POOR	MARGINAL	LOW
ADVANCED THIN FILMS									
SILICON CR-1	LOW	GOOD	FAIR	FAIR	MED	GOOD	GOOD	GOOD	V. HIGH
SILICON CR-2	LOW	GOOD	FAIR	FAIR	MED	FAIR	MED	GOOD	V. HIGH
GaAs CR-1	HIGH	EXCELLENT	GOOD	GOOD	LOW	GOOD	GOOD	FAIR	HIGH
GaAs CR-2	HIGH	EXCELLENT	GOOD	GOOD	LOW	FAIR	MED	FAIR	HIGH
GaAs CR>2	HIGH	EXCELLENT	GOOD	GOOD	LOW	POOR	POOR	FAIR TO GOOD	HIGH
CADMIUM SULFIDE	LOW	EXCELLENT	GOOD	POOR	LOW	GOOD	GOOD	GOOD	V. HIGH
COPPER INDIUM SELENIDE	LOW	EXCELLENT	GOOD	POOR	LOW	GOOD	GOOD	POOR	V. HIGH

BOEING

ORIGINAL PAGE IS
OF POOR QUALITY

PHOTOVOLTAIC SUMMARY

These are the conclusions with respect to photovoltaics at the end of Part I.

With respect to the cost of silicon solar cells, we found that the 20.5 billion 5 by 10 cm cells required for each solar power satellite would be manufactured in new automated factories which would be entirely different from today's solar-cell production facilities, and the cell cost would be more like the cost of today's high-volume semiconductor products. The "mature industry" approach to pricing indicated that the cost of the satellite would indeed be reasonable.

The weight and cost of the satellite was not too sensitive to solar cell performance. Practical satellites could be designed around solar cells having efficiencies even as low as 16.5 percent, which is achievable today.

In concentration ratio trades, the non-concentrating array always came out best from cost and weight standpoints. The key factor was the radiation degradation in reflectance of aluminized Kapton films. Project Able tests indicated that the 85 percent reflectance of the aluminized Kapton films would degrade to 63 percent, with most of the degradation occurring within the first few years of the 30-year projected satellite life.

Work done by Simulation Physics, Inc., showed that in solar cells the radiation damage caused by solar-flare protons can be annealed out, avoiding the loss of some \$16 billion of power sales revenue. Laser light, electron beams and infrared radiation are possible heating methods. Thermal annealing is worth developing.

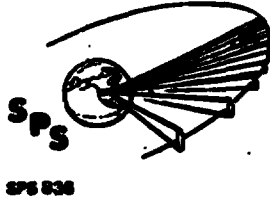
Low-earth-orbit turned out to be the most practical place to assembly to the solar power satellites, provided electric thrusters could be used to transfer the completed satellite to geosynchronous orbit. Geosynchronous-orbit assembly required shipping huge quantities of propellants to low-earth orbit. Essential to the low-earth-orbit assembly approach is the thermal annealing of radiation damage occurring during transit through the Van Allen radiation belts.

Gallium arsenide solar cells were found to be advantageous because of their probable 21 percent conversion efficiency and their moderate loss in performance as they became warmer. However, gallium availability turned out to be questionable. Gallium was not concentrated sufficiently in sea-water to be worth recovering. Gallium is at present a by-product of aluminum and zinc refining, with coal fly-ash being a potential source. The projected United States coal consumption and aluminum production will not be great enough to support the construction of several solar power satellites per year unless the gallium arsenide layer in the solar cells is made thin, say under 10 μm . ERDA has funded Battelle Northwest to carefully investigate gallium availability.

Some work has suggested that radiation damage in thin layers of gallium arsenide can be annealed out at fairly low temperatures - perhaps at only 125°C. Also, gallium arsenide cells are more resistant than silicon solar cells to radiation damage, making them more applicable to powering the transfer of a completed solar power satellite from low-earth orbit to geosynchronous orbit.

Thin film solar cells, many types of which are being developed by ERDA, are characterized by great but unproven potential. Their low weights and thin cross-sections make possible ideal satellite design. Some offer the potential of good efficiency, for example, 15 percent in single-crystal indium-phosphide/cadmium sulfide. However, the generation of sizeable crystals on thin films has not yet been realized. The best achieved efficiency in other than single-crystal cells has been around 8 percent for cadmium sulfide which has not yet been proven to be stable in performance.

ORIGINAL PAGE IS
OF POOR QUALITY



Part I – Photovoltaic Summary

BOEING

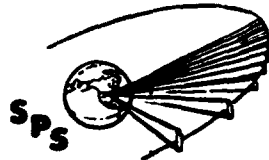
- SILICON COSTS NOT "TOO HIGH"
- SILICON SYSTEM NOT SENSITIVE TO CELL PERFORMANCE
- CR1 PREFERABLE TO CR2
- ANNEALING CRITICAL TO SILICON SYSTEM
- LEO ASSY & SELF POWER SHOW TO ADVANTAGE WITH ANNEALING
- GALLIUM SUPPLY & \$\$ IN QUESTION
- GAAS THIN FILM CRITICAL TECHNOLOGY
- IF GAAS SUPPLY & THIN FILM OK—GAAS ATTRACTIVE & NOT AS SENSITIVE TO ANNEALING OR LEO/GEO TRADE
- OTHER THIN FILMS LOOK COMPETITIVE BUT NEED IMPROVED DATA BASE

ORIGINAL PAGE IS
OF POOR QUALITY

D180-22876-7

PART I RECOMMENDATIONS

The conclusion of Part I of the study was the recommendation of a system to define to a greater depth for the reduction of uncertainties in size, mass and cost in Part II. The main recommendations were the result of trades conducted on the various candidates and the comparative factors discussed previously.



SPS-1630

D180-22876-7

Part 1 – Recommendations

BOEING

- **RECOMMEND SILICON, CR1, ANNEALABLE SYSTEM**
 - **BEST DATA BASE – LEAST AMOUNT OF EXTRAPOLATION**
 - **LOWEST SYSTEM COMPLEXITY**
 - **BEST CANDIDATE FOR REDUCTION OF UNCERTAINTIES**
 - **CR-2 ONLY PROVIDES A $CR_{off} \sim 1.31$**
 - **REFLECTOR/UNEVEN ILLUMINATION PROBLEMS**

- **CARRY GALLIUM ARSENIDE AS ADVANCED TECHNOLOGY SYSTEM**
 - **HIGHER EFFICIENCY – LOWER DEGRADATION**
 - **MATERIAL AVAILABILITY**
 - **THINNER CELLS REDUCE USAGE**

- **DISCONTINUE THIN FILM CANDIDATES**
 - **INSUFFICIENT DATA BASE**

PHOTOVOLTAIC SATELLITE—INITIAL PART II OBJECTIVES

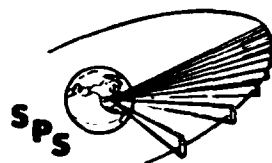
These program objectives pertain to the solar array for the initial Part II effort. An additional level of depth was needed for the solar array, array primary structure, and power distribution. To generate baseline designs, we adopted a cell size and type, a cover and substrate material, and an interconnecting technique. An important consideration was appropriateness to automated manufacture. With the blanket designed we could then proceed with preliminary designs of primary structure, and buses and control for carrying the power from the solar array to the rotary joint. Minimum manhours in orbital assembly was an important requirement of the structure.

Other areas requiring definition included microwave power transmission system, attitude control, secondary structure, and rotary joint. The rotary joint turned out to be sensitive to brush voltage drop, which represents heat that must be re-radiated away.

We investigated gallium arsenide solar cells further, particularly with respect to their use in concentrated sunlight, considering the reflectors, supporting structure, and performance during anticipated mis-orientations.

An important key issue in the use of silicon solar cells is annealability. Many years ago the U.S. Naval Research Laboratory demonstrated that radiation damage can be annealed out of silicon solar cells. However, no one has annealed cells repeatedly, so we do not know what is the unannealable fraction of radiation damage. More work in this field is recommended.

ORIGINAL PAGE IS
OF POOR QUALITY



SPS-1002

D180-22876-7

Photovoltaic Satellite Initial Part II Objectives

BOEING

■ IMPROVE REFERENCE SATELLITE DEFINITION

● PURSUE THOSE AREAS ALREADY DEFINED TO AN ADDITIONAL LEVEL OF DEPTH:

- SOLAR ARRAY
- PRIMARY STRUCTURES
- POWER DISTRIBUTION

● DEFINE THOSE SIGNIFICANT AREAS PREVIOUSLY ACCEPTED FROM JSC GREEN BOOK

- MPTS
- ATTITUDE CONTROL
- SECONDARY STRUCTURE
- ROTARY JOINT

■ PURSUE GAAS ISSUES OF SUPPLY AND HIGHER COSTS

■ PURSUE KEY ISSUES

- SILICON ANNEALING
- COST DATA BASE

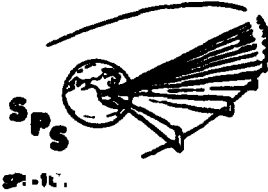
D180-22876-7

DECISION CRITERIA

Obviously a full preliminary design of the solar power satellite is not possible with the available funding. However, the available resources do permit in-depth explorations of those portions of the design that significantly contribute to the uncertainties of mass and cost.

As an example, previous work was hampered by lack of a data base for thin-film solar cells. Additional investigation revealed that at this time a data base on thin-film cells is not possible because the necessary inventions and developed processes aren't here yet. However, in other development work, the single-crystal silicon solar-cell technology had advanced to the point where 12.5 percent efficiencies are being obtained with 50 μm thick cells, and the COMSAT-invented technique of texturing solar-cell surfaces turned out to improve hardness to radiation.

Other sources of uncertainty, which resulted from design complexity and analytical difficulty, have likewise been resolved. The resulting array concept is one which is achievable with reasonable extrapolation of the present state-of-the-art, rather than requiring new invention.



Decision Criteria

BOEING

■ DESIGN SELECTION RATIONALE

- TIED TO STUDY PHASE OBJECTIVES
- LIMITED BY RESOURCES

■ REDUCTION IN THE UNCERTAINTY OF SYSTEM MASS & COST REQUIRES:

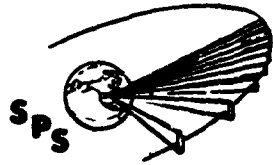
- REDUCTION OF TECHNICAL UNCERTAINTIES INTRODUCED BY;
 - LACK OF DATA BASE
 - DESIGN COMPLEXITY
 - ANALYTICAL DIFFICULTY
- WITHIN REASONABLE PERFORMANCE BOUNDS

D180-22876-7

PART II INFORMATION UPDATES

In an advancing technological society there is a continuous increase in technology items. Shown here are some of the areas that needed updates for the reference system selection. The charts following this will discuss the information updates in each area and show what effect, if any, that they have on the selected system.

D180-22876-7



SPS-1831

Part II Information Updates

BEING _____

- **THIN FILM REFLECTOR DEGRADATION**

- **LOWER RADIATION DEGRADATION FOR 2 MIL SILICON CELLS**

- **SOLAR CELL UPDATES**
 - **EFFICIENCIES**
 - **THIN FILM GALLIUM ARSENIDE BREAKTHROUGHS**

- **ANNEALING UPDATE**

D180-22876-7

THIN FILM REFLECTOR DEGRADATION UPDATES

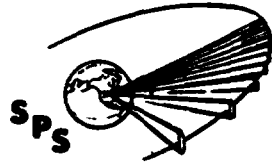
Recent data, from tests at JPL, show that there is an insignificant amount of thin film reflector degradation in a radiation environment similar to that in geosynchronous orbit. This is a significant change from the 30% degradation of reflectance that was used in the CR-1 vs CR-2 trade.

The effect of this update on the CR-1 vs CR-2 trade is also insignificant because the major portion of the performance degradation on the CR-2 system was due to the higher operating temperature not reflector degradation. The reflector degradation has a secondary effect.

The lower degradation of reflectance results in a higher FOE operating temperature for the solar cells. This resulted in an effective concentration ratio of 1.36 instead of 1.31 shown at the end of Part I.

D180-22876-7

Thin Film Reflector Degradation



SPS-1532

BOEING ———

- **LOWER DEGRADATION ON THIN FILM REFLECTORS**
 - **0% vs. 30% PROJECTED FROM PROJECT ABLE DATA**

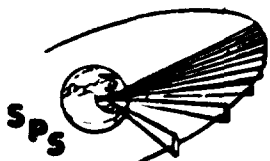
- **EFFECT ON CR1-CR"2" TRADE**
 - **PART I $CR_{off} = 1.31$ INCREASES TO $CR_{off} = 1.36$**
 - **CR1 STILL APPEARS TO BE BEST CHOICE FOR SILICON**

THIN CELLS EXHIBIT LOWER RADIATION DEGRADATION

A significant update was received in the area of radiation degradation of silicon solar cells. It had been stated previously that thinner solar cells exhibited lower radiation degradation but no information was available to demonstrate the effect of solar cell thickness on degradation.

Since we had gone to thinner solar cells (50 μm) to reduce system mass, it became necessary to reinvestigate the area of solar cell radiation degradation. A plot was made of radiation degradation at various fluences as a function of solar cell thickness. This data was obtained from JPL's "Solar Array Design Handbook." The curves that were developed, when extrapolated to a 2 mil cell thickness, showed a significant reduction in radiation degradation. Information was also published by Solarex on the radiation degradation characteristics of "ULTRA-THIN" 2 mil cells, also shown on this chart.

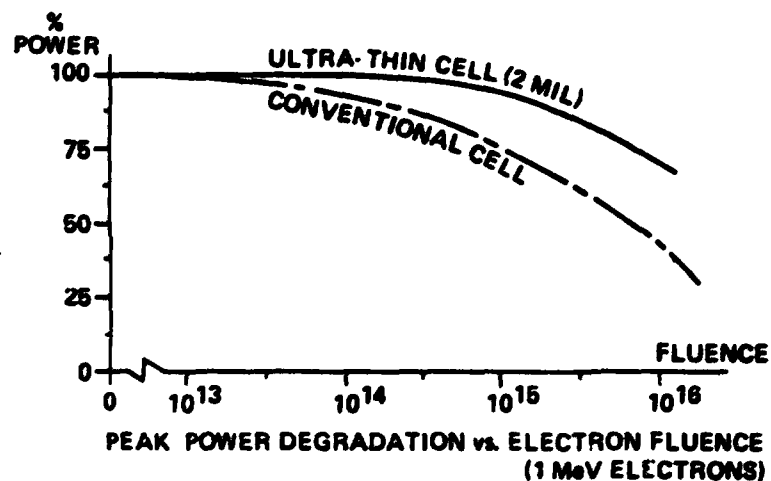
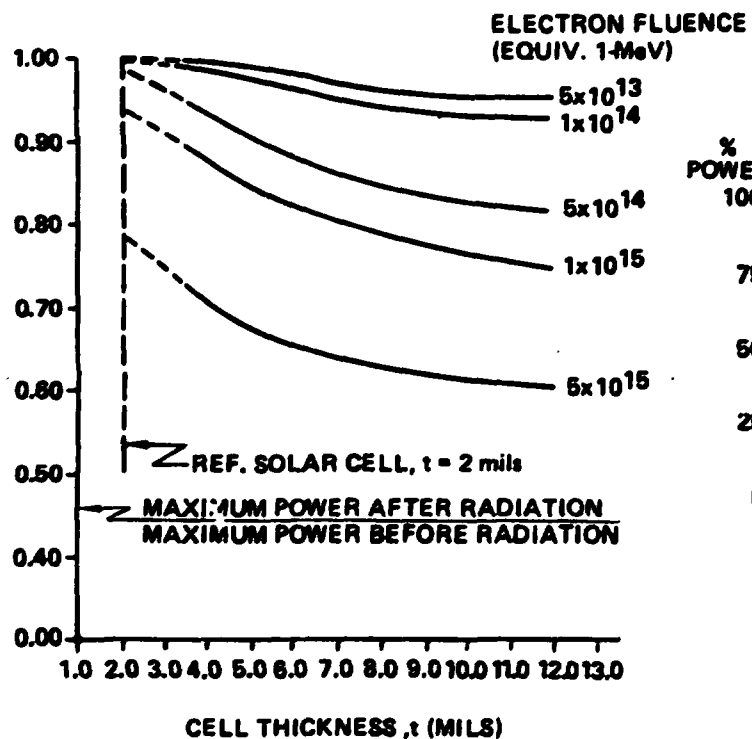
The effect of this data is that annealing, although still very advantageous, is not as critical an issue as previously reported.



Thin Cells Exhibit Lower Radiation Degradation

BOEING

SPS-1633



D180-22876-7

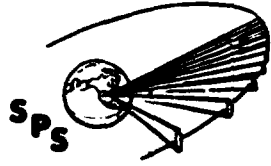
SOLAR CELL UPDATES

Other solar cell updates were recognized in the areas of cell efficiencies and in large grain growth on thin polycrystalline gallium arsenide films.

In silicon solar cells, an update was the achievement of 12.5 percent efficiency in 50 μm (2 mil) cells. Even though in our reference system, we used a 2 mil cell with 15.75 percent efficiency, an efficiency of 18 percent is probable by 1985 for this solar cell.

In gallium arsenide solar cells, John C. Fan of MIT's Lincoln Labs has achieved a 20.5 percent efficient homojunction solar cell in AM1 sunlight. He projects a 22 percent efficiency by optimizing the cell contacts.

A 16.2 percent efficiency has been reported in JPL's AMOS (polycrystalline) solar cell by Stirn and Yeh. Lincoln Labs has also grown 25 μm diameter crystallites on films 2 μm thick by heating with a laser beam.



SPS-1634

Solar Cell Updates

BOEING

- **SOLAR CELL EFFICIENCIES**

- **SILICON**

- 12.5% ACHIEVED FOR 2 MIL CELLS

- **GALLIUM ARSENIDE**

- 20.5% ACHIEVED IN HOMOJUNCTION CELLS
- 22% PROJECTED WITH OPTIMIZED CONTACTS
- 16.2% ACHIEVED IN SLICED POLYCRYSTALLINE CELLS

- **THIN FILM GALLIUM ARSENIDE**

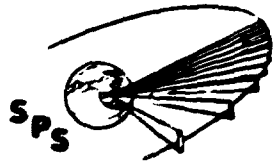
- **LARGE GRAIN GROWTH FROM LASER RECRYSTALIZED POLYCRYSTALLINE GaAs FILM**
- 25 μm GRAIN DIAMETER ON 2 μm THICK FILMS

ORIGINAL PAGE IS
OF POOR QUALITY

D180-22876-7

ANNEALING UPDATES

A technical effort is being accomplished by Boeing and Simulation Physics, Inc. under Boeing subcontract to achieve a better annealing data base. This effort is in work at this time and the results will be made available after more work has been accomplished.



SPS-1536

D180-22876-7

Annealing Updates

BOEING

- **TECHNICAL EFFORT—ANNEALABILITY OF RADIATION DAMAGE IN SILICON SOLAR CELLS***

- **LASER ANNEALING**

- **CONVENTIONAL SOLAR CELLS WITH ELECTROSTATICALLY BONDED 7070 GLASS COVERS**

- **TITANIUM SILVER CONTACTS**

- **DEEP JUNCTION SOLAR CELLS WITH ELECTROSTATICALLY BONDED COVERS**

- **50 μm SOLAR CELLS WITHOUT COVERS**

- **ELECTRON BEAM ANNEALING**

- **SOLAR CELLS WITH 75 μm COVERS**

*SIMULATION PHYSICS, INCORPORATED (SPIRE), UNDER BOEING SUBCONTRACT

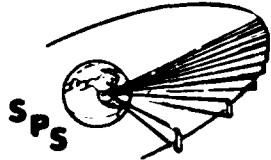
D180-22876-7

REDUCTION IN GALLIUM REQUIRED FOR CR>2 PHOTOVOLTAIC SYSTEM

Shown here is the possible reduction in the gallium required for a photovoltaic SPS by increasing the CR_g . A $CR_g = 6.0$ gallium requirement was calculated for a GaAs, CYLINDRICAL CPC system. For this case approximately 450 MT/satellite of gallium is required, so for a production of 4 satellites/year, 1800 MT/year of gallium would be needed.

Possible annual U.S. gallium production quantities are from "Availability of Gallium and Arsenic" by Dr. R. N. Anderson. A recovery of 30% of the gallium available from bauxite and coal fly-ash would supply the necessary amount of gallium for four SPS's per year.

D180-22876-7

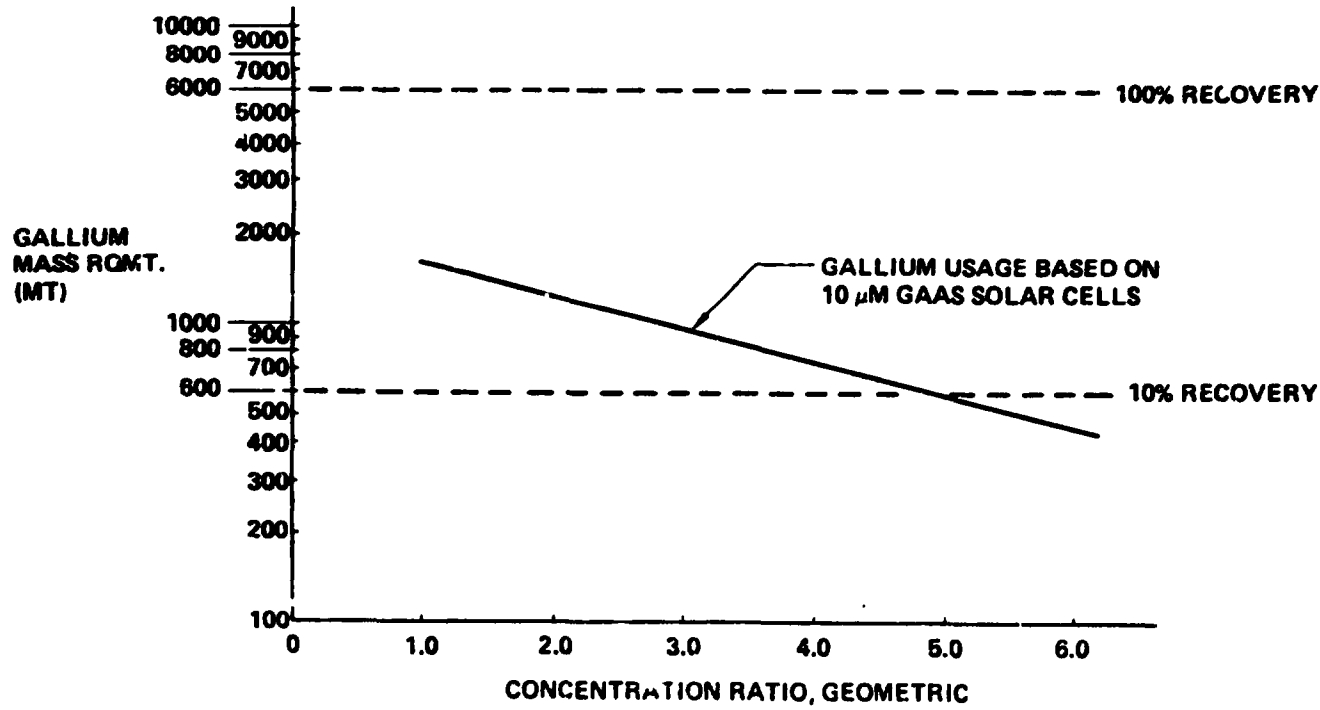


SPS-1028

Reduction in Gallium Required for CR > 2 System

BOEING

ANNUALLY AVAILABLE
GALLIUM FROM U.S. PRODUCTION
OF ALUMINUM AND COAL
FLY-ASH



PART II REFERENCE SYSTEM ENERGY CONVERSION/SIZING

These are the factors used in calculating the solar array power output. We start with solar cells having 15.75 percent efficiency. To this we add a 10 percent improvement, which could be achieved by any one of several means. For example, A. Meulenberg of COMSAT Laboratories estimates that the sawtooth cover that he invented will improve the efficiency of solar cells by 8 to 12 percent.

The blanket factors of 0.9453 account for the power losses shown. The individual elements of the blanket factors will change, but the product will probably remain around 0.9453.

The summer solstice loss accounts for the 23.5 degrees mis-orientation with respect to the Sun's rays. This loss could be avoided by having the satellite oriented perpendicular to the ecliptic plane, but the cost in thrusters and propellants required for attitude control in that mode shows to no real advantage.

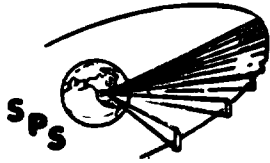
The aphelion intensity factor accounts for the reduced solar intensity when the Earth is at its aphelion, around the first part of July.

The temperature losses result from the solar cells operating between 36.5°C and 46°C, rather than at the 25°C at which cell efficiency is commonly tested.

The output is further reduced by 3 percent to account for radiation damage that cannot be removed by thermal annealing. In past tests, 95 percent of the radiation damage in solar cells has been annealed out, even though the cells had not been designed for thermal annealing. There is no theoretical reason why all of the radiation damage in solar cells cannot be annealed out, annealing temperatures of around 500°C being well below the 800°C region where diffusion of impurities starts. On the other hand, the operating plan for the solar power satellite involves repeated annealings, which have not been attempted by anyone, as far as we know.

The power requirement of 17.55×10^9 watts was based on supplying 16.43×10^9 watts to the slip rings and compensating for bus I-R losses. Another one percent was added to this power in the calculation of solar cell area to provide power regulation, auxiliary power, attitude control and energy storage.

The other items include the lost area factors considered for each case. This information was used in the formulation of final reference system sizing.



D180-22876-7

Part II Reference System Energy Conversion/Sizing

BOEING

SPS-1536

	OUTPUT = W/M ²
● BASIC CELL PERFORMANCE @ AMO-25°C (.1575)	213.1
● 10% IMPROVED PERFORMANCE DUE TO TEXTURED COVERS (.1733)	234.4
● BLANKET FACTORS (.9453) (STRING I ² R, UV LOSSES, & MISMATCH)	221.8
● SUMMER SOLSTICE COSINE LOSS (.9190)	203.6
● APHELION INTENSITY FACTOR (.9675)	197.0
● TEMPERATURE LOSSES (36.5°C @ SUMMER SOLSTICE = 0.9540)	188.0
● 30 YEAR NON-ANNEALABLE RADIATION DEGRADATION (0.970)	182.3
● POWER REQUIRED TO BUS (INCLUDES I ² R LOSS)	17.55 (10) ⁹ WATTS
● SOLAR CELL AREA (1% OVERSIZE FOR ENERGY STORAGE, ATTITUDE CONTROL REGULATION, AUX. PWR & ANNEALING CAPABILITY)	97.3 km ²
● ARRAY AREA (CELL, PANEL, STRING AND SEGMENT LOST AREAS)	102.5 km ²
● SATELLITE AREA (BEAM, CATENARY & ATTACHMENT LOST AREA FACTOR)	112.8 km ²

ORIGINAL PAGE IS
OF POOR QUALITY

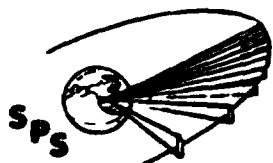
D180-22876-7

PHOTOVOLTAIC REFERENCE CONFIGURATION

This illustration shows the overall dimensions of the Photovoltaic Reference SPS. It is made up of 8 modules each 5300 meters by 2680 meters. Each of the modules are made up of 32-660 meter square bays. When assembled, the system will have an aspect ratio of four.

The basic bay size has decreased from a 680 meter square to a 660 meter square to compensate for the revised solar cell area requirements and lost area factors.

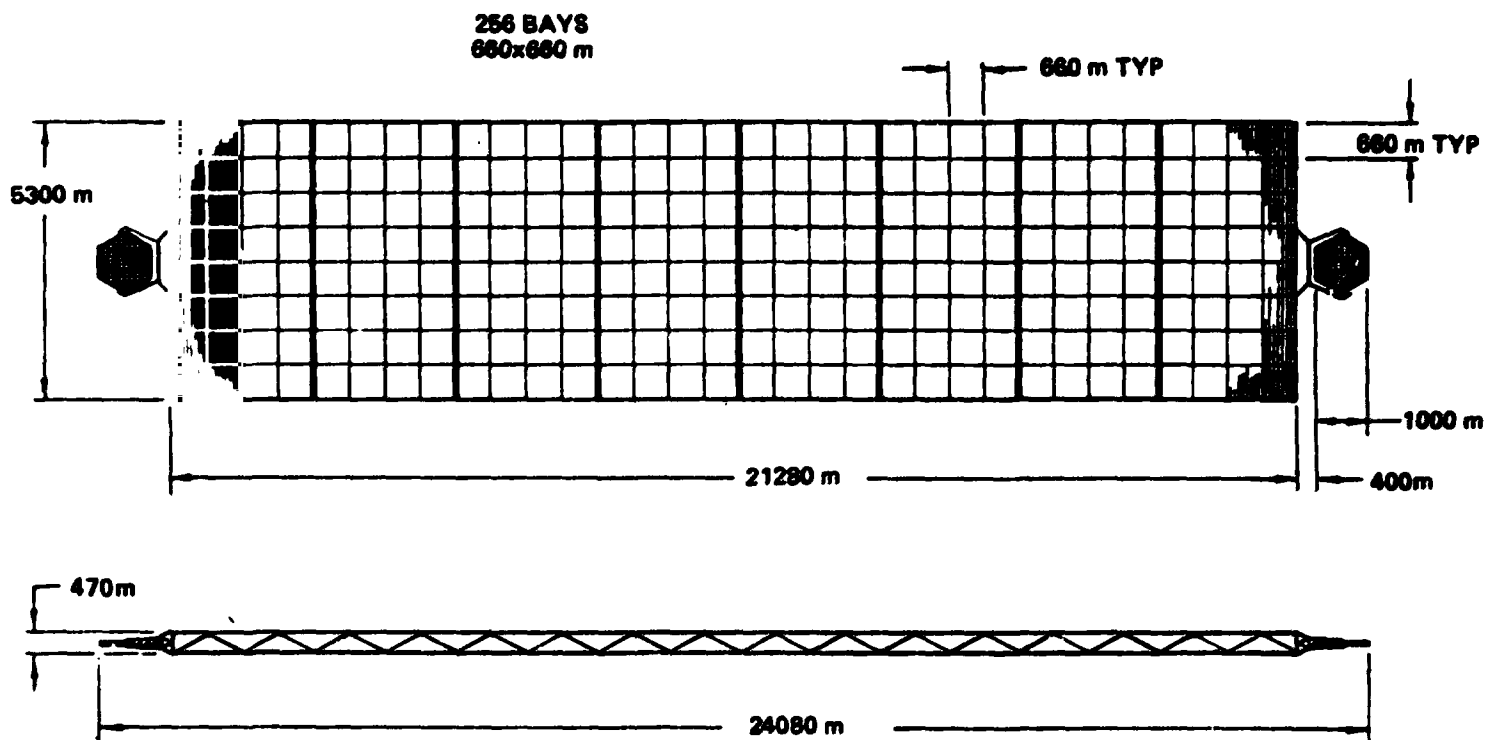
D180-22876-7



Photovoltaic Reference Configuration

SPS-1004

BOEING



TOTAL SOLAR CELL AREA: 97.34 Km²
TOTAL ARRAY AREA: 102.51 Km²
TOTAL SATELLITE AREA: 112.78 Km²
OUTPUT: 16.43 GW MINIMUM TO SLIPRINGS

LOW-COST ANNEALABLE BLANKET STRUCTURE

A silicon solar cell must be provided with a cover to increase front-surface emittance from around 0.25 to around 0.85, and to protect the cell from low-energy proton irradiation. Cerium-doped borosilicate glass is a good cover material because it costs only a fraction of the best alternate, 7940 fused silica, matches the coefficient of thermal expansion of silicon, and yet resists darkening by ultraviolet light. Borosilicate glass can be electrostatically bonded to silicon to form a strong and permanent adhesiveless joint. In ATS-6 flight tests the cells having integral 7070 borosilicate glass covers lost only 0.8 ± 1.1 percent of their output because of ultraviolet degradation. These cells had no cover adhesive. Other cells having cell-to-cover adhesives degraded twice as much. Jena Glaswerk Schott & Gen Inc., in West Germany expects to be able to manufacture 75 μm borosilicate glass sheets one meter wide by several meters long.

The cell cover is embossed during bonding with grooves which refract sunlight away from the grid lines and buses on the cell surface. COMSAT Labs expects an 8 to 12 percent increase in cell output from this feature in cell covers.

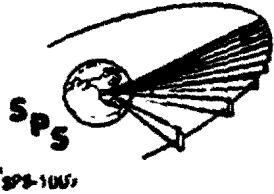
Solar cells only 50 μm thick recently made by Solarex had an air-mass-zero efficiency of 12.5 percent without a back-surface field or anti-reflection treatment. Texturing the sun-facing surface makes the incoming light arrive at the back surface of the cell at an angle of over 31° , so the light rays that have not been absorbed are reflected off the back surface with virtually no loss, the critical angle in a silicon-air junction being 15.3 degrees. This feature not only improves photon collection efficiency, when compared with thicker cells, by lengthening the light path in silicon for infrared photons, but also improves radiation resistance. Since all charge carriers are generated within 50 μm of the P-N junction which is 0.2 μm under the sun-facing surface, the cell can absorb radiation damage until the diffusion length in the bulk silicon is reduced to 50 μm by radiation-generated recombination centers.

The cells are designed with both P and N terminals brought to the backs of the cells. This feature makes it possible to use simple 50 μm silver-plated copper interconnections which are formed on the substrate glass. Complete panels are assembled electrically by welding together the module-to-module interconnections.

Glass was chosen for the substrate because it makes possible annealing out radiation damage by heating. With all glass-to-silicon bonds made by the electrostatic process there are no elements in the blanket which cannot withstand the 500°C annealing temperature which at present seems to be required. One researcher suggests that 500°C may not be needed for annealing out the radiation damage from solar-flare protons. However, his theory has not yet been confirmed by experiment.

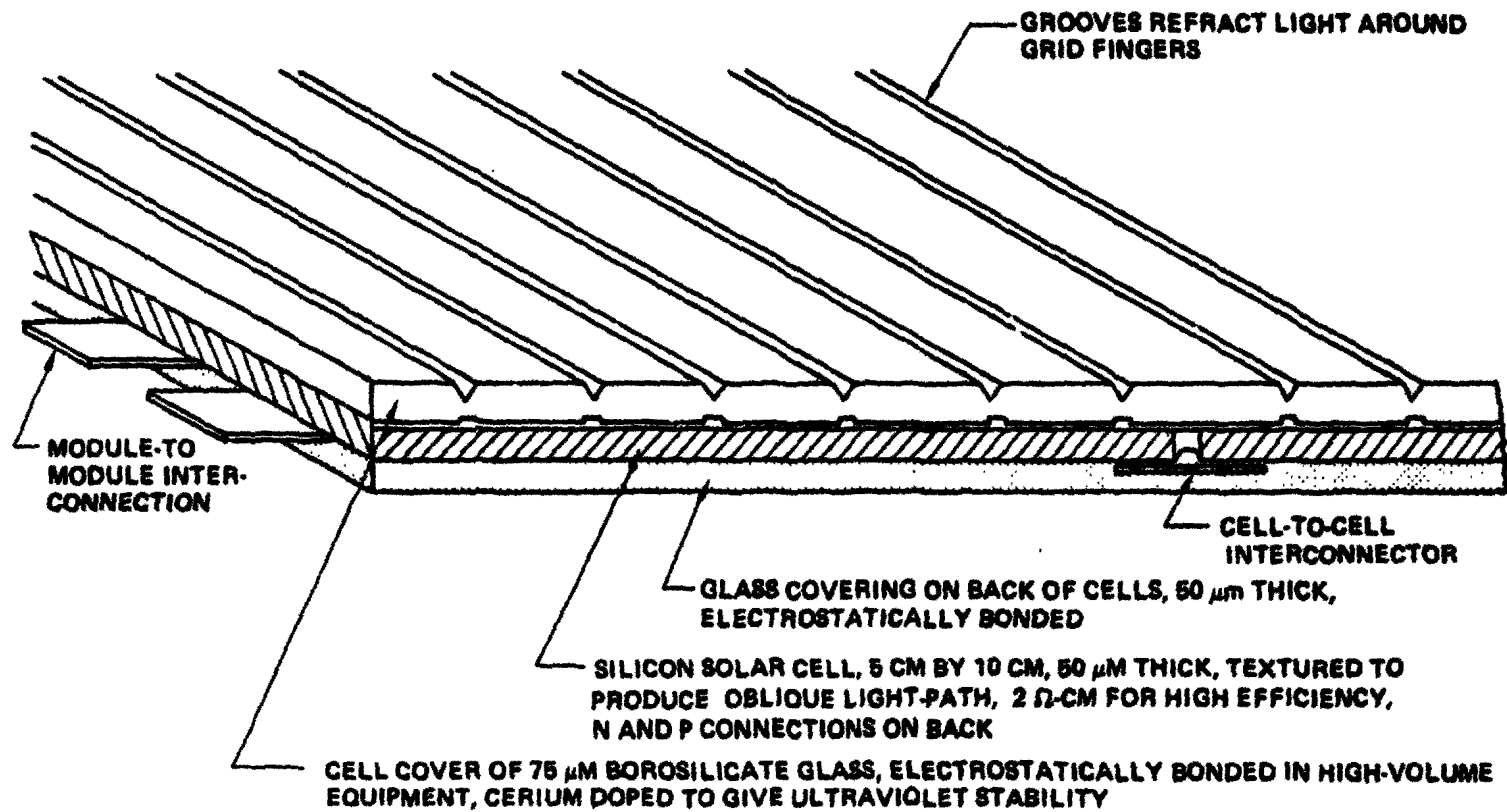
**ORIGINAL PAGE IS
OF POOR QUALITY**

D180-22876-7



Low Cost Annealable Blanket Structure

BEING



INTERCONNECTORS: 12.5- μm COPPER, WITH IN-PLANE STRESS RELIEF, WELDED TO CELL CONTACTS

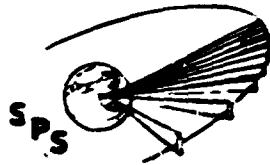
PHOTOVOLTAIC REFERENCE CONFIGURATION, SOLAR ARRAY FUNDAMENTAL ELEMENT, "BLANKET PANEL"

This is the basic panel adopted for design studies. It has a matrix of 252 solar cells, each 6.4 by 7.7 cm in size, connected in groups of 14 cells in parallel by 18 cells in series. The cells are electrostatically bonded between two sheets of borosilicate glass. Spacing between cell and edge spacings are as shown. Tabs are brought out at two edges of the panel for electrically connecting panels in series. Cells within the panel are interconnected by conducting elements printed on the glass substrate.

Important panel requirements were these:

- The panel components and processes should be compatible with thermal annealing at 500°C.
- Presence of charge-exchange plasma during ion-engine operation may necessitate insulating the electrical conductors on the panel.
- The panel design should be appropriate for the high-speed automatic assembly required for making the some 78 million panels required for each satellite.
- Low weight and low cost are important.

The glass-encapsulation technology, while not in use today, seems to be achievable by 1985. Simulation Physics has made excellent electrostatic bonds of covers to cells. Schott in West Germany is making thin microscope slides from borosilicate glass. The alternate panel design, using adhesives for bonding cells, covers and substrate, may also be feasible by 1985. Today polyphenylene sulfide adhesives can operate at 320°C and polyphenyl quinoxaline adhesives are good for 370°C. Also, some of our research suggests that a temperature of 500°C may not be needed for annealing out the cluster defects produced in solar cells by solar-flare protons.



D180-22876-7

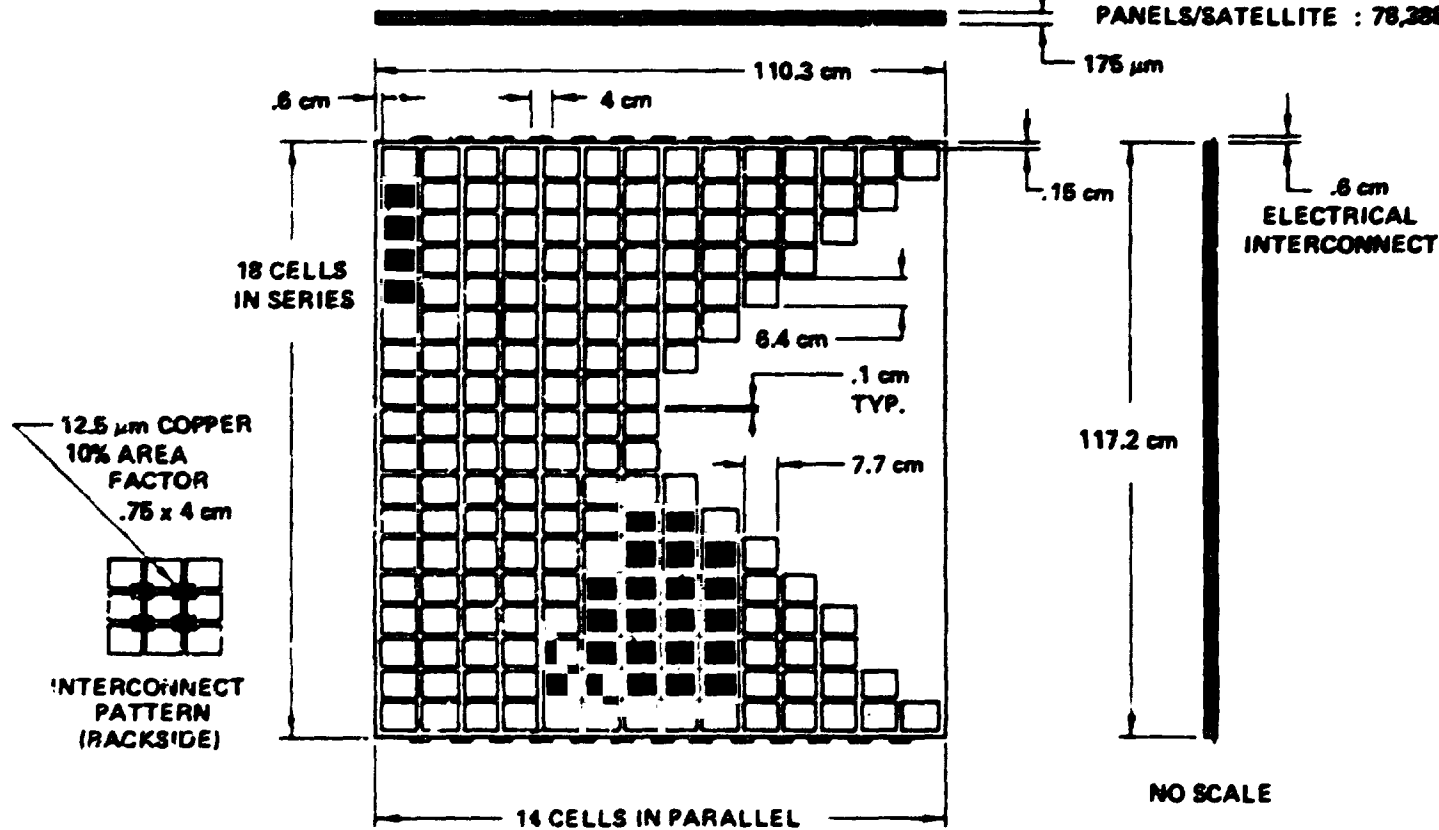
Photovoltaic Reference Configuration Solar Array Fundamental Element "Blanket Panel"

BOEING

SPS-1300

- 14 CELLS IN PARALLEL WILL TOLERATE 4 CELL FAILURES IN ANY ROW

CELLS/PANEL : 252
WGT/PANEL : 426 GRAMS
PANELS/BAY : 308,208
PANELS/SATELLITE : 78,208,736



NO SCALE

D180-22876-7

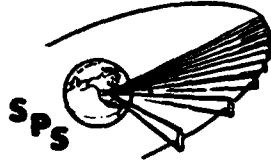
PHOTOVOLTAIC REFERENCE CONFIGURATION—PANEL TO ARRAY ASSEMBLY

Shown here is the way panels would be assembled to form larger elements of the solar array. The interconnecting tabs of one panel are welded to the tabs of the next panel in the string, and then the interconnections are covered with a tape that also carries structural tension between panels. After joining, the panels are accordion-folded into a compact package for transport to the low-Earth-orbit assembly station.

The 0.5 cm spacing between panels provides room for the welding electrodes, and also permits reasonable tolerances in the large sheet of 75 μm glass that covers the cells and the 50 μm sheets of substrate glass.

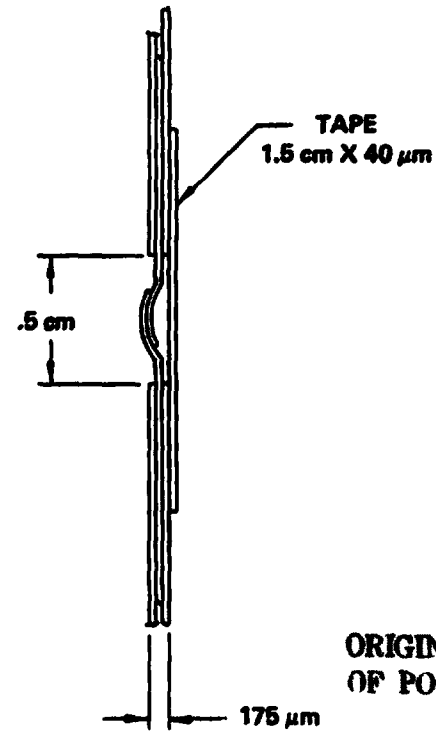
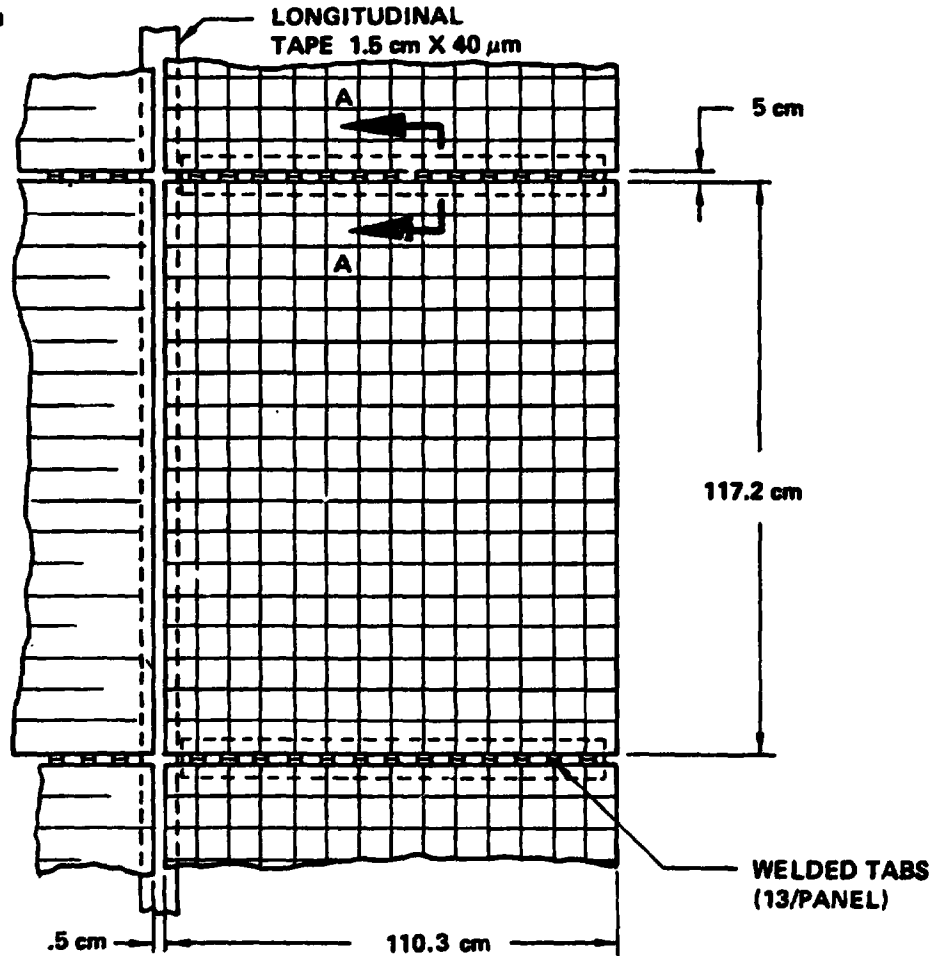
**ORIGINAL PAGE IS
OF POOR QUALITY**

Photovoltaic Reference Panel to Array Assembly



BEING _____

SPS-1391



SECT A-A

**ORIGINAL PAGE IS
OF POOR QUALITY**

D180-22876-7

PHOTOVOLTAIC REFERENCE-SOLAR ARRAY ARRANGEMENT AND ATTACHMENT

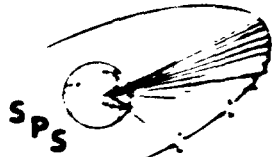
This illustration shows a typical 660 meter bay and the method by which the solar cell blankets are supported within the bay.

The solar array panels are supported by a main web support system which attaches to the satellite structure at 20 meter intervals around the perimeter of the 660 meter bay. Further web support is provided by the catenary.

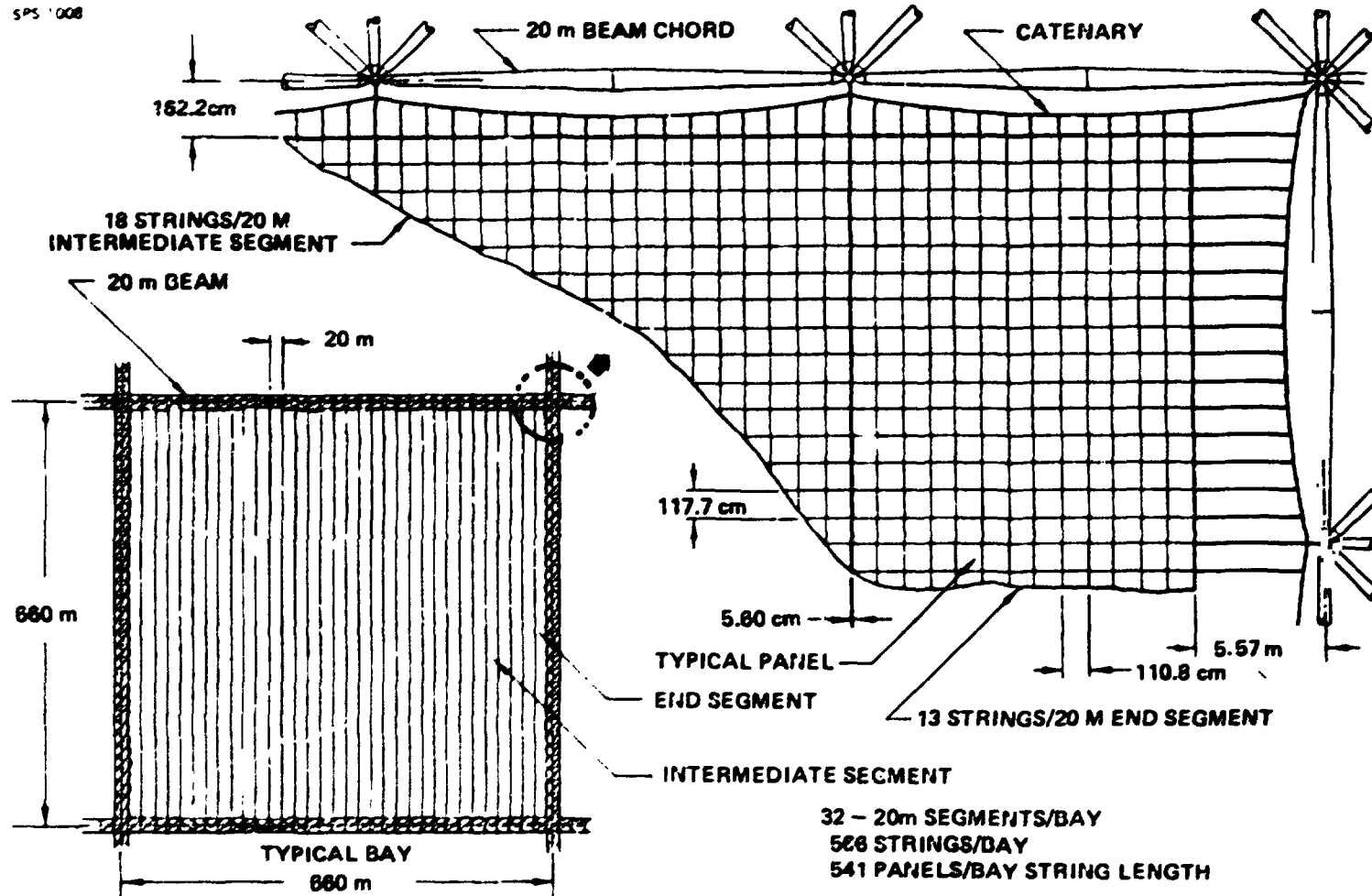
Thermal expansion and contraction are accommodated by use of a spring loaded piston cylinder that provides a constant force to the solar array support system. This arrangement also provides for a movement of up to 2 meters, in both x and y directions, which may occur due to LEO-GEO transfer acceleration of 10^{-4} g.

D180-22876-7

Photovoltaic Reference Solar Array Arrangement and Attachment



SPS 1008



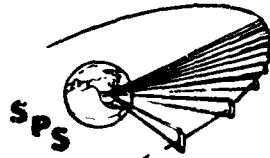
D180-22876-7

PHOTOVOLTAIC BLANKET WEIGHT BUILDUP

The top of the chart shows the weights for the solar array blanket as reported at the time of the Part I final presentation. These weights were based on a blanket having Kapton as a substrate.

Our latest blanket design is compatible with thermal annealing of radiation damage, resulting in a significant reduction in array area and consequently array weight and cost. The annealable blanket has a 50 μm glass substrate, electrostatically bonded to the solar cells to avoid adhesives and plastics that can be degraded by thermal annealing. The silicon solar cells are 50 μm thick, and the cell covers are 75- μm thick borosilicate glass, electrostatically bonded to the cells. Interconnections are printed on the substrate glass prior to bonding.

**ORIGINAL PAGE IS
OF POOR QUALITY**



D180-22876-7

Photovoltaic Blanket Weight Buildups

BOEING

SPS-1012

SILICON SOLAR CELL BLANKET WEIGHT @ PART I FINAL

ITEM	DENSITY (S.G.) (g/m ² /MIL)	THICKNESS (MILS)	AREA FACTOR	WEIGHT (g/m ²)
COVERS—FUSED SILICA	2.20	56.88	2.00/3.00	107.96/161.94
CELLS—SILICON	2.36	59.94	4.00	231.61
INTERCONNECTS—COPPER	8.94	227.08	0.50	22.71
SUPPORTING FILM—KAPTON*	1.42	36.07	2.00	32.46
ADHESIVE, CELLS TO FILM	1.40	35.56	0.50	16.00
ADHESIVE, KAPTON TO KAPTON	1.40	35.56	0.50	14.22
				62.68

8 MILS	2 MILS COVER	} 2 MILS BLANKET & INTERCONNECT	THEORETICAL WEIGHT	424.96/478.94
	4 MILS CELL		TOLERANCES & INSTALLATION (15 %)	63.74 / 71.86
			ESTIMATED ACTUAL WEIGHT	488.7/550.8

AVAILABLE BLANKET @ PART II MIDTERM

COVERS—FUSED SILICA	2.20	56.88	3.0	1.0	167.64
CELLS—SILICON	2.36	59.94	2.0	0.9607	115.17
INTERCONNECTS—COPPER	8.94	227.08	.5	0.100	11.35
SUBSTRATE—FUSED SILICA	2.20	56.88	2.0	1.0	111.76

7 MILS	3 MILS COVER	} 2 MILS SUBSTRATE & INTERCONNECTS	THEORETICAL PANEL WEIGHT	405.92
	2 MILS CELL		TOLERANCES ALLOWANCE (5%)	20.30
			ESTIMATED PANEL WEIGHT	426.22
			PANEL AREA FACTOR (.9913)	422.51
			SEGMENTS AREA FACTOR (.9972)	421.33
			JOINT/SUPPORT TAPES	2.93
			CATENARY SYSTEM	2.52
			ESTIMATED ARRAY WEIGHT	426.78

CELL AREA = 380,264 m²/BAY
 PANEL AREA = 395,843 m²/BAY
 ARRAY AREA = 400,434 m²/BAY
 NO. OF BAYS = 256

ORIGINAL PAGE IS
OF POOR QUALITY

PHOTOVOLTAIC REFERENCE CONFIGURATION—POWER COLLECTION

Long solar cell strings were adopted for the reference configuration to permit generating the required voltage, around 40 kV, directly from the solar array without intervening power electronics. The string length is around 5.1 km.

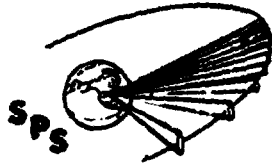
Current generated by the solar cells can be carried by conductors or by the solar cells themselves. The configuration shown here uses the solar cells to the maximum possible extent for carrying the current. It will be noted that no conductors are needed for bringing in the current from the edges of the array, the solar-cell strings being arranged in loops which start from one center bus, loop around the edge of the array, and return to the other bus at the center of the array.

Solar array power is controlled by vacuum circuit breakers near the buses. Voltage is controlled by turning groups of strings on or off, depending on load requirements.

Two sections of the array provide the required voltage at the slip-rings using the sheet conductor voltage drop to achieve the required voltage at the slip-rings. All solar cell strings are of the same design.

Power source 'A' provides power directly to the fifth stage of the Klystron depressed collector. Power source 'B' provides power directly to the fourth stage of the Klystron depressed collector and to the MPTS dc/dc converters which supply all other Klystron element power requirements.

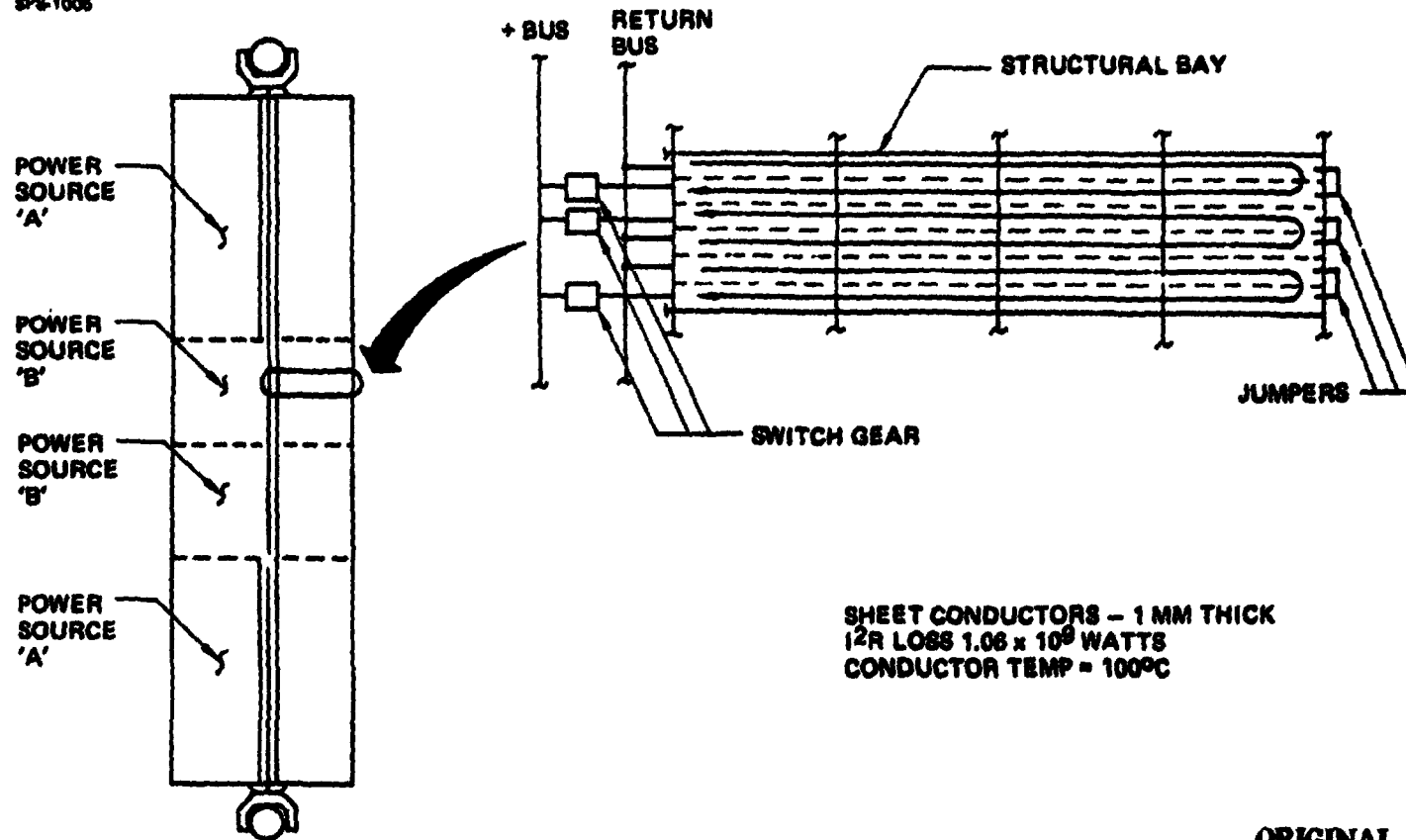
D180-22876-7



Photovoltaic Reference Power Collection

SPS-1006

BOEING



SHEET CONDUCTORS - 1 MM THICK
 I^2R LOSS 1.06×10^9 WATTS
CONDUCTOR TEMP = 100°C

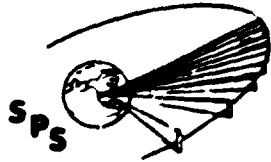
ORIGINAL PAGE IS
OF POOR QUALITY

D180-22876-7

ANTENNA SUPPORT AND MECHANICAL JOINT AND WEIGHTS

The Antenna Support structure and mechanical rotary joint are the structural interfaces between the basic satellite structure and the antenna yoke structure while providing for the 360° rotation of the antenna.

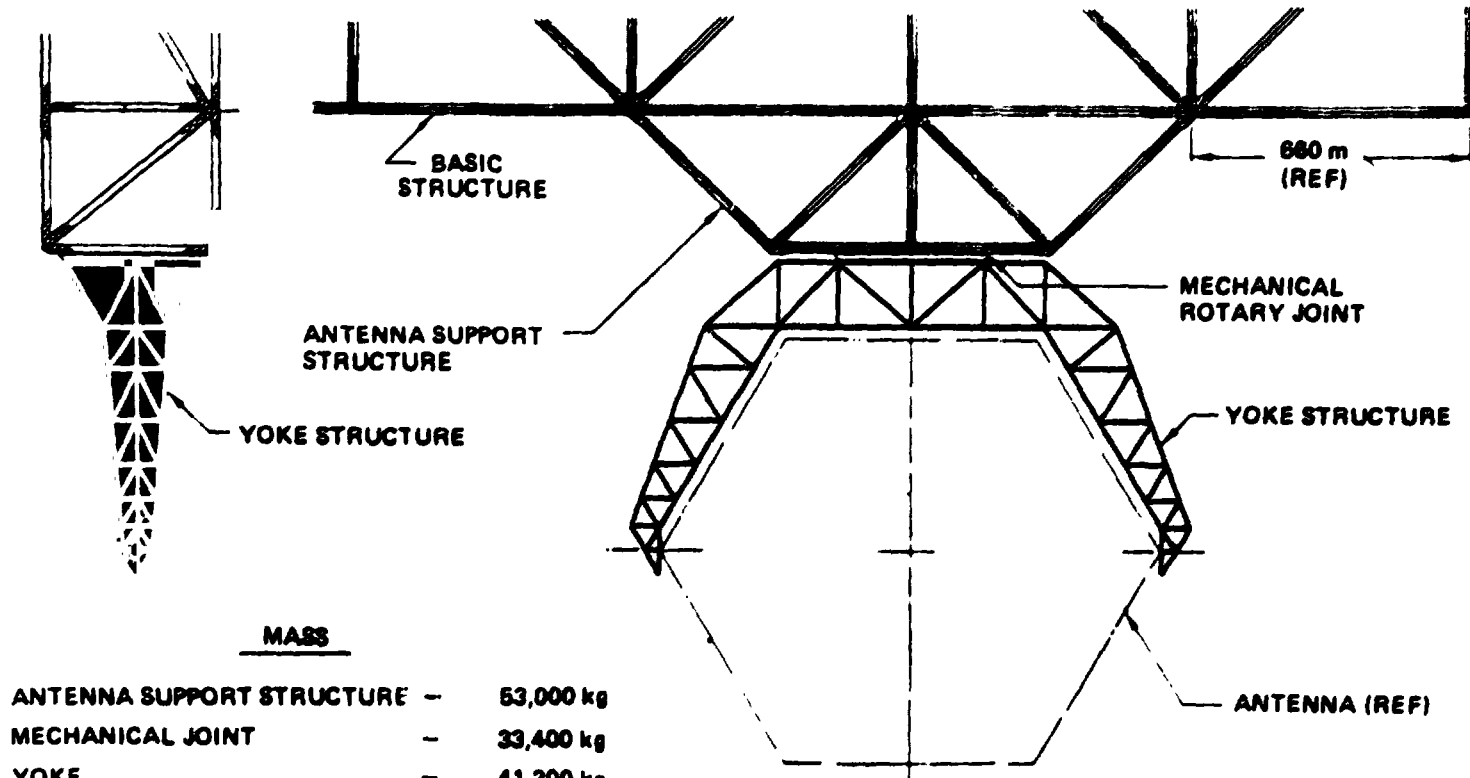
The Electrical Slip Rings are mounted at the center of the mechanical rotary joint and provide for energy transfer across the rotating connection. Flexible conductors provide for energy transfer across the elevation joint on the antenna yoke.



SPS-1018

Antenna Support and Mechanical Joint Weights

BOEING



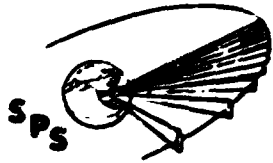
<u>MASS</u>	
ANTENNA SUPPORT STRUCTURE	- 53,000 kg
MECHANICAL JOINT	- 33,400 kg
YOKE	- 41,200 kg
TOTAL	- 127,600 kg

ORIGINAL PAGE IS OF POOR QUALITY

D180-22876-7

ROTARY JOINT AND MASS

The diameter of the rotary joint which was first designed was 350 meters. Subsequent analysis of the silver required for the con silver slip ring showed that over 5% of the silver reserves (known and projected) was required for large slip rings. The smaller design shown was developed to 1) reduce the required materials, and 2) to fit into the launch vehicle payload envelope. This will enable earth fabrication and check-out of the electrical slip ring prior to launch.



D180-22876-7

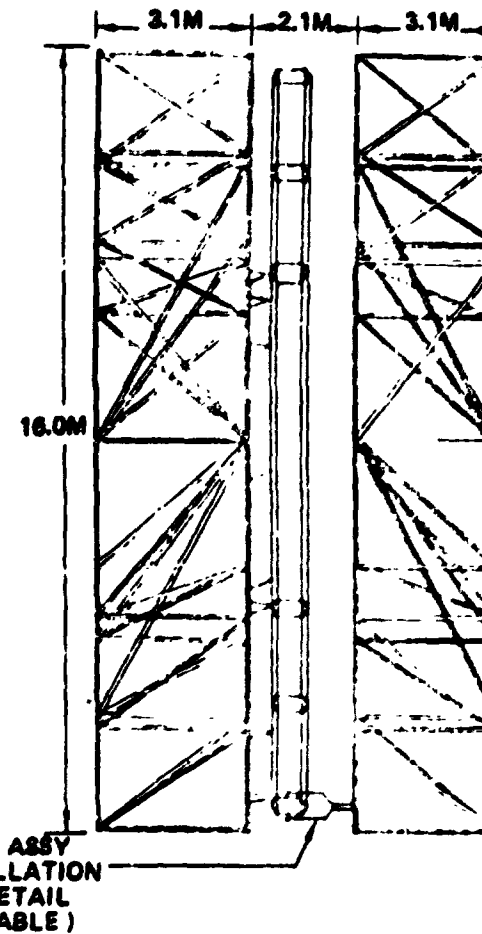
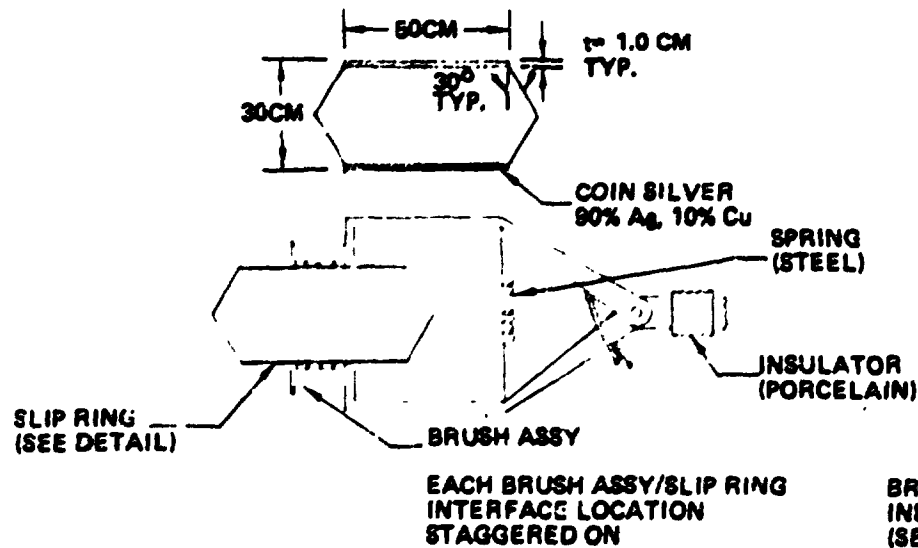
Electrical Rotary Joint and Mass

SPS-1022

BOEING

ELECTRICAL ROTARY JOINT MASS SUMMARY

SLIP RINGS	- 11,810 kg
BRUSH ASSEMBLY	- 1,970 kg
FEEDERS	- 3,840 kg
STRUCTURAL SUPPORT	- 900 kg
ASSY. & INSTL. HARDWARE	- 200 kg
CONTINGENCY ALLOWANCE	- 900 kg
TOTAL	- 19,800 kg

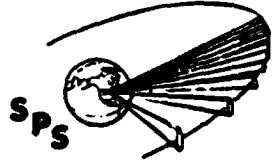


D180-22876-7

REFERENCE PHOTOVOLTAIC INSTRUMENTATION AND CONTROL SYSTEMS

A preliminary Instrumentation and Control list was compiled for the power generation, distribution, and transmission systems. A summary of the number of items in each major category for the power generation and distribution systems is shown.

**ORIGINAL PAGE IS
OF POOR QUALITY**



SPS-1699

D180-22876-7

Reference Photovoltaic Instrumentation and Controls

BOEING

	CONTROLS	INSTRUMENTATION
POWER GENERATION		
POWER SECTORS		1,152
SOLAR ARRAY STRINGS		36,224
POWER DISTRIBUTION		
SWITCH GEAR	420	1,680
MAIN BUS		4
ROTARY JOINT	104	149
DC-DC CONVERTERS		70
TOTALS*	524	39,279

ORIGINAL PAGE IS
OF POOR QUALITY

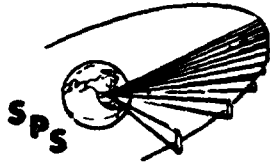
*DOES NOT INCLUDE STATIONKEEPING, HOUSEKEEPING, OR ENVIRONMENTAL CONTROL AND MONITORING SYSTEMS.

D180-22876-7

PHOTOVOLTAIC REFERENCE-ATTITUDE CONTROL

For an orientation perpendicular to the orbital plane the photovoltaic SPS attitude control equipment and propellant masses are listed along with the assumptions used in the calculations. A control authority margin of 20 percent was used in these calculations.

It was noted that the chemical propulsion requirement during equinoctial occultations resulted in a small mass penalty.



SPS-1023

D180-22876-7

Photovoltaic Reference Attitude Control

BOEING

THRUST PRODUCTION EQUIPMENT	23.3 MT
POWER PROCESSORS	90.0 MT
INSTALLATION HARDWARE	16.8 MT
NON REOCCURRING TOTAL	<u>130.1 MT</u>
ANNUAL PROPELLANT (ARGON)	48.0 MT/YEAR
1-YEAR TOTAL	<u>178.1 MT</u>

ASSUMPTIONS:

OPTIMIZED $I_{sp} \sim 20,000$ SEC

SINUSOIDAL DUTY CYCLE (50 MW PEAK, 32 MW AVG)

PERFECT CONTROL LAWS (NO WASTED PROPELLANT)

CHEMICAL PROPULSION FOR CONTROL IN EQUINOCTAL OCCULTATIONS
($I_{sp} \sim 400$ SEC REQUIRES 1.0 TO 1.5 MT/YEAR PROPELLANT)

D180-22876-7

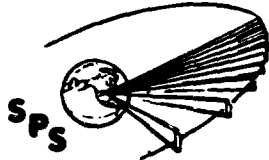
ANNUAL POWER VARIATION

The power output of a solar array depends on the intensity of illumination at the cells and the temperature of the cells, the maximum-power point of cells diminishing as the cells become hotter. In geosynchronous orbit the temperature of the solar cell is related to the intensity of sunlight for any given panel configuration.

The sun is brightest at its perihelion, which occurs around winter solstice when the orientation of the array is such that the sun's rays arrive at 23.5 degrees off of normal incidence. The worst-case illumination is at summer solstice where the 23.5-degree misorientation is accompanied by aphelion where the intensity of sunlight is 0.967 of average. However, the solar array temperature is also down, being 36.5°C rather than 46.0°C as at the spring and autumn equinoxes.

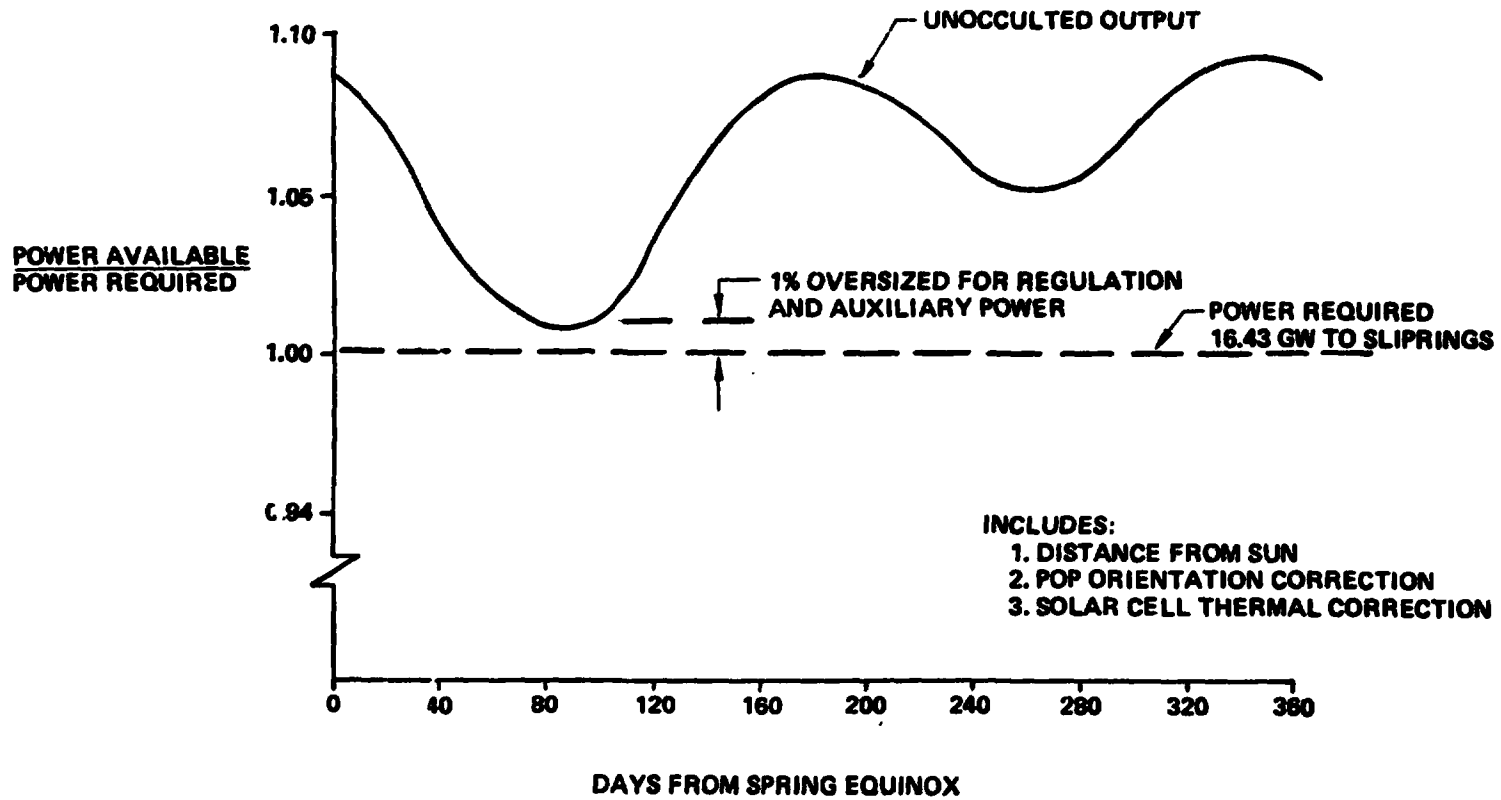
D180-22876-7

Annual Power Variation



SP8-1637

BOEING



PHOTOVOLTAIC REFERENCE CONFIGURATION NOMINAL MASS SUMMARY

The structural mass difference from previous analysis reflects a change in the structural concept and integration of the new sizing criteria for the Photovoltaic reference SPS. An all tubular beam section is now being used instead of a flat-tape, diagonally-stabilized, beam section used previously. The secondary structure has been incorporated into the primary structure. The bay size and member dimensions have been changed to be compatible with the new reference system.

The mechanical systems mass is composed of the mechanical rotary joint.

Investigation of the gravity-gradient torques and optimization of thrust I_{sp} led to a decrease in control system mass.

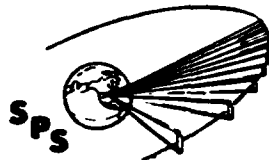
The mass of the solar cell blankets decreased due to a new blanket design consisting of 3.0 mil cover-glass, 2.0 mil silicon solar cells, and 2.0 mil silica substrate. Solar cell blanket decrease also resulted from lower radiation degradation of the 2.0 mil silicon solar cells.

The increase in power distribution system mass reflects a change from the no longitudinal bus bar configuration to no lateral bus bars and includes energy storage equipment.

The increase in MPTS mass reflects the inclusion of energy storage for antenna systems.

The growth used was 26.6% on the final configuration. This growth was the result of the uncertainty analysis that was performed.

**ORIGINAL PAGE IS
OF POOR QUALITY**



D180-22876-7

Photovoltaic Reference Configuration Nominal Mass Summary Weight in Metric Tons

SPS-1847

CR-2 (10 GW B.O.L.)

CR-1 (10 GW MINIMUM/30 YRS)

BOEING

COMPONENT	ORIENTATION	MIDTERM	CR-2 (10 GW B.O.L.)		CR-1 (10 GW MINIMUM/30 YRS)	
			PART I FINAL	PART I FINAL	PART II MIDTERM	PART II FINAL
1.0 SOLAR ENERGY COLLECTION SYSTEM	(38,616)	(59,313)	(49,512)	(56,357)	(56,184)	51,782
1.1 PRIMARY STRUCTURE	2,493	14,970	8,000	2,334	6103	5385
1.2 SECONDARY STRUCTURE	189	209	209	209	-	-
1.3 MECHANICAL SYSTEMS	40	40	40	40	67	67
1.4 MAINTENANCE STATION	85	-	-	-	-	-
1.5 CONTROL	340	340	340	340	150	178
1.6 INSTRUMENTATION/ COMMUNICATIONS	4	4	4	4	4	4
1.7 SOLAR-CELL BLANKETS	25,746	37,582	34,111	51,897	47,319	43,750
1.8 SOLAR CONCENTRATORS	5,149	2,978	3,276	-	-	-
1.9 POWER DISTRIBUTION	2,570	3,180	3,532	1,589	2451	2398
2.0 MPTS	15,371	15,371	15,371	15,371	(24,384)	25,212
SUBTOTAL	51,967	74,684	64,883	71,728	80,568	76,994
GROWTH (26.8%)	25,994	37,342	32,442	35,864	20,142	20,480
TOTAL	77,961	112,026	97,325	107,592	100,710	97,474

ORIGINAL PAGE IS
OF POOR QUALITY

D180-22876-7

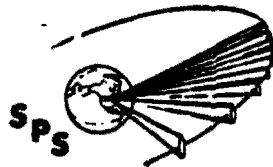
MASS/SIZE UNCERTAINTY ANALYSIS

An important part of this section of the study was to provide the results of the uncertainty analysis that was performed on the reference photovoltaic SPS. A plot of the results of the uncertainty analysis on size and mass is shown.

It should be noted that the reference point design had a rectenna output of 9.2 Gw instead of the 10.0 Gw that the uncertainty ellipses use. This was caused by a freeze in the energy transmission power requirements at the Part II mid term, to allow a more in-depth sizing analysis of the energy conversion systems. After this was done, changes occurred in the transmission system that lowered the rectenna output to 9.2 Gw.

The mass growth used in final mass summary was the mass growth shown on the uncertainty plot between the reference point design and the uncertainty analysis most probable mass point.

ORIGINAL PAGE IS
OF POOR QUALITY

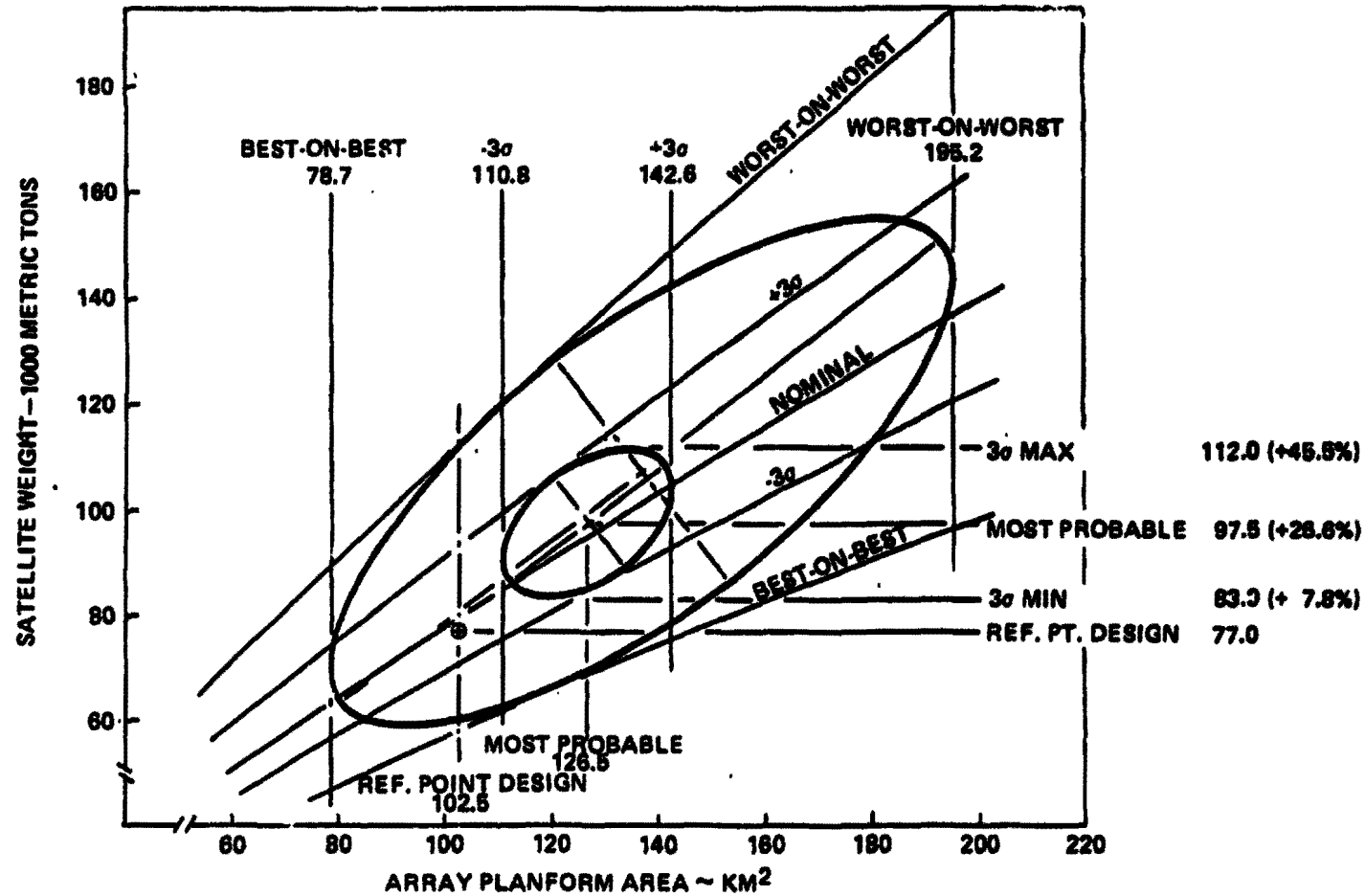


D180-22876-7

Mass/Size Uncertainty Analysis Results

SPS-1679

BRIND

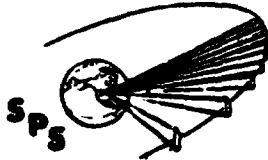


D180-22876-7

REFERENCE PHOTOVOLTAIC FINAL COST SUMMARY

The cost analysis on the photovoltaic SPS used a parametric cost model (PCM) to project the *theoretical first unit (TFU) cost*. A mature industry projection was applied to the TFU along learning curves to estimate the system costs for the various schemes shown.

The LEO construction advantage is readily seen along with the advantages of increased production rates.



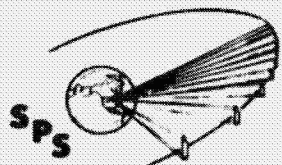
Reference Photovoltaic Final Cost Summary

SPS-1538

BOEING

WBS	NAME	1 SPS PER YEAR		4 SPS's PER YEAR	
		LEO CONST.	GEO CONST.	LEO CO' ST.	GEO CONST.
A1.01.01.00	MULTIPLE/Common PROD. COST (\$ x 10 ⁻⁶)	897	793	760	661
A1.01.01.01	ENERGY COLLECTION N/A	—	—	—	—
A1.01.01.02	ENERGY CONVERSION PROD. COST (\$ x 10 ⁻⁶)	3731	3588	2793	2686
A1.01.01.03	POWER DISTRIBUTION PROD. COST (\$ x 10 ⁻⁶)	138	133	82	79
A1.01.01.04	MPTS PROD. COST (\$ x 10 ⁻⁶)	2676	2676	1952	1952
SUB TOTAL (\$ x 10 ⁶)		7442	7190	5587	5378
INSTALLATION COST (\$ x 10 ⁻⁶)		7554	10906	5297	7648
TOTAL COST * (\$ x 10 ⁻⁶)		14,996	18,096	10,884	13,026

*INTEREST NOT INCLUDED

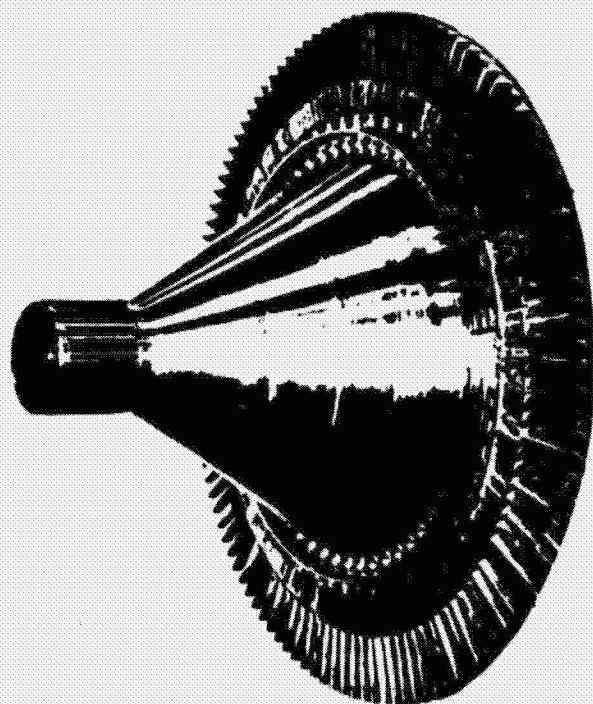


D180-22876-7

Thermal Engine SPS

SPS-1141

BOEING



PRECEDING PAGE BLANK NOT FILMED

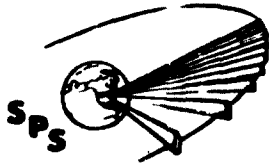
D. L. Gregory

Thermal Engine SPS

D180-22876-7

SUMMARY

Of the thermal engine systems studied, the potassium Rankine is the lightest near-term technology SPS option. Our study results show it to be lighter, with this technology, than steam Rankine, helium Brayton or thermionic SPS systems. In the area of solar concentrators, we had previously anticipated approximately 30% degradation in the baselined 30 year life of the SPS. More recent data has however, indicated that little or no degradation should be expected. Therefore, none has been baselined. An investigation of potential materials for thermal engine SPS usage has indicated that some of the best materials are in short supply. However, suitable options exist and these have been baselined. We have selected a turbine sizing of 32 megawatts. At this size, 576 turbines are required for a 10 GW output SPS. This turbine size is approximately that of the SST engine partially developed by General Electric for the American SST program, and is appropriate to the national fabrication capability. By the use of relatively small heat pipes it has been possible to configure a radiator system which is sufficiently immune to meteoroid penetration. At the end of this study phase we indicate that the mass of the thermal engine SPS is approximately 80,000 metric tons and that the average cost for one SPS at a rate of four per year is approximately 18 billion dollars or 1,800 dollars per kilowatt produced on the ground.



SPS-1501

D180-22876-7

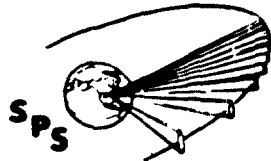
Summary

BOEING

- THE POTASSIUM RANKINE OFFERS THE LIGHTEST NEAR TERM THERMAL ENGINE SPS
- A PASSIVE SOLAR CONCENTRATOR WITHOUT ANTICIPATED DEGRADATION HAS BEEN BASELINED
- PROVEN, AVAILABLE MATERIALS ARE USED.
- A TURBINE SIZING OF 32 MW OUTPUT PERMITS MANUFACTURE BY ONLY A MODESTLY EXPANDED INDUSTRY.
- A HEAT PIPE RADIATOR SYSTEM HAS ADEQUATE METEOROID RESISTANCE
- THE SATELLITE MASS IS APPROXIMATELY 80,000 METRIC TONS
- THE SATELLITE COST FOR 112 UNITS IS ABOUT \$ 18B EACH

A RANGE OF THERMAL CONVERSION SYSTEMS WAS INVESTIGATED

The steam rankine SPS would be an extremely heavy option. This is primarily because the maximum turbine inlet temperature is in the neighborhood of 1,000 to 1,100 degrees Fahrenheit and the heat rejection temperature is near the condensation point of water. Consequently, the carnot efficiency is low and the realizable efficiency is even lower. Thermionic systems are also very heavy. This is because thermionic diodes and the interelectrode busbars required to connect them are heavy and the radiator system required for excess heat rejection from the thermionic diodes is also quite heavy. The Brayton SPS i.e. a helium closed cycle system, is a near competitor to the potassium Rankine system. However, it is only competitive in mass with very high turbine inlet temperatures, in the vicinity of 1,600 K i.e. 2,500°F. This turbine inlet temperature is only achievable with ceramic materials such as silicon carbide. This material is now in development but is not considered to be appropriate for baseline SPS use. We have emphasized the potassium Rankine SPS in Part II of this study and details of the results are concluded in the remainder of this presentation.



SPS-1502

D180-22876-7

A Range of Thermal Conversion Systems Was Investigated

BOEING

STEAM RANKINE

EXTREMELY HEAVY

THERMIONICS

VERY HEAVY

BRAYTON

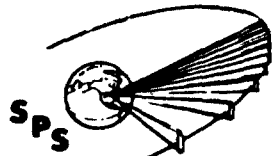
BEST WITH ADVANCED TECHNOLOGY

POTASSIUM RANKINE

EMPHASIZED

TECHNOLOGY TRENDS

In Part I of this study we put primary emphasis on the closed cycle helium Brayton system with very high turbine inlet temperatures achieved by the use of ceramic turbines. Also during Part I we were studying potassium rankine, steam rankine and thermionic systems. The potassium Rankine system was seen as the closest competitor to the Brayton. However, it was not until near the end of the Part I study that the temperature optimization of the potassium rankine system was completed. When the optimum cycle temperature ratio was identified it was found that the potassium rankine system was lighter than the Brayton SPS even with relatively modest turbine inlet temperatures for the Rankine SPS. Investigation of appropriate materials for the potassium rankine SPS led to the selection of a turbine inlet temperature of 1,242 K (1776°F).



SPS-1503

D180-22876-7

Technology Trends

BOEING

STUDY PART 1

SYSTEMS WITH HIGH TECHNOLOGY:

- TURBINE INLET TEMPERATURES TO 1850K (2510°F)
- SILICON CARBIDE TURBINE ASSEMBLIES

STUDY PART 2

SYSTEMS WITH LESS ADVANCED TECHNOLOGY:

- TURBINE INLET TEMPERATURES TO 1242K (1776°F)
- NIOBIUM/MOLYBDENUM TURBINE ASSEMBLIES

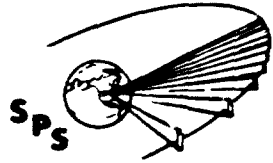
DUE TO INCORPORATION OF POTASSIUM RANKINE SYSTEM
WITH PROPER CYCLE TEMPERATURE RATIO, PART 2
SYSTEMS ARE LIGHTER THAN PART 1

D180-22876-7

REFERENCE RANKINE SPS DESIGN

A plan view of the thermal engine SPS is shown. This satellite has two 5 GW output rectennas located on the north-south axis of the satellite. The satellite is divided into 16 modules each of which has 36 turbogenerators, for a total of 576 per SPS. The satellite flies in a perpendicular-to-ecliptic plane orientation at all times.

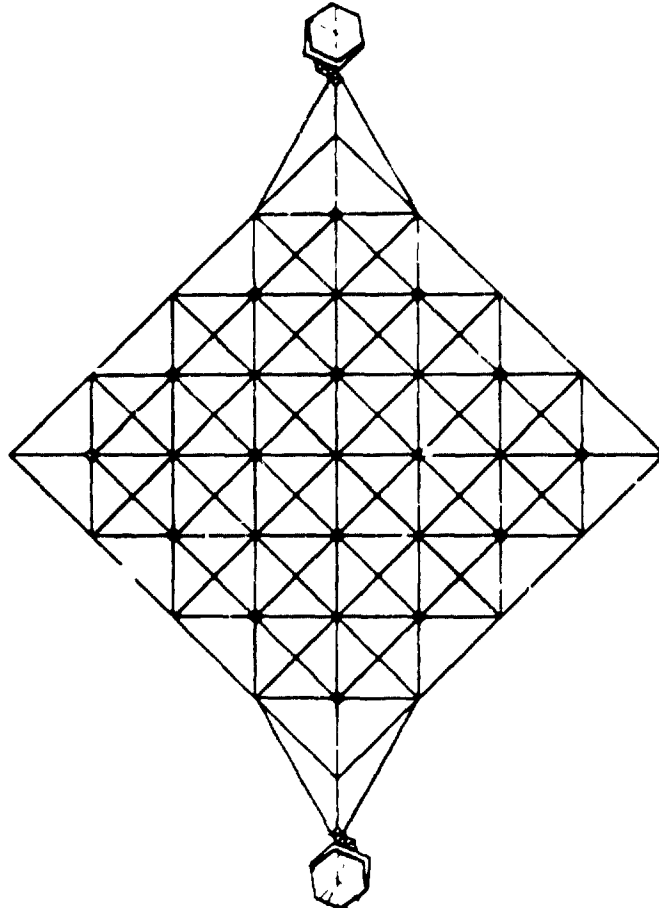
D180-22876-7



Reference Rankine SPS Design

SPS-1508

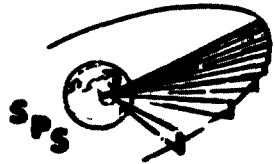
BOEING



- GROUND OUTPUT: MINIMUM OF 10 GW (TWO ANTENNAS)
- POTASSIUM RANKINE TURBINES (576/SPS)
- 16 MODULES
- "P.E.P." ORIENTATION
- CONCENTRATOR AREA: 119 km²
- SYSTEM MASS

RANKINE CYCLE SCHEMATIC

The working fluid in the potassium rankine loop is potassium vapor in a portion of the loop and liquid potassium in the remainder. Liquid potassium is introduced into the heat absorber tubes of the boiler located within the high temperature cavity absorber. Boiling produces potassium vapor which passes through the turbine and does the work of turning the generator which produces the useful power required for the SPS microwave transmitter and the power required to drive the electromagnetic pump. Potassium vapor leaving the turbine is cooled by the expansion in the turbine. It is introduced into the radiator system where it flows through the vapor manifold into potassium throughpipes which are cooled by sodium heat pipes. Condensation occurs in the throughpipes so that liquid potassium is collected in the radiator outlet manifold and flows to the electromagnetic pump.

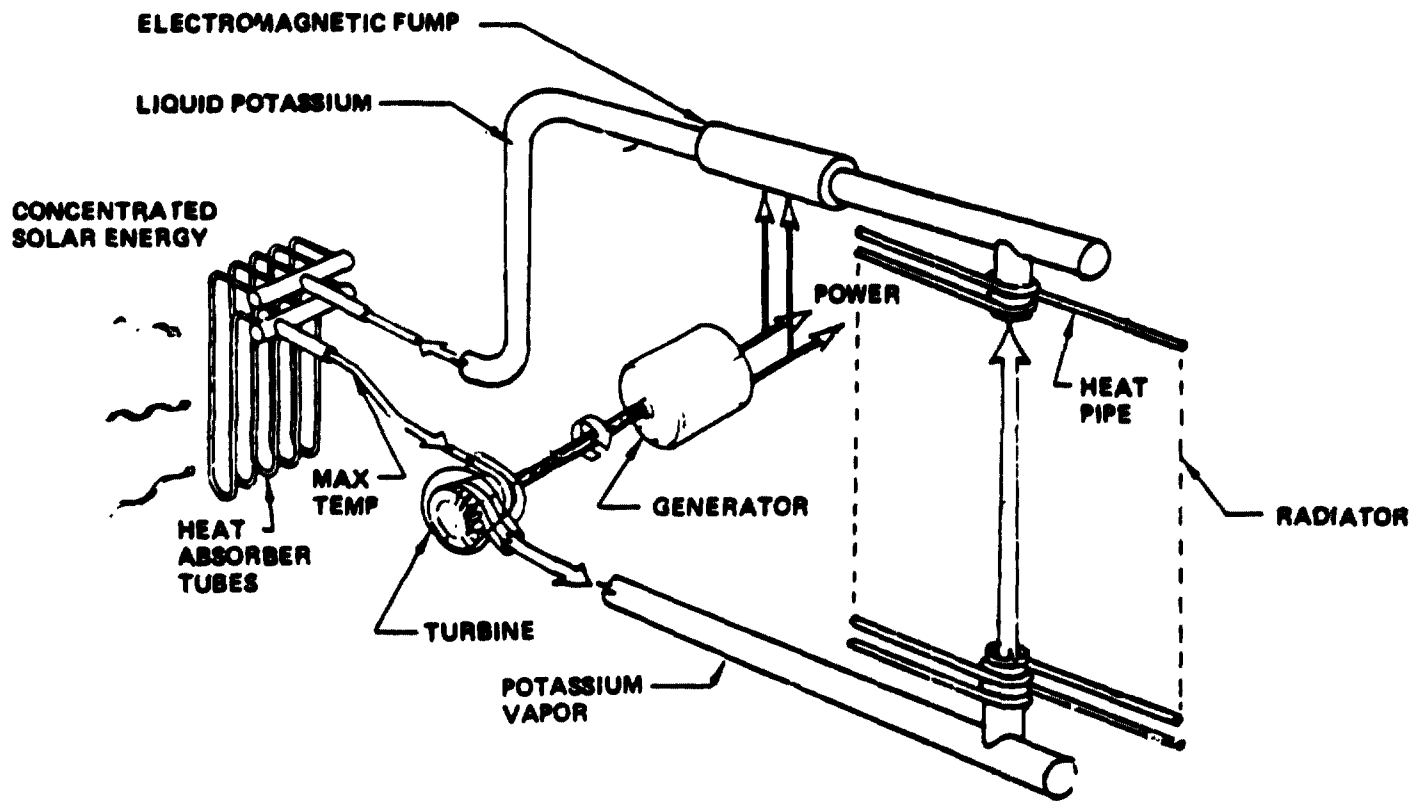


D180-22876-7

Rankine Cycle Schematic

SPS-1804

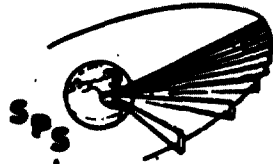
ORION



DATA BASE DRAWS HEAVILY ON DEMONSTRATED TECHNOLOGY

The General Electric Corporation, our subcontractor for Rankine turbines, produced the data shown on this chart. We have baselined a turbine efficiency of 80%. This was demonstrated in tests in the late 1960's at the Lewis Research Center. The 80% figure is probably quite conservative for large potassium turbines. In the area of erosion control three promising methods were demonstrated in the Lewis test. A total of nearly 800,000 hours of testing was accumulated relative to potassium systems. Note that this includes a total of more than 10,000 hours of running tests on turbines and more than 10,000 hours of electromagnetic feed pump testing.

Data Base Draws Heavily on Demonstrated Technology (General Electric Data)



SPS-1808

BEING

TURBINE EFFICIENCY: 80%; LeRe TESTS

EROSION CONTROL: THREE METHODS DEMONSTRATED

POTASSIUM HARDWARE:

	Potassium (800,000 hours testing)						Cesium (>23,000 hours testing) (b)	
	AirResearch	GE	JPL	NASA-Lewis	ORNL	PtW		Other ^a
	Testing hours accumulated							
Corrosion test systems:								
Boiling	1300	25 500	-----	-----	62 800	12 000	-----	3500
All-liquid	-----	-----	-----	-----	-----	-----	156 000	-----
Component test systems, boiling	5900	19 600	-----	1000	2 800	4 900	300	2400
Simulated powerplant systems	-----	-----	~1000	-----	10 200	-----	-----	-----
Boilers	7200	40 100	1000	1000	75 800	16 900	300	6000
Turbines	3050	10 100	-----	-----	5 000	-----	100	-----
Boiler feed pumps:								
Electromagnetic	7200	34 600	3600	1000	26 900	4 900	3 300	3600
Turbine driven	-----	-----	-----	-----	5 000	-----	-----	-----
Other pumps	5900	18 600	3600	1600	6 100	1 300	57 600	-----
Condensers	7200	40 100	~1000	1600	75 800	16 900	300	3600
Seals	3050	10 100	-----	-----	-----	-----	-----	-----
Bearing tests	3000	-----	-----	-----	4 500	-----	1 600	-----

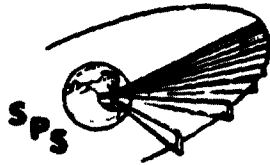
^aIncludes testing hours of Aerojet Nuclear, Allison, Rocketdyne, United Nuclear.

^bIncludes testing hours of Brookhaven, Aerojet Nuclear, Westinghouse Astronuclear.

ORIGINAL PAGE IS OF POOR QUALITY

MATERIAL AVAILABILITY

The abundance data given on this chart were drawn from Department of Interior publications for 1973. The first of the general rules shown states that since solar power satellites will not be available in large quantities until after the year 2000 it appropriate that we baseline materials that will still be sufficiently abundant in that time period. Our baseline SPS quantity for this study was 112 units, probably sufficient for U.S. electrical needs in the early part of the 21 century. However, more units may ultimately be required for the United States, and up to a 1000 units or more for the world. Therefore, it is probably appropriate that we do not baseline for SPS use a material such that 112 satellites would use over 5% of any world material resource. Rule 3 tends to minimize the impact of SPS incorporation and the concomitant industrialization required. Turbine wheels and blades for potassium Rankine turbines are baselined as using molybdenum, a wrought material. Silicon carbide could also be used, however, this material is in its very early development stage and its probably too advanced to baseline. Turbine housing materials must be ductal and weldable. Tantalum alloys would be ideal, however world resources are not adequate. Therefore, we have selected niobium, also called columbium, for the baseline material. Cesium would be an ideal rankine cycle working fluid. It would result in the turbines having fewer stages and a smaller disc diameter. However, the supplies of cesium are clearly not adequate for large scale SPS usage. Potassium, an abundant material has been baselined.



D180-22876-7

Material Availability

SPS-1146

- GENERAL RULES: 1) MATERIAL TO BE PREDICTED TO BE "SUFFICIENTLY ABUNDANT" IN 2020.
- 2) SPS TO NOT USE OVER 5% OF WORLD RESOURCES OF ANY MATERIAL
- 3) CURRENT WORLD PRODUCTION RATE ADEQUATE FOR ONE SPS/YEAR

- TURBINE WHEEL/BLADE MATERIAL (NEED ~ 6000 MT/SPS)
(WROUGHT MATERIAL)

<u>MATERIAL</u>	<u>STATE OF ART</u>	<u>WORLD RESOURCES (MT)</u>	<u>PRODUCTION RATE (MT/YR)</u>
MOLYBDENUM (TZM)	DEVELOPED	29,000,000	91,000
SILICON CARBIDE	EARLY TEST	VERY ABUNDANT	VERY SMALL

- TURBINE HOUSING MATERIAL/BOILER TUBES (NEED 4000 TO 7000 MT/SPS)
(WELDABLE DUCTILE MATERIAL)

<u>MATERIAL</u>	<u>STATE OF ART</u>	<u>WORLD RESOURCES (MT)</u>	<u>PRODUCTION RATE (MT/YR)</u>
TANTALLUM (T111)	DEVELOPED	100,000	PERHAPS 1,000
NIوبيUM (C103)	DEVELOPED	17,000,000	ABOUT 20,000
SILICON CARBIDE	EARLY TEST	VERY ABUNDANT	VERY SMALL

- RANKINE CYCLE WORKING FLUID

<u>MATERIAL</u>	<u>STATE OF ART</u>	<u>WORLD RESOURCES (MT)</u>	<u>PRODUCTION RATE (MT/YR)</u>
CESIUM	DEVELOPED	100,000	≈ 8
POTASSIUM	DEVELOPED	> 10 ⁹	10,000,000

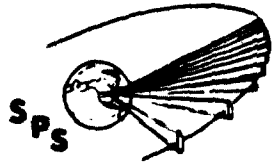
*MT = METRIC TON/SPS

MODULES CONSIST OF CONCENTRATOR AND FOCAL POINT ASSEMBLIES

The solar concentrator is made up of a structural system supporting a large number of plastic film reflector facets and is a segment of a sphere. The reflected light is concentrated into the focal point assembly which mounts to the concentrator by four cavity support arms. These arms are made up of graphite epoxy tube sections forming a 20 meter beam. The thruster systems required for self power transport to geosynchronous orbit in the LEO construction option are located at the 3 points shown.

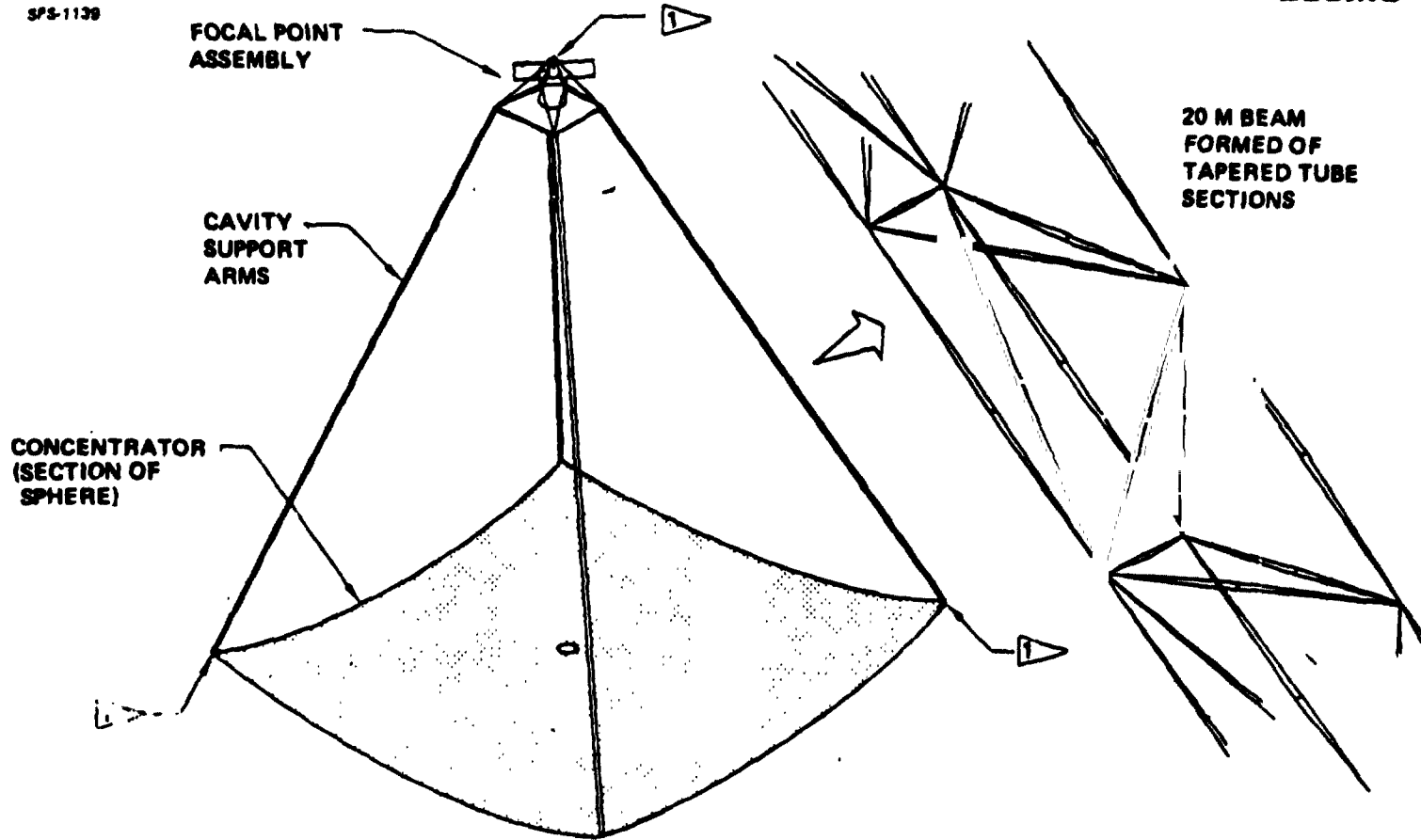
D180-22876-7

Modules Consist of Concentrator & Focal Point Assemblies



SPS-1139

BEING



FOCAL POINT ASSEMBLY

CAVITY SUPPORT ARMS

CONCENTRATOR (SECTION OF SPHERE)

20 M BEAM FORMED OF TAPERED TUBE SECTIONS



LOCATION OF ORBIT TRANSFER SYSTEM FOR SELF POWER (LOAD CONDITION IS $1 \times 10^{-4} g$ ORBIT TRANSFER)

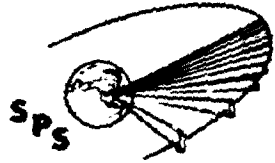
D180-22876-7

CONCENTRATOR FRAME ELEMENT

The concentrator structure which supports the reflector facets is made up of a large number of tetrahedral elements which are in turn composed of a number of tapered graphite epoxy tubes, jointed as shown. The graphite epoxy tubes can be nested to provide a high density payload for transportation.

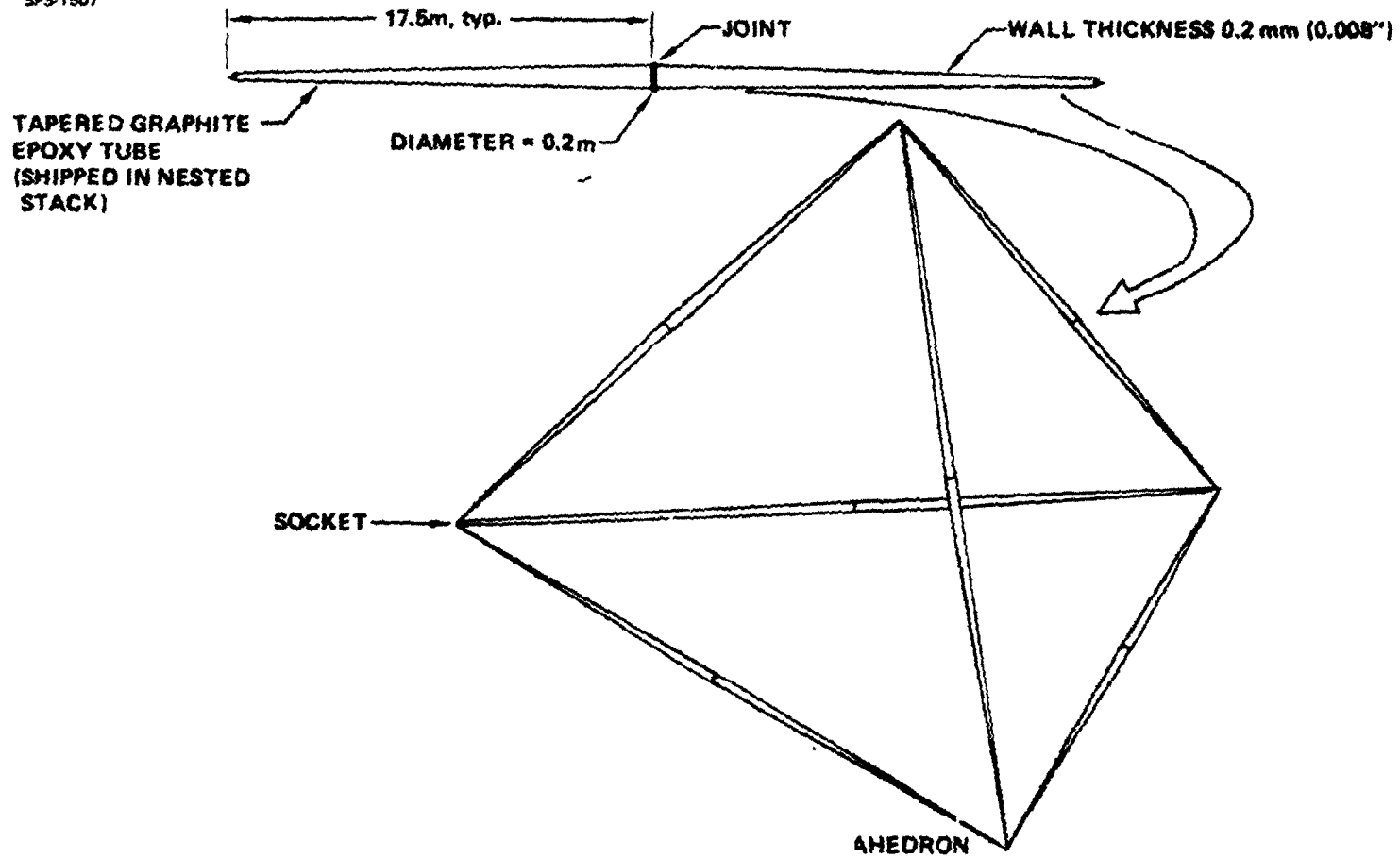
D180-22876-7

Concentrator Frame Element



SPS-1507

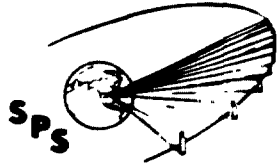
BEING



D180-22876-7

CONCENTRATOR FRAME

This is a photo of a "Toothpick Model" of a portion of the concentrator frame. It is seen that this structure is composed of repetitive tetrahedrons. A curved surface is required. This is formed by making the lower members of any tetrahedron larger than the upper members of the adjacent tetrahedron so that a bidirectional curvature is produced.

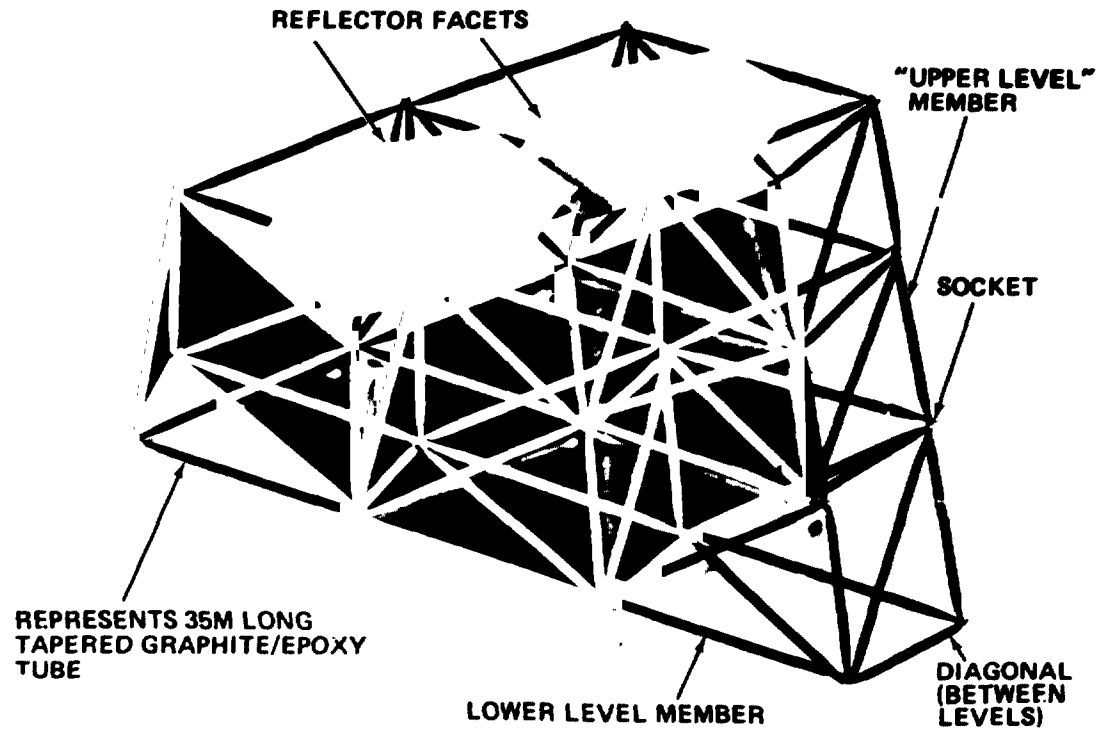


SPS-1296

Facet Support Structure

BOEING

(TOOTHPICK MODEL)

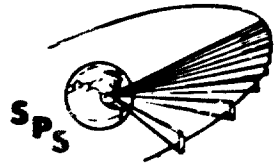


D180-22876-7

REFLECTOR FACET

The reflector facets are hexagons of thin aluminized Kapton. The Kapton is 3 micrometers thick. It is tensioned by 3 rigid end members, pulled outward by bridles. This tensioning system causes the three edge members to be coplanar, so that a flat reflector is produced. The rocker arm and spring canister systems which pull outward on the bridle are mounted to the concentrator frame. A "scallop" at the three free edges of the facet controls wrinkling at the facet edges.

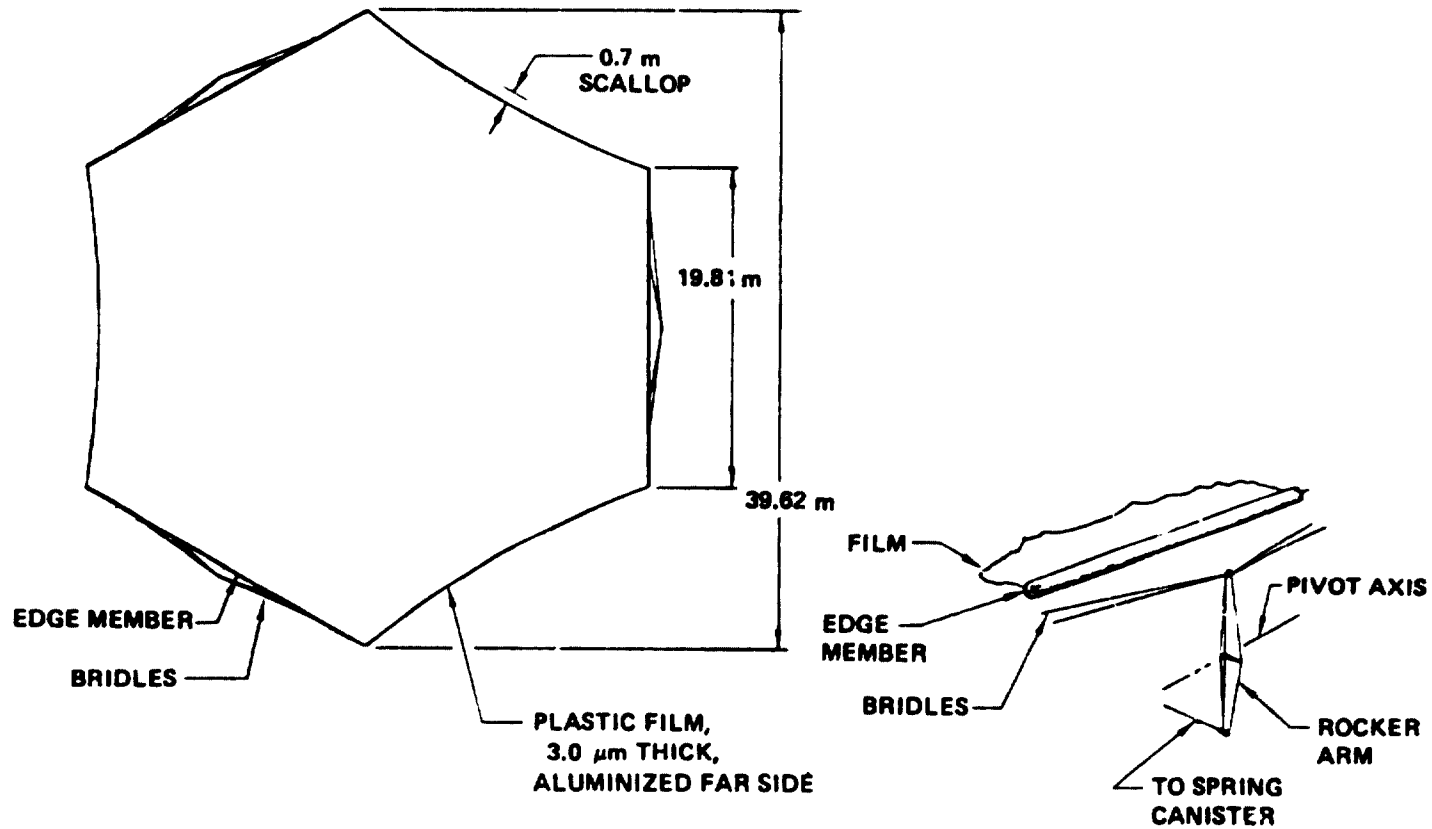
D180-22876-7



Reflector Facet 1000 M² of Reflecting Area

BOEING

SP3-1-64



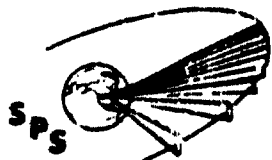
D180-22876-7

REFLECTOR FACET MOUNTING

The three bridles of the reflector facet are attached to the rocker arms which mount to the midpoint of the concentrator tube structural elements. The springs, contained in canisters, provide the pull that causes the rocker arm to tension the plastic film. Note then that the facet is mounted directly to the concentrator support structure and does not include radial arm and a hub system as shown in Part I of this study.

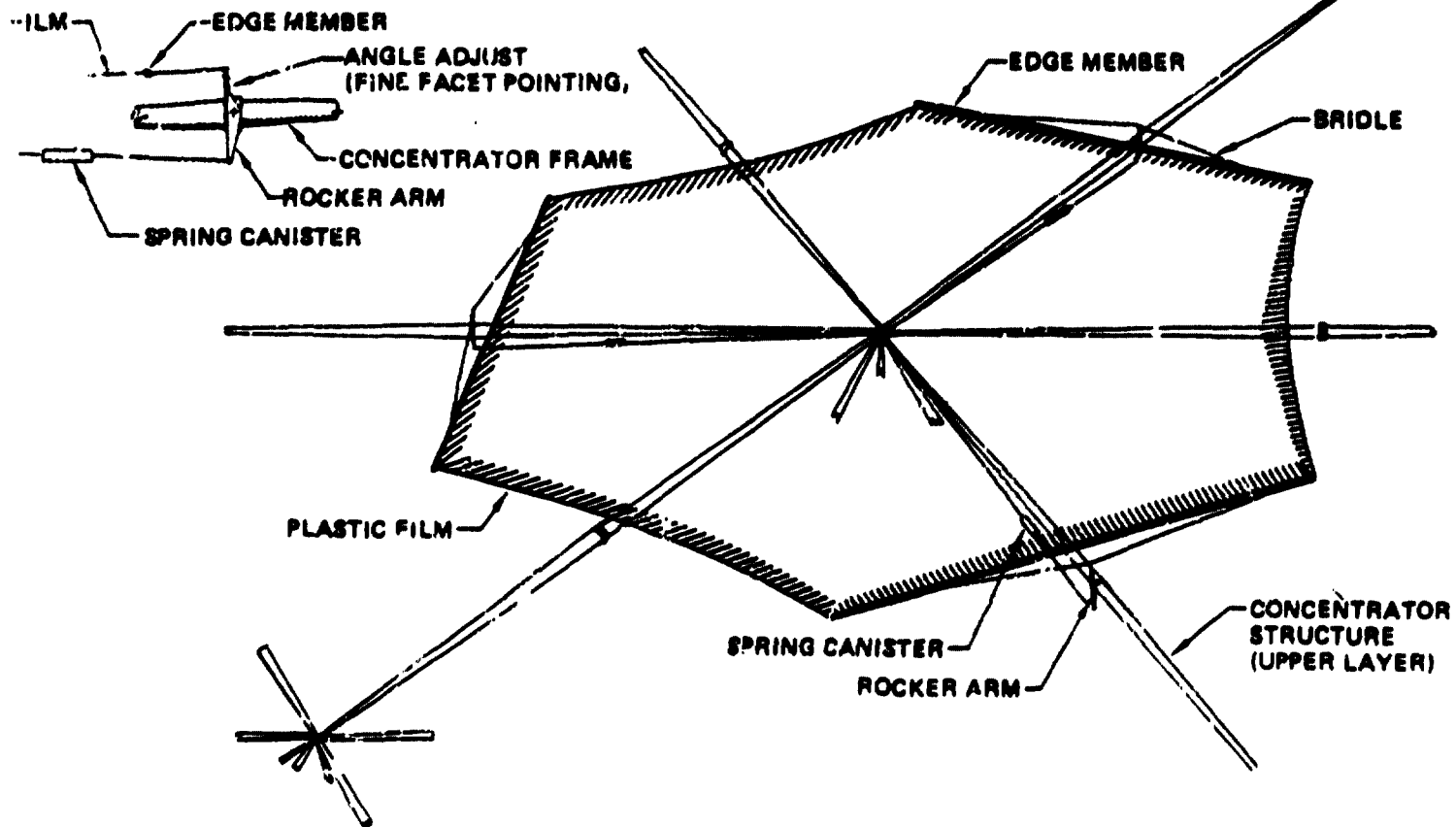
D180-22876-7

Reflector Facet Mounting



JPS 1508

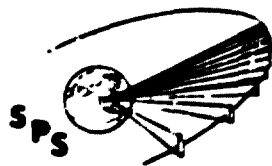
30210



D180-22876-7

PLASTIC FILM FOR FACET

The plastic film material is aluminized Kapton. DuPont Corporation, the manufacturer of Kapton, believes that a thickness of 3 micrometers is producible by nearly standard roll methods and will demonstrate this in tests in late 1977. Data from project .B7.E has shown a potential degradation of reflector film specular performance of approximately 30% due to the radiation encountered, first in a self-power transfer from low orbit to high orbit, and then 30 years of operation in geosynchronous orbit. Tests performed for the solar sail program at the Jet Propulsion Laboratory have indicated however that this degradation mode will probably not occur, and that the degradation previously seen is an artifact of the test method itself. We consequently do not forecast radiation degradation. We do anticipate approximately 2.25% degradation due to meteoroid impacts in 30 years of reflector film operation. Our reflectivity baseline is .90 for a reflector cone angle of .22 degrees. This is relatively conservatively selected since even higher reflectivities are probably achievable.



SPS-1500

D180-22876-7

Plastic Film For Facet

BOEING

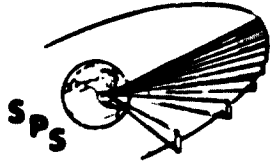
- **BASELINE MATERIAL IS ALUMINIZED KAPTON, 3 μ M (0.00012") THICK.**
- **DUPONT BELIEVES 2 μ M IS ROLLABLE.**
- **BASED ON PROJECT ABLE TEST DATA, 30% DEGRADATION OF SPECULAR REFLECTIVITY HAD BEEN PREDICTED.**

PROJECT ABLE TEST WAS WITH MONO-ENERGETIC PROTONS AT VERY HIGH DOSE RATES.

- **SOLAR SAIL WORK AT JPL INDICATES THAT THE THRESHOLD OF MECHANICAL AND REFLECTANCE DEGRADATION FOR KAPTON IS AT $\sim 5 \times 10^{10}$ RADS.**
THE SPS DOSE, INCLUDING SELF POWER TRANSFER, WILL BE $\sim 10^9$ RADS.
- **HENCE NO RADIATION DEGRADATION IS NOW FORECAST.**
- **0.90 REFLECTIVITY IS BASELINED BASED ON BOEING ENG. & CONCT. DIV. TESTS. 0.84 IS PROBABLY ACHIEVABLE WITH 100 Å SILVER OVERCOAT ON ALUMINUM.**

CAVITY & COMPOUND PARABOLIC CONCENTRATOR

Each of the 16 modules of the thermal engine SPS is equipped with the assembly shown at its focal point. Reflected sunlight from the reflector facets enters the CPC at its aperture and by reflections reaches the cavity absorber which contains the boiler tubes for the thermal engine. The CPC is made up of a framework supporting a single layer of molybdenum foil. A reflectivity of .8 is baselined for this foil due to the use of a rhenium reflective coating. The walls of the cavity absorber are composed of a framework system supporting 5 layers of molybdenum multifoil. Selection of the number of layers was based on a mass optimization trade. Heavy cavity walls leak relatively little energy to space and therefore require somewhat smaller concentrators. Thin walls are lighter but require larger solar concentrators. Five layers is approximately optimum. The purpose of the CPC is to allow a relatively large reflector facet image to fit within the aperture; also the large aperture of the CPC accommodates satellite pointing errors and some distortion in the framework in the solar concentrator.

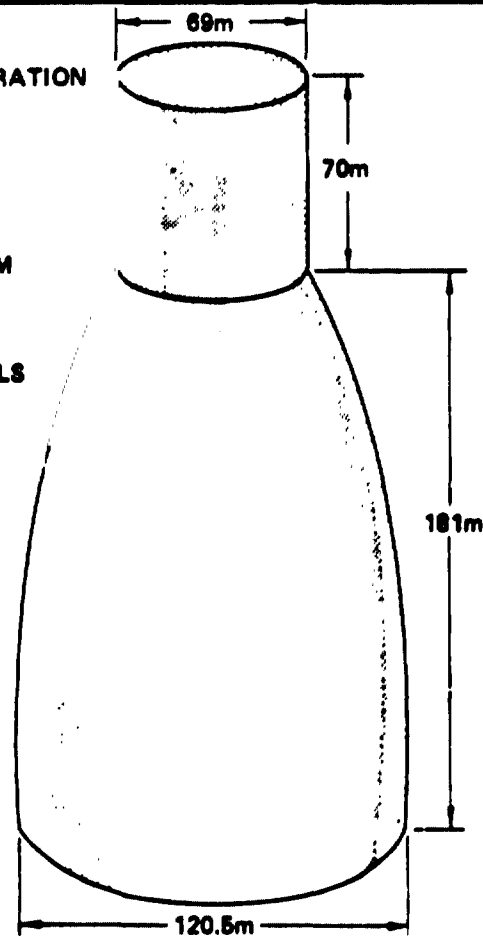


Cavity and Compound Parabolic Concentrator (CPC)

BOEING

SPS-1510

- CPC GEOMETRIC CONCENTRATION RATIO IS 3.05
- CPC LIGHT ACCEPTANCE ANGLE = 30°.
- CAVITY WALLS ARE 5 LAYERS OF MOLYBDENUM MULTIFOIL.
- ALL BOILER TUBES MOUNT ON CAVITY INTERIOR WALLS
- CPC WALLS ARE MOLYBDENUM FOIL WITH RHENIUM INTERIOR COATING.



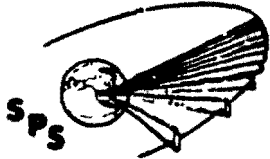
- CPC ACCEPTS LARGER IMAGE FROM FACETS:

- ALLOWS FEWER, LARGER FACETS
- ACCEPTS POINTING ERRORS & DISTORTIONS.

D180-22876-7

CPC APERTURE DOOR

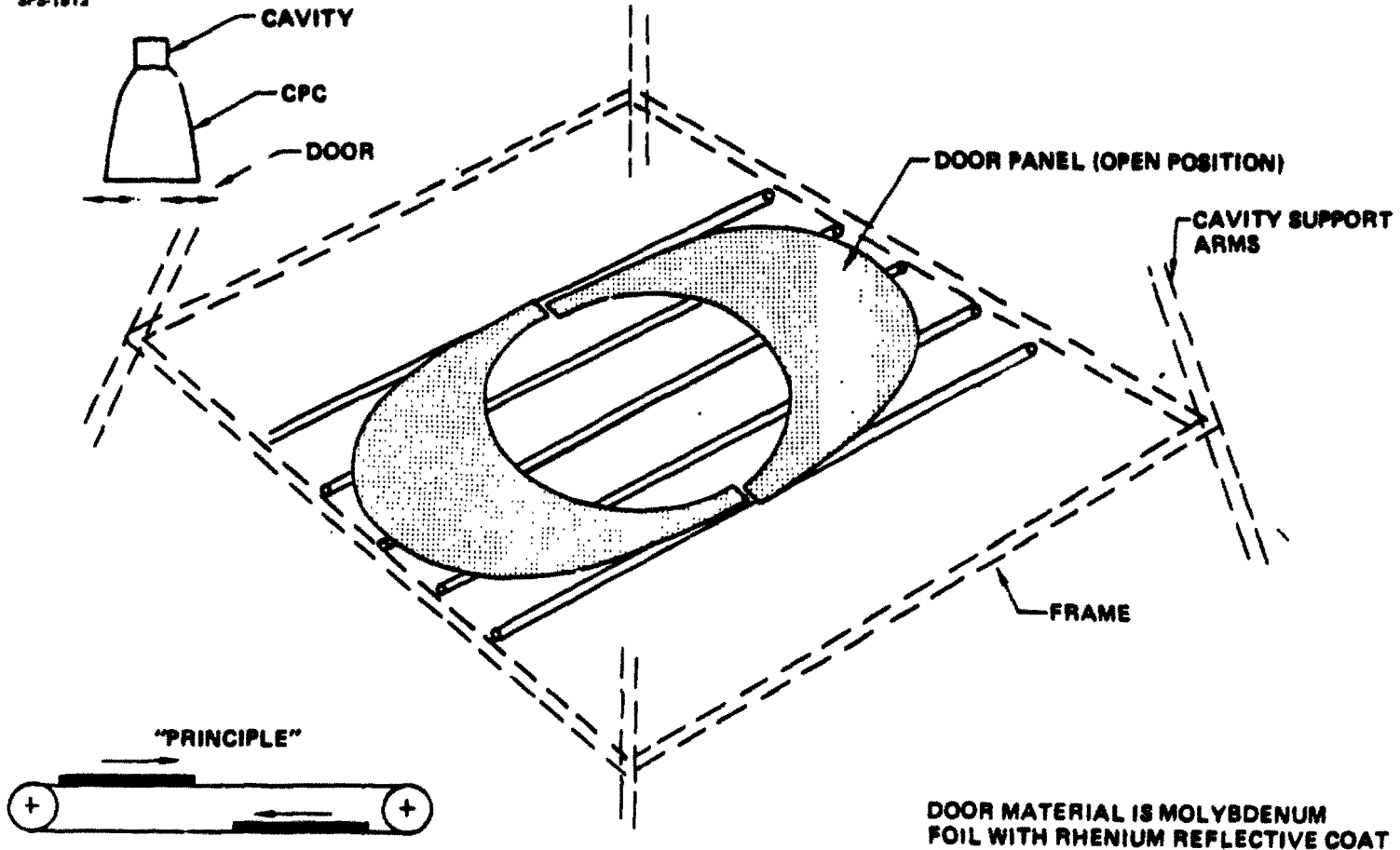
This door assembly allows a variation in turbine output power while maintaining a constant orientation with respect to the sun. The door is composed of molybdenum foil panels mounted on cables driven by pulley assemblies attached to the cavity support arm frame. The doors are shown in the open position. The rhenium reflective coating on the doors is used to maintain a low temperature for the door panels when they are fully closed and exposed to the full output of the solar concentrator assembly.



CPC Aperture "Door" Maintains Correct Cavity Temperature Despite Varying Power Output

BOEING

SPS-1812



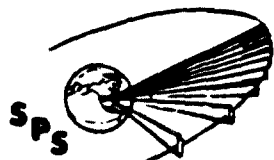
D180-22876-7

FOCAL POINT ASSEMBLY

The primary equipment of the focal point assembly is shown. The cavity absorber assembly and CPC are supported by a steel trussing framework system. A vertical steel tubing framework system. A vertical steel tubing framework member on each side of the cavity supports the turbogenerator assemblies. 18 turbogenerators are mounted on each side of the cavity. One radiator assembly is provided per turbogenerator and extends directly outward, either to left or right, from that turbogenerator. The radiator assembly which cools the generator is mounted above the cavity.

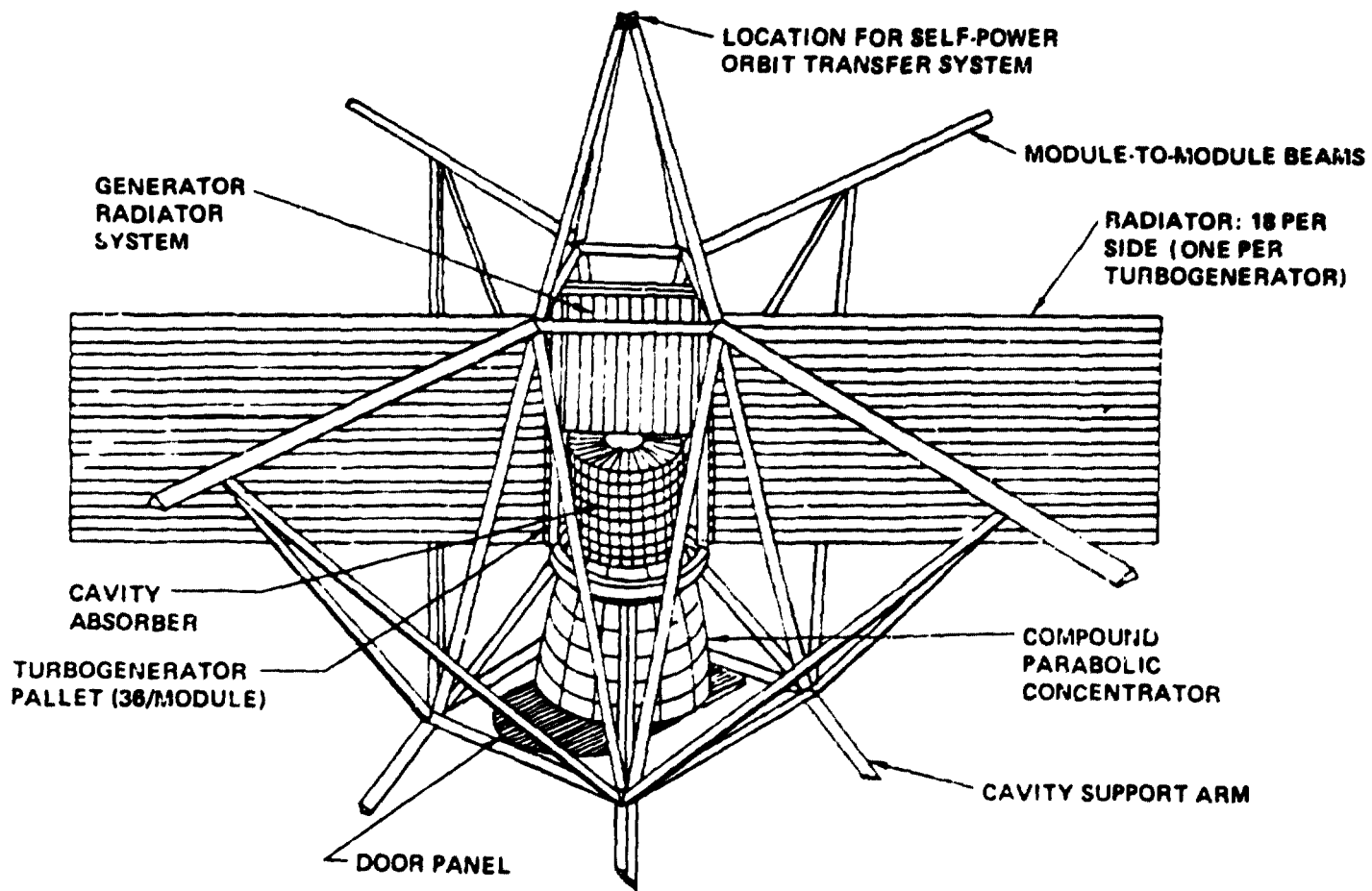
D180-22876-7

Focal Point Assembly



SPS-163E

BOEING



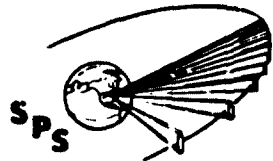
D180-22876-7

SYSTEM FLOW SCHEMATIC

Liquid potassium from the electromagnetic pump enters the boiler tubes which are located within the high temperature cavity assembly. Vapor from the boiler enters the double ended turbine and is exhausted into a single tapering radiator vapor duct. Some pertinent parameters for various points around the flow loop are given at the bottom of the chart. Note that while the vapor duct is relatively large in diameter, the pressures are quite low.

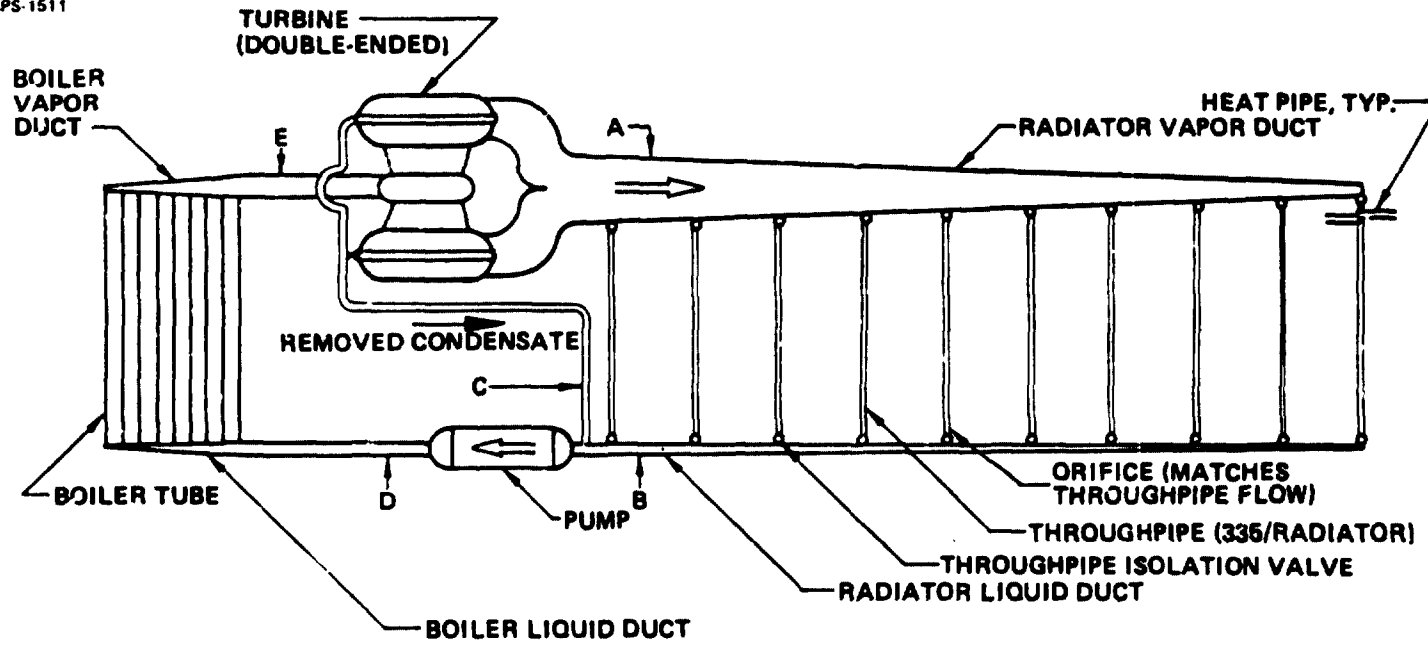
D180-22876-7

System Flow Schematic (Not to Scale)



SPS-1511

BOEING



LOCATION	PRESSURE		FLOW RATE		TEMPERATURE		DUCT M	DIA FT
	kPa	PSI	kg/s	lbm/s	K	°F		
A	37.9	5.50	74.67	164.6	932	1218	1.60	5.25
B	16.8	2.43	74.67	164.6	932	1218	0.28	0.92
C	37.9	5.50	9.23	20.3	928	1210	0.10	0.33
D	676	98.0	83.90	185.0	929	1212	0.145	0.48
E	531	77.0	83.90	185.0	1242	1776	0.55	1.80

D180-22876-7

ZERO "G" 2-PHASE FLOW

WHILE THERE ARE CERTAIN ADVANTAGES TO RECIRCULATION TYPE BOILERS OPERATING UNDER GRAVITY CONDITIONS, ZERO GRAVITY CONDITIONS FAVOR THE USE OF ONCE-THROUGH BOILING AND DELIVERY OF DRY, SLIGHTLY SUPER-HEATED VAPOR.

THE CONDENSATION OF LIQUID IN THE TURBINE DURING EXTRACTION OF HEAT FROM THE VAPOR IS A SPECIAL CASE INVOLVING NEED FOR LIQUID EXTRACTION DEVICES TO CONTROL DROPLET EROSION DAMAGE. IT IS CONSIDERED SEPARATELY, ELSEWHERE.

IN THE CONDENSER, LIQUID IS SWEEPED ALONG THE INSIDE LENGTH OF THE TUBES BY THE MUCH HIGHER VELOCITY OF THE VAPOR. THE TUBE MIGHT BE TAPERED ALONG ITS LENGTH TO MAINTAIN HIGH VAPOR VELOCITY, BUT THIS IS NOT NECESSARY. S. SAWOCHKA, NEAR THE 1965 TIME PERIOD, CONDUCTED EXPERIMENTS ON UPWARD FLOW CONDENSATION OF POTASSIUM IN VERTICAL, CONSTANT DIAMETER TUBES; THE PERFORMANCE OF THESE CONDENSER TUBES WAS NOT ADVERSELY EFFECTED BY A 1 "G" FORCE ACTING TO RESTRICT SWEEPING OF LIQUID CONDENSATE BY THE HIGH VELOCITY VAPOR.

POSSIBLE THERMAL FATIGUE CRACKING IN CONDENSERS UNDER 2-PHASE FLOW HAS BEEN CONSIDERED. IN AIR-COOLED METAL VAPOR CONDENSERS FOR LAND BASED APPLICATIONS, THE POOR AIR-SIDE HEAT TRANSFER COEFFICIENTS CONTROLLED HEAT TRANSFER; THUS THE ALTERNATE PRESENCE OF EITHER A LIQUID OR A VAPOR PHASE AT A GIVEN POINT ON THE CONDENSER TENDED TO CAUSE THERMAL FLUCTUATIONS AND POSSIBLE THERMAL FATIGUE. THIS POSSIBILITY OCCURRED SINCE THE HOT SIDE HEAT TRANSFER FILM COEFFICIENTS VARIED APPRECIABLY IN THE PRESENCE OF A LIQUID OR A VAPOR PHASE. IN THE SPS A HIGH HEAT TRANSFER FILM COEFFICIENT ON THE COLD SIDE OF THE CONDENSER TUBE WILL CONTROL THE METAL TEMPERATURE AND PREVENT SUCH ABRUPT THERMAL FLUCTUATIONS.

DURING PRIOR RANKINE CYCLE SPACE POWER SYSTEM STUDIES, THE PROBLEMS OF 2-PHASE FLOW WERE RECOGNIZED AND PLAUSIBLE SOLUTIONS AND REASONABLE APPROACHES TO THESE SOLUTIONS WERE PROPOSED.

D180-22876-7



ZERO "G" 2-PHASE FLOW



BOILER

- ONCE-THROUGH BOILING HEAT TRANSFER DEMONSTRATED
- BOILER VAPOR OUTPUT IS IN THE SUPERHEAT REGIME
- NO LIQUID PHASE EXPECTED FROM BOILER

TURBINE

- LIQUID EXTRACTION METHODS USED:
 - TO REMOVE LIQUID
 - TO CONTROL DROPLET EROSION

CONDENSER

- HIGH VAPOR VELOCITY SWEEPS LIQUID PHASE
- 1 "G" UPWARD CONDENSER FLOW AND LIQUID REMOVAL DEMONSTRATED EXPERIMENTALLY
- TAPERED CONDENSER TUBES OPTIONAL
 - TO MAINTAIN VAPOR VELOCITY
 - NOT NEEDED FOR LIQUID SWEEPING

PUMPS

- SUBCOOLING OF LIQUID TO PUMP
 - ASSURES LIQUID PHASE
 - PREVENTS PUMP CAVITATION

D180-22876-7

ELECTROMAGNETIC BOILER FEED PUMPS

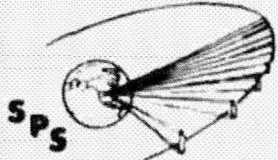
ELECTROMAGNETIC (EM) PUMPS HAVE BEEN USED EXTENSIVELY IN THE PUMPING OF LIQUID METALS. THEY HAVE THE ADVANTAGES OF ABSENCE OF SEALS AND BEARINGS, OPERATING RELIABILITY AND REDUCED MAINTENANCE REQUIREMENTS.

FOR THE RANKINE CYCLE SPACE POWER PROGRAM, A LIGHT WEIGHT (425 LBS.) ELECTROMAGNETIC BOILER FEED PUMP, CAPABLE OF OPERATING AT A LIQUID METAL TEMPERATURE UP TO 1400°F, WAS DESIGNED, BUILT AND TESTED FOR 10,000 HOURS. IT PUMPED 1000°F POTASSIUM AT FLOW RATES UP TO 3.25 LB/SEC AT A DEVELOPED HEAD OF 240 PSI, A NPSH OF 7 PSI AND AN EFFICIENCY OF 16.5%. THE PUMP FEATURED A T-111 ALLOY HELICAL PUMP DUCT AND A HIGH TEMPERATURE STATOR WITH A 1000°F MAXIMUM OPERATING TEMPERATURE; THE STATOR MATERIALS CONSISTED OF HIPERCO 27 MAGNETIC LAMINATIONS, 99% ALUMINA SLOT INSULATORS, TYPE "S" GLASS TAPE INTERWINDING INSULATION AND NICKEL-CLAD SILVER CONDUCTORS JOINED BY BRAZING IN THE END TURNS. PUMP WINDINGS WERE COOLED BY LIQUID NaK AT 800-900°F.

LARGE SIZE ANNULAR LINEAR EM PUMPS ARE UNDER DEVELOPMENT FOR THE LIQUID METAL FAST BREEDER REACTOR. A 14,500 GPM (1502 LB/SEC) PUMP HAS BEEN BUILT AND IS AWAITING TEST; PUMPS OF LARGER SIZES HAVE BEEN CONSIDERED IN THE RANGE OF 30,000; 70,000; 80,000 AND 130,000 GPM (3108; 7573; 8289 AND 13,470 LB/SEC). WEIGHT AND COST ESTIMATES FOR COMMERCIAL LAND BASED VERSIONS OF THESE PUMPS HAVE BEEN INITIATED. WHILE THESE PUMPS WERE DESIGNED FOR HANDLING SODIUM AT ABOUT 858°F, THEIR DEVELOPMENT INDICATES PUMP SCALE-UP EXPERIENCE WELL ABOVE THAT OF THE EARLIER HIGHER TEMPERATURE BOILER FEED PUMPS FOR RANKINE SPACE POWER SYSTEMS.

SINCE THE DESIGN TECHNOLOGY FOR EM PUMPS IS WELL-DEVELOPED AND RELATIVELY LARGE PUMPS HAVE BEEN BUILT, THE DESIGN AND PRODUCTION OF PUMPS OF THE REQUIRED SIZE AND OPERATING CHARACTERISTICS FOR THE SPS SHOULD BE A STRAIGHTFORWARD ENGINEERING PROBLEM. THE USE OF HIGHER PUMP VOLTAGES AND IMPROVED HIGH TEMPERATURE ELECTRICAL INSULATION, MAGNETIC AND CONDUCTOR MATERIALS WILL BE REQUIRED UTILIZING EXPERIENCE GAINED IN THE DESIGN AND TEST OF THE 1400°F BOILER FEED EM PUMP.

PUMPING AT LOW NPSH HAS BEEN DEMONSTRATED AND AVOIDANCE OF CAVITATION IN THESE PUMPS CAN BE CIRCUMVENTED BY (1) SUBCOOLING OF THE CONDENSED POTASSIUM TO MINIMIZE POSSIBILITY OF CAVITATION (ONLY VERY LOW ENERGY LOSSES ARE INVOLVED), (2) MINIMIZING CONDENSATE RETURN LINE PRESSURE LOSSES AND (3) RELIANCE UPON THE DYNAMIC PRESSURE HEAD OF THE HIGH VELOCITY CONDENSING POTASSIUM VAPOR TO HELP SUPPORT THE MINIMUM NPSH REQUIRED TO PREVENT CAVITATION.

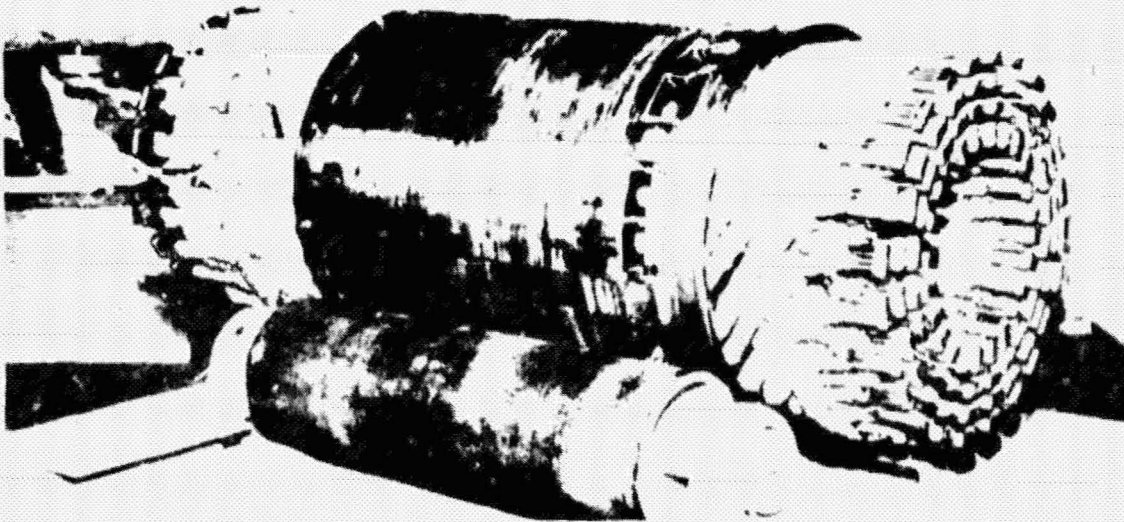


SPS-1232

Electromagnetic Pumps

BOEING

- NO MOVING PARTS
- NO RUBBING SEALS
- RELATIVELY HEAVY (APPROXIMATELY 100 TIMES HEAVIER THAN MECHANICAL)
- RELATIVELY LOW EFFICIENCY (17% VS. 80%, MECHANICAL)
- GOOD DATA BASE



- 10,000 TEST HOURS
- 17% EFFICIENCY
- UP TO 1033 K (1400°F)

D180-22876-7

ALKALI METAL VAPOR TURBINE

THE CONCEPTUAL DESIGN OF THE 31.7 MW_e, FIVE STAGE, DOUBLE FLOW ALKALI METAL VAPOR TURBINE IS BASED ON TECHNOLOGY DEVELOPED FOR SMALLER SCALE SPACE POWER TURBINES.

IT FEATURES HYDRODYNAMIC LUBRICATED LIQUID METAL PIVOTED PAD JOURNAL AND THRUST BEARINGS. IN ADDITION, THE TURBINE SHAFT LEADING TO THE GENERATOR WOULD FEATURE AN ESSENTIALLY ZERO LEAKAGE POTASSIUM SEAL OF A TYPE ON WHICH EXPERIMENTAL TESTING HAS BEEN ACCOMPLISHED; IN SMALLER SCALE SEAL TESTS OVER 100 HOURS IN DURATION, IT WAS ESTIMATED THAT THE LEAKAGE OF POTASSIUM WOULD NOT BE OF ENGINEERING SIGNIFICANCE IN OVER 10,000 HOURS OPERATION.

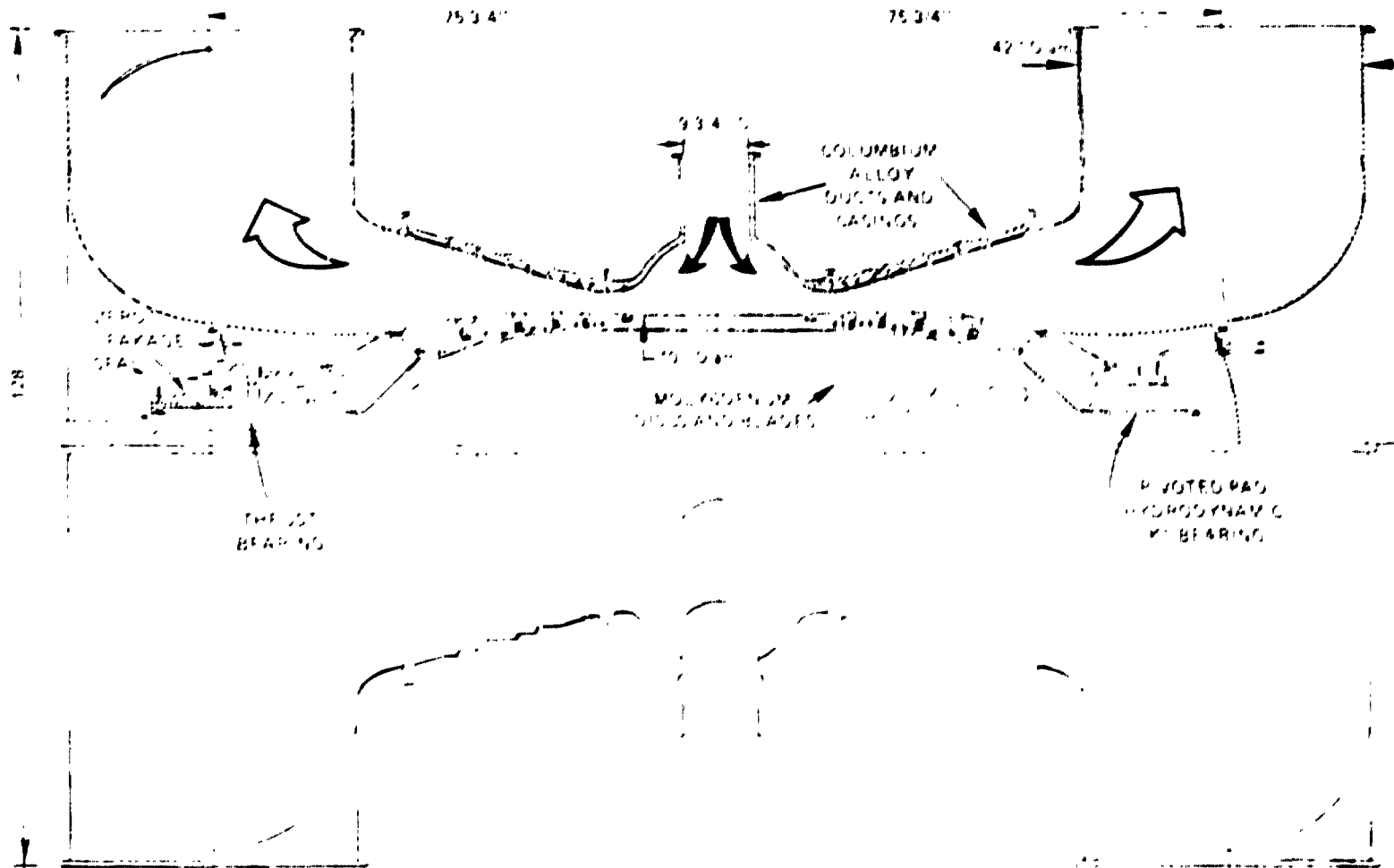
LIQUID EXTRACTION DEVICES, AS SHOWN IN DETAIL ON OTHER PAGES, CAN BE INCORPORATED IN THE DESIGN USING VANE TRAILING EDGE DROPLET EXTRACTION OR TRAILING EDGE TURBINE ROTOR DROPLET EXTRACTION.

THE SELECTION OF THE SUGGESTED MODULAR SIZE PROVIDES A NOMINAL POINT IN THE DESIGN, PRODUCTION AND TEST OF THE ALKALI METAL VAPOR TURBINES NEEDED FOR RANKINE CYCLE SOLAR POWER SATELLITES.

D180-22876-7



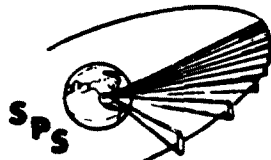
ALYALITE METAL VAPOR TURBINE



D180-22876-7

GENERATORS

Each potassium Rankine turbine turns a generator as shown here. These generators produce either 41,000 or 39,000 volts direct current as required by the microwave transmitters. The generators are oil cooled using coolant passages through both the rotor and stator. Although they are quite efficient the generators must dissipate waste heat at such a rate that their own surface area is not sufficient for this dissipation therefore external radiators are used. A high copper temperature is advantageous to reduce the area and mass of these radiators.



D180-22876-7

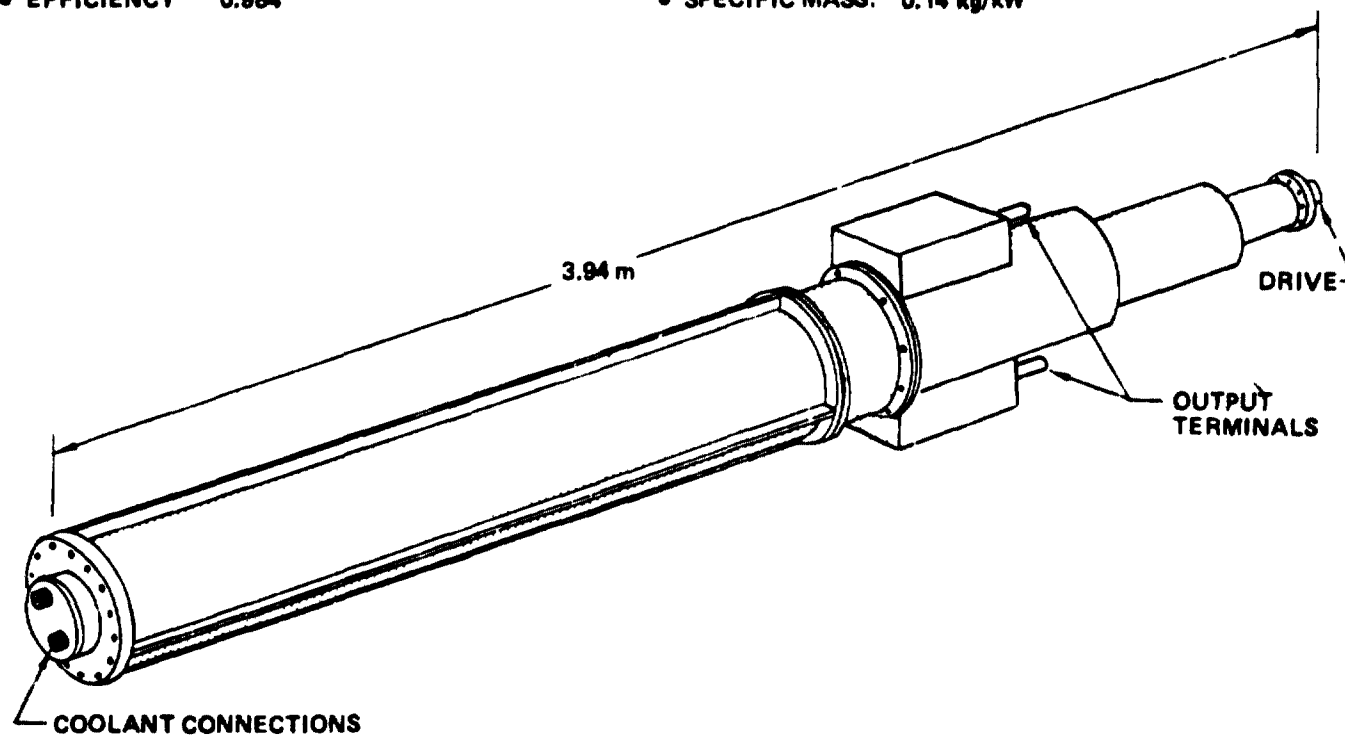
Generators

BOEING

SPS-1813

- OUTPUT 31.43 MW
- ROTOR SPEED 7500 RPM
- COOLANT OIL (DC-200)
- EFFICIENCY 0.984

- VOLTAGES: EITHER 41000 OR 39000 VDC, NOMINAL
- COPPER TEMP: 478K (400°F)
- DUTY CYCLE: CONTINUOUS
- SPECIFIC MASS: 0.14 kg/kW

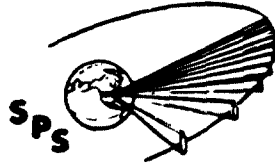


PRIMARY DATA BASE: AIRESEARCH MFG. CO. OF CA. STUDY FOR AIR FORCE, CONTRACT F33615-75-C-2071

D180-22876-7

TURBOGENERATOR PALLETS

These pallets mount one turbine, one generator and electromagnetic pump and an associated auxiliaries. The structure of this pallet is designed to allow launching of the unit preassembled that is at least a 5 g acceleration capability is required.

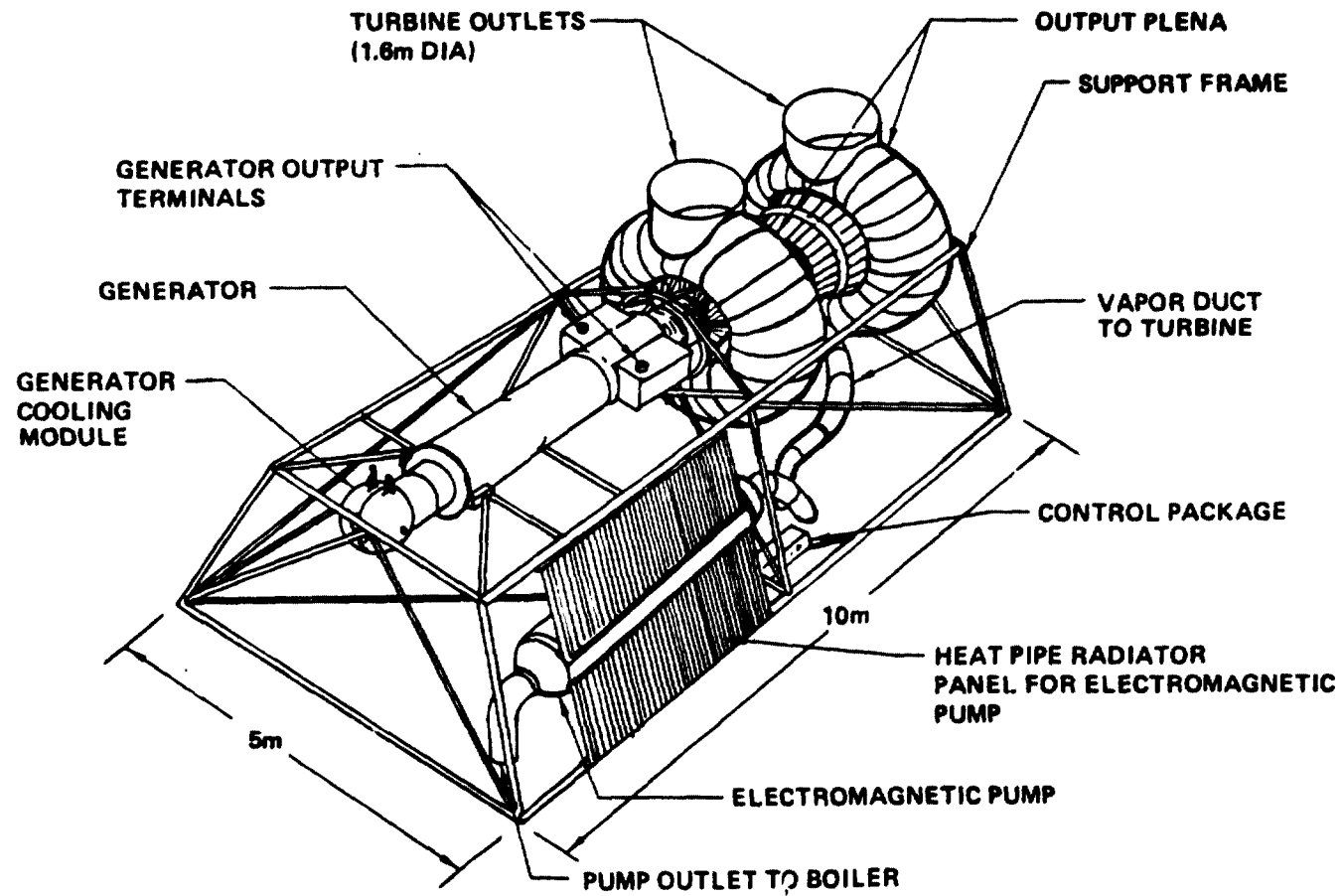


SPS-1636

D180-22876-7

Turbogenerator Pallet

BOEING

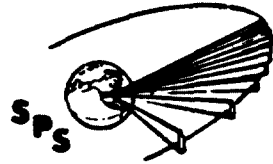


D180-22876-7

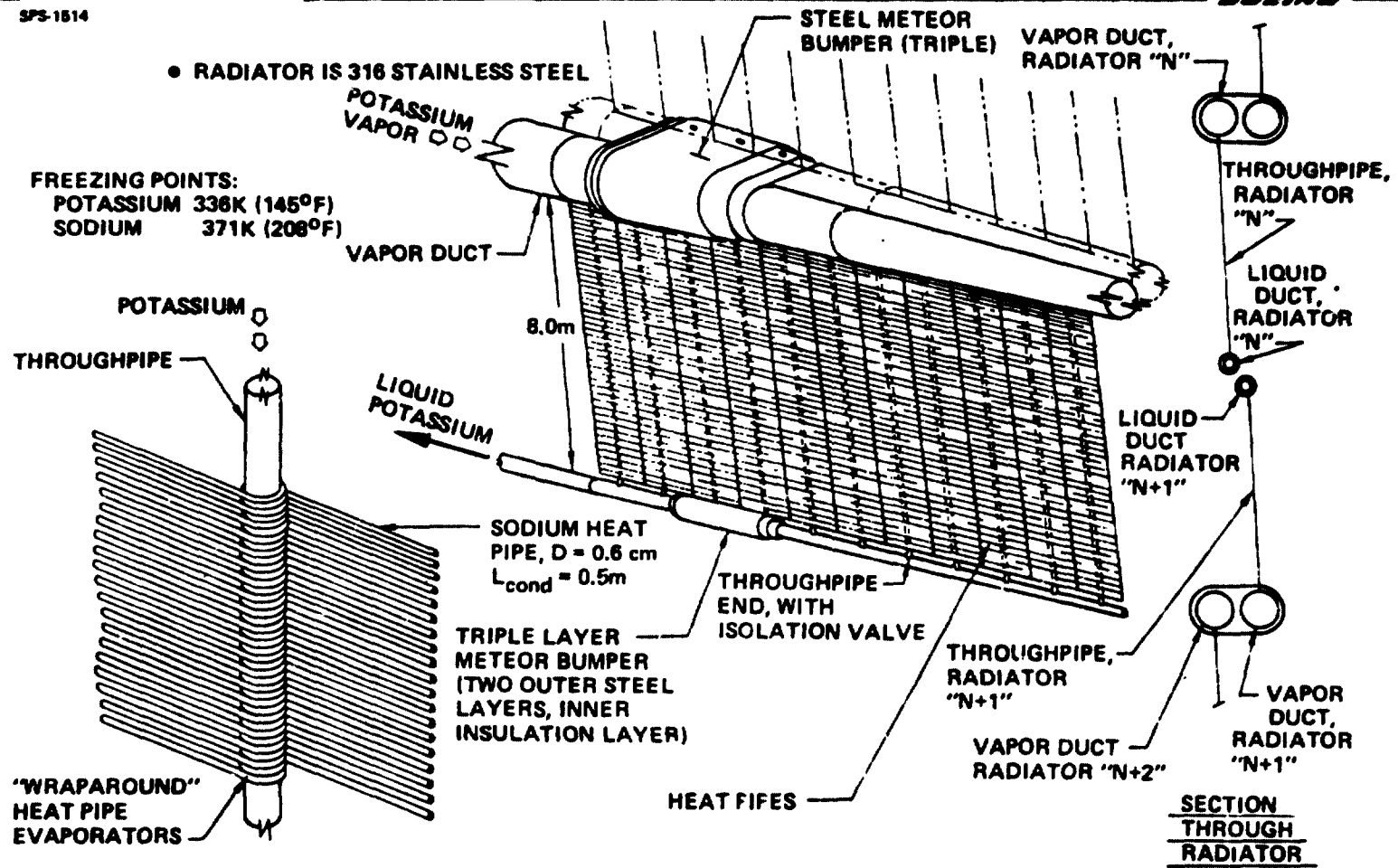
PRIMARY RADIATOR SYSTEM

Shown here is a segment of the radiator for one generator. A vapor duct is at the top and the liquid return duct is at the bottom. The heat pipe panels with their throughpipes pass between the ducts. Also shown are the triple layers of meteoroid bumper installed on the ducting. At the lower left is a detail of the throughpipes and the wraparound sodium heat pipes. These sodium heat pipes are spaced apart such that their centerlines are 1.6 diameters from each other. This spacing is an optimum compromise between greater spacing, which would improve heat radiation, and reduced spacing which would reduce manifold mass by requiring fewer through pipes. On the right is a cross section through two adjacent radiator systems showing how the vapor ducts share common meteoroid protection systems for a reduction in bumper mass.

Primary Radiator System



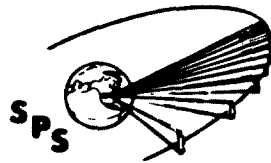
SPS-1514



D180-22876-7

RADIATOR MASS

A breakdown is given here of the radiator mass elements per engine and for the entire SPS. Note that the heat pipes and the potassium for the fill of the radiator systems dominates this mass statement. The heat pipe shell thickness is driven by meteoroid protection requirements and is such as to allow approximately 10% of the heat pipes to be penetrated and thereby made inoperable in 30 years of geosynchronous operation. Because the heat pipes wrap the throughpipes they provide significant throughpipe protection, however, approximately 3% of the throughpipes can be expected to be holed in 30 years of operation. The radiator is consequently oversized by 13 percent.



SPS-1634

D180-22876-7

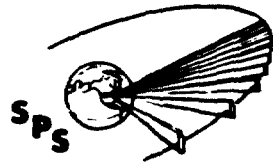
Radiator Mass

BOEING

	PER ENGINE KG	PER SPS 10 ⁶ KG
MANIFOLDS	3895	2.24
VAPOR DUCT	(1240)	(0.71)
LIQUID DUCT	(216)	(.12)
METEOROID PROTECTION	(2439)	(1.40)
THROUGHPIPES	1500	0.86
THROUGHPIPES (335/ENGINE)	(790)	(.46)
ISOLATION VALVES	(710)	(.41)
HEAT PIPES	13,299	7.66
SHELL	(10,838)	(6.24)
WICK	(1729)	(0.99)
SODIUM	(732)	(0.43)
<u>POTASSIUM</u>	<u>8046</u>	<u>4.63</u>
TOTAL	26,740	15.39

POWER BUDGET

This is a breakdown of the system power requirements aboard the SPS. The generators require 16.43 GW. Additional utilizations within the system bringing the busbar total to 17.913 GW. The power distribution losses are those associated with resistance affects within the distribution busbars. The pumping power is that required to operate the electromagnetic potassium pumps. The attitude control power is a maximum value and corresponds to the time period when maximum thrust is required to maintain the perpendicular-to-ecliptic plane orientation. The total output can be produced by 570 of the generators. 576 generators are installed allowing approximately a 1% margin. It is anticipated that the microwaves transmitters will degrade in output and required power input by approximately 2% in the course of a year. Consequently in one year about 3% of the turbogenerator systems could be automatically shutdown by malfunction detection systems without impacting the power output of the microwave transmitter.



SPS-1518

D180-22876-7

Power Budget

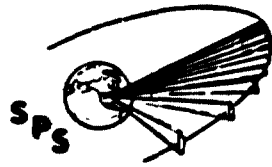
BOEING

TRANSMITTERS	<u>10⁶ kW</u> 16.430
POWER DISTRIBUTION	0.898
PUMPING	0.282
ATTITUDE CONT, MAX	0.300
MISC.	<u>0.003</u>
BUSBAR	17.913

570 GENERATORS AT 31.426 MW_e EACH
(576 INSTALLED)

SYSTEM EFFICIENCY CHAIN

The 17.913 GW required for busbar power as indicated by the previous chart is the beginning point for this system efficiency chain. The generators have an efficiency of 98.4%. This requires that the turbines have a shaft output of 18.204 GW. Since the turbines and the rest of the system have an overall cycle efficiency of 0.189, a power level of 96.317 GW must be added to the potassium flow within the boilers of the cavity absorber. A breakdown of the losses associated with the cavity absorber is also given. For example, 5% of the energy entering the cavity is reflected back out again. This is based on tests of "bench model" absorbers for ground solar power programs. The five layers of insulation making up the cavity walls allow a heat loss of approximately 1.2 GW. The hot walls of the cavity reradiate energy back out through the aperture. Some of this passes directly to space and some of it is reflected to space from the solar concentrator. Other losses, such as heat losses through the walls of the manifolds, connecting the boilers to the turbines, amount to approximately 1.1 GW. The CPC also has losses due to energy absorbed rather than reflected by its walls. The end of life reflectivity of the plastic film facets is 0.877. This is the reflectivity after a reduction of 2.25% due to meteoroid scouring, in 30 years of operation.



SPS-1818

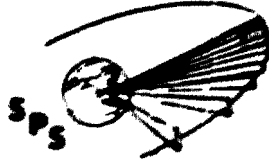
System Efficiency Chain

	<u>10⁹ kW</u>
BUSBAR (GENERATOR OUTPUT) (GEN. EFFICIENCY = 0.984)	17.913
TURBINE SHAFT OUTPUT (CYCLE EFFICIENCY = 0.189)	18.204
POWER ADDED TO POTASSIUM	96.317
SOLAR ENERGY INTO CAVITY	112.397
(REFLECTION LOSS, 5%)	(5.620)
(LOSS THROUGH INSULATION)	(0.500)
(RERADIATION THROUGH APERTURE)	(8.836)
(MISC, I.E., MANIFOLD HEAT LOSS)	(1.124)
INTO SECOND STAGE CONCENTRATOR (CPC REFLECTIVITY = 0.865)	129.939
IMPINGING UPON PLASTIC FILM (FILM END-OF-LIFE REFLECTIVITY = 0.877)	148.079

D180-22876-7

"PERPENDICULAR TO ORBIT PLANE" ORIENTATION

Some advantages and disadvantages of a PEP orientation are given. PEP has been selected primarily because moving facets are not required. However, other benefits accrue as shown. The disadvantage of the additional seasonal antenna axis are somewhat offset by two advantages relative to microwave power transmission. The first of these is that rectennas can be switched without polarization loss even if the antennas are at different longitudes without moving the satellite along the geosynchronous path. Additionally, the seasonal antenna axis can be used to provide antenna tilt to compensate for Faraday rotation caused by the ionosphere.



SPS-1712

“Perpendicular-to-Ecliptic Plane” Orientation

BEHIND

DISADVANTAGES

- HIGHER PROPELLANT CONSUMPTION (UNLESS CONFIGURATION IS INERTIALLY SYMMETRIC, USES MAGNETIC TORQUING OR SOLAR PRESSURE EFFECTS)
- BEST PERFORMANCE REQUIRES TIGHTER ATTITUDE CONTROL LIMITS (E.G., 0.1° , NOT 0.5°)
- REQUIRES ADDITIONAL (SEASONAL) AXIS ON ANTENNA
- 300 MW PEAK POWER REQUIRED TO OPERATE THRUSTERS

ADVANTAGES

- FACETS NEED NOT FOLLOW SEASONAL SUN MOTION
- ELIMINATES COSINE EFFECT ON SIZING
- FACETS NEED NOT BE SPACED APART TO ALLOW MOTION
- LOWER METEOROID FLUX ON RADIATORS
- ADDITIONAL ANTENNA AXIS PERMITS TRANSMISSION TO VARIOUS RECTENNA LONGITUDES WITHOUT POLARIZATION LOSS (FROM GIVEN ORBIT LONGITUDE)
- ADDITIONAL ANTENNA AXIS PERMITS COMPENSATION FOR DIURNAL IONOSPHERIC FARADAY POLARIZATION ROTATION
- RADIATOR IS ALWAYS EDGE ON TO THE SUN
- CONSTANT THERMAL ENVIRONMENT FROM FIXED SOLAR ORIENTATION

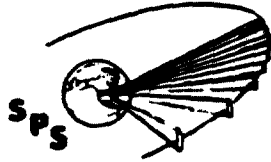
D180-22876-7

ANTENNA JOINT STRUCTURE FOR PEP SPS

The additional, seasonal axis and dog-leg structure required for PEP operations is shown. Slip-rings need not be used at the seasonal axis pivot. Flat cables which are wound during one year of operation and unwound during an annual shutdown period are instead baselined.

D180-22876-7

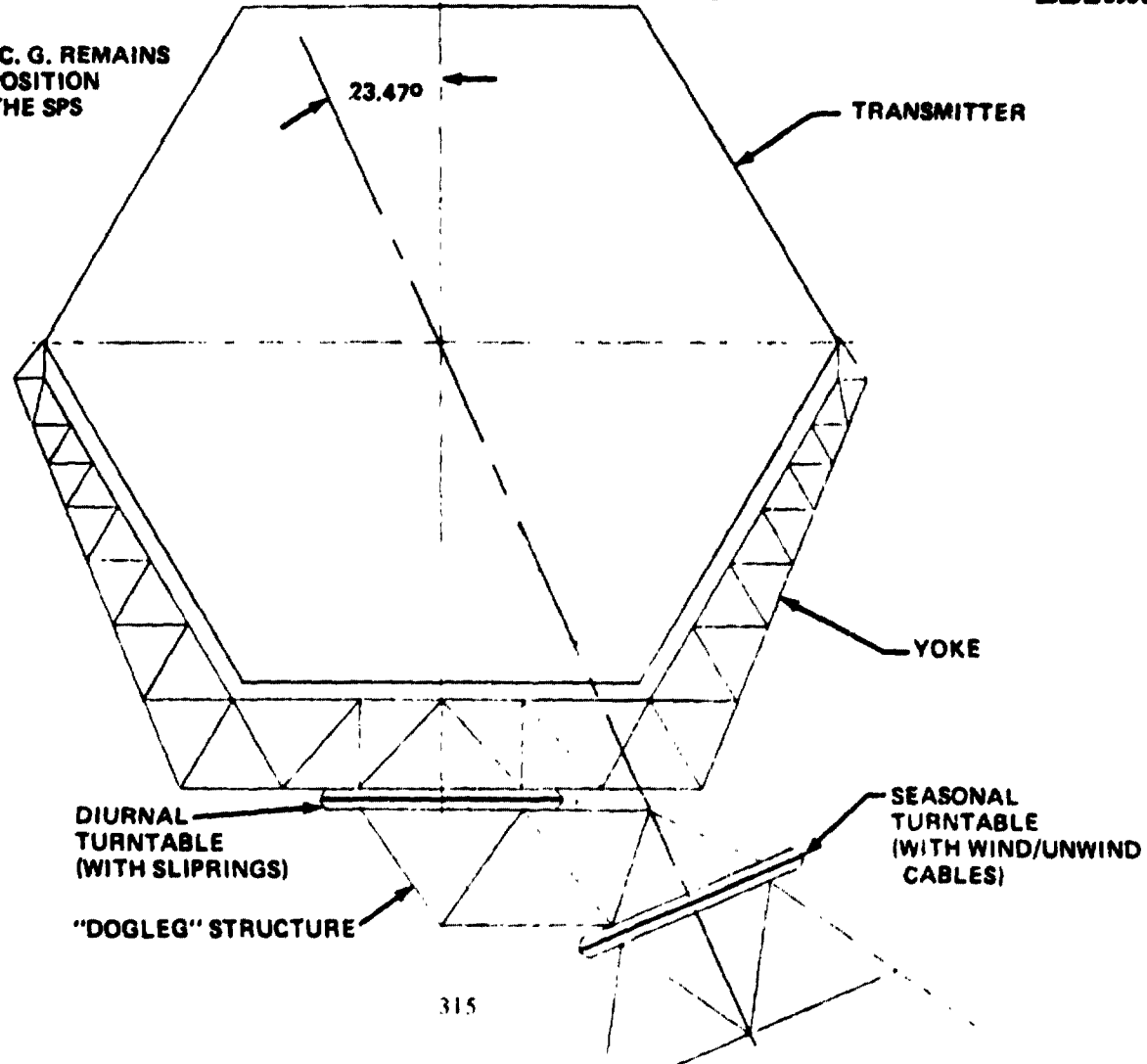
Antenna Joint for "P.E.P." SPS



SPS-1236

BOEING

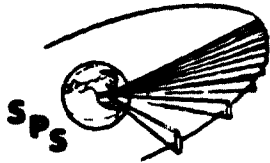
NOTE: TRANSMITTER C. G. REMAINS
IN CONSTANT POSITION
RELATIVE TO THE SPS



D180-22876-7

POTASSIUM RANKINE SPS MASS STATEMENT

This is a breakdown of the Part II final mass. Prominent elements in this mass are the transmitters, the turbines, the radiator systems, the structure (primarily the facet support structure) and the potassium inventory for the system. The turbine mass was estimated by General Electric and represents a value which is probably correct to within +20% and -40%.



SPS-1633

D180-22876-7

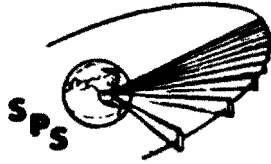
Potassium Rankine SPS Mass Statement

BOEING

	<u>10⁶ kg</u>
STRUCTURE	6.976
FACETS	1.837
RADIATOR (W/O POTASSIUM)	10.768
POV DIST	4.760
SW, GEAR	0.218
GENERATORS, ACCESSORY PACK	2.508
GENERATOR RADIATORS	1.140
TURBINES	13.755
PUMPS, PUMP RADIATORS	0.984
BOILERS & MANIFOLDS	3.296
CAVITY ASSYS	1.000
CPCS	0.299
LIGHT DOORS	0.075
MONITOR, COMMAND & CONTROL	0.100
ATTITUDE CONTROL	1.200
START LOOPS, CONTROLS	0.250
ANTENNA SUPPORT	0.286
MISC, INCLUDING STORAGE	0.200
POTASSIUM INVENTORY	6.058
POWER GENERATION	55.660
ANTENNAS	24.384
SPS	80.044

SUMMARY-THERMAL ENGINE SPS

Final conclusions of the thermal engine work of this study are given here. It was determined that the potassium Rankine cycle thermal engine is the lightest of the potential approaches investigated. At the beginning of this study the solar concentrators involved steerable facets with individual power supplies, sensors and servo mechanisms. These have been eliminated by using a perpendicular-to-ecliptic orientation and a concentrator dish of the requisite curvature. Instead of electromechanical pumps, composed of an electric drive motor and a pump with the requisite seal between them (which could be subject to leakage), we now utilize electromagnetic pumps. Although somewhat heavy, the low pumping power associated with potassium Rankine makes these potentially low-failure-rate pumps practical. Although certain materials such as silicon carbide and tantalum may offer advantages for thermal engine SPS they are either too advanced or insufficiently abundant to allow them to be baselined. The materials selected are in common use and resource data indicates that there is enough to allow a significant thermal engine program to be accomplished. The perpendicular-to-ecliptic plane orientation is critical in allowing the fixed reflector facets. This requires somewhat more thruster power, but is a proper orientation for the thermal engine SPS. The turbines themselves, at their size of approximately 32 megawatts, use forgings which can be produced by existing U.S. industry. Generally low industrialization is therefore required for the thermal engine SPS. The nation's current production capability is probably adequate to produce one SPS per year.

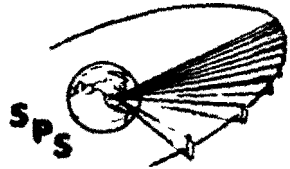


SPS-1617

Summary – Thermal Engine SPS

BOEING

- RANKINE CYCLE IS LIGHTEST AND SIMPLEST
- SYSTEM IS LARGELY PASSIVE
 - FIXED CONCENTRATOR
 - ELECTROMAGNETIC PUMPS
- PROVEN MATERIALS WITH NECESSARY ABUNDANCE ARE USED
- THE SATELLITE SHOULD FLY P.E.P.
- TURBINES SIZED FOR EXISTING INDUSTRY; GENERALLY LOW "INDUSTRIALIZATION"



SPS-1703

D180-22876-7

BOEING

Construction and
Transportation

Construction and Transportation

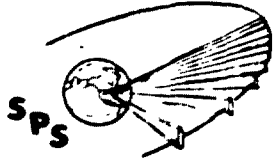
PRECEDING PAGE BLANK NOT FILLED

CONSTRUCTION/TRANSPORTATION AGENDA

In this section of the briefing, the construction and transportation systems are discussed together from the standpoint of how they relate to the two main issues of the study which are the comparison of 1) the power generation systems and 2) the location for their construction. The power generation system comparison will be presented using the LEO construction option. The GEO construction option has also been studied and it could be presented at this time as well as both construction option at the same time. But in order to focus most clearly on the differences in the construction and transportation characteristics for the two power generation options this portion of the briefing will be confined to the LEO construction approach. In summary, the outcome of the power generation comparison is not influenced by the construction location. Resulting from the power generation comparison will be a judgement as to which is the preferred system from the construction and transportation standpoint. This concept will then be used in the comparison of the construction location options. Again, both power generation systems have been investigated for both construction locations.

The construction splinter meeting will focus on more detailed definition of construction bases and the staging depot including such factors as sizing, configuration, crew modules, and mass and cost data. Additional data will be provided on the construction equipment and requirements imposed by this equipment. Finally, several key trades will be presented relative to the antenna construction location and satellite installation as well as structural assembly of the satellite itself.

The transportation splinter meeting will be held at a separate time and will include data on self-power flight control.



SPS-1612

D180-22876-7

Construction/Transportation Agenda

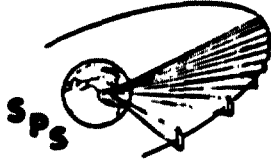
BOEING

- **MAIN BRIEFING** **ELDON DAVIS**
 - **POWER GENERATION SYSTEM COMPARISON
(USING LEO CONSTRUCTION)**
 - **CONSTRUCTION LOCATION COMPARISON
(USING BEST POWER GENERATION SYS)**

- **SPLINTER MEETING** **KEITH MILLER
ELDON DAVIS**
 - **CONSTRUCTION BASE AND STAGING DEPOT DEFINITION**
 - **CONSTRUCTION EQUIPMENT DETAIL**
 - **TRADES**
 - **ANTENNA CONST. LOCATION AND SATELLITE INSTALL.**
 - **STRUCTURE ASSEMBLY**
 - **CONSTRUCTION BASE SIZING**
 - **SELF POWER FLIGHT CONTROL**

**ASSUMPTIONS AND PHILOSOPHY
CONSTRUCTION AND TRANSPORTATION**

The key assumptions and philosophy used in the construction and transportation analysis are indicated. Most of these items are self explanatory but a few require a brief explanation. Item 1 was specified in the Statement of Work. Item 2 deals with the actual amount of useful time available for construction taking into account that personnel do not work literally an entire shift (coffee breaks etc), and allowances also included for machine down time. Item 3 is specified to indicate no construction operations were investigated which used the satellite itself to support construction equipment. Item 5 relates to the case where a given type of machine operation such as a solar array deployer was analyzed to determine its required construction rate in LEO construction and then this same value was used for the GEO construction approach. Item 6 deals with the thought that wherever practical, parallel construction operations were performed in order to reduce the construction rates of the equipment and at all times an attempt was made to eliminate the cases where several operations had to occur simultaneously to finish a given task. Item 9 primarily deals with the task of indexing the satellite or the terminal phase of bringing together large items such as satellite modules or antennas using propulsive devices. Item 10 identifies the two stage ballistic/ballistic system as the reference cargo launch vehicles although two stage winged/winged systems were also investigated.



SP2 1830

Assumptions and Philosophy Construction and Transportation

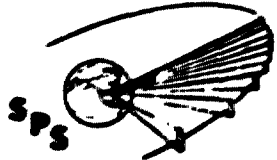
BOEING

1. ONE YEAR CONST TIME (INCL 30 DAYS TEST AND C/O)
2. PRODUCTIVITY FACTOR OF 0.75
3. FACILITIZED CONSTRUCTION WITH ASSEMBLY LINE TYPE OPERATIONS
4. COMPONENTS MANUFACTURED ON EARTH, ASSEMBLED IN SPACE
5. SIMILAR CONST EQUIP USE SAME RATES FOR ALL CONST OPTIONS
6. PARALLEL AND DECOUPLED CONSTRUCTION WHEREVER PRACTICAL
7. CONST. ACCOMPLISHED USING CREW OPERATED OR MONITORED EQUIP/MACHINES - NO "HANDS ON" OPERATIONS
8. CREW WORK SCHEDULE
10 HOURS PER DAY
6 DAYS PER WEEK
90 DAY STAYTIMES
9. NO FREE FLYING INDEXING OR DOCKING OF LARGE SYSTEMS OR MOVEMENT OF CARGO AROUND FACILITY
10. REFERENCE CARGO LAUNCH VEHICLE—TWO STAGE BALLISTIC/BALLISTIC
11. SHUTTLE GROWTH (LIQUID BOOSTER) USED FOR LEO CREW DELIVERY
12. ORBIT TRANSFER SYSTEMS USED ION ELECTRIC OR LO_2/LH_2 PROPULSION

D180-22876-7

PHOTOVOLTAIC SATELLITE CONFIGURATION

The next two charts illustrate the reference photovoltaic and thermal engine satellites to be constructed and transported. The referenced 10 GW photovoltaic satellite consists of 8 satellite modules, which when assembled have an overall length of 21.6 kilometers. Approximately 1300 kilometers of 20 meter beam is assembled. 112 square kilometers of solar array is installed along with 65 kilometers of powerbus. Construction of two antennas involves fabrication of structure and the placement of 1.6 square kilometers of radiating surface.

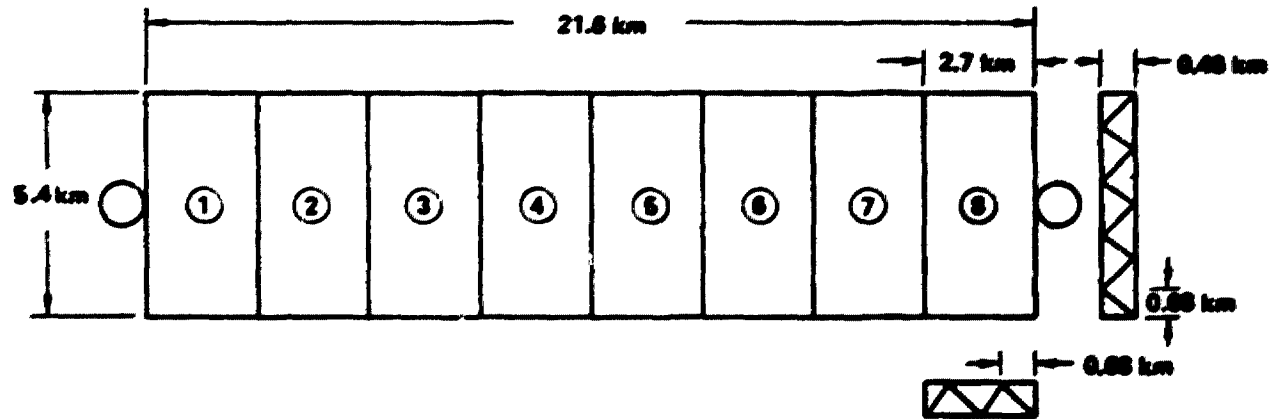


D180-22876-7

Photovoltaic Satellite Configuration

SPS-1218

BEING



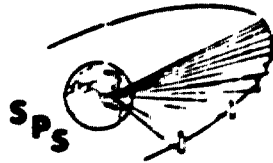
- EIGHT MODULES
- 97 MILLION kg
- 1300 km OF 20 KI BEAM
- 102 km² OF SOLAR ARRAY
- 65 km OF POWER BUSES
- 1.6 km² OF ANTENNA SURFACE AREA

THERMAL ENGINE SATELLITE CONFIGURATION

The thermal engine satellite consists of 16 modules which when assembled have a planform dimension of 12.8 kilometers on a side resulting in an area 29% greater than the photovoltaic satellite. A key distinguishing feature of this configuration relative to the photovoltaic satellite is that the depth of the satellite is considerably greater. Key component characteristics are also indicated with the only one directly comparable to the photovoltaic satellite being that of the structure which is approximately 2.5 times greater in length although in this case the majority of this beam is 10 meter size rather than 20 meter.

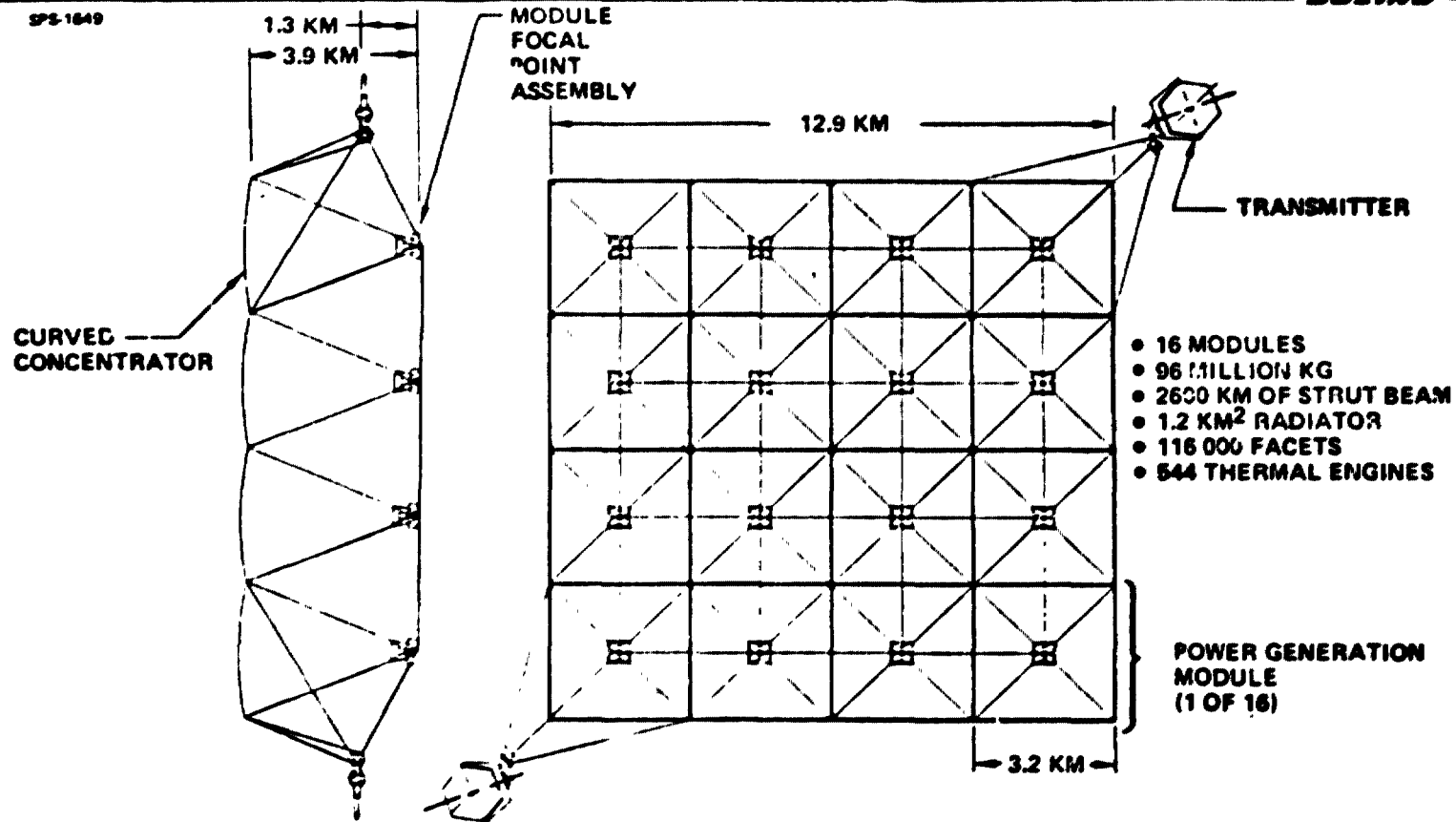
D180-22876-7

Thermal Engine Satellite Configuration



SPS-1649

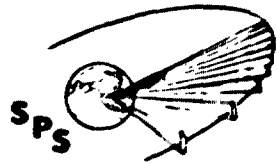
BOEING



D180-22876-7

POWER GENERATION SYSTEM COMPARISON

The principal areas which will be used to compare the two power generation systems are indicated. These areas have been selected to emphasize the differences between the two satellites. The approach used in the briefing will be to compare both power generation system options for a given item of comparison at the same time or in two consecutive charts rather than going all the way through the photovoltaic satellite and then the thermal engine satellite followed by a comparison at the end.



D180-22876-7

Power Generation System Comparison

SPS-1614

BOEING

AREAS OF COMPARISON

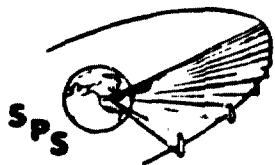
- CONSTRUCTION BASE CONFIGURATION
- SATELLITE AND ANTENNA CONSTRUCTION OPERATIONS
- FINAL ASSEMBLY OPERATIONS
- CONSTRUCTION EQUIPMENT
- CREW REQUIREMENTS
- CONSTRUCTION SYSTEM MASS AND COST
- LAUNCH SYSTEM
- ORBIT TRANSFER SYSTEM
- TRANSPORTATION COST

D180-22876-7

**LEO CONSTRUCTION CONCEPT
PHOTOVOLTAIC SATELLITE**

The first comparison to be made is that of the overall construction/transportation concept for each satellite. As indicated earlier, the LEO construction approach will be used in making the power generation system comparison. In the case of the photovoltaic satellite, eight modules and two antennas are constructed at the LEO base. All modules are transported to GEO using self-power electric propulsion. Two of the modules will transport an antenna while the remaining six modules will be transported alone. The GEO operation requires berthing (docking) the modules to form the satellite and deployment of the solar arrays not used for the transfer, followed by the rotation of the antenna into its desired operating position.

D180-22876-7

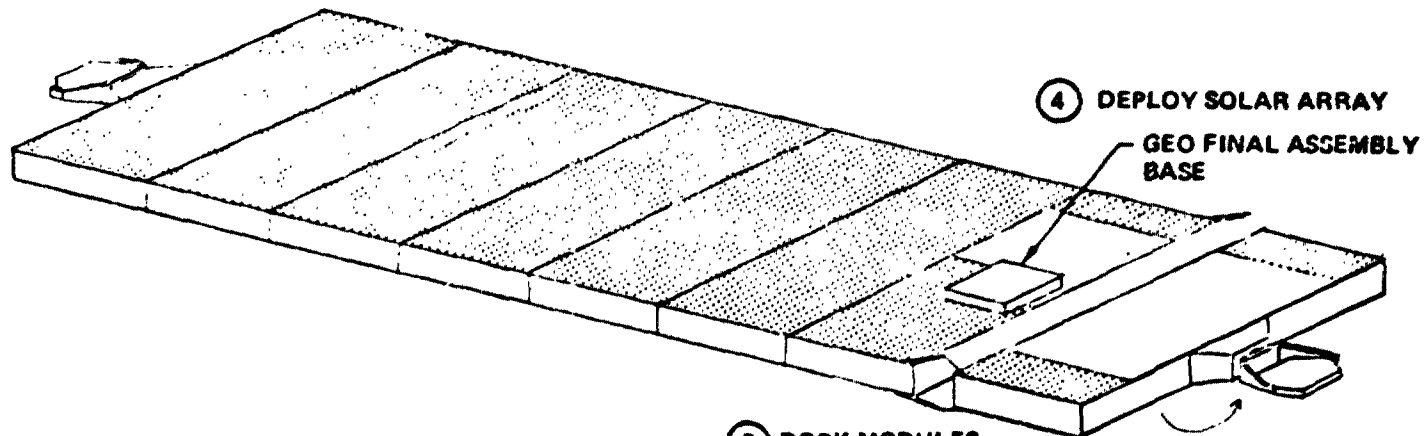


LEO Construction Concept Photovoltaic Satellite

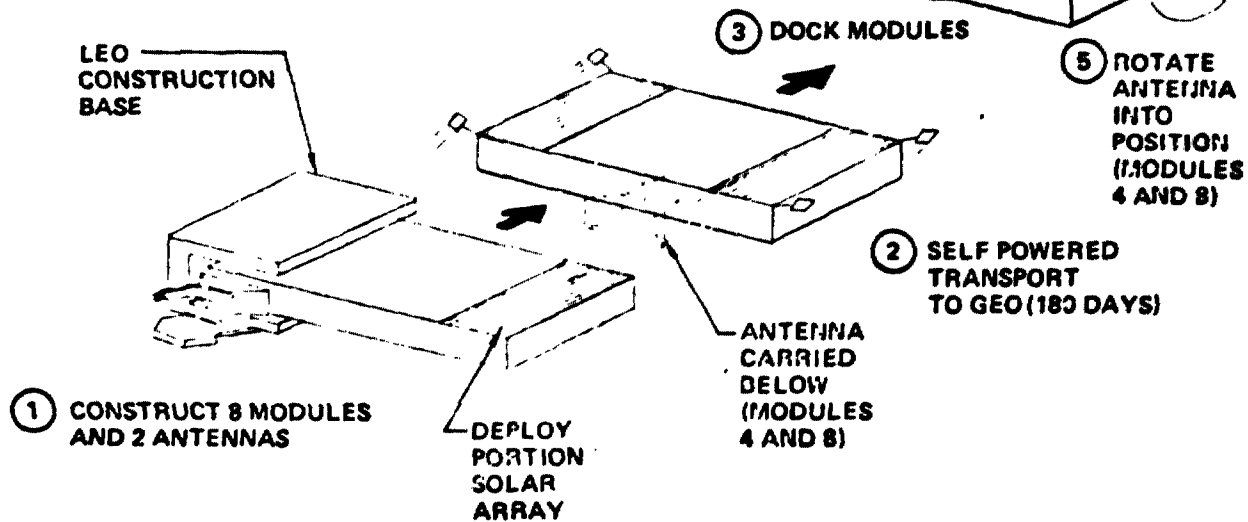
BEING

SPS-1383

GEO



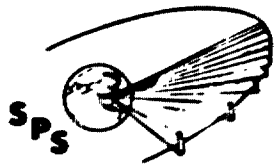
LEO



D180-22876-7

**LEO CONSTRUCTION CONCEPT
THERMAL ENGINE SATELLITE**

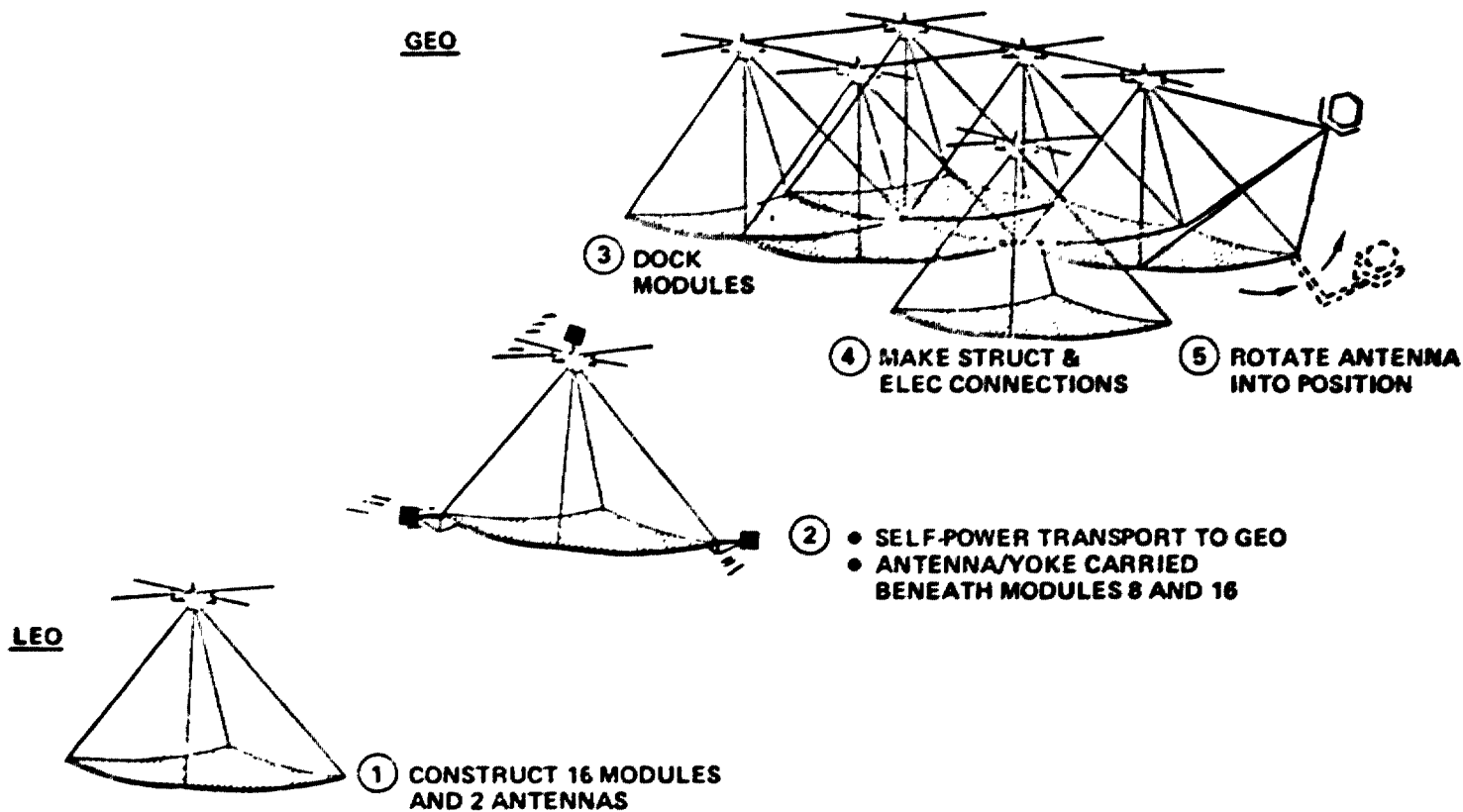
The thermal engine LEO construction concept is similar to the photovoltaic satellite with the exception that 16 modules are constructed in LEO with 14 of these being transported alone and again 2 modules each taking up an antenna. Berthing is again required at GEO, however, no reflector facets require deployment since they are not affected by radiation when passing through the Van Allen belt so consequently are deployed while in LEO in order to simplify the construction operations at GEO.



SPS-1496

LEO Construction Concept Thermal Engine Satellite

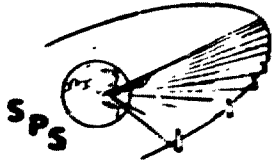
BOEING



D180-22876-7

LEO BASE CONSTRUCTION TASKS

The construction operations to be performed at the LEO construction base are 1) assemble the structure to form a module 1/8 the size of the total satellite. 2) install solar arrays. 3) install power bus system. 4) install orbit transfer system. 5) install subsystems and 6) construct two antennas with their yoke and rotary joints.



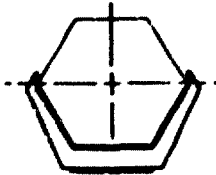
D180-22876-7

LEO Base Construction Tasks

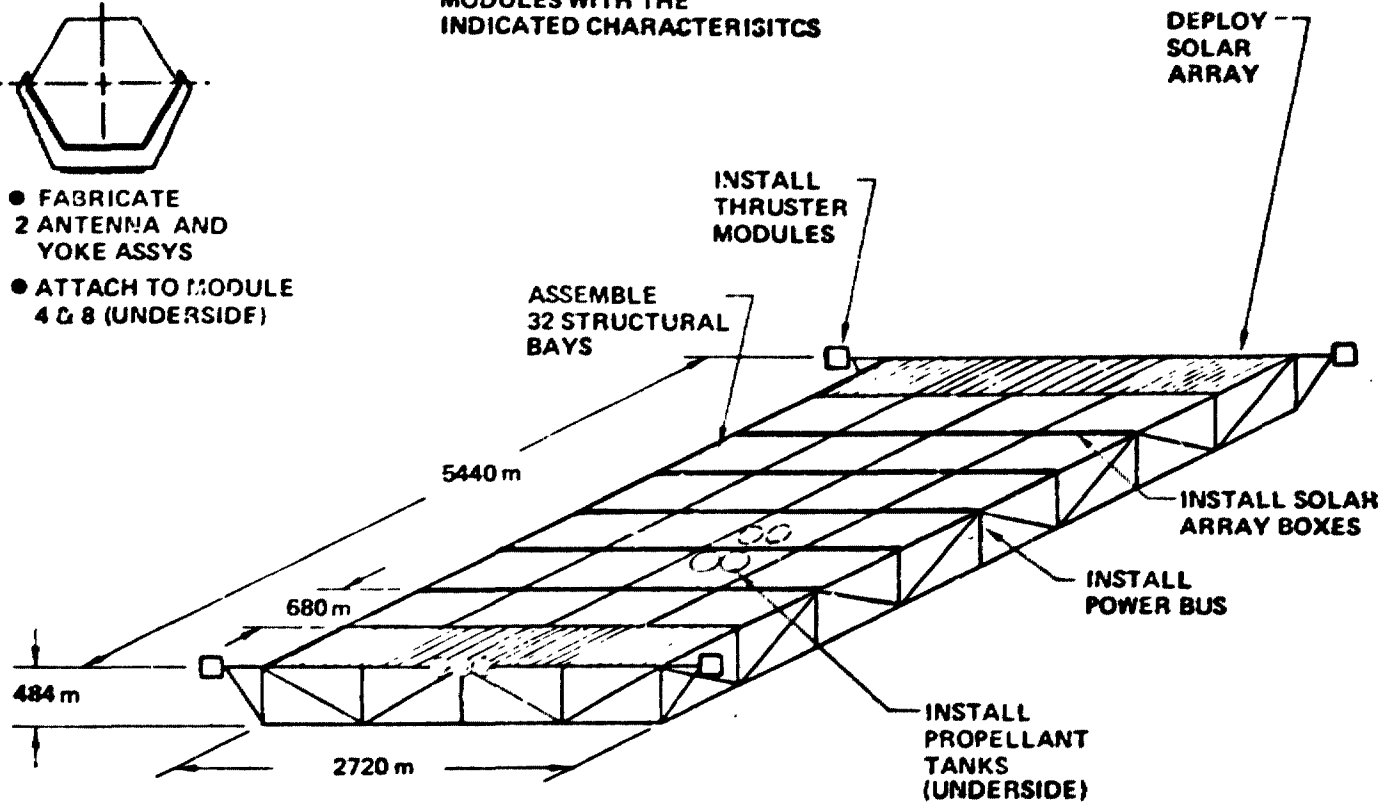
SPS-1130

BOEING

- CONSTRUCT 8 SATELLITE MODULES WITH THE INDICATED CHARACTERISTICS



- FABRICATE 2 ANTENNA AND YOKE ASSYS
- ATTACH TO MODULE 4 & 8 (UNDERSIDE)



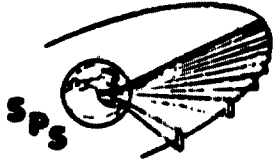
D180-22876-7

**LEO BASE CONSTRUCTION TASKS
THERMAL ENGINE SATELLITE**

The construction tasks associated with thermal engine satellite modules are indicated. The key difference compared to the photovoltaic construction task primarily relates to the difference in the power generation devices (i.e., reflectors and thermal engines/radiators instead of solar arrays).

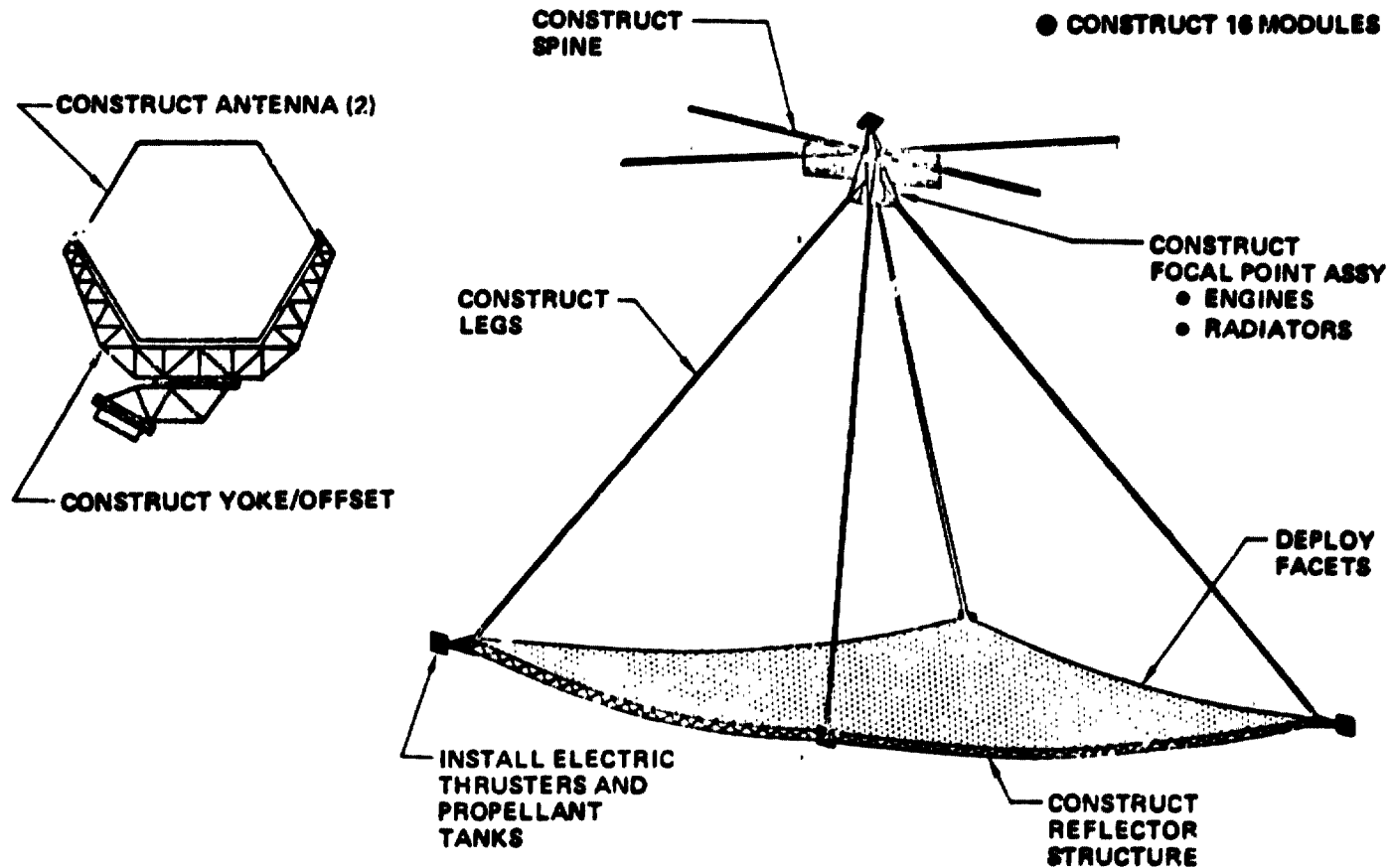
D180-22876-7

LEO Base Construction Tasks Thermal Engine Satellite



SPS-1416

BEING

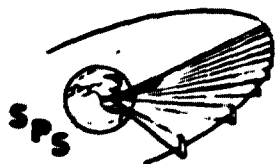


D180-22876-7

**LEO CONSTRUCTION BASE
PHOTOVOLTAIC SATELLITE**

The construction base for the photovoltaic satellite consists of two connecting facilities with one used to build the modules and the other to build the antenna. The module construction facility is an open ended structure which allows the four bay wide module to be constructed with only longitudinal indexing. There are two internal working bays. The aft bay is used for structural assembly using beam machines and joint assembly machines attached to both the upper and lower surfaces of the facility. Solar array and power distribution are primarily installed from equipment attached to the upper facility surface in the forward bay. The satellite module is supported by movable towers located on the lower surface of the facility. These towers are also used to index the module as it is being fabricated.

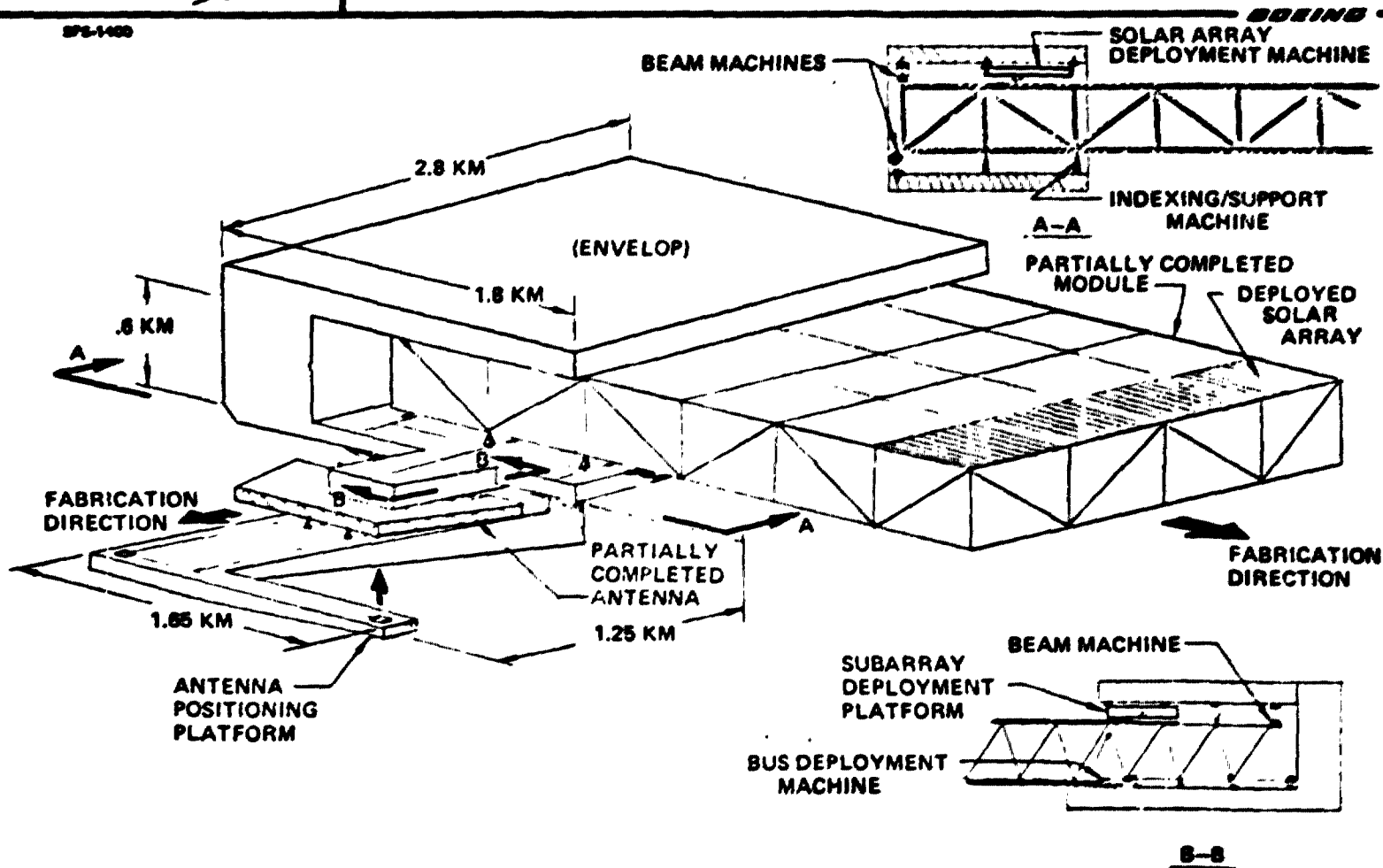
The antenna facility is configured to enclose four bays of antenna in width and four rows of bays in length. The minimum plan-view shape of the facility is obtained through use of a 60 degree parallelogram. This shape is the result of the basic unit of the primary structure being triangular in shape and the resulting angular indexing. The lower surface of the facility is used to support beam machines, joint assembly machines, support indexing machines and bus deployment equipment. The upper surface is used to support beam machines, joint assembly machines and a deployment platform that is used to deploy the secondary structures and antenna subarrays.



D180-22876-7

LEO Construction Base Photovoltaic Satellite

SPS-1400



D180-22876-7

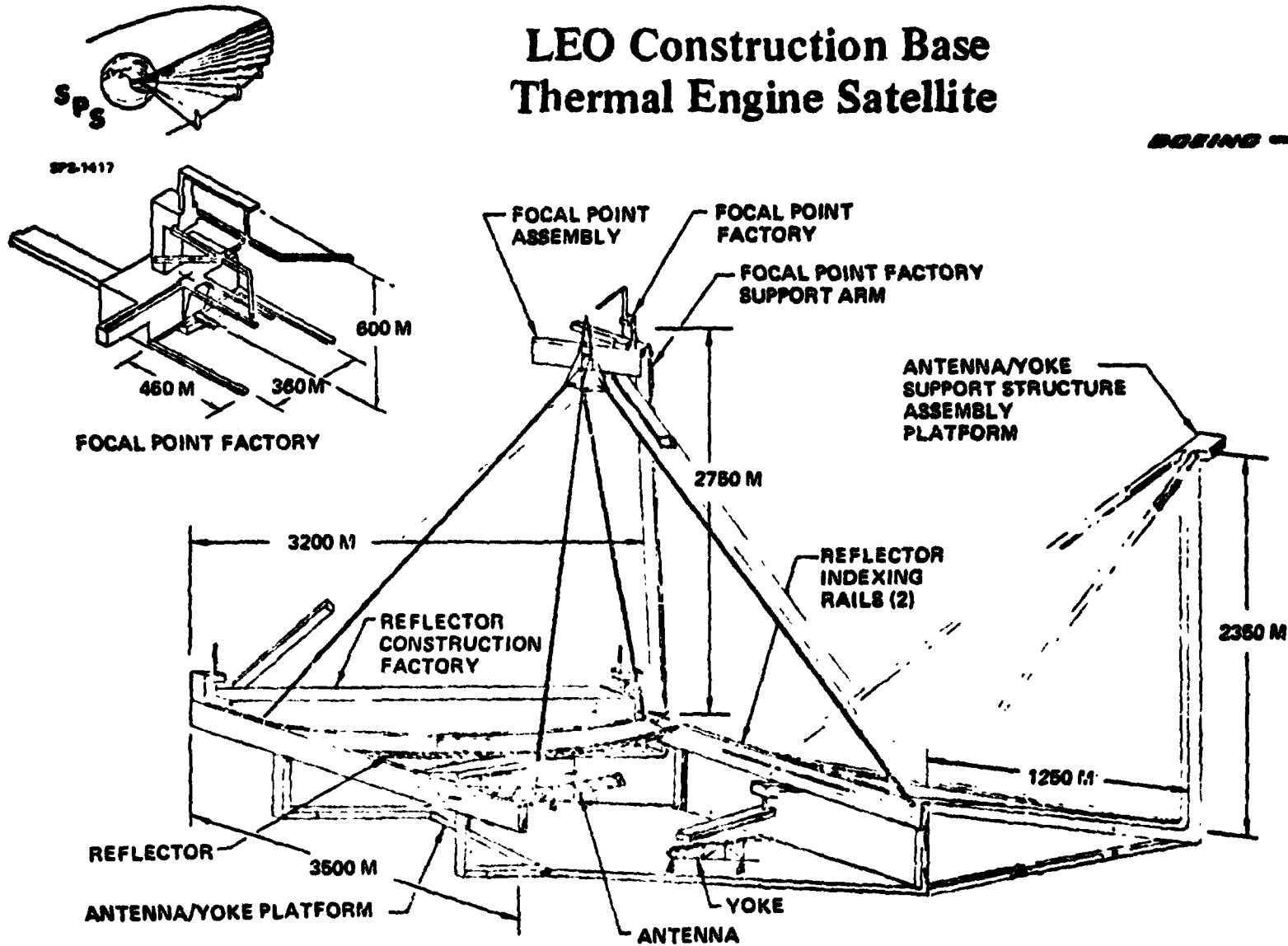
**LEO CONSTRUCTION BASE
THERMAL ENGINE SATELLITE**

The thermal engine satellite construction base has been designed to in effect surround the thermal engine satellite module and as a result consists of some rather large dimensions. The construction operations are performed in three separate levels or areas of the base. At the lower level is located the antenna construction facilities and those provisions necessary to construct the antenna yoke. Immediately above this area is the reflector construction factory which includes equipment necessary to construct reflector structure and install reflecting facets. Deployment of the constructed reflectors is accomplished using indexing devices moving down two side rails. These rails are also used to support beam machines used to construct the four supporting legs between the reflector surface and the focal point. At the upper level of the construction base is located the focal point factory which has the task of constructing the CPC cavity, installing the thermal engines, constructing radiators and the spine which serves as the power distribution system. A fourth area, although only used in the construction of two modules is the assembly platform used to form the antenna structure support point for the antenna.

D180-22876-7

LEO Construction Base Thermal Engine Satellite

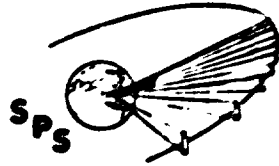
BOEING



D180-22876-7

**MODULE CONSTRUCTION SEQUENCE
PHOTOVOLTAIC SATELLITE**

The construction sequence associated with the structure, solar array and power buses consists of initially building the first end frame of the structure. This end frame is indexed forward one structural bay length at which time machines can form the remainder of the structure in each of the bays. The first row of four bays is then indexed forward to allow construction of the fifth structural bay in parallel with installation of solar arrays in bay 1 through 4. Solar array installation and construction of structure occurs simultaneously across the width of the module, although neither operation depends on the other. At the completion of 16 bays or four rows of bays in length, the power buses and propellant tanks are installed. Construction of the structure and installation of solar arrays of the remaining four bay lengths of the module are done in a similar manner to that previously described. Thruster modules for the self-power system are attached to each of the four corners of the module.

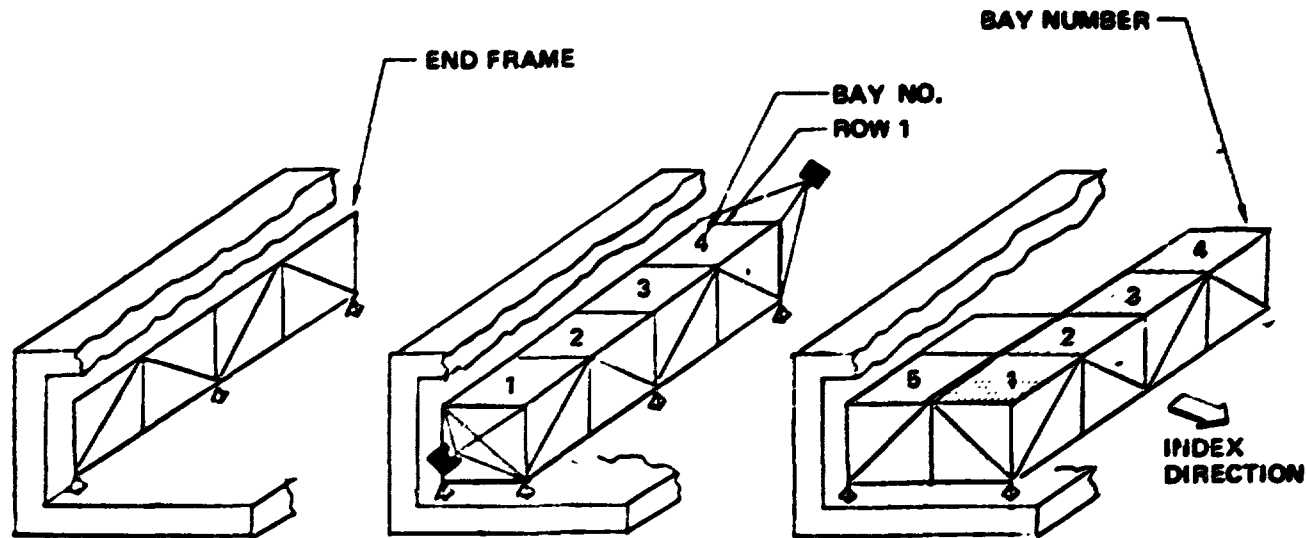


SPS-1221

D180-22876-7

Module Construction Sequence Photovoltaic Satellite

BOBING



①

- CONST END FRAME
- INDEX 1 BAY LENGTH

②

- CONST BAY 1 - 4 STRUCTURE
- INSTALL THRUSTER MODULES
- INDEX 1 BAY LENGTH

③

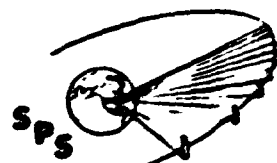
- DEPLOY SOLAR ARRAY AND CONST NEXT ROW OF STRUCTURE
- INSTALL BUSES AT END OF 4th ROW AND PROP. TANK
- INDEX 1 BAY LENGTH
- INSTALL SOLAR ARRAY CONTAINERS & FAB STRUCT

**REFLECTOR CONSTRUCTION OPERATIONS
THERMAL ENGINE SATELLITE**

The construction sequence for the power generation portion of the thermal engine satellite module is done using two charts. The first of these construction operations deals with the formation of the reflector surface. The principal elements involved in this operation are the factory itself and the structural machines, reflector deployment machines and indexing devices. The complexity of this operation and the machines themselves is better appreciated by the fact that the shape of the reflector surface is a portion of a sphere and in addition the structure forming the shape consists of interconnecting tetrahedrons. To accomplish this task, the structure and reflector machines are attached to the underside of the reflector factory and run on tracks. The spherical reflector shape is obtained by having the reflector factory move up and down in elevation and rotate about its longitude axis. Movement of the factory occurs after the machines make each transit across the factory length. Five structural and reflector machines are required in order to satisfy the timeline requirements.

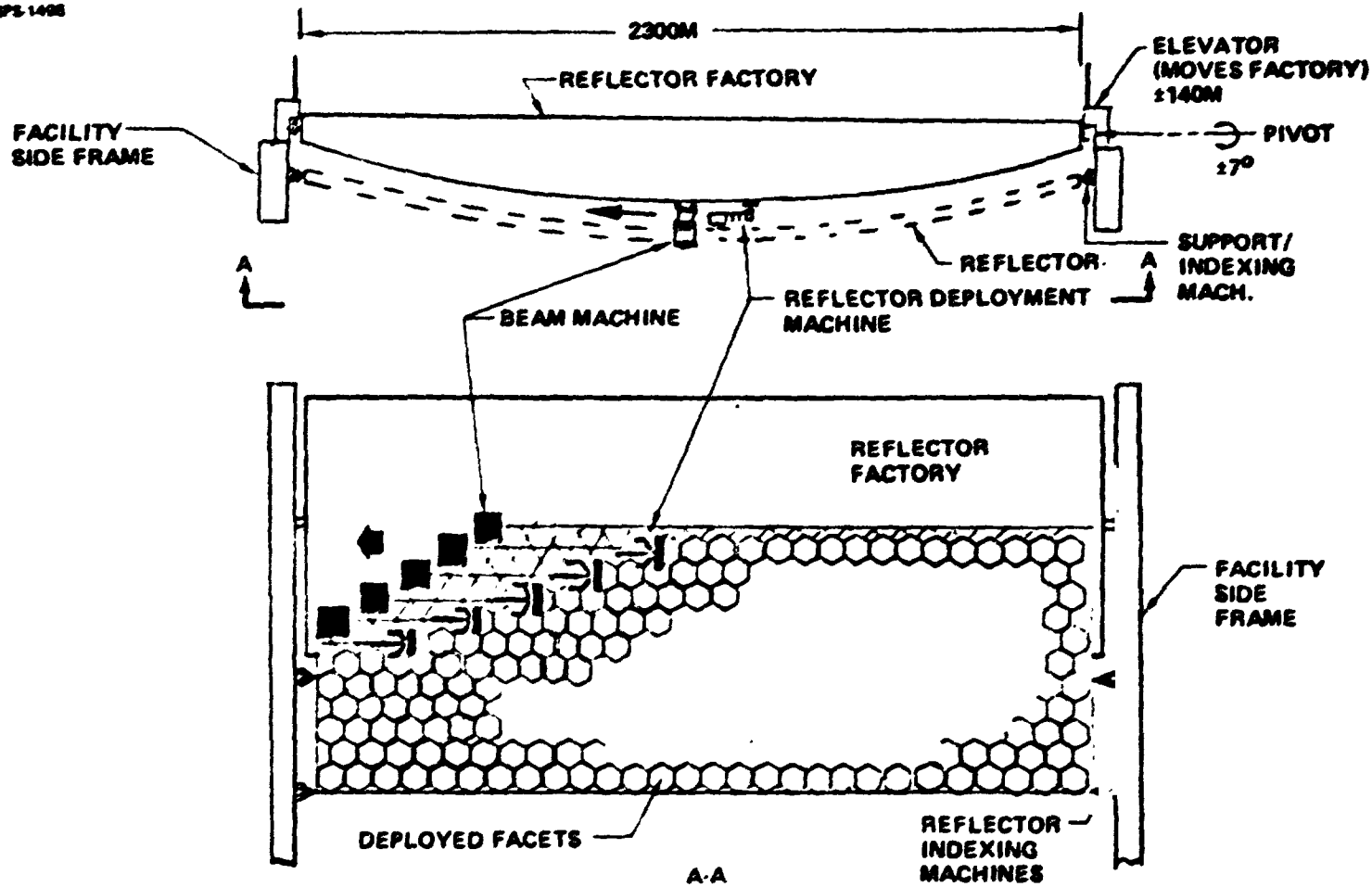
D180-22876-7

Reflector Construction Operations Thermal Engine Satellite



SPS-1498

BOEING

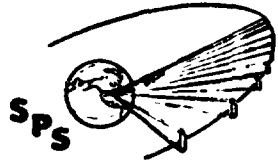


D180-22876-7

**FOCAL POINT ASSEMBLY OPERATIONS
THERMAL ENGINE SATELLITE**

The other major operation in constructing the thermal engine satellite occurs at the top of the construction base where the focal point equipment is constructed and installed. Shown here are the major individual operations to occur against a background of the focal point assembly factory. The point to be kept in mind is that all of these operations are going on simultaneously. At several points in time, major subassemblies are brought together and finally all elements are then connected to form the complete unit. At that point, the factory is moved away and the focal point can be attached to the support legs coming up from the reflector surface.

D180-22876-7

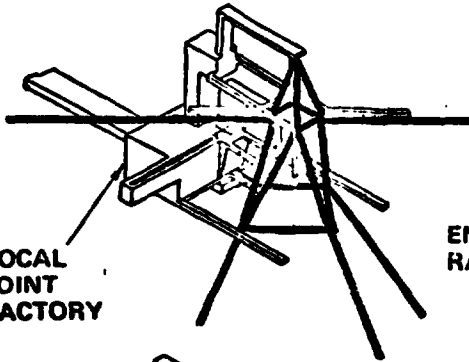


SPS-1497

Focal Point Assembly Operations Thermal Engine Satellite

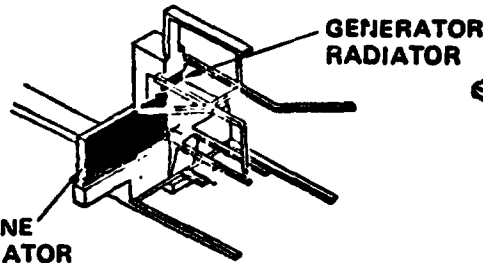
BOEING

• FRAME AND SPINES



FOCAL
POINT
FACTORY

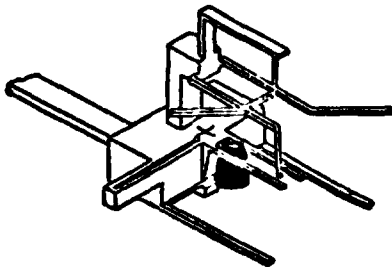
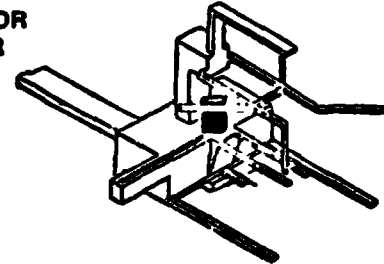
• RADIATORS AND
ENGINE INSTALL



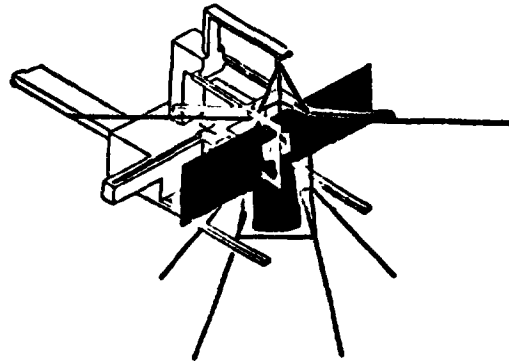
ENGINE
RADIATOR

GENERATOR
RADIATOR

• CAVITY



• CPC



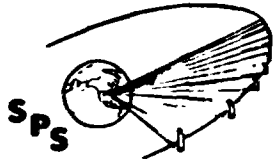
• COMPLETED FOCAL POINT ASSEMBLY

D180-22876-7

**ANTENNA/YOKE/MODULE ASSEMBLY
PHOTOVOLTAIC SATELLITE**

Construction of antenna and yoke for each satellite is essentially the same, and for that reason specific operations associated with this task are not covered at this time. In both cases, each antenna requires six months of construction time. A point of difference however, is where and when these elements are constructed and how the assembled antenna/yoke is attached to the satellite for transportation.

In the case of the photovoltaic satellite as shown here, the yoke for the antenna is constructed in the module construction facility because of its large dimensions. When using this approach however, it requires the yoke to be made in between the third and fourth module and between the seventh and eighth modules. Following yoke construction, it is moved to the side of the module facility. At that time either the fourth or the eighth module will be constructed. During the construction of these modules, the antenna is completed so that it can then be attached to the yoke. After five bays of either the fourth or eighth module have been completed, the antenna/yoke combination can then be attached to the module in its required location. Construction of two more rows of bays puts the antenna outside the facility where it then can be hinged under the module for its transfer to GEO.



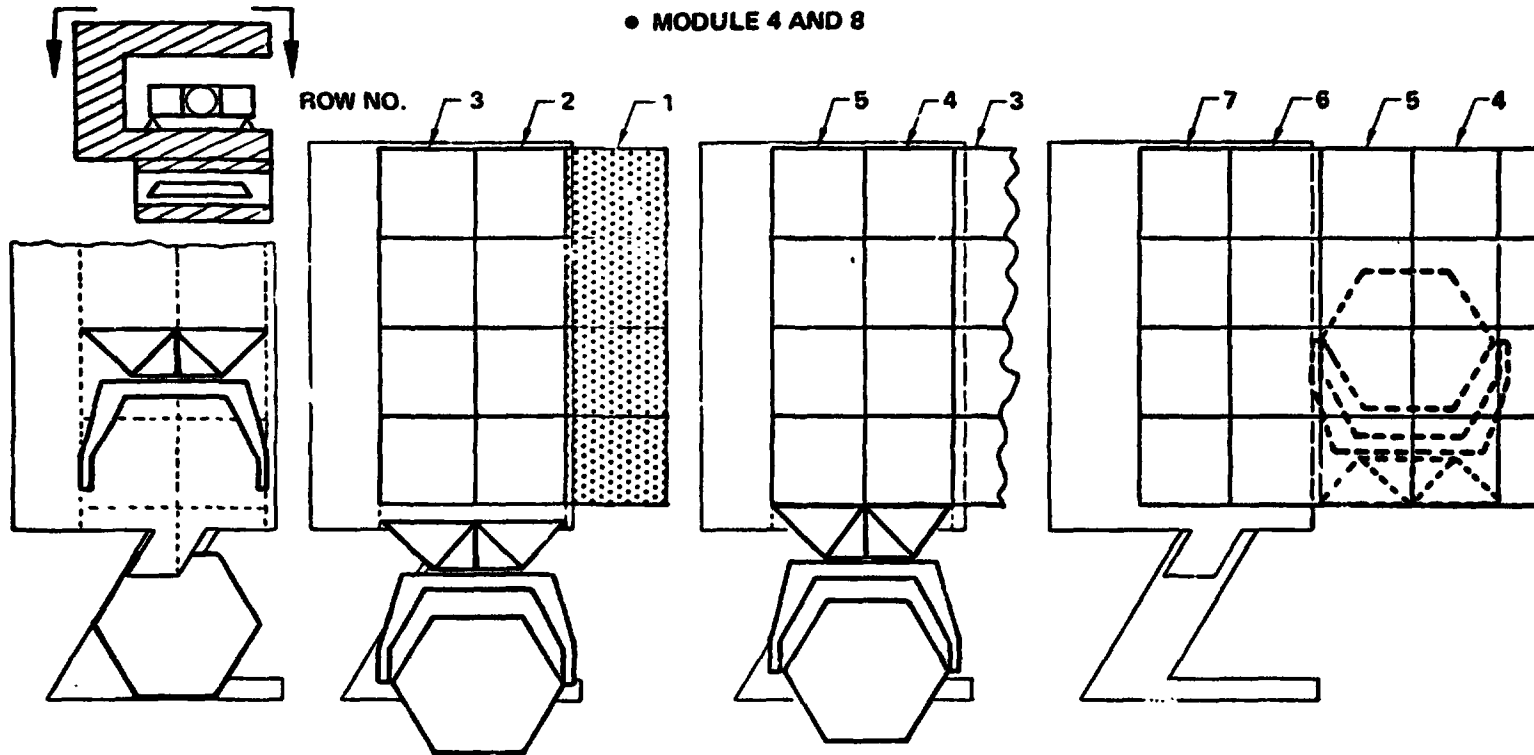
D180-22876-7

Antenna/Yoke/Module Assembly Photovoltaic Satellite

SPS-1402

BOEING

• MODULE 4 AND 8



- ① • ASSEMBLE YOKE & ROTARY JOINT (BETWEEN MODULE 3 & 4 AND 7 & 8)
• MOVE YOKE TO SIDE OF FACILITY

- ② • CONST 3 ROWS OF BAYS
• COMPLETE ANTENNA
• ATTACH ANTENNA TO YOKE

- ③ • COMPLETE 5 ROWS OF BAYS
• ATTACH ANTENNA SYS. TO MODULE

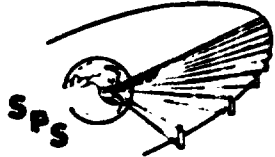
- ④ • CONST ROW 6 & 7
• ROTATE ANTENNA UNDER MODULE
• CONST ROW 8

D180-22876-7

**ANTENNA/YOKE/MODULE ASSEMBLY
THERMAL ENGINE SATELLITE**

Construction of the antenna elements of the thermal engine satellite occur at the lower level of the construction base. The support structure for the yoke and the hinge linkage used to position the antenna are different from the photovoltaic satellite. In the case of the support structure, there is an offset which allows the proper pointing of the antenna while the satellite flies PEP rather than POP as in the case of the photovoltaic satellite. The hinge linkage used to position the satellite is made following the yoke. Assembly of the antenna, yoke and hinge linkage into one unit is followed by the attachment of this unit to the underside of the reflector surface for the transfer to GEO.

D180-22876-7

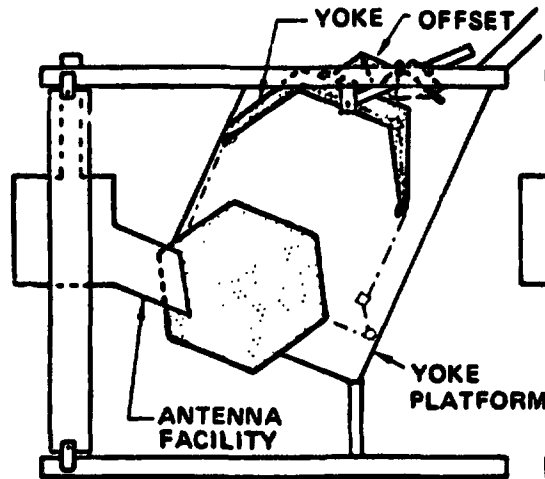


Antenna/Yoke/Module Assembly Thermal Engine Satellite

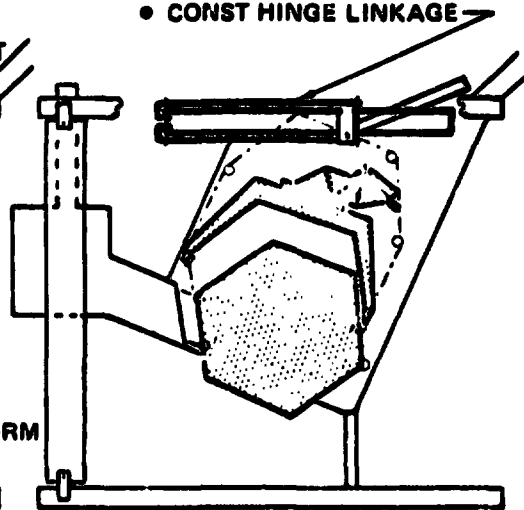
BOEING

SPS-1419

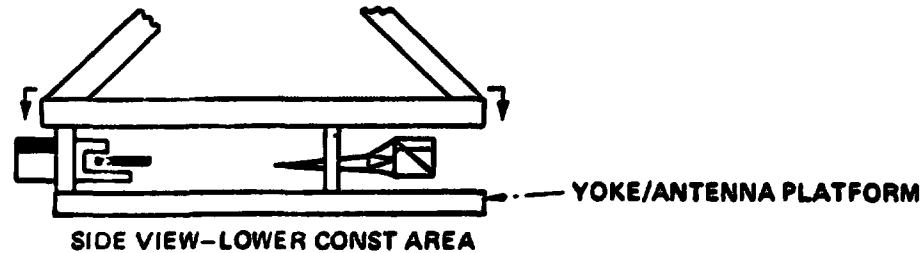
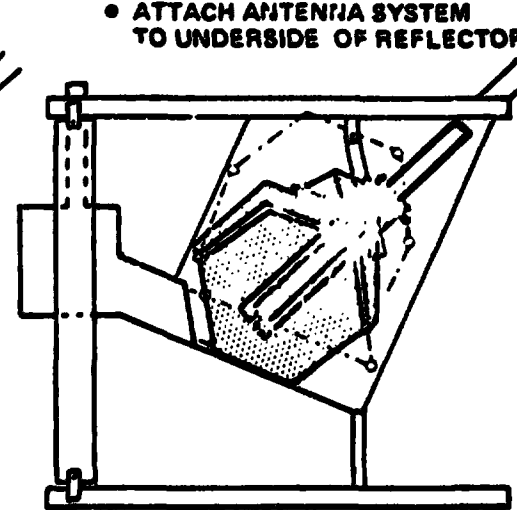
- ① • CONST YOKE, OFFSET AND ANTENNA



- ② • REPOSITION YOKE, OFFSET AND ANTENNA
• CONST HINGE LINKAGE



- ③ • ATTACH ANTENNA/YOKE & HINGE LINKAGE
• ATTACH ANTENNA SYSTEM TO UNDERSIDE OF REFLECTOR

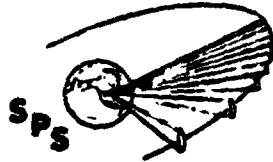


D180-22876-7

**GEO BASE CONSTRUCTION TASKS
PHOTOVOLTAIC SATELLITE**

Several key and distinguishing construction tasks are required by each satellite once GEO is reached. In the case of the photovoltaic satellite, an additional task is required in that those solar arrays not deployed for transfer now require deployment. This operation requires a final assembly platform that can support four solar array deployment machines as shown. The other tasks to be performed at GEO are shown on subsequent charts.

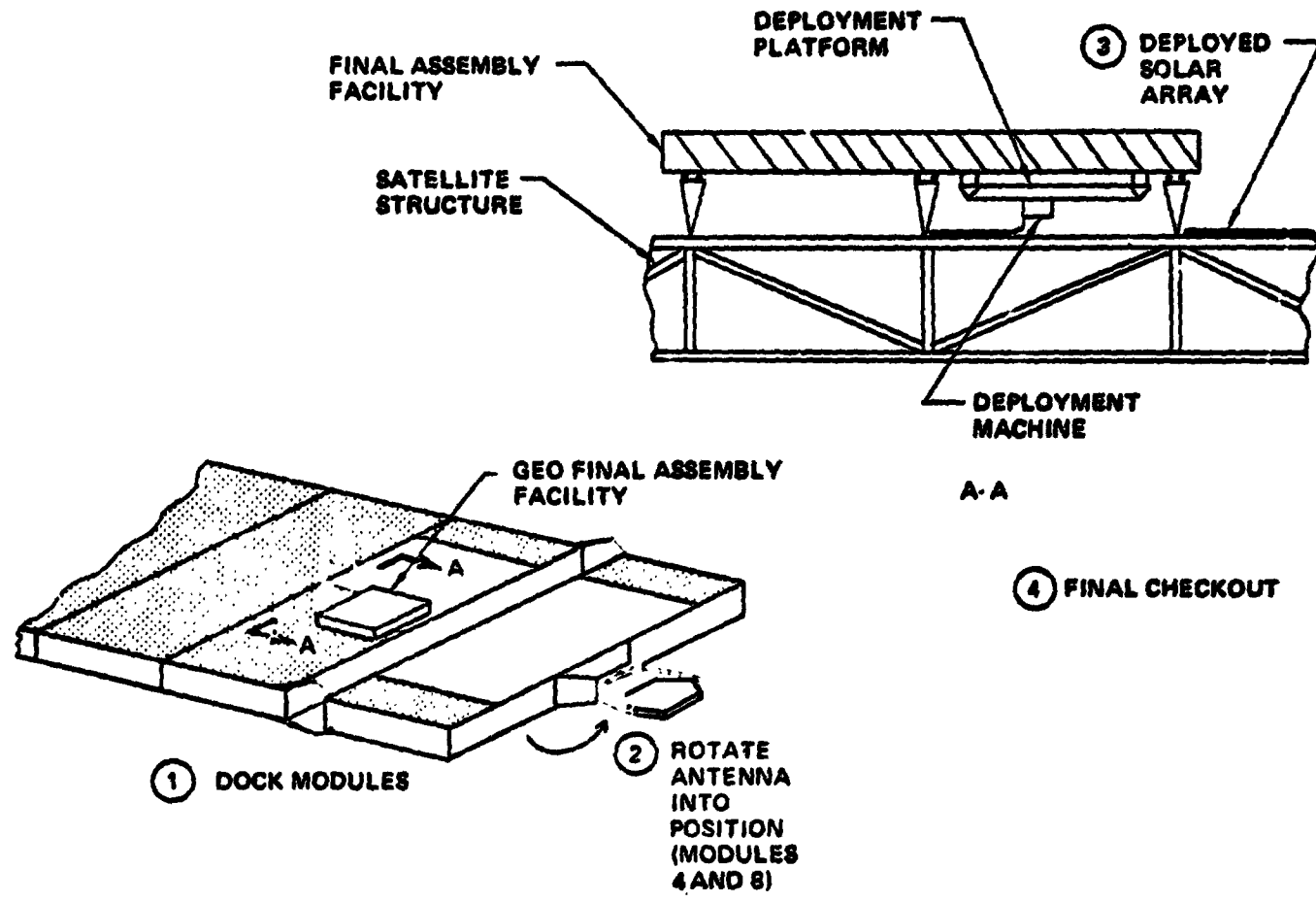
D180-22876-7



SPS-1412

GEO Base Construction Tasks

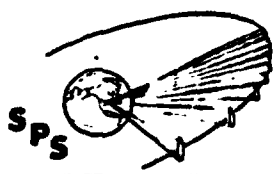
BEING



D180-22876-7

**GEO BERTHING CONCEPT
PHOTOVOLTAIC SATELLITE**

The first operation to occur once the modules reach GEO is that of the berthing (or docking) of the modules. In the case of the photovoltaic satellite, the modules are berthed along a single edge as indicated. The major equipment used to perform these berthing operations are shown. The concept employs the use of four docking systems with each involving a crane and three control cables. Variations in the applied tension to the cables allows the modules to be pulled in, provide stopping control and provides attitude control capability. Also required in this concept is an attitude control system involving thrusters which are not shown.

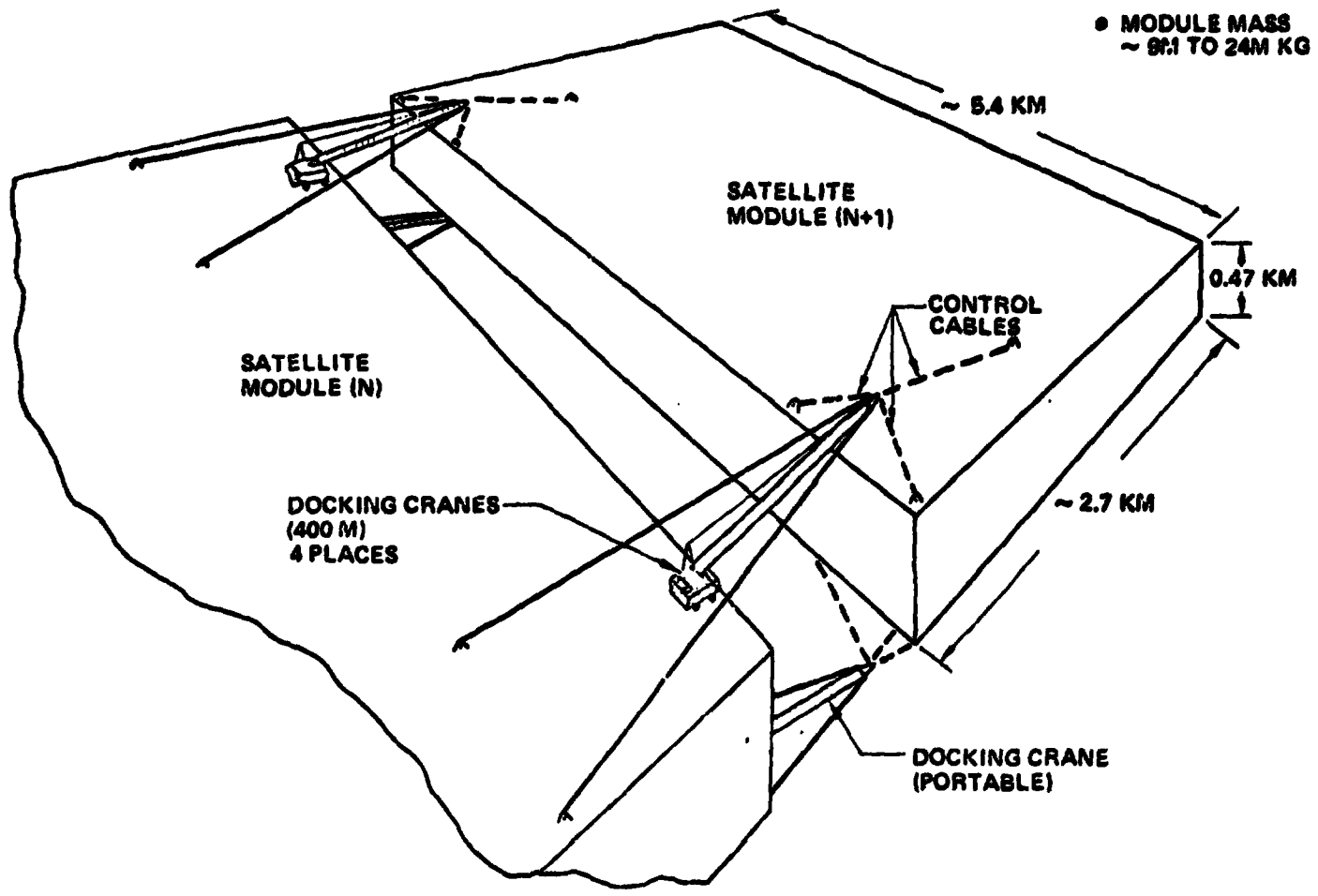


D180-22876-7

GEO Berthing Concept Photovoltaic Satellite

BOEING

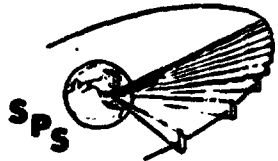
SPS-908



D180-22876-7

**GEO BERTHING CONCEPT
THERMAL ENGINE SATELLITE**

Berthing operations associated with the thermal engine satellite modules requires both single edge and two edge (corner) berthing as indicated. To accomplish the berthing operation, two facilities are employed. Each is provided with a crane system similar to those described for the photovoltaic concept. One of the facilities is located at the upper portion of the module while the second is near the plane of the reflector so that forces can be applied around the cg of the module. Movement of one of these facilities from module to module occurs by releasing one attachment point and pivoting around the other until the desired location is reached.



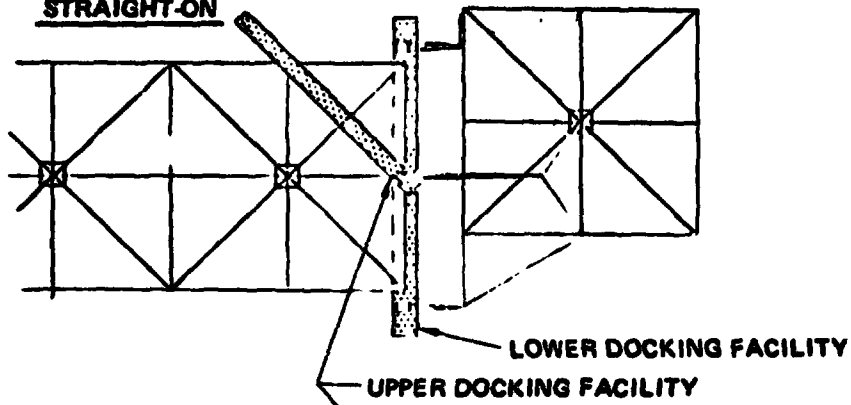
D180-22876-7

GEO Berthing Concept Thermal Engine Satellite

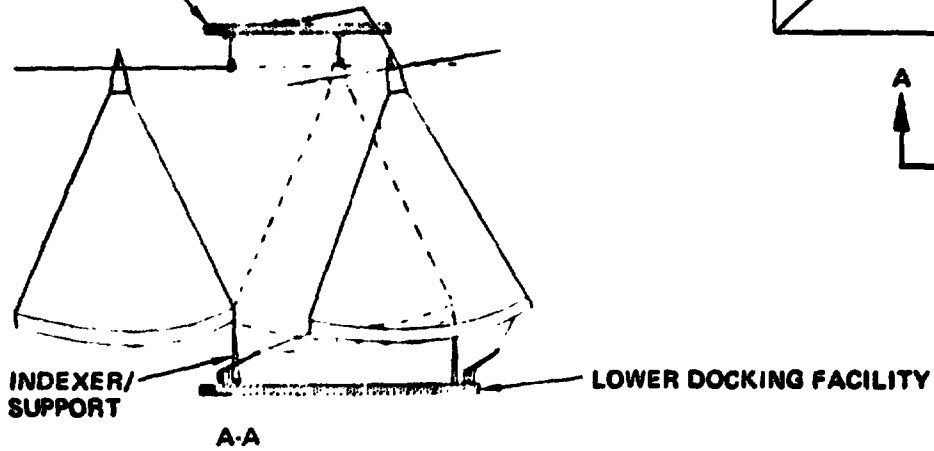
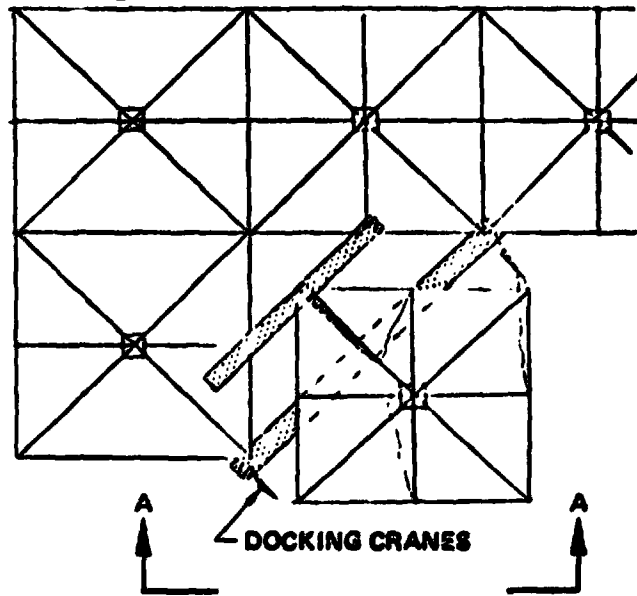
BOEING

SPS-1498

STRAIGHT-ON



CORNER



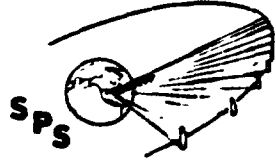
D180-22876-7

**ANTENNA FINAL INSTALLATION
PHOTOVOLTAIC SATELLITE**

Comparison of the antenna final assembly installation operations associated with the satellite also illustrates some differences in terms of complexity of the required mechanisms. In the case of the photovoltaic satellite, the antenna is attached below the module and uses a single hinge line. Once GEO is reached, the antenna is rotated into position followed by the final structural and electrical connections.

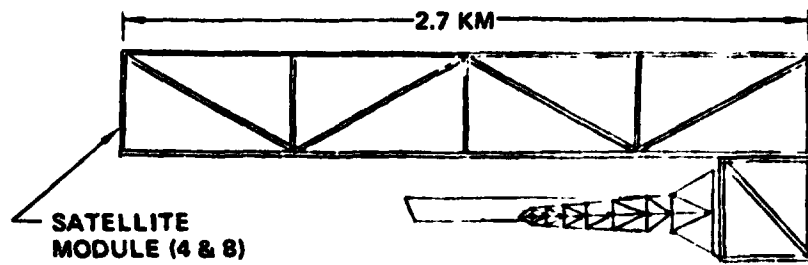
D180-22876-7

Antenna Final Installation Photovoltaic Satellite



SPS-1487

BOEING



- ①
- CONSTRUCT IN LEO
 - TRANSPORT TO GEO



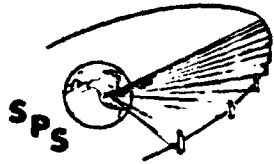
- ②
- ROTATE ANTENNA SYSTEM INTO POSITION
 - MAKE STRUT AND ELEC CONNECTIONS



D180-22876-7

**ANTENNA FINAL INSTALLATION
THERMAL ENGINE SATELLITE**

Placement of the thermal engine satellite antenna requires similar operations except that 3 hinge lines are required as shown rather than one. This condition is a result of the long distance between the transfer position of the antenna and the final position for the operational phase.



D180-22876-7

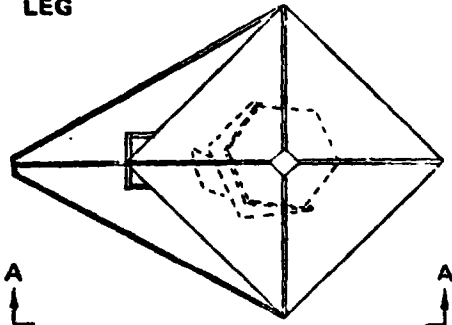
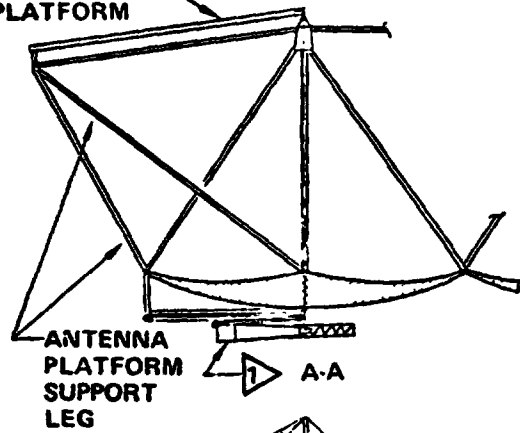
Antenna Final Installation Thermal Engine Satellite

BOEING

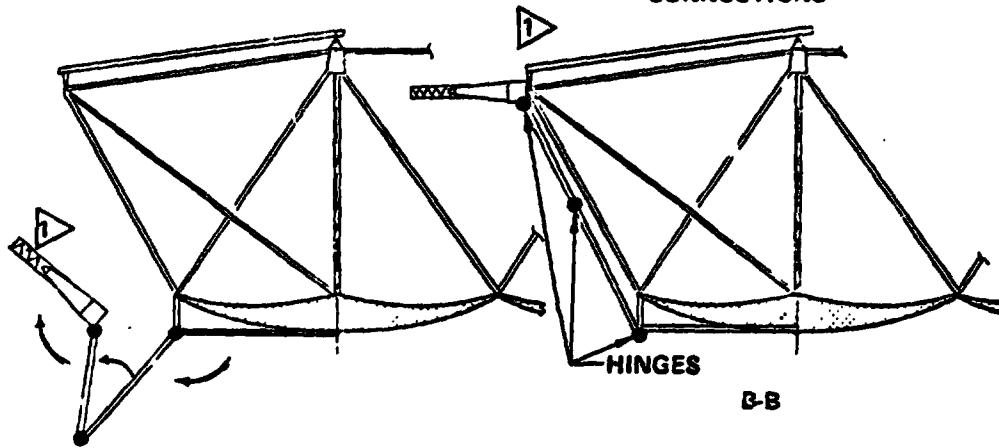
SPS-1433

- ① •TRANSPORT TO GEO
•DOCK TO OTHER MODULES

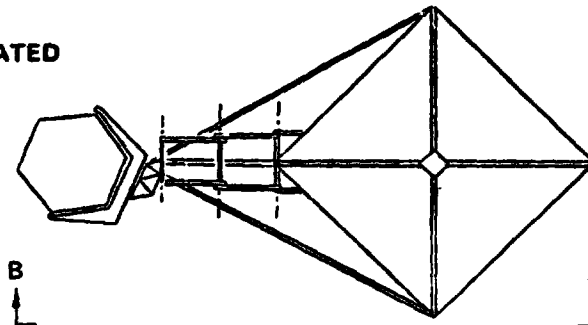
FINAL
ASSEMBLY
PLATFORM



- ② ROTATE INTO
POSITION



① ANTENNA SHOWN ROTATED
23.5 DEG CCW



- ③ MAKE STRUCTURAL
AND ELECTRICAL
CONNECTIONS

HINGES

B-B

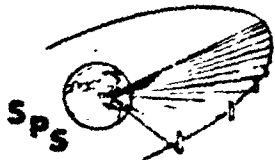
D180-22876-7

**MAJOR CONSTRUCTION EQUIPMENT
PHOTOVOLTAIC SATELLITE**

The major construction equipment associated with the photovoltaic satellite are illustrated along with some of the key characteristics such as quantity, mass and dimensions. Again, because the antenna itself is common to both satellite systems its special equipment is not shown although this material has been presented in the Part II Midterm and is included in the final documentation. The beam machine shown is indicative of the structural concept which uses two beam machines to form all the main structure. Accordingly, it has both translation as well as rotational capability. The dimensions and mass indicated are indicative of the segmented beam approach although machines fabricating thermally formed continuous cord structure could also be attached to the same frame.

Crane manipulator systems are primarily used to form the structural beam joints. Although the size indicated is most common, several 250 meter units are also required in the construction of the antenna yoke as well as several 20 meter cranes. Two man control cabins with manipulators are located at the end of the crane which is itself attached to a moving platform.

The principal difference between the indicated solar array machine and those illustrated in previous briefings is that the gantry itself is located approximately 50 meters below the facility beams since that is the location of the upper surface of the satellite. Further discussion on these machines will occur in the splinter meeting and in the final documentation.



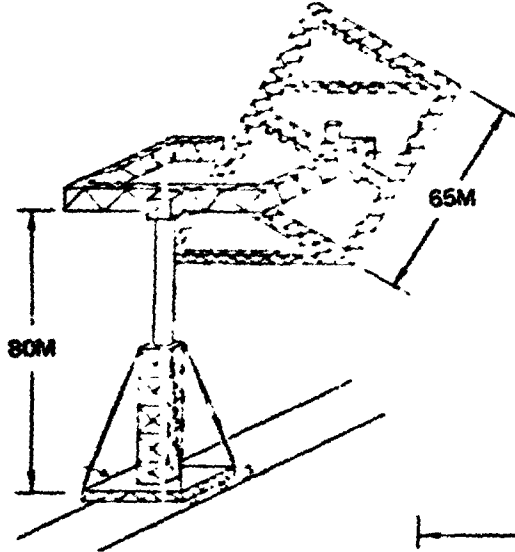
D190-22876-7

Major Construction Equipment Photovoltaic Satellite

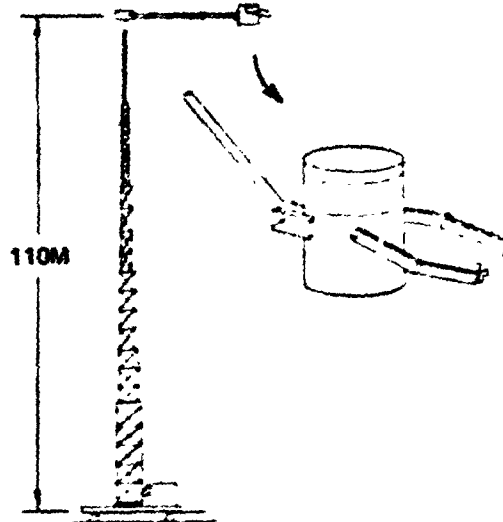
BOEING

SPS-1499

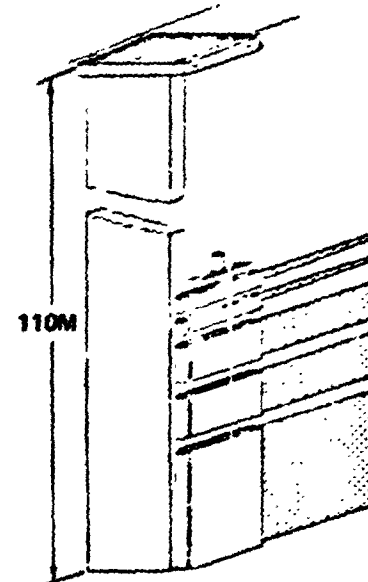
- BEAM MACHINE
 - (2) 20M - 20 000 kg
 - (2) 5M - 7 500 kg



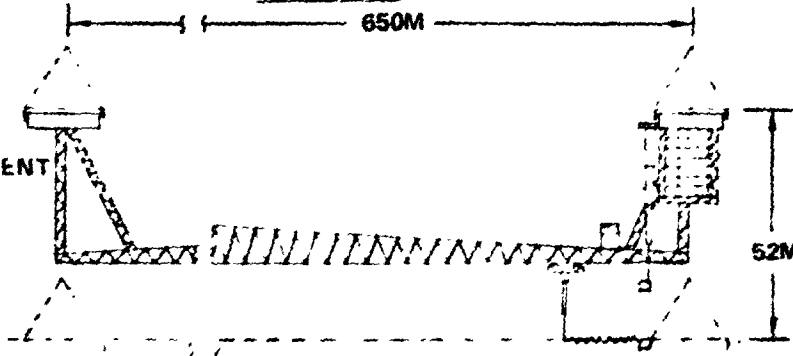
- CRANE/MANIPULATOR
 - 8 UNITS
 - 8 000 kg



- POWER BUS INSTALL
 - 1 UNIT
 - 7 000 kg



- SOLAR ARRAY DEPLOYMENT
 - 4 UNITS
 - 12 000 kg (Ea)



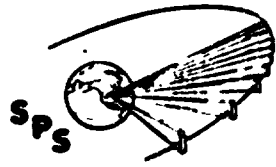
D180-22876-7

**MAJOR CONSTRUCTION EQUIPMENT
THERMAL ENGINE SATELLITE**

The thermal engine satellite requires several machines similar to the photovoltaic equipment but in addition requires several different units. Beam machines are also required with the key difference being the quantity and also the need of a 10 meter beam machine. Crane/manipulator units are approximately the same. Formation of the reflector (facets surface) requires a special structure machine and a facet deployment machine.

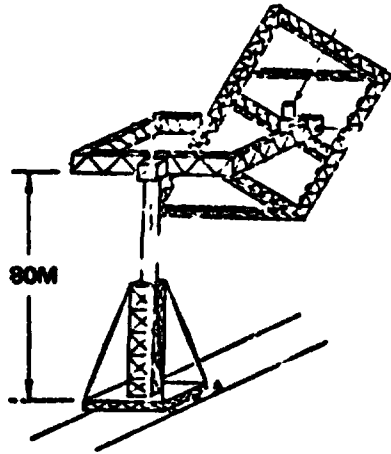
D180-22876-7

Major Construction Equipment Thermal Engine Satellite

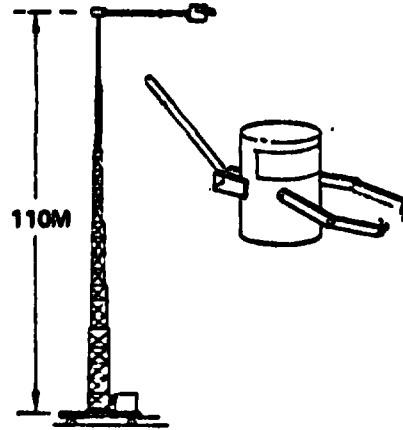


SP8-1500

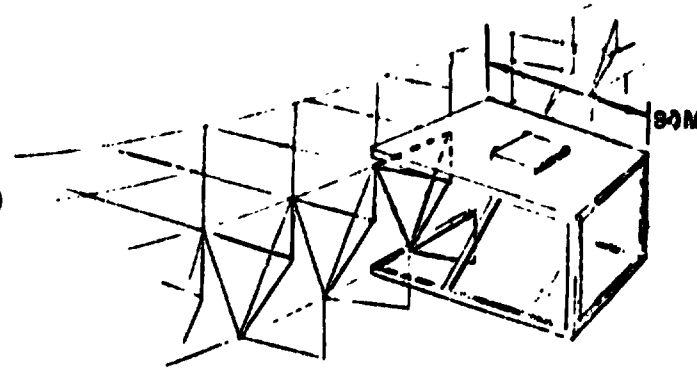
BEING



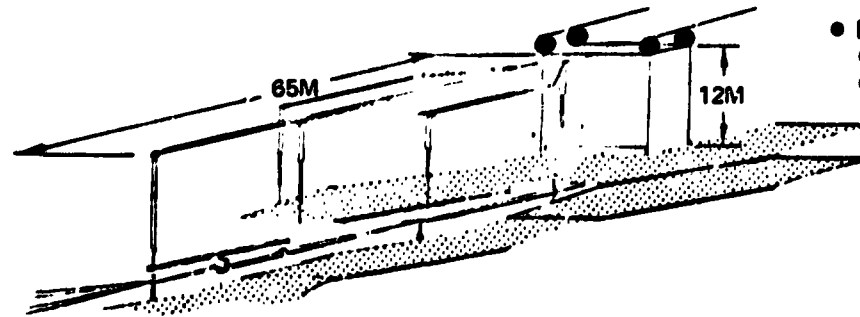
- BEAM MACHINE
 - (3) 20M - 20 000 kg
 - (4) 10M - 11 000 kg
 - (7) 5M - 7 000 kg



- CRANE/MANIPULATOR
 - 21 UNITS
 - 7 500 Kg (EA)



- FACET STRUCT MACHINE
 - 5 UNITS
 - 30 000 kg (EA)



- FACET DEPLOYMENT MACHINE
 - 5 UNITS
 - 13 000 kg (EA)

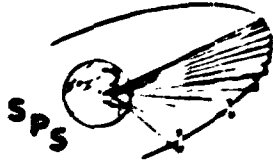
D180-22876-7

**MAJOR CONSTRUCTION EQUIPMENT
THERMAL ENGINE SATELLITE**

In addition to individual machines, the thermal engine satellite construction operation requires several mini-factories involving numerous pieces of equipment. Examples of these small factories are as follows: the formation of the CPC and cavity where cranes, manipulators, welders, conveyors and control cabins are required; a radiator factory that welds the 20 meter length sections of pipe into 350 meter lengths and then attaches the radiators (heat pipe) panels to the main pipes; in addition, engine installation is required including a connection of power busses between the engines and finally, the spine assembly that consists of machines to build structure running between module focal points and machines to assemble and attach the major power busses to that structure.

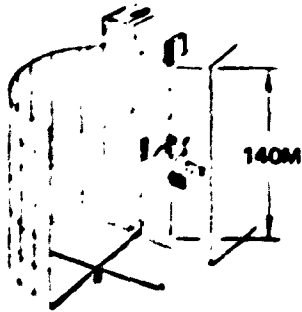
D180-22876-7

Major Construction Equipment Thermal Engine Satellite

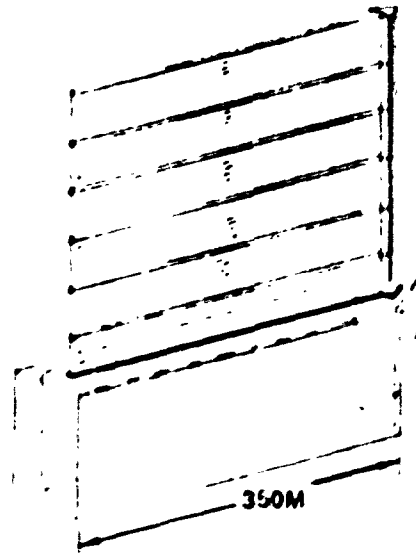


SPS 1601

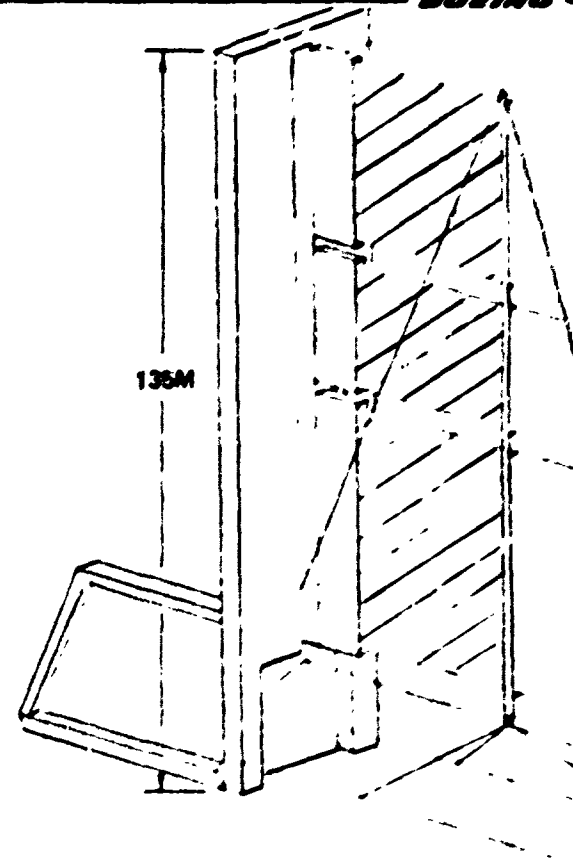
BOEING



- CAVITY AND CPC
ASSY EQUIPMENT
- 1 EACH
- 28 000 kg



- RADIATOR AND
THERMAL ENGINE ASSY
AND INSTALL EQUIP
- 27 000 kg

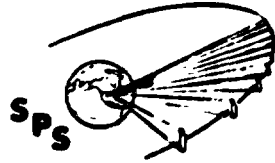


- SPINE ASSY MACHINE
- TWO UNITS
- 28 000 kg

D180-22876-7

**CREW SIZE AND DISTRIBUTION
LEO CONSTRUCTION**

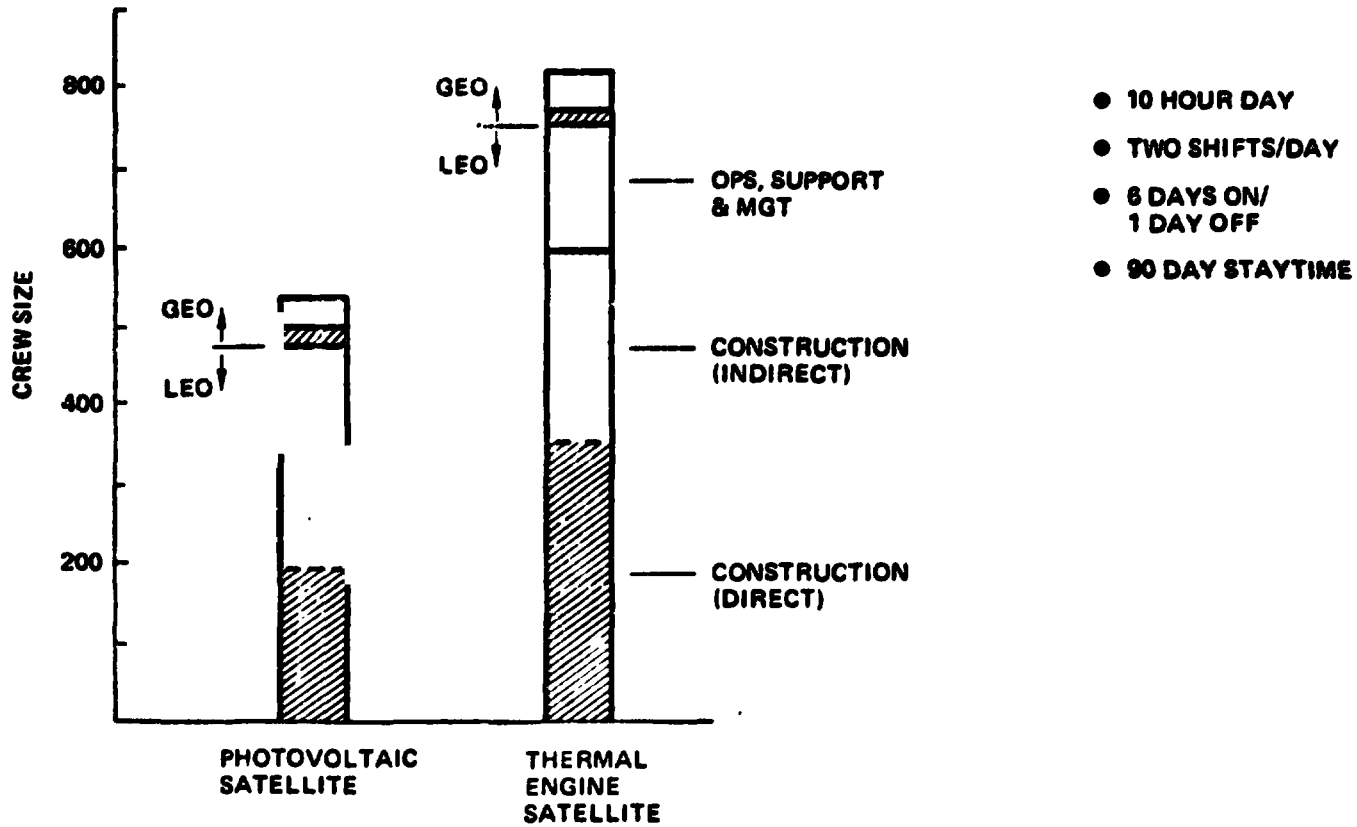
The difference in crew size and distribution of crew is indicated for the two satellite concepts. The crew size for all orbital personnel indicates the photovoltaic satellite requires approximately 300 fewer people with all this difference occurring in the low Earth orbit construction base. The principal reason for the larger crew requirements for the thermal engine satellite is due to more construction operations required and of course this then contributes to the construction (indirect) personnel and the support personnel manloadings.



SP2-1480

Crew Size and Distribution LEO Construction

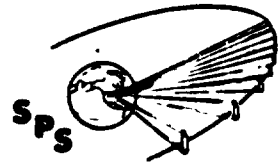
BOEING



D180-22876-7

CONSTRUCTION ROM MASS SUMMARY

ROM mass estimates are presented for the construction bases as well as crew rotation/resupply. In the case of the LEO construction bases, the photovoltaic satellite is lighter by approximately 3 million kilograms. The major contributors to the thermal engine mass is the large foundation (structure) along with three extra crew modules due to the 300 additional people and of course as previously described additional construction equipment. GEO final assembly bases are approximately equal. Differences in the annual crew rotation resupply requirements reflects the difference in the 300 man crew size



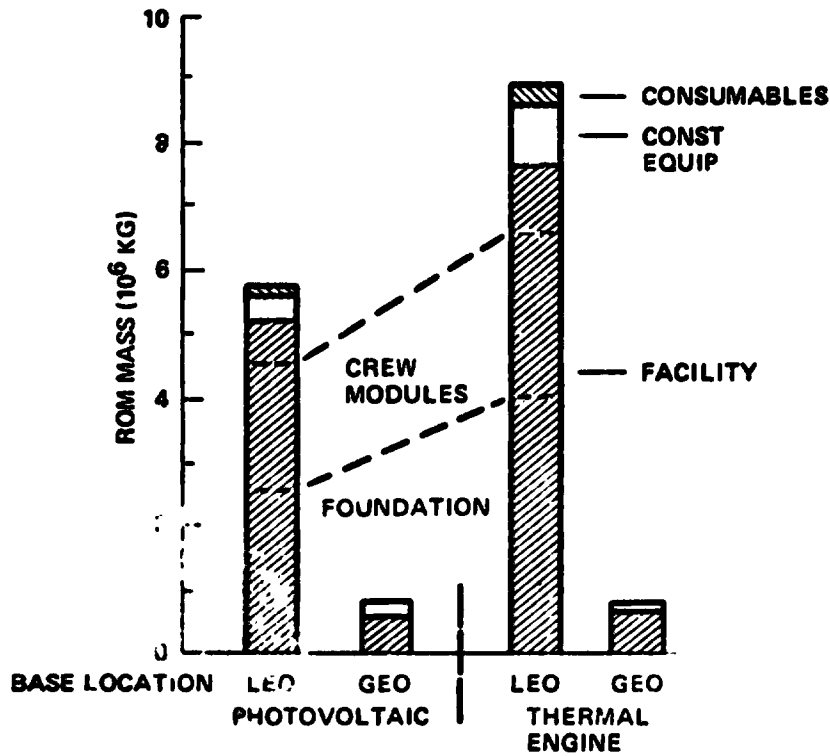
SPS-1616

Construction Mass Summary

BOEING

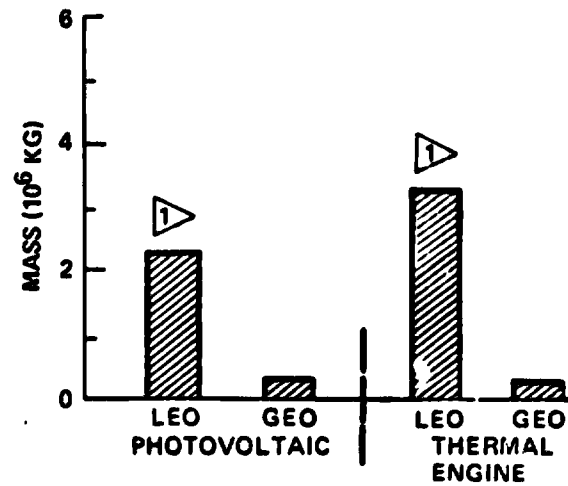
● LEO CONSTRUCTION

CONSTRUCTION BASES



CREW ROTATION/RESUPPLY

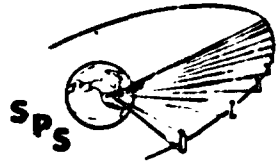
- ANNUAL
- CARGO, CREW, VEHICLES AND MODULES
- ▷ INCLUDES GEO SUPPLIES



D180-22876-7

**CONSTRUCTION BASE ROM COST
FIRST SET**

Comparison of the unit cost of the first set of construction bases indicates over a 4 billion dollar savings for the photovoltaic satellite. These values reflect a 90% learning factor applied to each major end item. Transportation costs are not included in this particular chart. In the case of the thermal engine satellite, the principal difference in the facility cost is the three extra crew modules and of course the large difference in construction equipment quantity and mass contributes the difference in cost. The wrap-around factor is applied to the sum of the facility construction equipment cost.



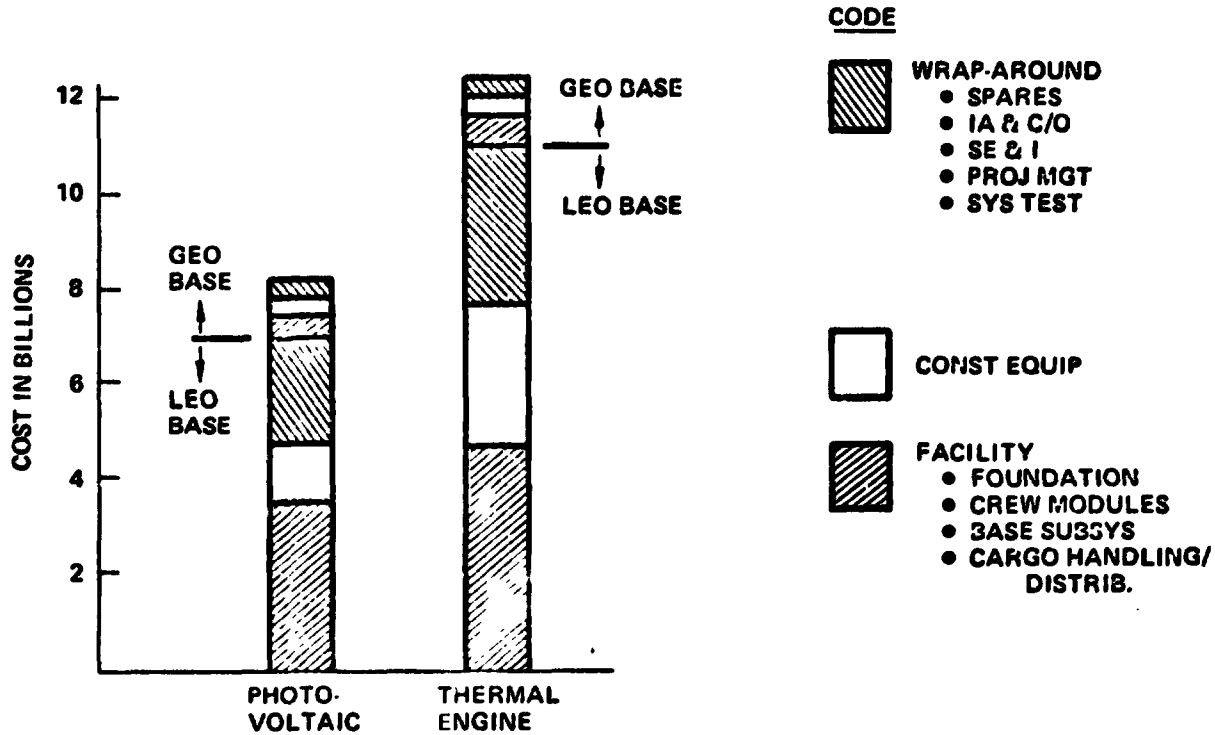
SPS-1608

D180-22876-7

Construction Base ROM Cost First Set

BOEING

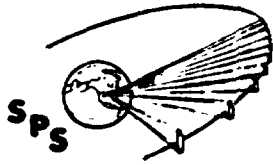
- 1 SATELLITE PER YEAR
- 90% LEARNING



D180-22876-7

TRANSPORTATION SYSTEM DIFFERENCES

Several key transportation differences occur when comparing the two satellites as shown in this chart. Each of these differences are further described in subsequent charts.



SPS-1613

Transportation System Differences

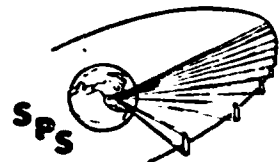
BOEING

<u>TRANSPORTATION FUNCTION</u>	<u>DIFFERENCE</u>	<u>REASON</u>
<ul style="list-style-type: none"> • SATELLITE LAUNCH SYSTEM • TWO STAGE BALLISTIC 	<ul style="list-style-type: none"> • PAYLOAD SHROUD P/V – REUSABLE T/E – EXPENDABLE 	<ul style="list-style-type: none"> • SATELLITE COMPONENT DENSITY
<ul style="list-style-type: none"> • CREW LAUNCH SYSTEM • SHUTTLE GROWTH 	<ul style="list-style-type: none"> • NUMBER OF FLTS 	<ul style="list-style-type: none"> • MORE PEOPLE IN ORBIT
<ul style="list-style-type: none"> • SATELLITE LEO-GEO SYSTEM • SELF POWER 	<ul style="list-style-type: none"> • T/E HAS LESS SATELLITE DESIGN IMPACT • LESS GRAVITY GRADIENT TORQUE 	<ul style="list-style-type: none"> • NO OVERSIZING AND USE OPER. VOLT. • LOWER INERTIAS
<ul style="list-style-type: none"> • CREW/SUPPLIES LEO-GEO • TWO STAGE LO₂/LH₂ OTV 	<ul style="list-style-type: none"> • NONE 	

COMPONENT PACKAGING DENSITY IMPACT

A most significant factor in the launch aspect of power satellites is the component packaging density and its impact on the number of launches required and/or the type of payload shroud that is used. In terms of the component density of the photovoltaic satellite, an average density of approximately 95 kilograms per cubic meter is indicated. The current 23 meter by 17.5 meter payload envelope with a volume utilization factor of 0.7 requires a density of 93 kilograms per cubic meter in order to reach a mass limited condition.

The thermal engine satellite density is approximately 66 kilograms per cubic meter primarily due to radiators, reflecting facets and antenna subarrays. Should the antenna subarrays be divided into a waveguide/structure section and klystron tube section, the density would go up to 76 kilograms per cubic meter. This approach however, requires assembly of the subarrays in orbit which is not deemed desirable at this time. Consequently, the thermal engine concept presents a difficult case for achieving mass limited launch conditions. The number of flights for the photovoltaic satellite reflect mass limited launch conditions. The thermal engine system is shown for both an expendable shroud large enough to reach a mass limited condition and a reuseable shroud option. Launch cost for these options are compared in the third set of bars. For the thermal engine system, the expendable shroud shows approximately a 300 million dollar savings per satellite as compared with a reuseable shroud due to the low unit cost (2 million dollars) for the expendable shroud when large quantities are procured. It should be mentioned however, that the thermal engine satellite will also utilize reuseable shrouds for the delivery of crew and supplies and delivery of construction requirements.

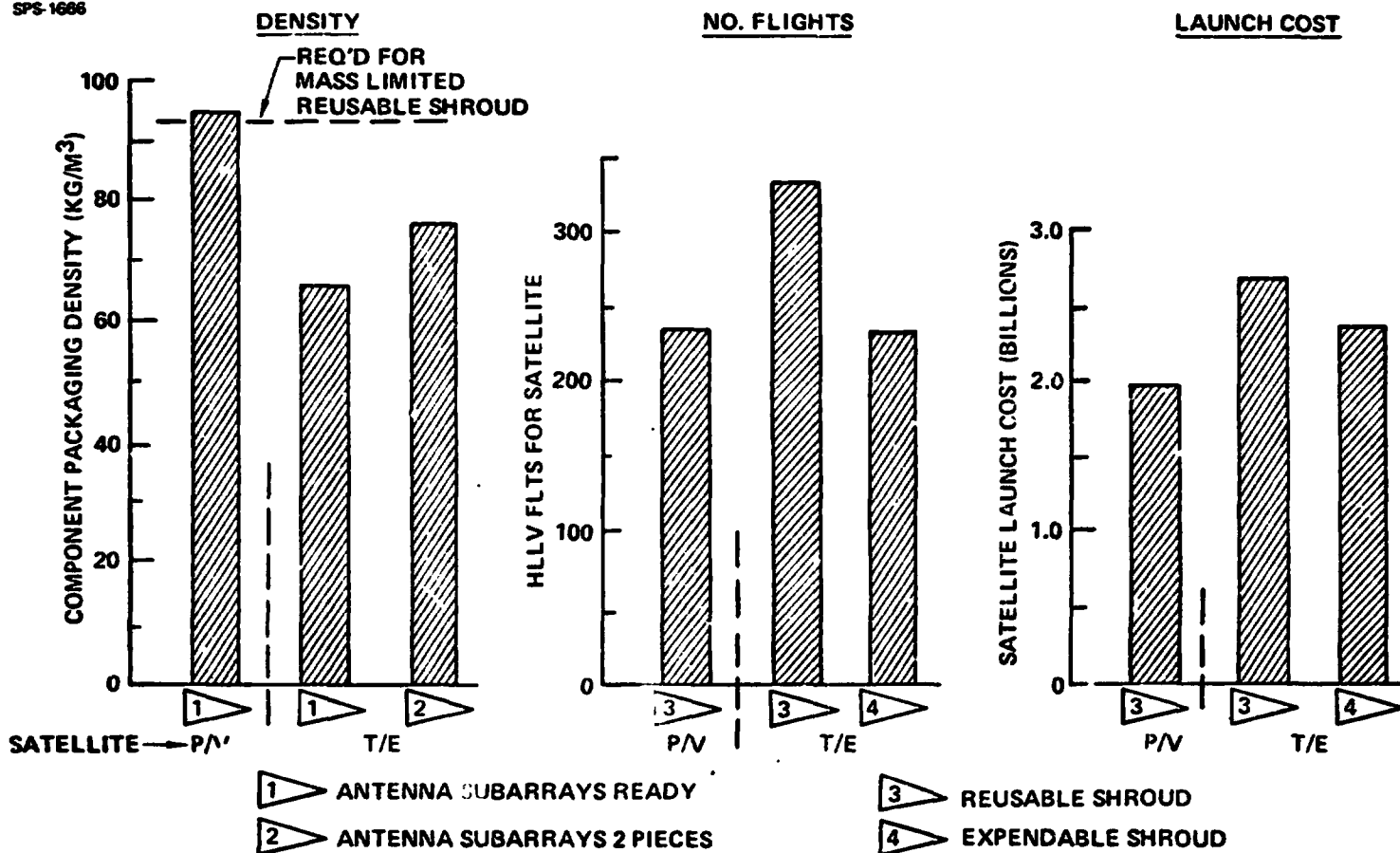


D180-22876-7

Component Packaging Density Impact

BOEING

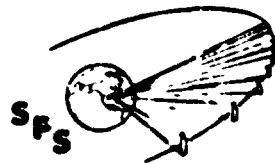
SPS-1686



D180-22876-7

SATELLITE LAUNCH VEHICLE

A comparison of the launch and reentry configuration for the two satellites is presented. The 35 meter expendable shroud required for the thermal engine systems is judged to be nearing the upper length limit without giving excessive bending loads during the launch. It should also be mentioned that although the expendable shroud is heavier than the reusable unit the system is jettisoned after the dynamic pressure level has fallen to zero. Consequently, payload capabilities of the two launches are judged to be nearly equal. As a result of using the expendable shroud, the docking system must be attached directly to the payload rack and then return on subsequent reusable shroud flights.



D, 80-22876-7

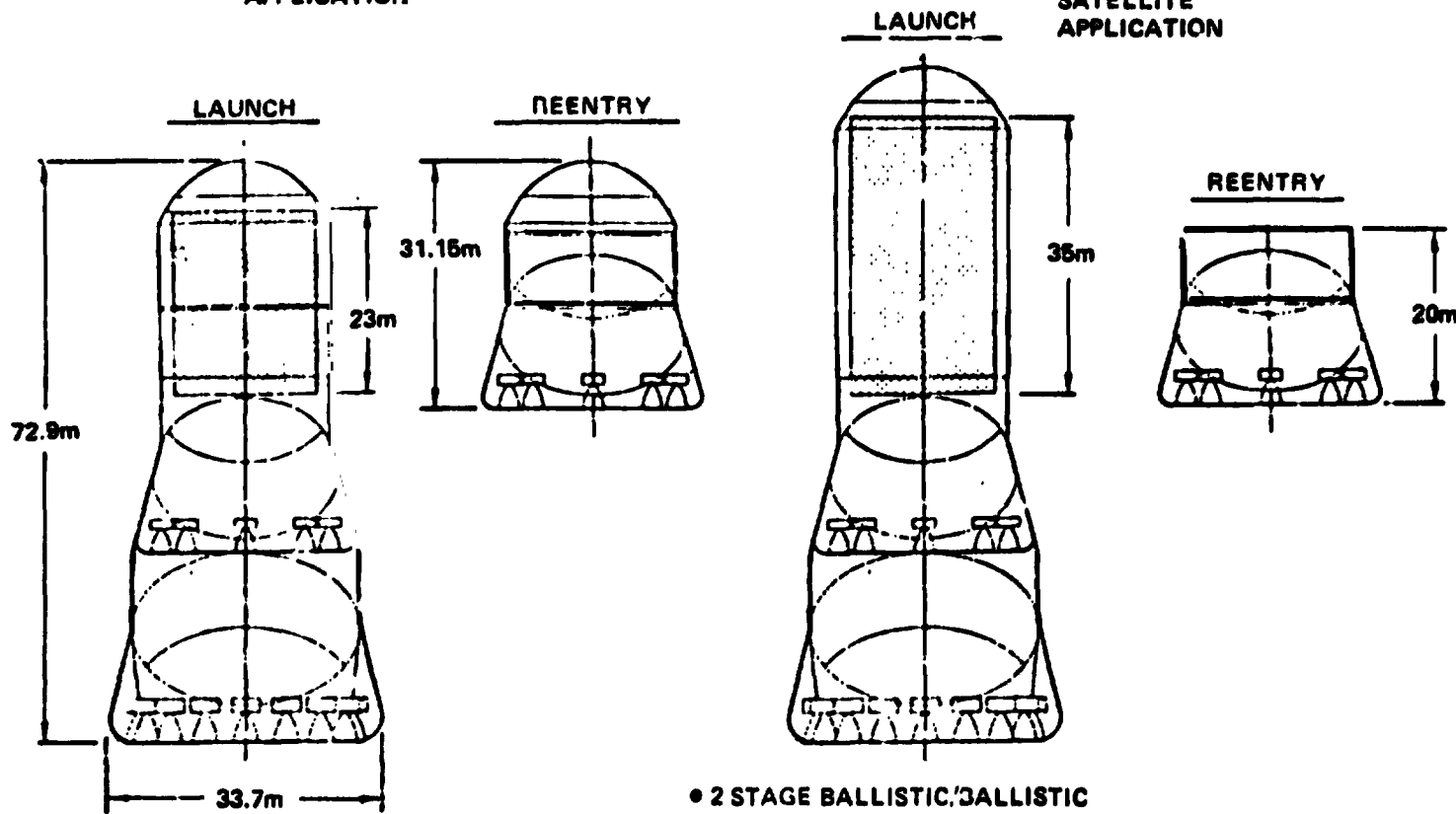
Satellite Launch Vehicle

D'S-1621

BOEING

PHOTOVOLTAIC SATELLITE APPLICATION

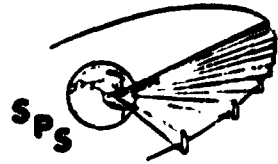
THERMAL ENGINE SATELLITE APPLICATION



- 2 STAGE BALLISTIC/BALLISTIC
- GLOW = 10.4×10^6 Kg
- PAYLOAD = 0.39×10^6 Kg

**SELF-POWER CONFIGURATION
PHOTOVOLTAIC SATELLITE**

b. transfer of the satellite modules from LEO to GEO involves the use of electric propulsion using power provided by the module (thus the name self-power). The characteristics associated with self-power of a photovoltaic module are shown for both those modules transferring antennas and those that do not. The general characteristics indicate a 5% oversizing of the satellite to compensate for the radiation degradation occurring during passage through the Van Allen belt and the inability to anneal out all of the damage after reaching GEO. It should also be emphasized at this point, only the arrays needed to provide the required power for transfer are deployed. The remainder of arrays are stowed within radiation proof containers. Cost optimum trip times and I_{sp} values are respectively 180 days and 7,000 seconds. Flight control of the module when flying a PEP attitude during transfer results in large gravity gradient torques at several positions in each revolution. Rather than provide the entire control capability with electric thrusters which are quite expensive, the electric system is sized only for the optimum transfer time with the additional thrust provided by LO_2/LH_2 thrusters. This penalty actually is quite small since by the time 2,500 kilometer altitude is reached the gravity gradient torque is no longer a dominating factor.

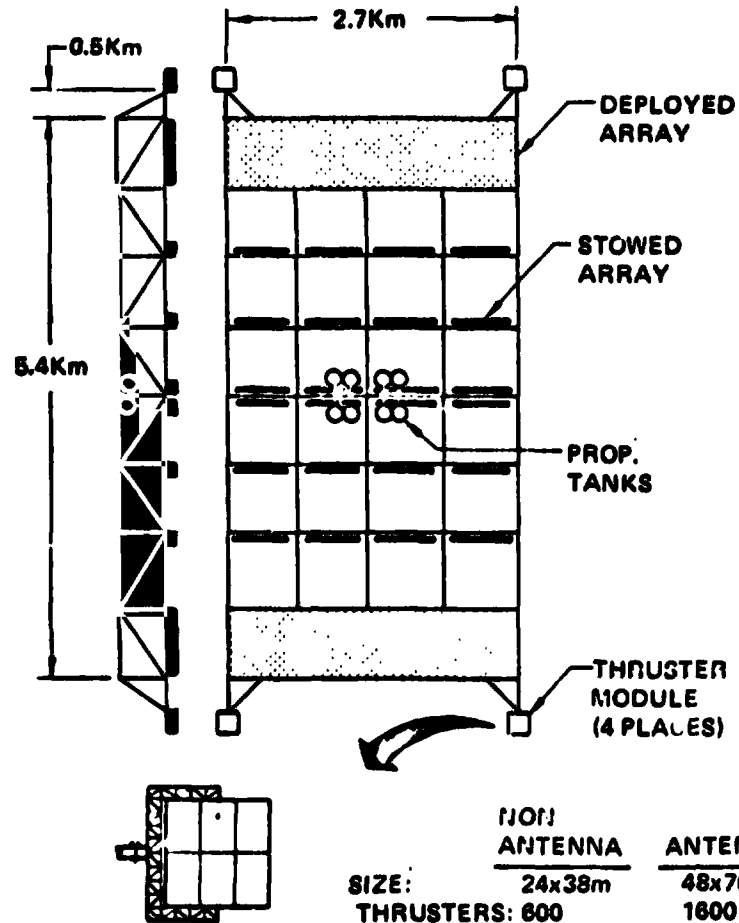


D180-22876-7

Self Power Configuration Photovoltaic Satellite

BOEING

SPS-1619



GENERAL CHARACTERISTICS

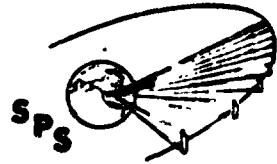
- 5% OVERSIZING (RADIATION)
- TRIP TIME = 180 DAYS
- ISP = 7000 SEC

MODULE CHARACTERISTICS	NON ANTENNA MODULE	ANTENNA MODULE
• NO. MODULES	6	2
• MODULE MASS (10^6 KG)	8.7	23.7
• POWER REQ'D (10^6 Kw)	0.3	0.81
• ARRAY %	13	36
• OTS DRY (10^6 KG)	1.1	2.9
• ARGON (10^6 KG)	2.0	5.6
• LO ₂ /LH ₂ (10^6 KG)	1.0	2.8
• ELEC THRUST (10^3 N)	4.5	12.2
• CHEM THRUST (10^3 N)	12.0	5.0

	NON ANTENNA	ANTENNA
SIZE:	24x38m	48x76m
THRUSTERS:	600	1600

**SELF-POWER CONFIGURATION
THERMAL ENGINE SATELLITE**

Self-power of the thermal engine satellite modules are for the most part similar to the photovoltaic modules from a performance standpoint although there are some distinguishing differences in terms of satellite design impact. One example of this is that no oversizing of the thermal engine modules is required since the reflector facets and engines are not sensitive to radiation as are the solar arrays. A second point is that the voltage generated by the satellite can be the same as the operating satellite voltage (since no plasma losses occur as in the case of solar arrays) and thus a minimum power distribution penalty occurs. From a propulsion standpoint, three thruster modules are used rather than four and although all facets are deployed in LFO, only a portion of these are required for the transfer. Gravity gradient torque associated with this configuration, are considerably lower due to the inertia characteristics of the module and consequently the chemical thrust required and the amount of LO_2/LH_2 propellant are considerably less than in the case of the photovoltaic satellite module.

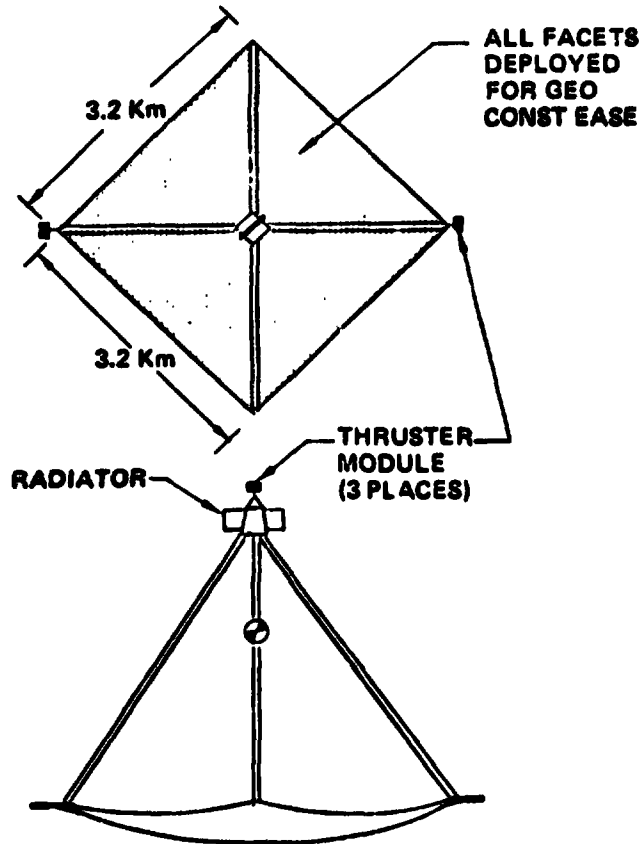


D180-22876-7

Self Power Configuration Thermal Engine Satellite

BOEING

SPS-1618



GENERAL CHARACTERISTICS

- NO OVERSIZING
- TRIP TIME = 180 DAYS
- ISP = 7000 SEC

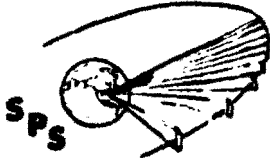
<u>MODULE CHARACTERISTICS</u>	<u>NCN ANTENNA MODULE</u>	<u>ANTENNA MODULE</u>
● MODULES	14	2
● MODULE MASS	4.1	19.1
● POWER REQ'D (10^6 Kw)	0.14	0.65
● FACETS REQ'D %	27	74
● OTS DRY (10^6 Kg)	0.5	2.35
● ARGON (10^6 Kg)	1.0	4.5
● LO_2/LH_2 (10^6 Kg)	0.2	0.94
● ELEC THRUST (10^3 N)	2.1	9.8
● CHEM THRUST (10^3 N)	2.1	9.8

INCLUDES 14% TO COVER LOSSES

**CREW ROTATION/RESUPPLY TRANSPORTATION
POWER GENERATION COMPARISON**

The major transportation system elements and the number of flights associated with crew rotation/resupply is presented. A shuttle growth vehicle using a liquid booster delivers up to 75 crewmen per flight to LEO. Cargo in terms of crew and base supplies as well as propellant and OTV hardware is delivered by the satellite launch vehicle. The OTV used for crew rotation/resupply is a two-stage LO_2 / H_2 system with each stage having identical propellant capacity.

Crew LEO delivery flights and supply flights are different as a result of the difference of 300 people required to construct the two satellites. The GEO bases are nearly the same. No difference occurs in the OTV operation.



SPS-1616

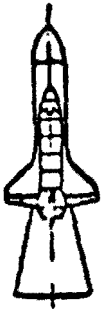
D180-22876-7

Crew Rotation/Resupply Transportation Power Generation System

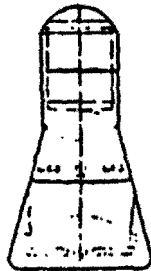
BOEING



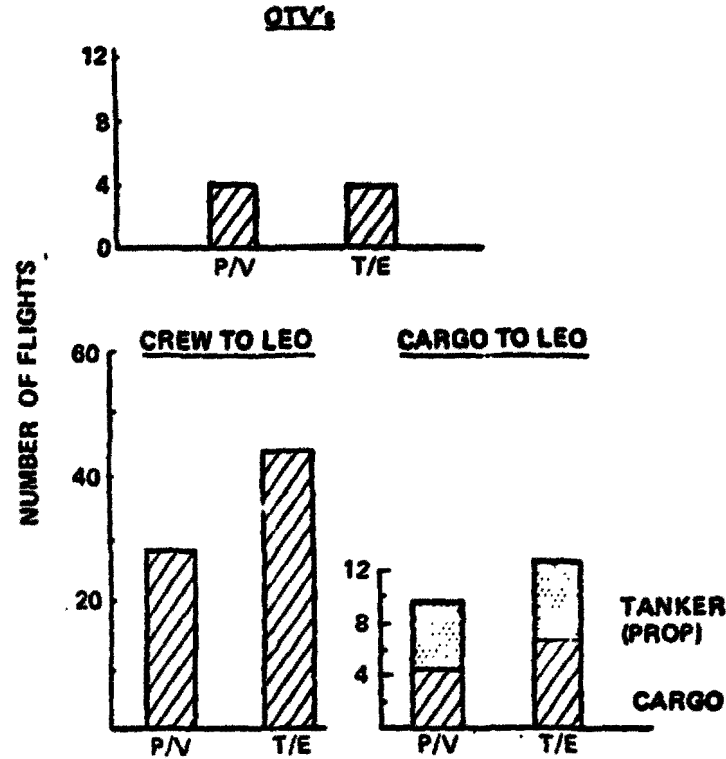
- CREW/CARGO TO GEO
- 2 STAGE LO₂/LH₂ OTV
- W_g = 495 000 Kg



- CREW TO LEO
- SHUTTLE GROWTH
- 75/FLT



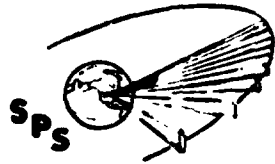
- CARGO, PROP & OTV's
- 2 STAGE BALLISTIC



D180-22876-7

**TRANSPORTATION COST
PHOTOVOLTAIC vs THERMAL ENGINE SATELLITE**

The total transportation cost of the photovoltaic and thermal engine satellite effort is presented. The costs are broken down to illustrate the differences for the three major transportation operations although the magnitude of the cost of the three are quite different. In the case of the satellite transportation costs, the primary reason for the thermal engine being greater is its need to use an expendable shroud in order to achieve a mass limited launch condition. Crew rotation/resupply differences are reflecting the difference in numbers of flights to get an extra 300 people to LEO in the case of thermal engine satellites. Construction base transportation differences are primarily due to the larger mass of the thermal engine construction base as well as the volume limited condition of the construction equipment itself and the fact that the thermal engine concept uses considerably more equipment. It should be remembered however, that this initial placement will most likely last for 20 years in terms of the facility and 10 years for the construction equipment so that facility transportation costs can be considered as amortized.



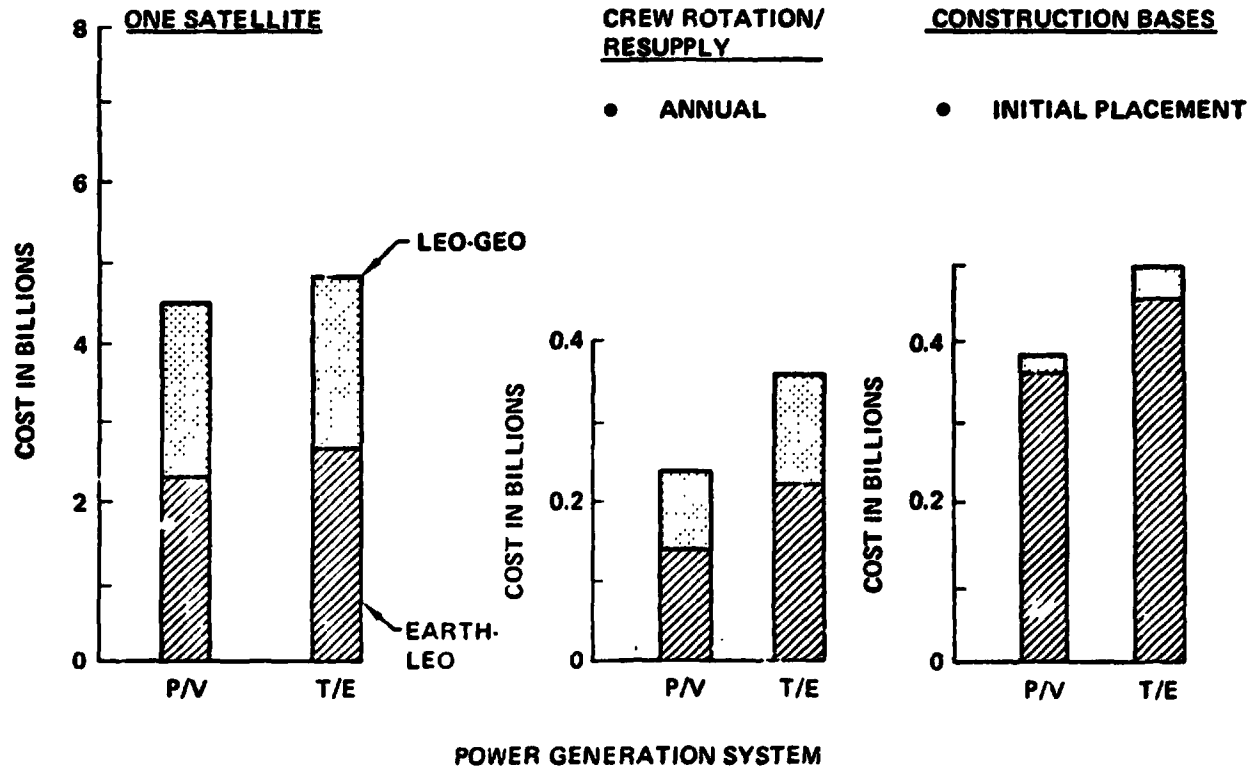
SPS-1000

D180-22876-7

Transportation Cost Photovoltaic vs Thermal Engine

BOEING

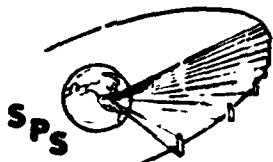
- 4 SATELLITES/YEAR
- LEO CONSTRUCTION



D180-22876-7

**CONSTRUCTION/TRANSPORTATION SUMMARY
GENERATION SYSTEM COMPARISON**

A summary comparison of the photovoltaic and thermal engine satellite is presented with an indication of which concept is preferred relative to the various construction and transportation parameters discussed on prior charts. Compared in this manner, it appears that the photovoltaic satellite has a clear advantage in terms of less complex facilities, construction operations and construction equipment, all leading to a lower construction cost and in addition has lower transportation costs.



D180-22876-7

Construction/Transportation Summary Power Generation Comparison

BOEING

SPS-1625

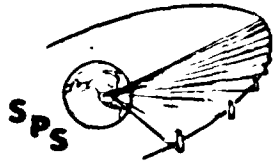
✓ FOR MOST PROMISING CONCEPT

<u>COMPARISON PARAMETER</u>	<u>PHOTO-VOLTAIC</u>	<u>THERMAL ENGINE</u>	<u>RATIONALE</u>
1. BASE CONFIGURATION	✓		<ul style="list-style-type: none"> • SMALLER • LESS COMPLEX
2. SATELLITE CONSTRUCTION	✓		<ul style="list-style-type: none"> • LESS COMPLEX • FEWER OPERATIONS
3. ANTENNA CONSTRUCTION		NO DIFFERENCE	
4. FINAL ASSEMBLY OPS	✓		<ul style="list-style-type: none"> • DOCKING & ANTENNA INSTALL LESS COMPLEX
5. CONSTRUCTION EQUIP	✓		<ul style="list-style-type: none"> • FEWER TYPES AND LESS COMPLEX
6. CONSTRUCTION SYSTEM MASS AND COST (UNIT)	✓		<ul style="list-style-type: none"> • LIGHTER (3.2M Kg; 33%) • CHEAPER (\$4.0B; 33%)
7. CREW REQUIREMENTS	✓		<ul style="list-style-type: none"> • 300 FEWER PEOPLE • \$110M LESS/YR (33%)
8. LAUNCH SYSTEM	✓		<ul style="list-style-type: none"> • HIGH DENSITY COMPONENTS ALLOW REUSABLE SHROUD
9. SATELLITE ORBIT TRANSFER		✓	<ul style="list-style-type: none"> • LESS IMPACT ON SATELLITE DESIGN
10. SATELLITE TRANSPORTATION COST	✓		<ul style="list-style-type: none"> • CHEAPER (\$300M; 6%)

D180-22876-7

**CONSTRUCTION LOCATION COMPARISON
PHOTOVOLTAIC SATELLITE**

Comparison of the major construction and transportation parameters associated with LEO and GEO construction will be done using the photovoltaic satellite due to it being judged to offer the best characteristics in terms of construction and transportation. The principle areas to be used in comparing the two construction locations options are indicated. As in the case of comparing the power generation system options, the two construction location concepts will be compared at the same time or on consecutive charts for a given item of comparison.



D180-22876-7

Construction Location Comparison Photovoltaic Satellite

BOEING

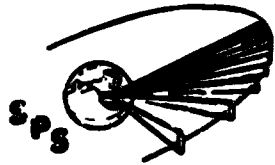
SPS-1624

- FACILITIES
- SATELLITE (MODULE) AND ANTENNA CONST. OPERATIONS
- CONSTRUCTION EQUIPMENT
- CREW REQUIREMENTS
- ENVIRONMENTAL FACTORS
- CONSTRUCTION MASS AND COST
- SATELLITE DESIGN IMPACT
- ORBIT TRANSFER COMPLEXITY
- LAUNCH OPERATIONS
- TRANSPORTATION COST

D180-22876-7

**LEO CONSTRUCTION CONCEPT
PHOTOVOLTAIC SATELLITE**

To establish a framework from which to conduct the comparison of LEO vs GEO construction, an overall summary of each construction concept is presented in the next two charts. In the case of the photovoltaic satellite, eight modules and two antennas are constructed in the LEO facilities. All modules are transported to GEO using self-power. Two of the modules will transport an antenna while the remaining six modules go up alone. GEO operations require berthing of the modules to form the complete satellite and the deployment of the solar arrays not used for the transfer.



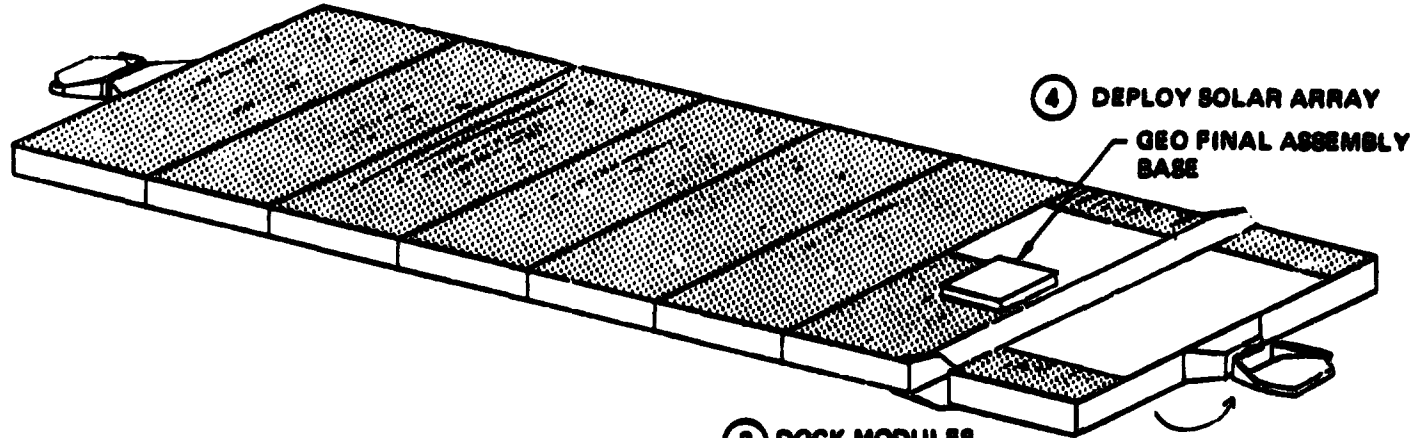
D180-22876-7

LEO Construction Concept Photovoltaic Satellite

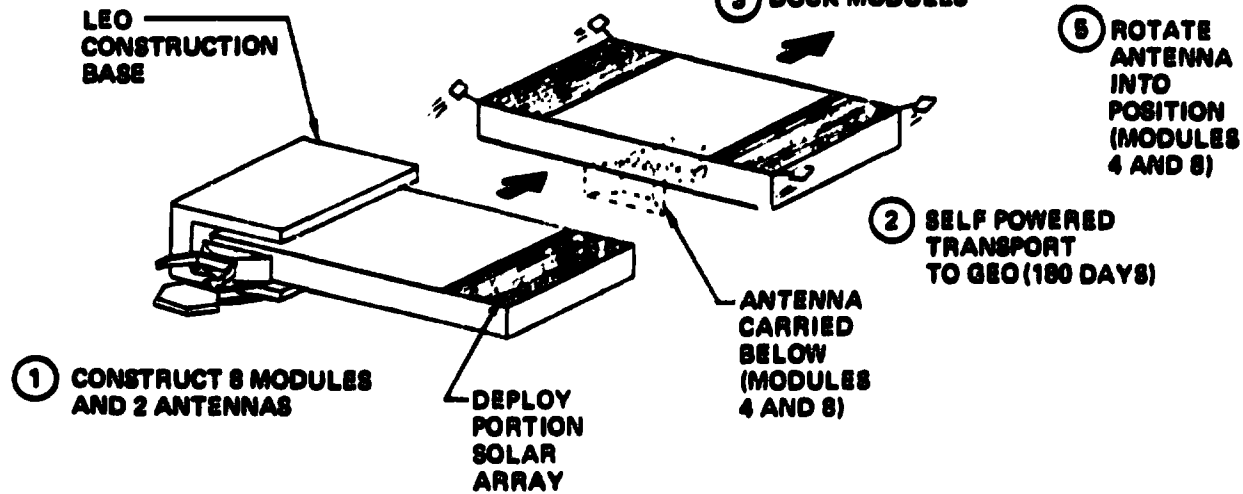
BOEING

SPS-1383

GEO



LEO

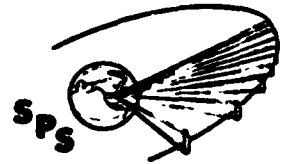


GEO CONSTRUCTION CONCEPT

The GEO construction concept begins with a staging depot, which has the capability to transfer payloads from a launch vehicle to orbit transfer vehicles and to house and maintain the orbit transfer vehicle fleet. Transfer of all payloads between LEO and GEO is accomplished using LO₂/LH₂ OTV's. Construction of the entire satellite including antenna is done at GEO. The reference satellite for the GEO construction option is a monolithic design rather than modular as in the case of LEO construction. The effect of this difference as well as others is discussed on subsequent charts.

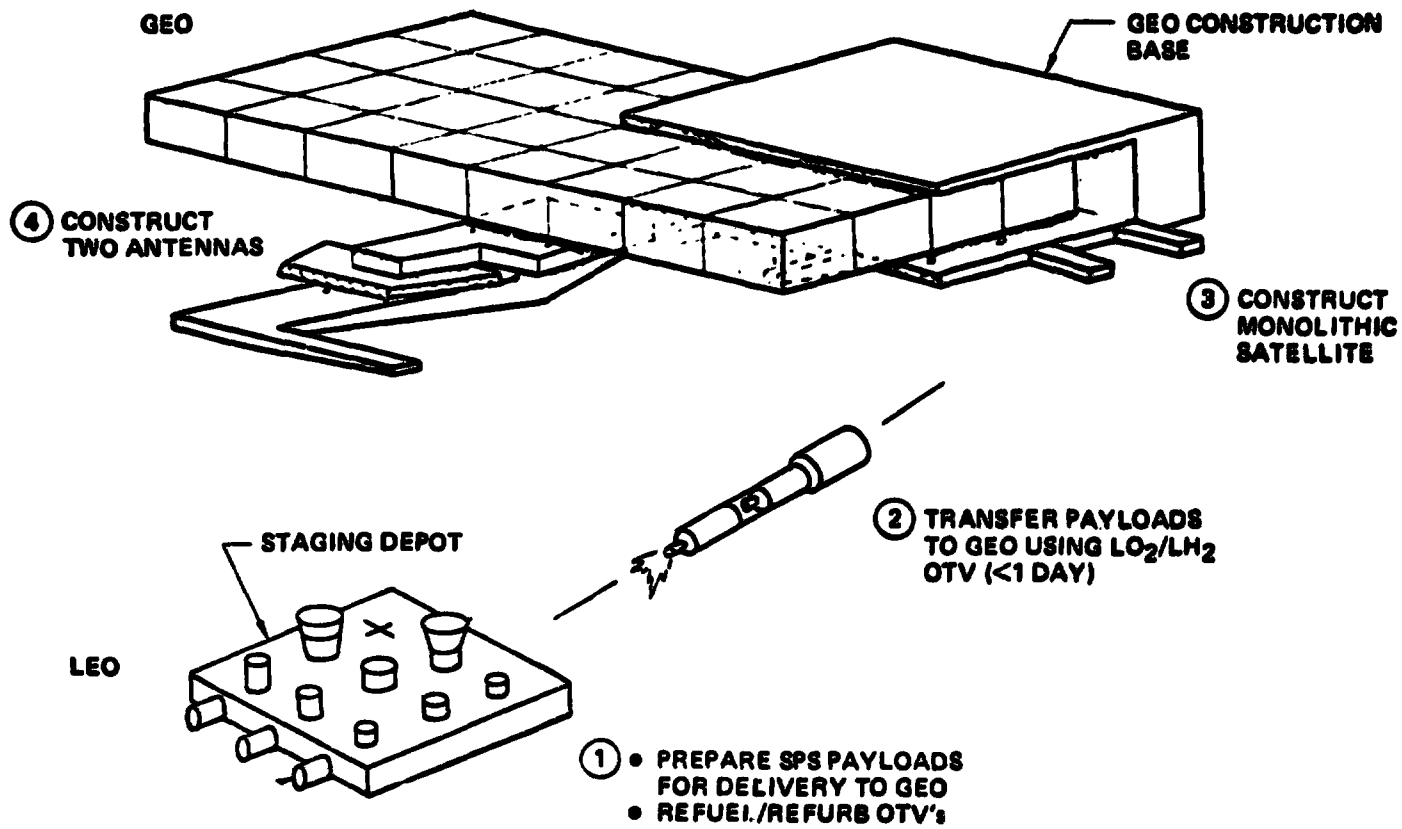
D180-22876-7

GEO Construction Concept



SPS-1802

BOEING ———



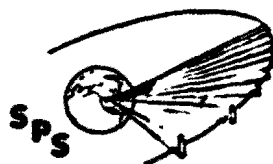
D180-22876-7

**ORBITAL BASES
LEO CONSTRUCTION CONCEPT**

Two principal bases are required for the construction of each satellite in the LEO construction option. The bases for the photovoltaic option have been described earlier in the comparison of the two power generation system concepts. In summary, however, the LEO construction base consists of two connecting facilities, with one used for construction of satellite modules, while the other is used to construct the antennas. The GEO base provides basing for cranes used in the berthing of the modules and supports solar array deployment machines.

D180-22876-7

Orbital Bases LEO Construction Concept

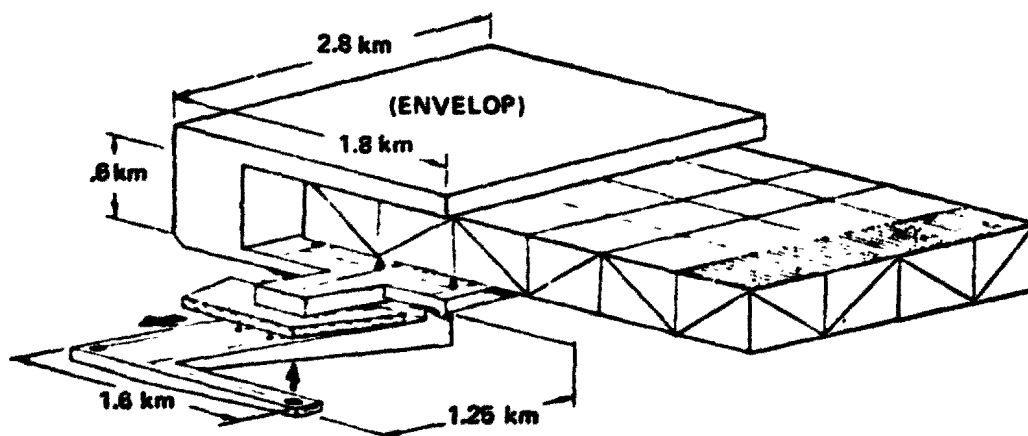
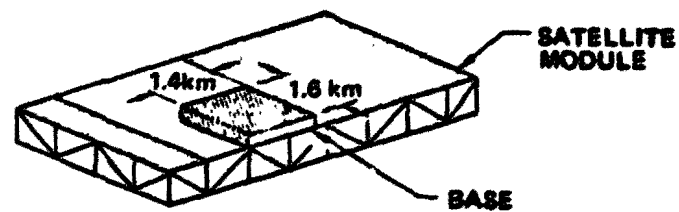


SPS-1528

ORING ———

● **GEO FINAL ASSEMBLY BASE**

- MASS: 855 000 kg
- CREW SIZE: 65



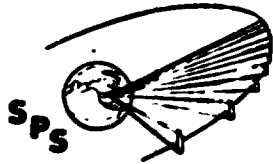
● **LEO CONSTRUCTION BASE**

- MASS: 5 900 000 kg
- CREW SIZE: 480

**ORBITAL BASES
GEO CONSTRUCTION CONCEPT**

The GEO construction base has been sized to construct a satellite in one year and consequently, results in the same overall size as the base for LEO construction. This approach does result in moving the satellite construction facility in two directions rather than one. This has been judged to be more cost effective than having a full width facility and additional construction equipment and have this equipment sit idle half of the time. Additional discussion on this subject will occur in subsequent charts. Mass difference for this construction base compared to the base for LEO construction primarily reflects the additional mass required for shielding protection against solar flares. Other significant differences in the GEO construction base are the outriggers on the satellite facility to allow lateral direction indexing in addition to the movement of the antenna facility from one end of the satellite to the other. Again, both of these differences are the subject of subsequent charts.

The staging depot located in LEO in this construction option is sized to support the construction of one satellite per year, and accordingly requires one SPS component OTV flight per day, based on a five day a week launch and flight schedule. As such, the depot must provide accommodations for three launch vehicle payloads, one being the SPS components and the other two being propellant tankers used to refuel the orbit transfer vehicles. Since the orbit transfer vehicle propellant loading requires slightly more propellant than can be provided by two tankers, a storage tank is also provided at the staging depot and is refueled every fourth OTV flight. Other docking accommodations are provided for a dedicated OTV used for GEO crew rotation/resupply on a once per month basis. This operation also requires docking for supply modules and crew transfer vehicles. The operational crew size for the staging depot is 75 which can be accommodated in one module similar to the crew modules used in the GEO construction base. A transient crew quarters module is also provided to accommodate the 160 personnel rotated with each crew flight to the GEO base. A maintenance module is also included at this base for repair work primarily on the transportation systems.



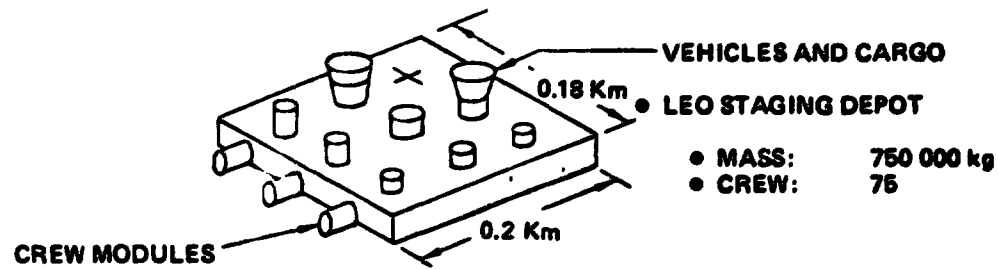
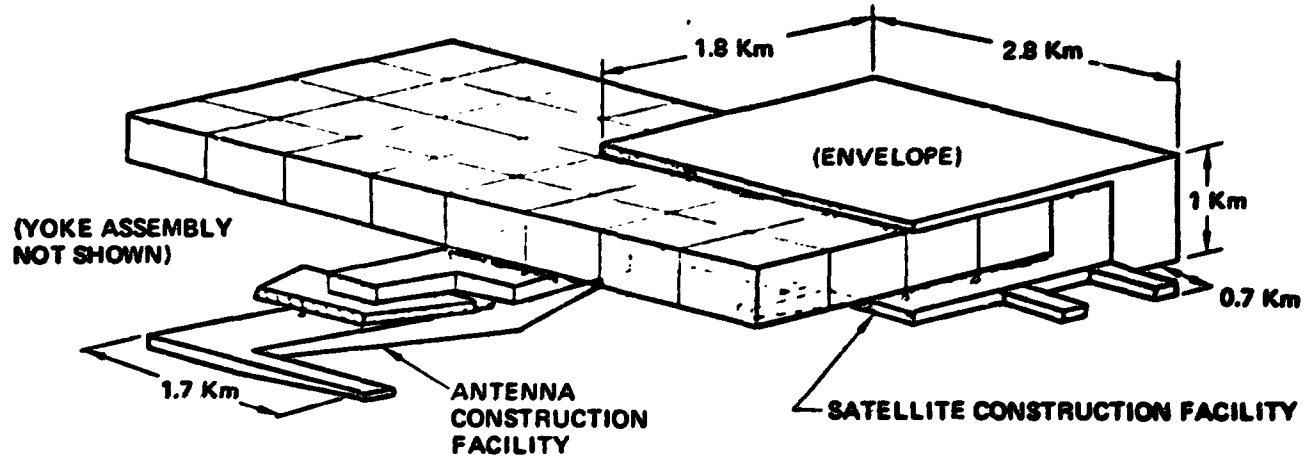
SPS-1413

D180-22876-7

Orbital Bases GEO Construction

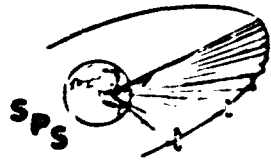
BOEING

- GEO CONSTRUCTION BASE
- MASS: 6 500 000 kg
- CREW: 480



**SATELLITE CONSTRUCTION OPERATIONS
LEO CONSTRUCTION CONCEPT**

The LEO construction operations associated with the photovoltaic satellite have previously been shown and described. In this chart the operations are illustrated in a slightly different manner in order to show a more direct comparison with the GEO constructed satellite. Each satellite module is four bays wide and eight bays long. The module facility is four bays wide and consequently can construct a complete width of the module and results in indexing the module only in the longitudinal direction



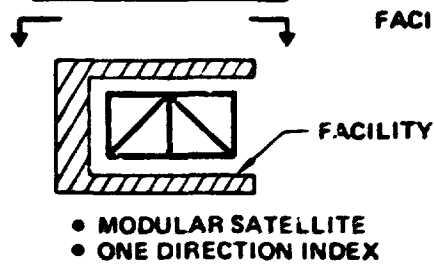
D180-22876-7

Satellite Construction Operations LEO Construction Concept

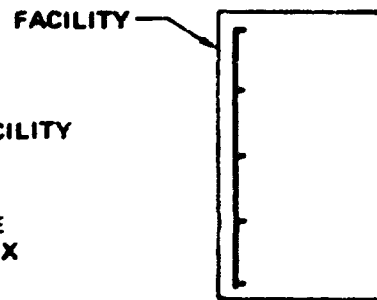
SPS-1400

BOEING

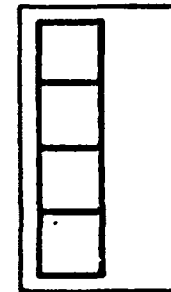
LEO OPERATIONS



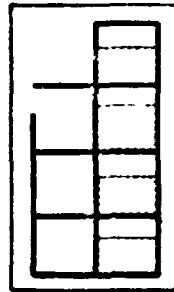
- ① • CONST END FRAME
• INDEX FWD 1 BAY



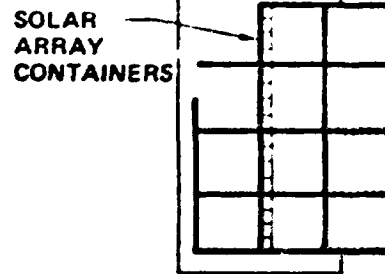
- ② • CONST 4 BAYS OF STRUCT
• INDEX FWD 1 BAY



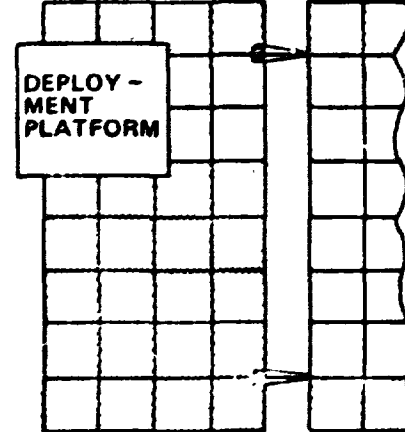
- ③ • DEPLOY ARRAY
• CONST STRUCT BAYS
• INDEX FWD 1 BAY



- ④ • INSTALL ARRAY
CONTAINERS
• CONST STRUCT BAYS
• INSTALL BUS AT END
OF 4TH ROW



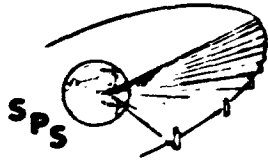
GEO OPERATIONS



- BERTH MODULES
- DEPLOY SOLAR ARRAY

**SATELLITE CONSTRUCTION OPERATIONS
GEO CONSTRUCTION CONCEPT**

The GEO constructed satellite is monolithic in design (although it could also be modular, if so desired) and as a result has a construction width of eight bays. In order to obtain this width with the same size facility (least mass and cost) as a LEO construction base, indexing of the satellite is required in two directions as indicated. In general, four bays of the satellite are under construction at one time. With their completion, those bays are moved laterally and the remaining four bays of that row are constructed. When a given row is completed, it is then indexed in a longitudinal direction and the construction operation is repeated. In order to accomplish the lateral indexing in only two steps, outriggers have been added to the side of the satellite facility to enable indexing of four bays outside the construction envelope.



D180-22876-7

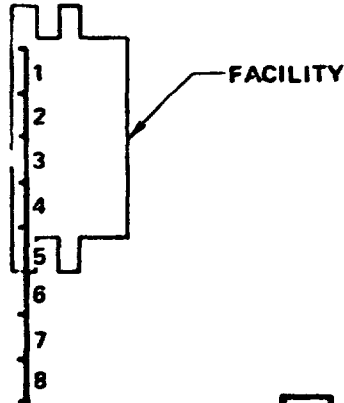
Satellite Construction Operations GEO Construction Concept

BOEING

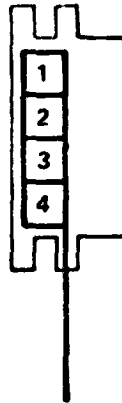
SPS 1471

- MONOLITHIC SATELLITE
- TWO-DIRECTION INDEXING

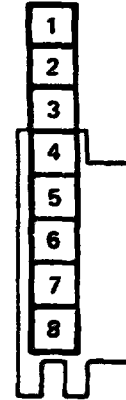
- ① ● CONST END FRAME - 4 BAYS
● INDEX Laterally
● CONST END FRAME - 4 BAYS



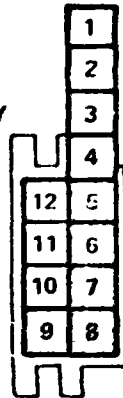
- ② ● INDEX FWD 1 BAY
● CONST BAY 1-4



- ③ ● INDEX LAT. 4 BAYS
● CONST BAY 5-8
● INDEX FWD 1 BAY



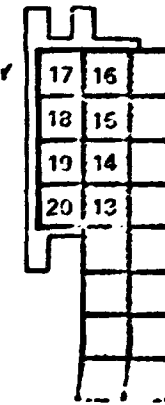
- ④ ● INDEX FWD 1 BAY
● DEPLOY ARRAY BAY 5-8
● CONST BAY 9-12
● INDEX LAT. 4 BAYS



- ⑤ ● DEPLOY BAY 1-4
● CONST BAY 13-16
● INDEX FWD 1 BAY



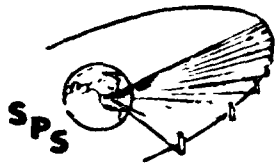
- ⑥ ● DEPLOY ARRAY BAY 13-16
● CONST BAY 17-20



**ANTENNA CONSTRUCTION AND INSTALLATION
LEO CONSTRUCTION**

Antenna construction and installation also presents some significant differences in the two construction location options. Again, the photovoltaic LEO construction approach has been presented in the power generation system comparison, but is shown here in a manner to make a more direct comparison with the GEO construction approach. In summary, the yoke support structure of an antenna is made in the module facility and in between the third and fourth modules or between the seventh or eighth modules depending on whether it is the first antenna or second antenna being built. The antenna is made in its facility which remains permanently attached to the module facility. Construction of either the fourth or eighth module is then partially completed and the antenna and yoke attached at its proper location. Following module construction completion, the antenna is rotated under the module for transfer to GEO. Once GEO is reached, the antenna is rotated back up to its operating position.

**ORIGINAL PAGE IS
OF POOR QUALITY**



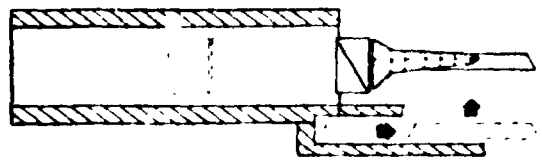
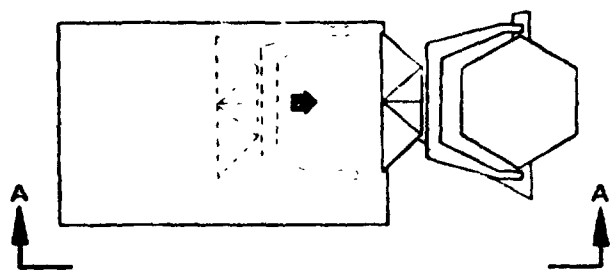
SPS-1492

D180-22876-7

Antenna Construction and Installation LEO Construction

BOEING

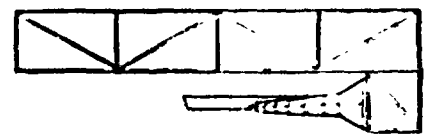
LEO OPERATIONS



A-A

- CONST YOKE
- CONST ANTENNA
- ATTACH YOKE/ANTENNA
- ATTACH ANTENNA SYS/MODULE

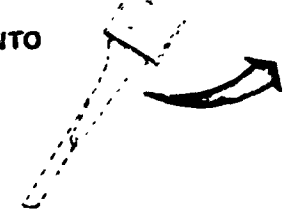
GEO OPERATIONS



● GEO TRANSFER POSITION



● ROTATE INTO POSITION

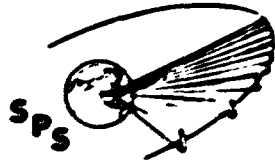


ORIGINAL PAGE IS
OF POOR QUALITY

**ANTENNA CONSTRUCTION AND INSTALLATION
GEO CONSTRUCTION CONCEPT**

The GEO construction concept also utilizes separate satellite and antenna facilities. However, in the reference case indicated, the antenna facility with antenna is required to free-fly to the opposite end of the satellite and back. It should be noted at this point, that the antenna construction/installation approach indicated has been judged to be one of the best, if not the best, option for this particular task. Eight other options, involving variations of the antenna facility remaining attached, others with it independent, and also two separate antenna facilities were investigated and are reported in the final documentation.

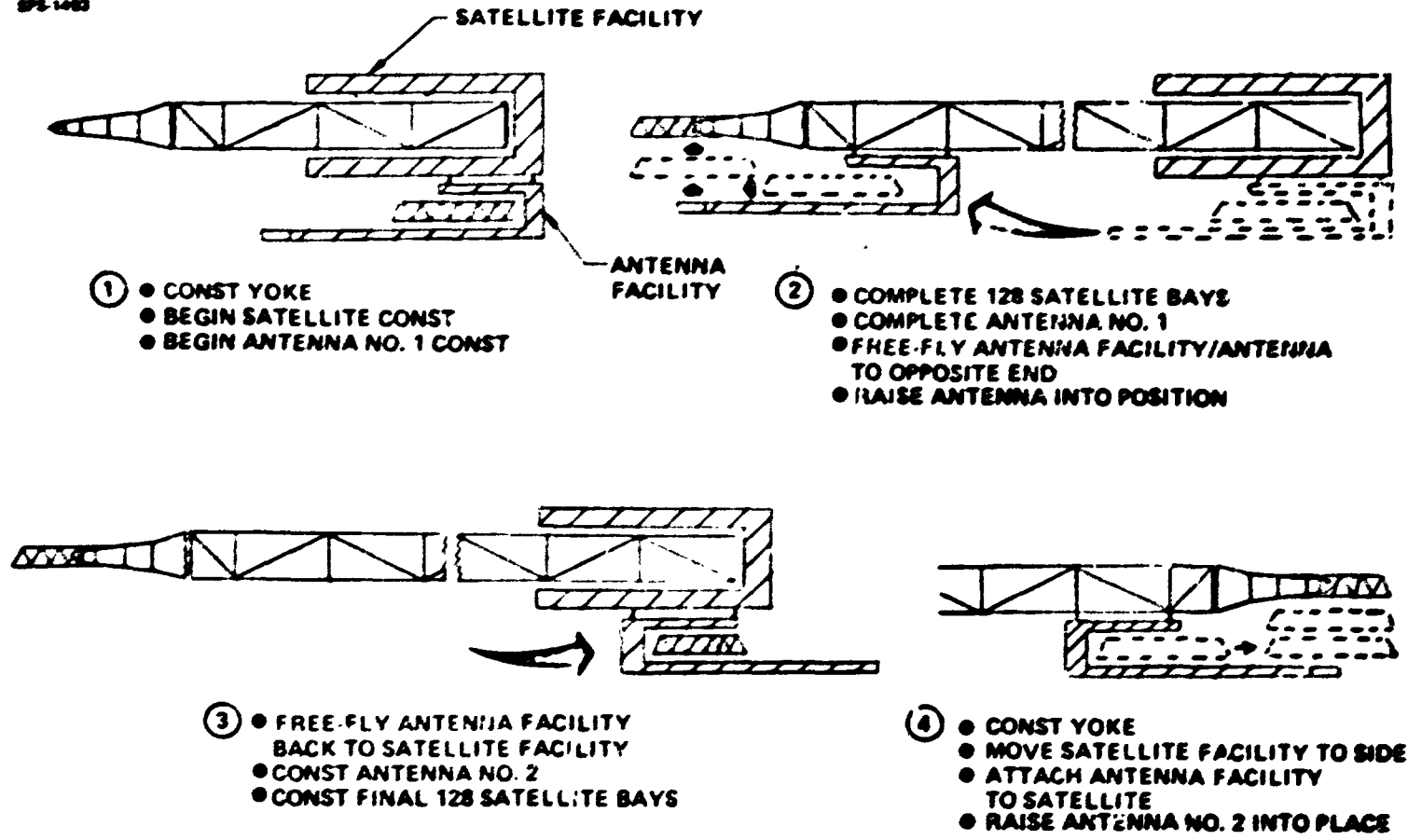
In summary, the reference approach consists of the first antenna being made while the first half of the satellite is constructed including the yoke and support structure. At that point, the antenna facility with antenna is flown to the end of the satellite and docked and the antenna then attached to the yoke. The antenna facility is then flown back to the satellite facility (the short term separation of the two facilities simplifies the logistics problem in terms of supplying antenna components as well as living quarters for the crew). The remaining half of the satellite is then constructed, including a second yoke, while the antenna facility constructs the second antenna. Indexing of the satellite facility to the extreme edge of the satellite allows the antenna facility to be positioned to enable placement of the antenna into the yoke.



SPS-1480

Antenna Construction and Installation GEO Construction Concept

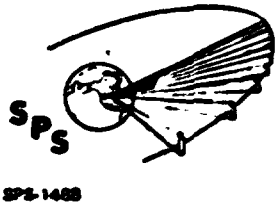
BOEING



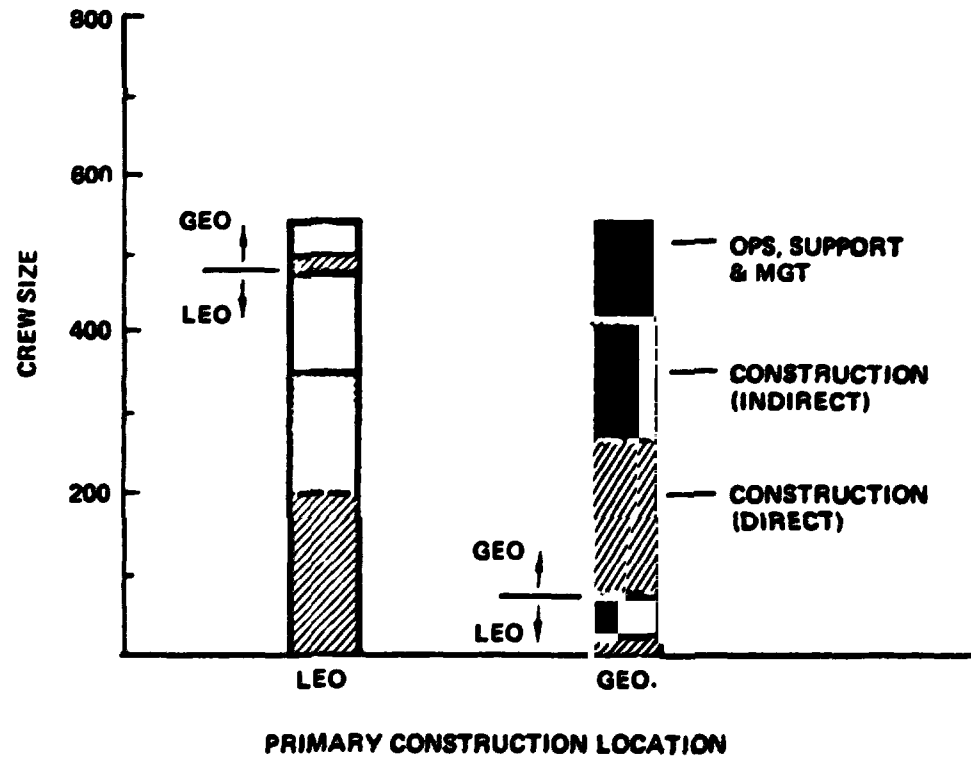
CREW SIZE AND DISTRIBUTION

There is essentially no difference in orbital crew size between the two construction location concepts, although the distribution of personnel is considerably different. Crew size for the main construction base indicates 480 people in LEO concept while this same number is required in GEO for the GEO concept. Staging depot and final assembly manning requirements are also found to be nearly the same.

Crew Size and Distribution



BOEING —



ENVIRONMENTAL FACTORS SUMMARY

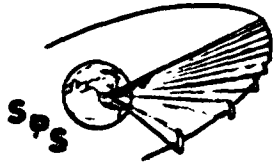
Several key environmental factors should be considered when comparing the two construction location options. A summary of these factors is presented plus an additional chart dedicated to the topic of collision with man-made objects.

The principal difference between the two construction location options, in terms of natural radiation, is the large amount of solar flare shielding which must be provided for all crew modules located at GEO. Steady-state radiation would make EVA at GEO considerably worse than at LEO although only a bare minimum of suit EVA is anticipated in either case.

Occultations of the construction base at LEO occur 15 times a day, while a base at GEO is only occulted 88 times per year. The principal effects of occultation are on the electrical power supply and thermal aspects of the structure. In the case of power requirements, the GEO option requires less power due to not having to recharge nickel hydrogen batteries used for the occultation. The penalty for the larger power system is relatively small however when one is in the era of low mass, low cost solar arrays. Although a GEO base is certainly more continuously illuminated, the construction base itself produces shadows. Consequently, both construction locations require a large amount of power for lighting purposes. Use of graphite/epoxy structure in both the satellite as well as the construction base structure should minimize the impact of thermal effects.

Most construction concepts will orient the construction base so it is passively stable for attitude control and minimize gravity gradient torque. Although the LEO construction case required considerably more orbit keeping/attitude control propellant per day, it still results in less than one HLLV launch per year for this propellant makeup.

Large amounts of debris from man-made space systems have resulted in some concern regarding LEO construction. The analysis conducted has indicated the potential is greater with construction in LEO, however, simple avoidance maneuvers can reduce the probability of being hit to near zero. The next chart discusses this topic in more detail.



D180-22876-7

Environmental Factors Summary

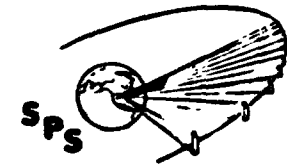
SPS 1011

BOJING

<u>FACTOR</u>	<u>LEO BASE</u>	<u>GEO BASE</u>
<ul style="list-style-type: none"> ● RADIATION <ul style="list-style-type: none"> ● SOLAR FLARE ● EVA 	<p>2-3 GM/CM² SO. ATLANTIC ANOMALY RESTRICTION</p>	<p>20-25 GM/CM² (115 000 KG/100 PEOPLE) STEADY STATE IS WORSE</p>
<ul style="list-style-type: none"> ● OCCULTATION <ul style="list-style-type: none"> ● BASE POWER REQ'TS: ● LIGHTING: ● THERMAL EFFECTS: 	<p>3600 KW</p>	<p>2500 KW</p> <ul style="list-style-type: none"> ● REQ'D AT BOTH LOCATIONS (Δ OF 100-150 KW) ● NO SIGNIFICANT DIFFERENCE IF GRAPHITE EPOXY IS USED
<ul style="list-style-type: none"> ● GRAVITY GRADIENT & DRAG: 		<ul style="list-style-type: none"> ● GRAVITY GRADIENT CONST MODE USED FOR BOTH LOCATIONS ● LEO PROP REQ'T GREATER BY 800 KG/DAY
<ul style="list-style-type: none"> ● COLLISION WITH MAN-MADE OBJECTS 		<ul style="list-style-type: none"> ● POTENTIAL GREATER FOR LEO BUT AVOIDANCE MANEUVERS ● REDUCE PROBABILITY TO NEAR ZERO

COLLISIONS WITH MAN-MADE OBJECTS

The collision analysis has been done for an environment predicted for the year 2000, including an addition of 500 objects per year since 1975. Results of this analysis indicated that the LEO construction approach could have forty additional collisions if no preventive action is taken. However, as indicated at the Part 2 mid-term briefing, rescheduled orbit altitude corrections can essentially eliminate the problem of collision with little or no additional penalty. Thrust initiation or termination during orbit transfer can also be used to prevent collisions. In summary, there should be no difference between the two concepts regarding the number of collisions although the LEO construction approach does require slightly different operations, including the use of the tracking and warning systems.



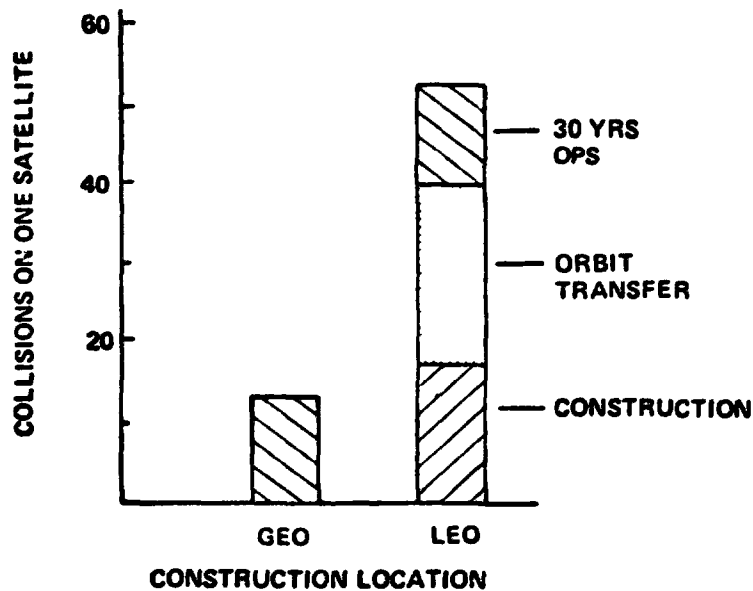
SPS-1605

Collisions with Man Made Objects

BOEING

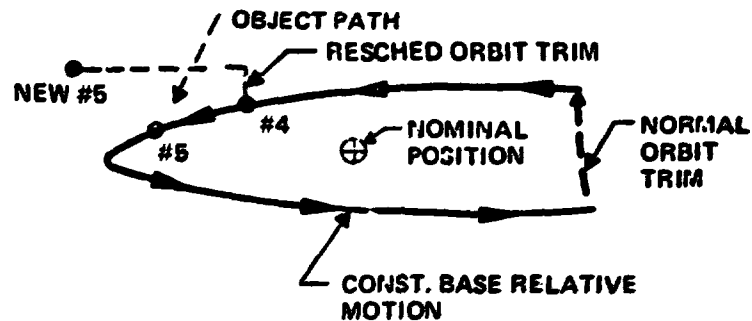
NO PREVENTATIVE ACTION

- YEAR 2000 ENVIRONMENT



PREVENTIVE ACTION

- CLEAN UP GEO ENVIRONMENT
- RESCHEDULE ORBIT ALTITUDE ADJUSTMENT FOR AVOIDANCE DURING CONSTRUCTION



- TERMINATE OR INITIATE THRUST FOR AVOIDANCE DURING TRANSFER

- EXPECTED COLLISIONS:

NEAR ZERO

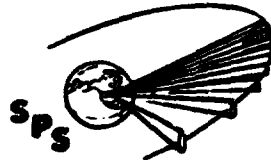
**SATELLITE DESIGN IMPACT SUMMARY
LEO CONSTRUCTION**

The design impact on the satellite for the case of LEO construction and self-power has been described earlier in the description of the photovoltaic satellite. A summary of the key impact areas is presented at this time. In the area of solar array, an oversizing of 5 percent has been included to compensate for the inability to completely anneal out all the damage to the cells caused by radiation occurring during transfer and for the mismatch in voltage output between the damaged and undamaged cells.

The structural impact includes both that of modularity and oversizing. Modularity includes additional vertical members used around the perimeter of the satellite module and lateral beams at the end of the modules as well as the penalties for the transfer of the 15 million kg antenna supported underneath the module. (It should be noted that all module structure has been sized to that dictated by the modules used to transfer the antenna.)

The power distribution penalty is related to the additional length of bus caused by the oversizing of the array. The total mass penalty for a LEO constructed satellite is approximately 4.2 million kg for the selected self-power transportation system. It should be noted however that the array oversizing and power distribution penalty depend on the particular performance characteristics selected for the self-power system.

D180-22876-7






SPS-1620

Satellite Design Impact Summary LEO Construction

BOEING 

SELF POWER TRANSFER

<u>IMPACT</u>	<u>REASON</u>	<u>PENALTY</u>
● SOLAR ARRAY	● OVERSIZING FOR RADIATION DEGRADATION	● 2.75M Kg 
● STRUCTURE	● MODULARITY ● OVERSIZING	● 1.07M Kg ● 0.34M Kg 
● POWER DISTRIBUTION	● EXTRA LENGTH DUE TO OVERSIZING	● 0.07M Kg 

 FUNCTION OF SELF POWER PERFORMANCE CHARACTERISTICS

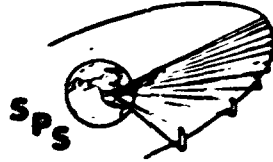
**TRANSPORTATION REQUIREMENTS
LEO VERSUS GEO**

Transportation requirements associated with the payloads of each construction location concept are shown, there is no OTV propellant mass included.

The difference in satellite mass only reflects the structural mass penalty of the additional vertical and lateral members and loads caused by transfer of the antenna. Oversizing and power distribution penalties are all a function of orbit transfer characteristics and consequently are chargeable to the orbit transfer system itself.

Differences in crew and supply requirements delivered to LEO primarily reflect additional orbit keeping/attitude control propellant requirements. The key difference, however, is in the mass which must be delivered to GEO.

Facility transportation requirements reflect the initial placement task as well as in the case of the GEO bases (both options), that mass that must be moved to the longitude location where the next satellite is to be constructed. The principal difference in the two main construction bases is that the six crew modules in the GEO concept each have approximately 115 000 kg of additional mass for solar flares shelters.

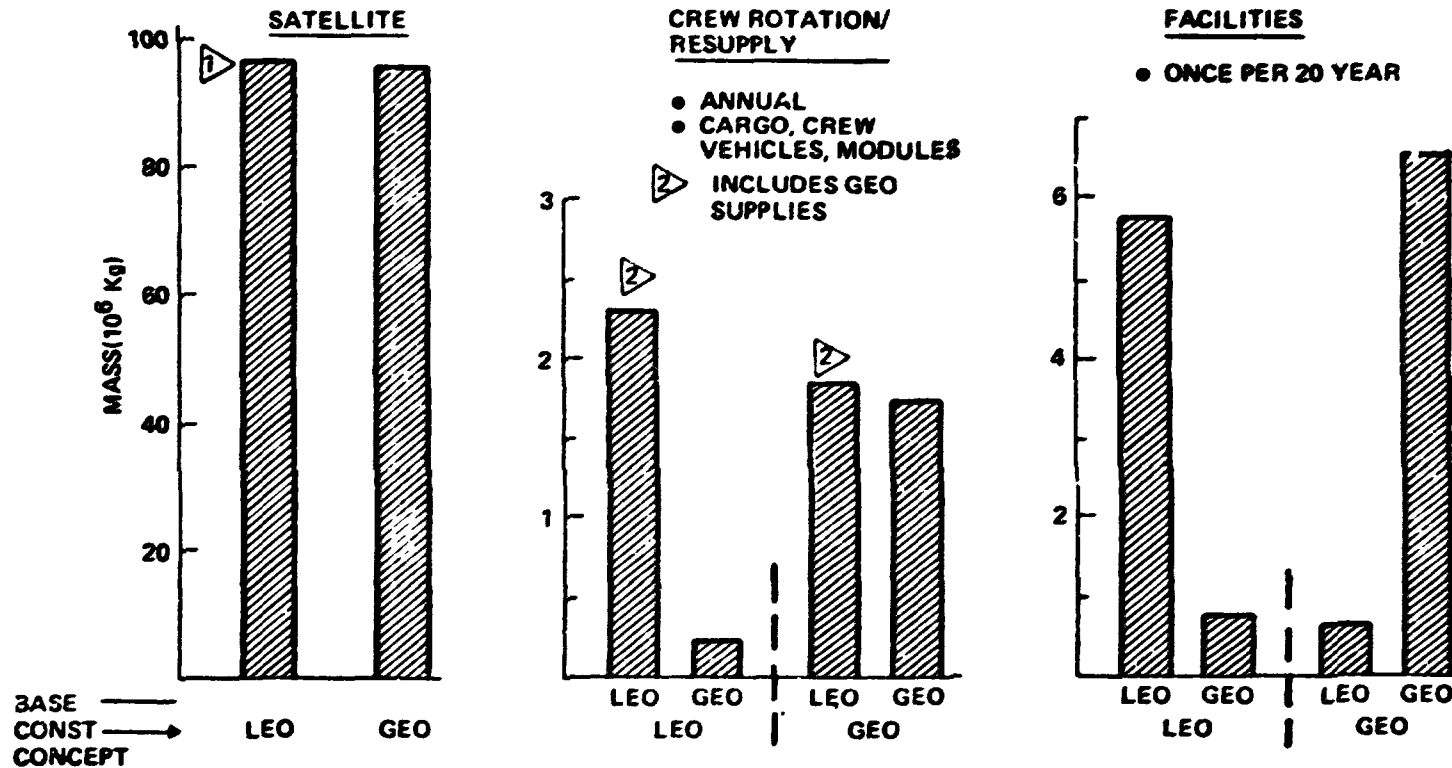


SPS-1604

Transportation Requirements LEO vs GEO

BOEING

● PHOTOVOLTAIC SATELLITE



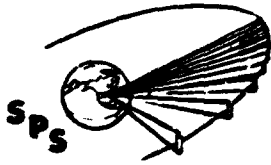
△ INCLUDES STRUCT. MODULARITY AND ANTENNA TRANSFER PENALTY, OVERSIZING AND POWER DISTRIB. CHARGEABLE TO ORBIT TRANSFER

D180-22876-7

**SELF POWER CONFIGURATION
PHOTOVOLTAIC SATELLITE**

The self power orbit transfer system used in the LEO construction approach has previously been shown in the power generation system comparison. In summary, electrical power generated by the solar arrays is used to power ion electric thrusters which use argon propellant. LO_2/LH_2 thrusters are also included to provide attitude control during all occultations and during short periods of time early in the transfer (up to 2 500 km altitude) when thrust required to counter gravity grading torque is greater than that provided by electric thrusters.

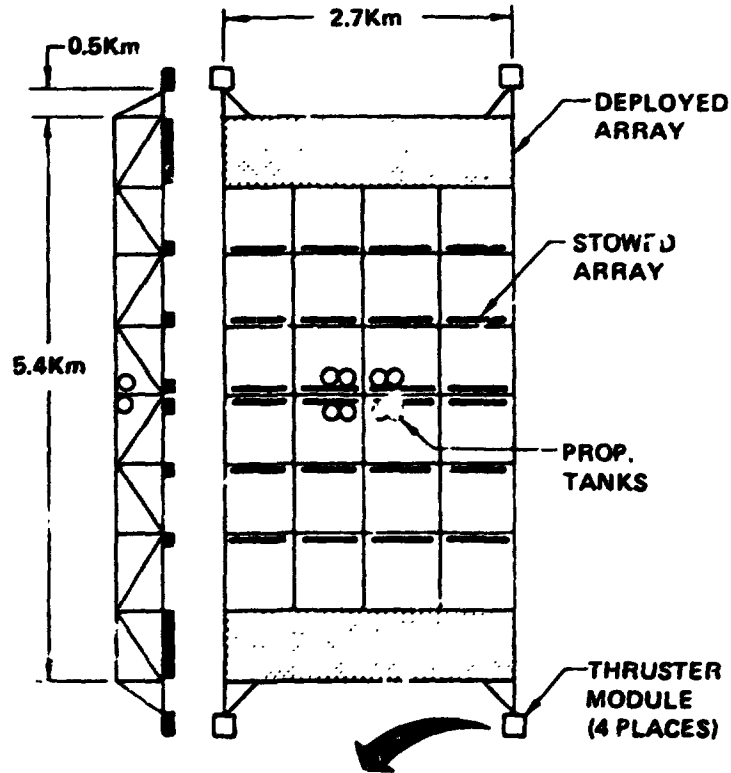
The cost optimum trip time and I_{sp} are respectively 180 days and 7,000 seconds. Variation in number of thrusters, propellant tanks, etc do occur in the design to compensate for the case of whether a module is being transported alone or with an antenna.



Self Power Configuration Photovoltaic Satellite

BOEING

SPS-1010



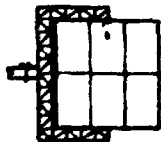
GENERAL CHARACTERISTICS

- 5% OVERSIZING (RADIATION)
- TRIP TIME = 180 DAYS
- ISP = 7000 SEC

MODULE CHARACTERISTICS

- NO. MODULES
- MODULE MASS (10^6 KG)
- POWER REQ'D (10^6 Kw)
- ARRAY %
- OTS DRY (10^6 KG)
- ARGON (10^6 KG)
- LO_2/LH_2 (10^6 KG)
- ELEC THRUST (10^3 N)
- CHEM THRUST (10^3 N)

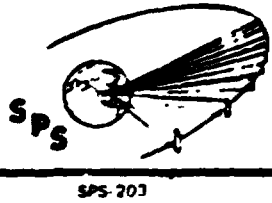
	NON ANTENNA MODULE	ANTENNA MODULE
• NO. MODULES	6	2
• MODULE MASS (10^6 KG)	8.7	23.7
• POWER REQ'D (10^6 Kw)	0.3	0.81
• ARRAY %	17	36
• OTS DRY (10^6 KG)	1.1	2.9
• ARGON (10^6 KG)	2.0	5.6
• LO_2/LH_2 (10^6 KG)	1.0	2.8
• ELEC THRUST (10^3 N)	4.5	12.2
• CHEM THRUST (10^3 N)	12.0	5.0



	NON ANTENNA	ANTENNA
SIZE:	24x38m	48x76m
THRUSTERS:	600	1800

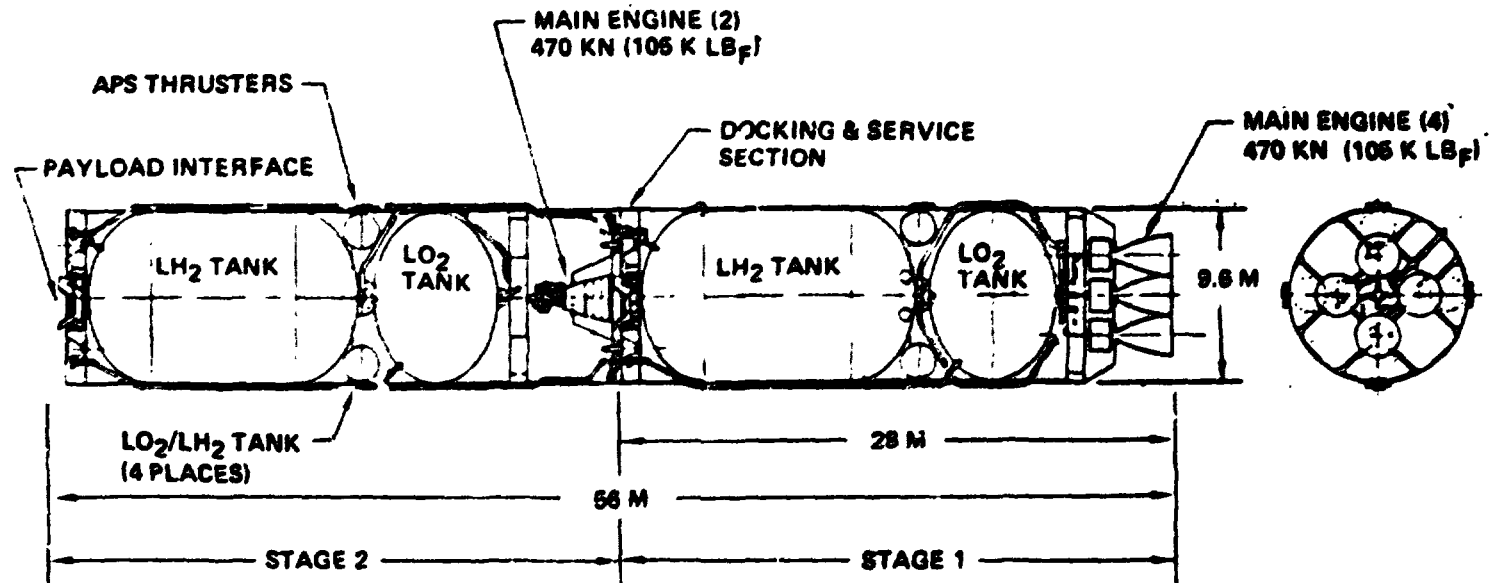
**SPACE BASED COMMON STAGE OTV
GEO CONSTRUCTION**

The GEO construction OTV is a space based common stage (2-stage) system with both stages having identical propellant capacity. The first stage provides approximately 2/3 of the delta V requirement for boost out of low earth orbit at which point it is jettisoned for return to the low earth orbit staging depot. The second stage completes the boost from low earth orbit as well as providing the remainder of the other delta V requirements to place the payload at GEO and the required delta V to return the stage to the LEO staging depot. Subsystems for each stage are identical in terms of design approach. The basic difference includes the use of four engines in the first stage due to thrust-to-weight requirements of approximately 0.15. The second stage requires additional auxiliary propulsion due to its maneuvering requirements in the docking of the payload to the construction base at GEO. The OTV shown has been sized to deliver a payload taken directly from the launch vehicle (400 000 kg). As a result, the OTV startburn mass is approximately 890 000 kg with the vehicle having an overall length of 56 meters.



D180-22876-7

Space Based Common Stage OTV GEO Construction

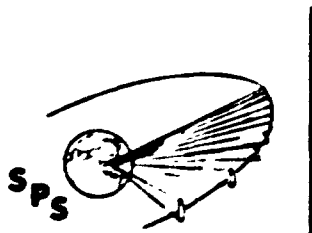


- PAYLOAD CAPABILITY = 400,000 KG
- OTV STARTBURN MASS = 890,000 KG
- STAGE CHARACTERISTICS (EACH)
 - PROPELLANT = 415,000 KG
 - INERTS = 29,000 KG (INCLUDING NONIMPULSE PROPELLANT)
- 290 OTV FLIGHTS PER SATELLITE

D180-22876-7

**FLIGHT OPERATIONS
SELF POWER ORBIT TRANSFER**

Flight operation differences between the two orbit transfer vehicle options is influenced by their orbit transfer time. In the case of the self power system for LEO construction, as many as 1200 revolutions around the Earth occur prior to reaching GEO when using a 180 day transfer. The flight schedule including a 40 day construction phase indicates as many as five modules can be in transit at any one time for the case of 8 modules per satellite.

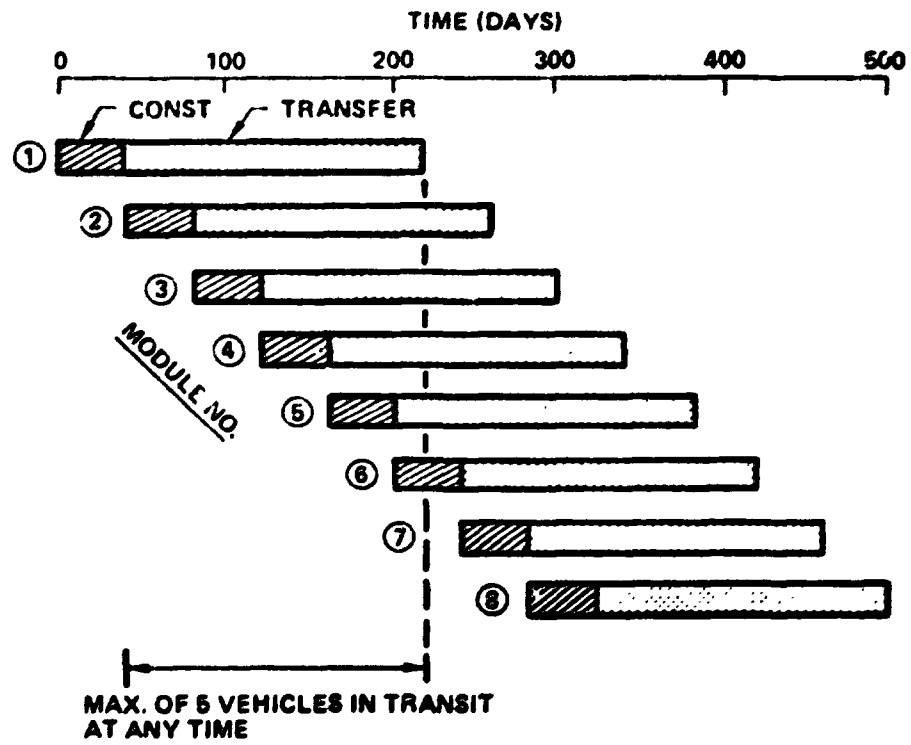
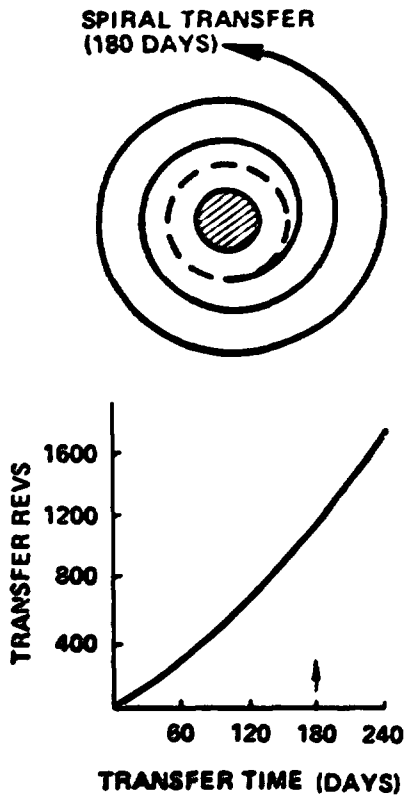


D180-22876-7

Flight Operations Self Power Orbit Transfer

SPS-1609

BOEING



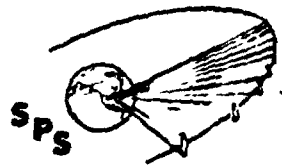
D180-22876-7

**FLIGHT OPERATIONS
CHEMICAL ORBIT TRANSFER**

The mission profile for the common stage LO_2/LH_2 OTV for GEO construction results in a 40 hour mission requirement for the first stage and 85 hours for a second stage which delivers the payload. These times include about 12 hours for refueling and refurbishment of each stage. With the requirement of one OTV flight per day with the GEO construction option, a total of two lower stages and four upper stages are required. Operated in this manner, as many as six independently operating stages can be in flight at one time.

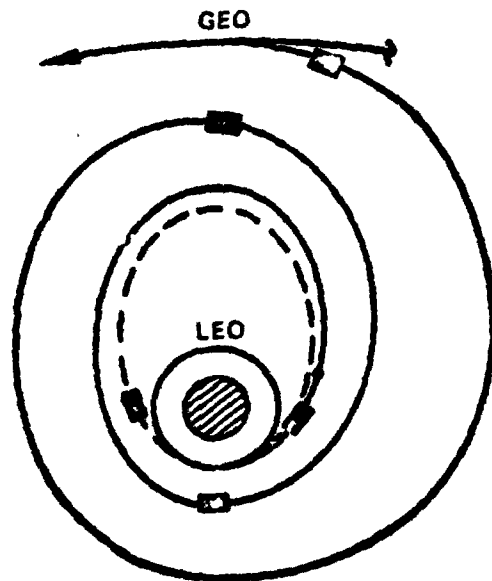
D180-22876-7

Flight Operations Chemical Orbit Transfer

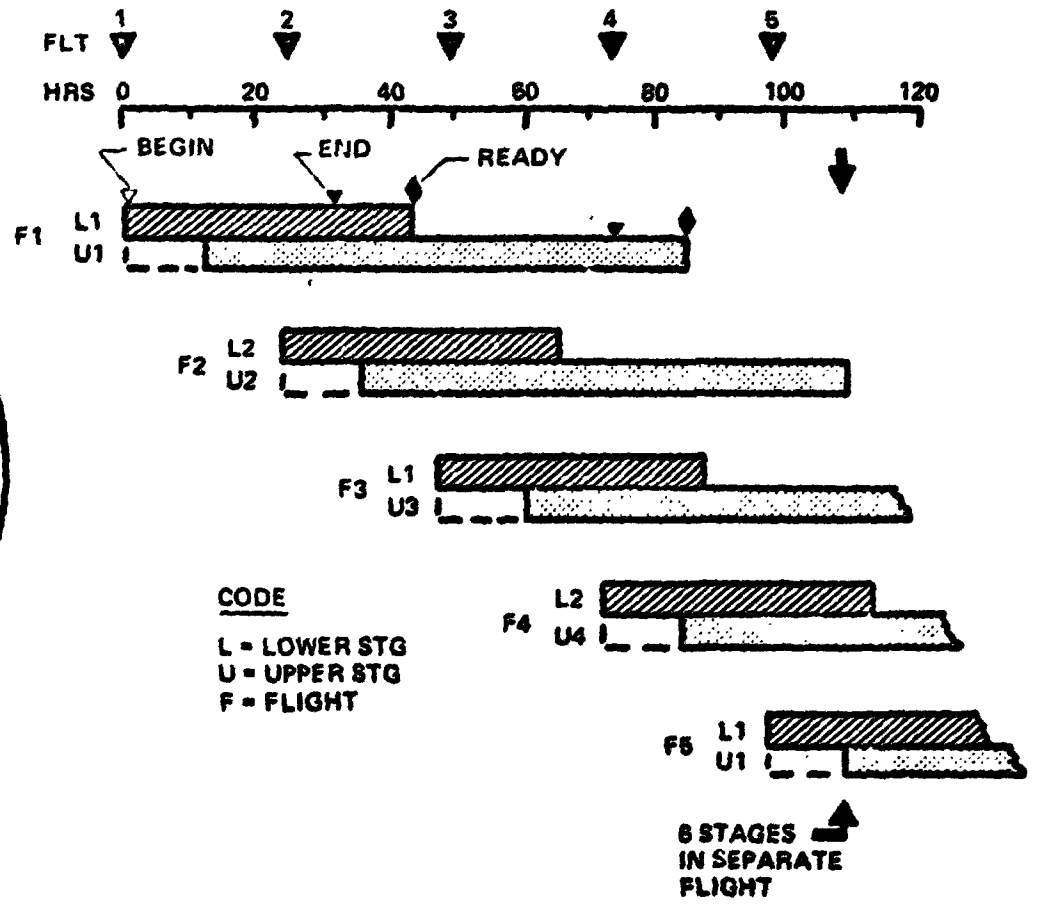


SP2-1610

MISSION PROFILE

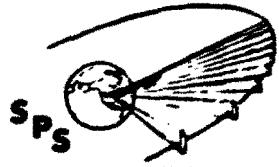


- STG 1 - - - - -
- STG 2 - - - - -
- MAJOR BURN -
- SEPARATION •



CREW ROTATION/RESUPPLY TRANSPORTATION

Crew rotation/resupply systems consist of a shuttle growth vehicle for delivery of personnel to LEO and the standard two-stage ballistic/ballistic launch vehicle for delivery of supplies and propellant to LEO. Crew and supply delivery between LEO and GEO use a two-stage LO₂/LH₂ OTV. The OTV for the LEO concept is about 1/2 as large as that for the GEO concept and requires one-third as many flights because of the significantly fewer people at GEO. Since the total orbital crew size for the two concepts is about the same number of delivery flights to LEO are also the same. Cargo flights to LEO, however, are three times greater for the GEO approach primarily due to the large OTV propellant requirements.



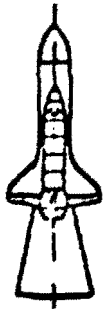
Crew Rotation/Resupply Transportation

SPS-1603

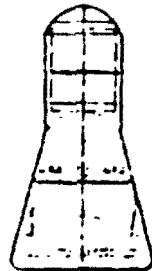
BEING



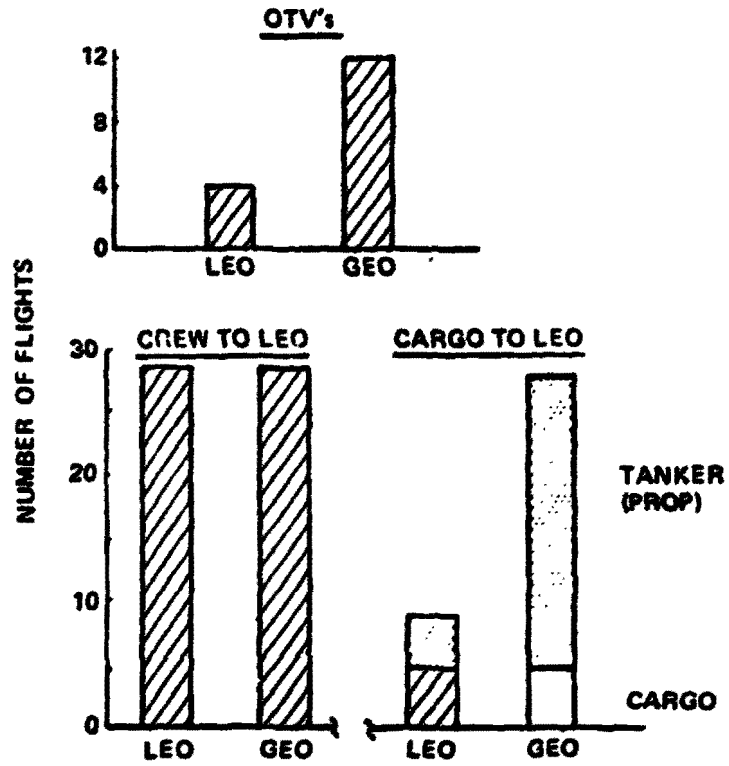
- CREW/CARGO TO GEO
- 2 STAGE LO₂/LH₂ OTV
- LEO CONST OTV
 - W_S = 495 000 Kg
- GEO CONST OTV
 - W_S = 890 000 Kg



- CREW TO LEO
- SHUTTLE GROWTH
- 76/FLT

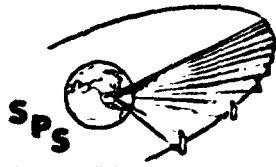


- CARGO, PROP & OTV's
- 2 STAGE BALLISTIC



TOTAL CARGO MASS TO LEO

Total cargo mass requirements to LEO reflect both the payload requirements indicated earlier and the OTV propellant and hardware requirements. For the three system elements that require transportation, payload requirements are not too different, however, the inclusion of the orbit transfer system requirements add significantly to the total mass which must be delivered by the HLLV. Again, it should be emphasized that the satellite transportation requirements are by far the most dominating.

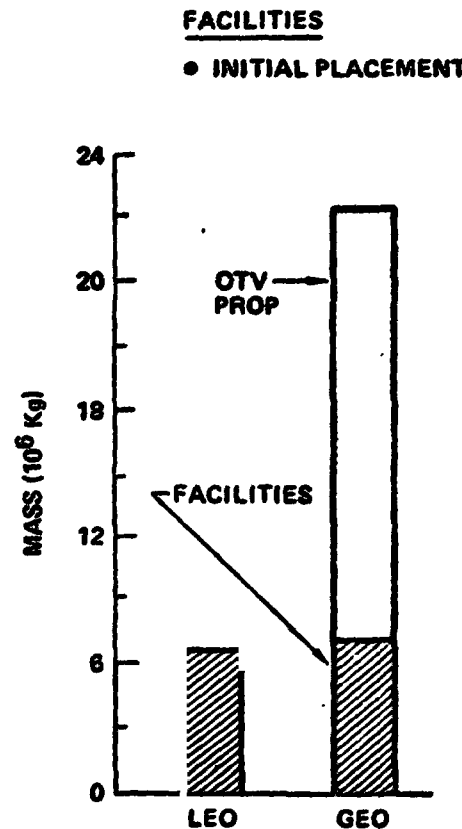
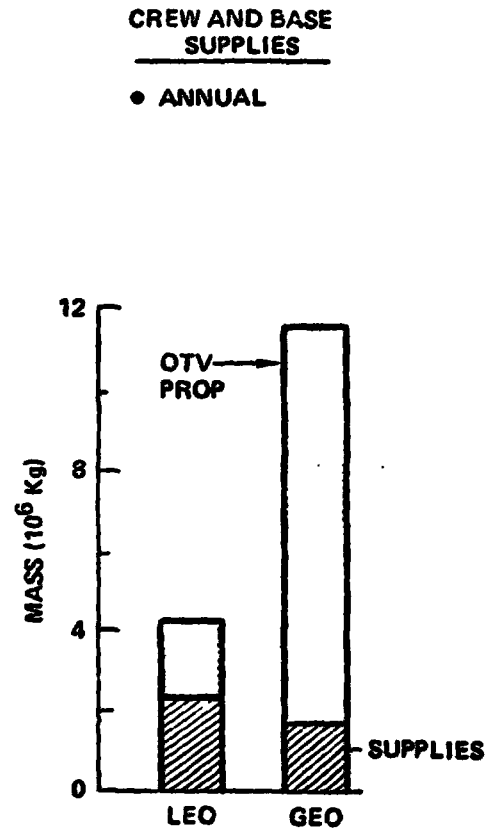
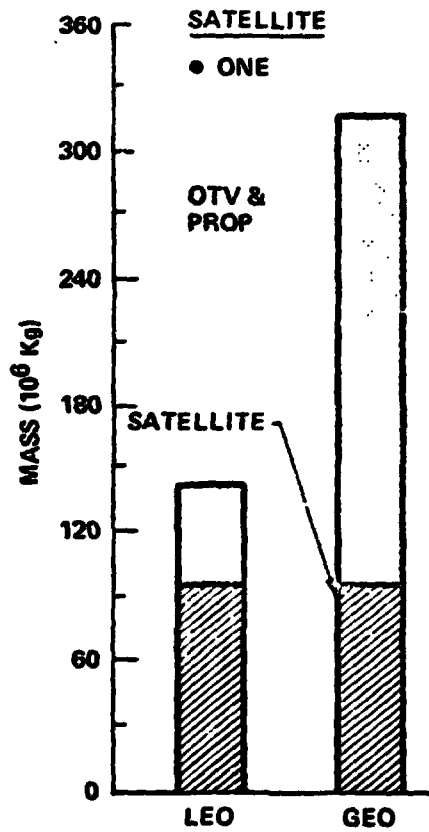


SPS-1608

Total Cargo Mass to LEO

BOEING

• ONE SATELLITE PER YEAR

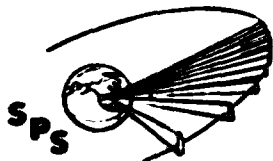


CONSTRUCTION LOCATION

D180-22876-7

SPS CARGO LAUNCH VEHICLE

As previously stated, the reference cargo launch vehicle is a two-stage ballistics/ballistic device using LO_2/RP in stage one and LO_2/LH_2 in stage two. GLOW for this system is approximately 10.5 million kg for the case of delivering 391 000 kg to the construction base or the staging depot located in LEO with orbit characteristics of 477 km altitude and 31 degrees inclination. Vehicle operations include first stage separation at a relative velocity of 2970 meters per second and downrange water landing approximately 815 km. The second stage delivers the payload to the LEO base, docks and returns one day later and also uses a water landing.

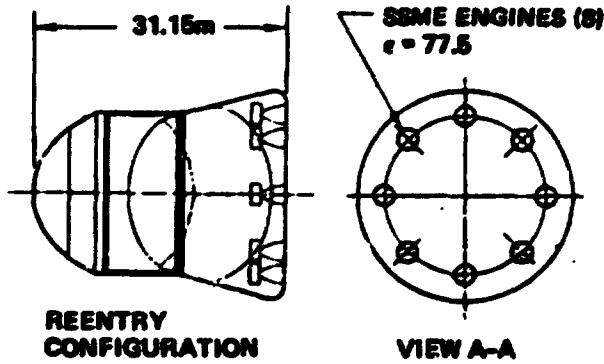


D180-22876-7

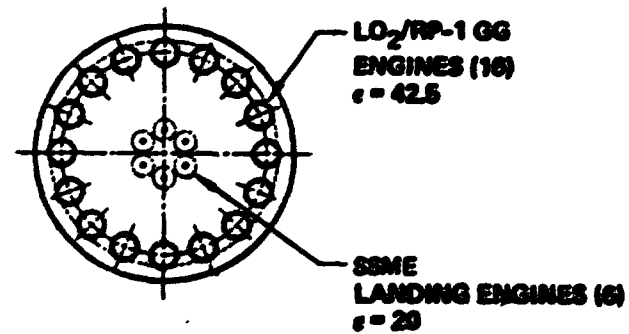
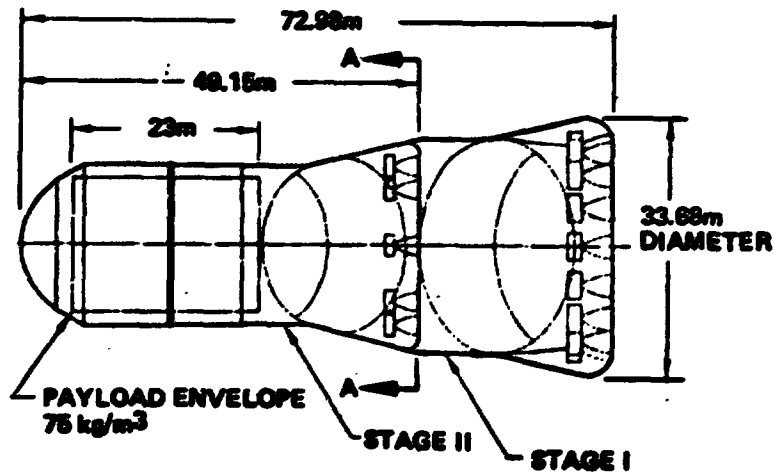
SPS Cargo Launch Vehicle

SPS-008

BOEING

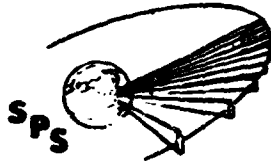


GLOW	10.472×10^6 kg
BLOW	8.243×10^6 kg
W_{P_1}	7.456×10^6 kg
ULOW	1.838×10^6 kg
W_{P_2}	1.479×10^6 kg
PAYLOAD	0.381×10^6 kg
T/W AT LIFTOFF	1.30



NUMBER OF HLLV LAUNCHES

A most significant impact in the area of launch operations is the difference in the number of launches required to support each construction location option. The number of flights indicated here are only those relating to the delivery of satellite components and orbit transfer provisions for the satellite and are for the case of constructing four satellites per year. As would be expected from the transportation requirements chart presented earlier, the LEO construction option requires only one half as many Earth launches as the GEO construction option.

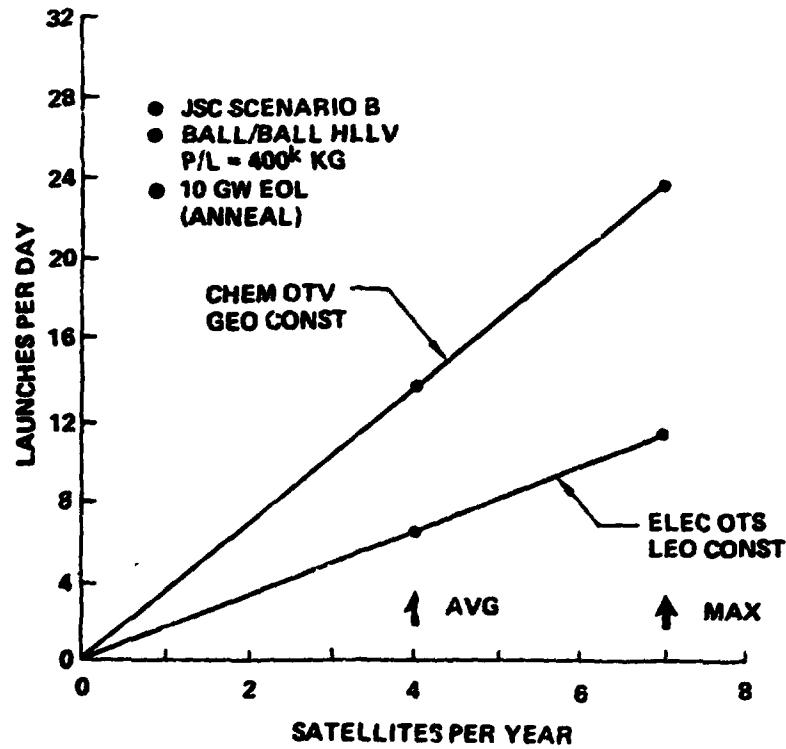


SPS 700

D180-22876-7

Number of HLLV Launches

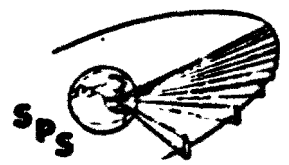
BOEING



**TRANSPORTATION COSTS
LEO VERSUS GEO**

Total transportation cost for the three major system elements is presented. Cost is related to that associated with one satellite, but reflect rates associated with four satellites per year. The Earth-LEO bar increments reflect the cost of getting payloads to LEO. Accordingly, the LEO-GEO increment relates to cost of refueling orbit transfer vehicles and their unit cost. In the case of satellite delivery, the interest increment relates to the self power trip time of 180 days and the additional interest accrued. (Note: Revenue is not lost, only delayed 180 days - the same revenue period still exists.)

The dominating factor in this comparison is that satellite transportation with LEO construction using self-power provides a \$2 billion (33% savings) over the GEO construction approach. Crew rotation/resupply transportation cost are also \$150 million (36%) lower for the LEO construction concept along with a \$200 million savings for the initial placement of the construction bases.

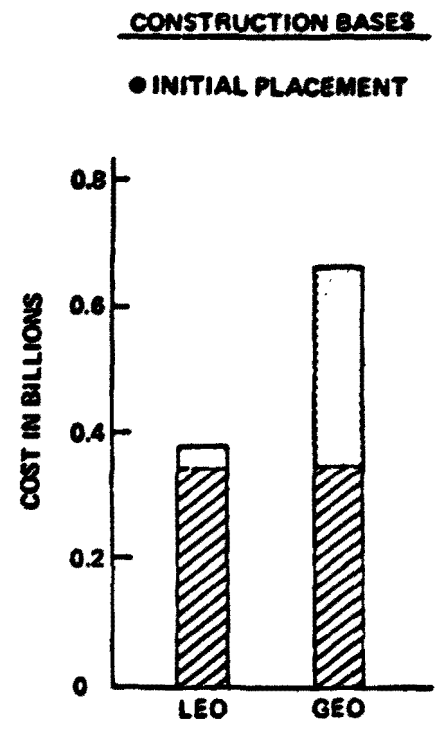
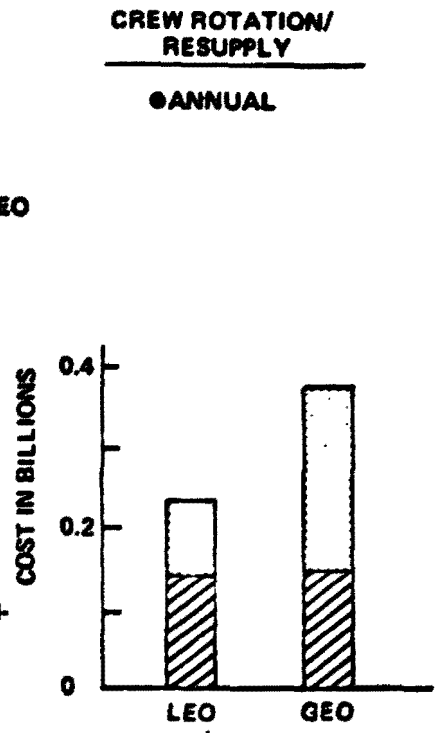
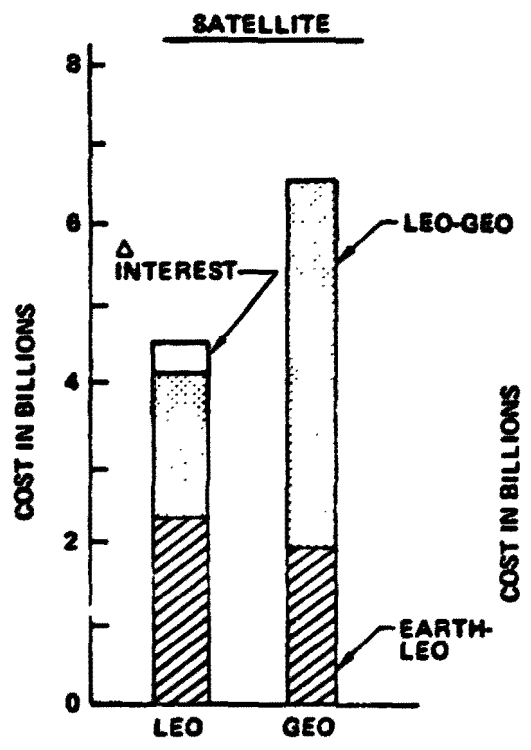


SPS-1007

Transportation Cost LEO vs GEO

BOEING

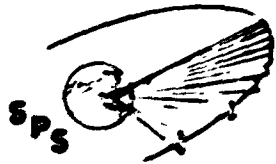
● 4 SATELLITES/YEAR



CONSTRUCTION LOCATION

CONSTRUCTION LOCATION SUMMARY

A summary comparison of the LEO and GEO construction locations is presented with an indication of which approach is most desirable. Compared in this manner, a number of parameters result in no significant differences between the two construction location options. However, a number of parameters give a clear indication that LEO construction is most desirable. Most notable among these being transportation costs, simplified launch operations, and reduced construction base mass and costs. One parameter has been judged to be in favor of the GEO construction approach (the impact on satellite design) although this data is then fed into the transportation comparison which still favors the LEO construction approach.



D180-22876-7

Construction Location Summary

SPS 1622

BOEING

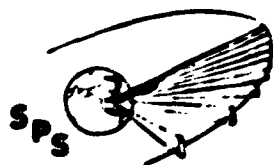
<u>COMPARISON PARAMETER</u>	<u>LEO</u> <u>LOCATION</u> <u>GEO</u>	<u>RATIONALE</u>
● FACILITIES	NO SIGNIF. DIFFERENCE	● SAME CONST BASE ● STAGING DEPOT vs FINAL ASSY FACILITY
● SATELLITE (PWR GEN) CONST	NO SIGNIF. DIFF.	● 1 vs 2 DIRECTION INDEXING OFFSET BY MODULE DOCKING
● ANTENNA INSTALLATION	✓	● ANTENNA FACILITY DOESN'T MOVE
● CONSTRUCTION EQUIP	NO SIGNIF. DIFF.	
● CREW REQUIREMENTS	✓	● SAME SIZE BUT MAJORITY AT LEO
● ENVIRONMENTAL FACTORS	NO SIGNIF. DIFF.	● ALL FACTORS CAN BE HANDLED WITH ACCEPTABLE SOLUTIONS
● CONSTRUCTION MASS & COST	✓	● LIGHTER (0.5M Kg; 7%) ● CHEAPER (\$0.5B; 8%)
● SATELLITE DESIGN IMPACT		● NO Δ OVERSIZING, MODU- LARITY OR POWER DIST. PENALTY
● ORBIT TRANSFER COMPLEX	NO SIGNIF. DIFF.	● APPROX SAME NO. VEHICLES IN FLIGHT
● LAUNCH OPERATIONS	✓	● ONE-HALF AS MANY LAUNCHES
● TRANSPORTATION COST	✓	● CHEAPER (\$2B; 33%)

✓ INDICATES MOST PROMISING CONCEPT

D180-22876-7

CONSTRUCTION/TRANSPORTATION CONCLUSIONS

The conclusions regarding the issues of power generation system comparison and construction location comparison as influenced by construction and transportation factors show a distinct advantage for a photovoltaic satellite (CR=1) constructed in low earth orbit and transported to GEO using self power.



SPS-1622

Construction/Transportation Conclusions

BOEING

- **THE PHOTOVOLTAIC SATELLITE (CR - 1) OFFERS SIGNIFICANT ADVANTAGES**
 - **LESS COMPLEXITY IN FACILITIES AND CONSTRUCTION EQUIP**
 - **SMALLER CONSTRUCTION CREW**
 - **LOWER CONSTRUCTION COST**
 - **LOWER TRANSPORTATION COST**

- **LEO CONSTRUCTION OFFERS A SIGNIFICANTLY LOWER TRANSPORTATION COST**
OTHER FACTORS ARE COMPARABLE:
 - **CONSTRUCTION OPERATIONS**
 - **SATELLITES IN EITHER CASE REQUIRE ELECTRICAL PROPULSION AND 3 AXIS ATTITUDE CONTROL**
 - **ENVIRONMENTAL FACTORS CAN BE HANDLED WITHOUT EXCESSIVE PENALTIES**